An Assessment of Uncertainties in the Analysis of the Impact of Climate Change on Flooding

A thesis submitted for the degree of Doctor of Philosophy

Department of Meteorology

Ralph James Ledbetter

May 2012

Declaration

I confirm that this is my own work and the use of all materials from other sources has been properly and fully acknowledged.

Ralph Ledbetter

Abstract

This thesis aims to address the role of uncertainty in climate change impact studies, with particular focus on the impacts of climate change on UK flooding. Methods are developed to quantify the uncertainty associated with climate variability, hydrological model parameters and flood frequency estimation. Each is evaluated independently, before being combined to assess the relative importance of the different sources of uncertainty in the 'top down' impact study framework over multiple time horizons.

The uncertainty from climate variability is addressed through the creation of a resampling methodology to be applied to global climate model outputs. Through resampling model precipitation, the direction of change for both mean monthly flows and flood quantiles are found to be uncertain with large possible ranges.

Hydrological model parameter uncertainty is quantified using Monte Carlo methods to sample the model parameter space. Through sensitivity experiments, individual hydrological model parameters are shown to influence the magnitude of simulated flood quantile changes. If a larger number of climate scenarios are used, hydrological model parameter uncertainty is small only contributing up to 5% to the total range of impacts.

The uncertainty in estimating design standard flood quantiles is quantified for the Generalised Pareto distribution. Flood frequency uncertainty is found to be most important for nearer time horizons, contributing up to 50% to the total range of climate change impacts. In catchments where flood estimation uncertainty is less important, global climate models are found to contribute the largest uncertainty in the nearer term, between 40% and 80% of the total range, with emissions scenarios becoming increasingly important from the 2050s onwards.

Acknowledgements

Table of Contents

List of Figures

List of Tables

List of Abbreviations

5RP	Five Year Return Period Flood
20RP	Twenty Year Return Period Flood
50RP	Fifty Year Return Period Flood
AM	Annual Maxima
AR4	IPCC Fourth Assessment Report
BFI	Base Flow Index
CMIP3	Third Couple Model Intercomparison Project
FAR	IPCC First Assessment Report
DYNIA	Dynamic Identifiability Analysis
GCM	Global Climate Model
GL	Generalised Logistic Distribution
GLUE	Generalised Likelihood Uncertainty Estimation
GP	Generalise Pareto Distribution
IPCC	Intergovernmental Panel on Climate Change
LAM	Limited Area Model
MOC	Atlantic Meridional Overturning Circulation
MORECS	UK Met Office Evapotranspiration Calculation System
NAO	North Atlantic Oscillation
NRFA	National River Flow Archive
NS	Nash Sutcliffe Flow Criterion
PDM	Probability Distributed Moisture Model
POT	Peaks Over Threshold
POT3	POT With Average of Three Peaks a Year
PPE	Perturbed Physics Ensemble

List of Abbreviations

PWM	Probability Weighted Moments
RCM	Regional Climate Model
RCP	Representative Concentration Pathways
RMME	Resampled Multi Model Ensemble
SE	Standard Error of Estimate
SRES	Special Report on Emissions Scenarios
TAR	IPCC Third Assessment Report
UKCIP	UK Climate Impacts Programme
UKCP09	UK Climate Projections 2009

CHAPTER 1

Introduction

1.1 Rationale

Fluvial flooding is the most frequently occurring natural hazard in the UK, with £800 million projected to have been spent on river and coastal flood risk management in 2010-2011 (Pitt Review, 2008). This is in response to the first decade of the 21st century which was characterised by numerous widespread and localised flood events (e.g. Autumn 2000 (Marsh, 2001), Boscastle 2004, Summer 2007 (Faulkner et al., 2008) and Cumbria 2009 (Stewart et al., 2010)). The impact of flood events in the UK is often severe, due in part to 2 million properties being at risk from flooding; valued at over £200 billion (FORESIGHT, 2004). Furthermore despite spending £800 million per annum managing the risk posed by flooding, the average annual damage as a consequence of flooding is £1.4 billion. Understanding and managing the risk of flooding in the present day is clearly of socio-economic benefit, however increasing focus is being placed on understanding the changing risk of future flooding in response to climate change (Evans et al., 2008).

Anthropogenic emissions of greenhouse gases are considered by the Intergovernmental Panel on Climate Change (IPCC) as *very likely* to cause an increase in global temperatures over the course of the 21st century (IPCC, 2007). One impact resulting from an increase in global temperatures will be an intensification of the global hydrological cycle (Huntington, 2006), which in turn will lead to changes in the pattern and magnitude of precipitation (Bates et al., 2008). The changes in precipitation will have a wide impact on hydrological systems (Wagener et al., 2010); although to date there is no evidence in UK observed river flows for a change in current flood risk (Robson, 2002, Mudelsee et al., 2003, Hannaford and Marsh,

2008). This is a result of a lagged response of the climate to the increases in anthropogenic emissions (IPCC, 2007), meaning the effects of climate change on hydrological systems will not be detectable until further into the future (Wilby, 2006). In light of this a number of climate change impact studies have sought to predict how future changes in climate may impact on flooding (Cameron et al., 2000, Reynard et al., 2001, Prudhomme et al., 2002, Prudhomme et al., 2003, Cameron, 2006, Kay et al., 2006, Dankers and Feyen, 2008, Dankers and Feyen, 2009, Kay and Jones, 2011); with a general consensus that there is likely to be an increase in the magnitude and frequency of flood events in the UK as a result of climate change.
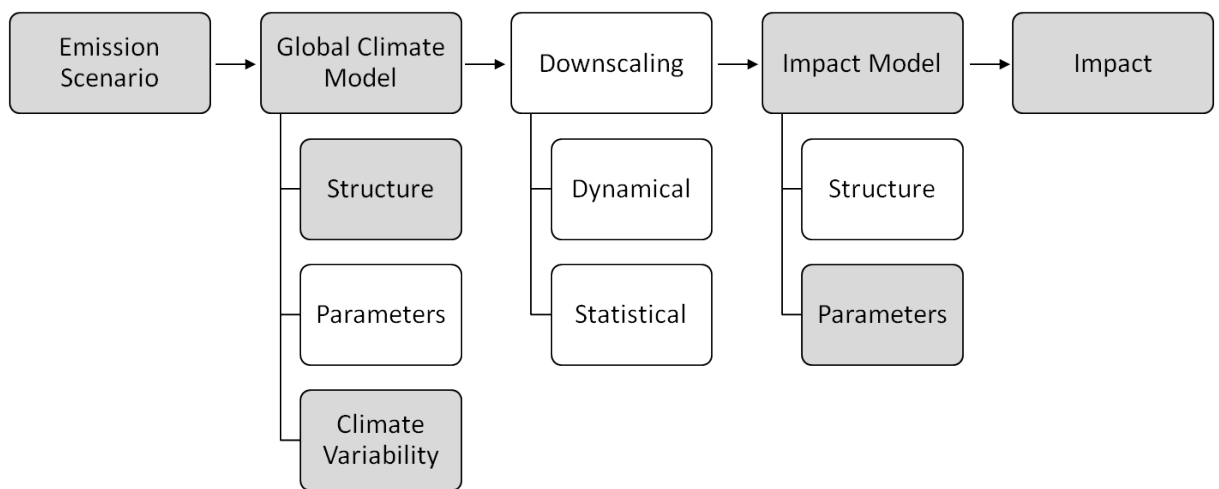
Figure 1.1 Schematic of 'top down' impact study framework. Shaded boxes are components which are addressed in this thesis.

Typically most climate change flood impact studies adopt a 'top down' framework (as detailed in Carter (2007) and outlined in Figure 1.1) where an emissions scenario, which describes a plausible rate of future greenhouse gas emissions, is used to force a global climate model (GCM). The GCM is a computational representation of the Earth, simulating the future response of the atmosphere and oceans over vertical and horizontal grids to changes in external forcings (e.g. greenhouse gas emissions). The resolution of a GCM grid cell is large (i.e. several degrees) requiring the GCM outputs to be downscaled for catchment scale hydrological analysis. Downscaling uses methods that are either dynamical; using a higher resolution climate model, or statistical; where empirical relationships are derived between larger and smaller scale climate variables. The downscaled climate time series are input to a hydrological impact model, with a flood impact analysis undertaken on the simulated river

flow time series. Each component of this 'top down' framework contributes a degree of uncertainty in any calculated changes in the impact response (Wilby et al., 2009).

The different components of uncertainty in the 'top down' framework need to be quantified in combination with one another to provide robust information to inform adaptation decisions (Wilby et al., 2008). There are a small number of studies which have attempted such an analysis (Wilby and Harris, 2006, New et al., 2007, Kay et al., 2009); however no study to date has separated the relative importance of uncertainties when assessed in combination with each other over multiple time horizons.

1.2 Research Objectives

The overarching aim of this thesis is to understand the role of uncertainty in the components of the 'top down' climate change impact study framework when assessing the impact on UK fluvial flooding. The literature review in the next chapter identifies a number of research gaps in the context of the following main research objectives:

1. Explore methods for quantifying the uncertainty associated with each component of the climate change impact study framework; specifically, as identified in Chapter 2, the role of climate variability, hydrological model parameter uncertainty and flood frequency analysis uncertainty.
2. Identify the relative importance of the uncertainty associated with each component in the 'top down' climate change impact study framework at different time horizons.
3. Develop methods for presenting future projections and their inherent uncertainties in a practical context.

The specific components of uncertainty in the 'top down' framework which are addressed in this thesis are highlighted in Figure 1.1. The research gaps identified from the literature review which contribute to the research objectives are presented in Chapter 2 and summarised as part of the thesis outline in the next section.

1.3 Thesis Structure

This thesis is structured in order to address the outlined research objectives, as schematised in Figure 1.2. A literature review on the 'top down' climate change impact study framework for flooding will be undertaken in the next chapter, Chapter 2, to identify a number of current research gaps and provide the scientific context for the thesis. The data and methods that are

required to undertake a climate change impact assessment on UK flooding are presented in Chapter 3. From Chapter 4 onwards, the thesis is structured in line with the 'top down' climate change impact study framework.
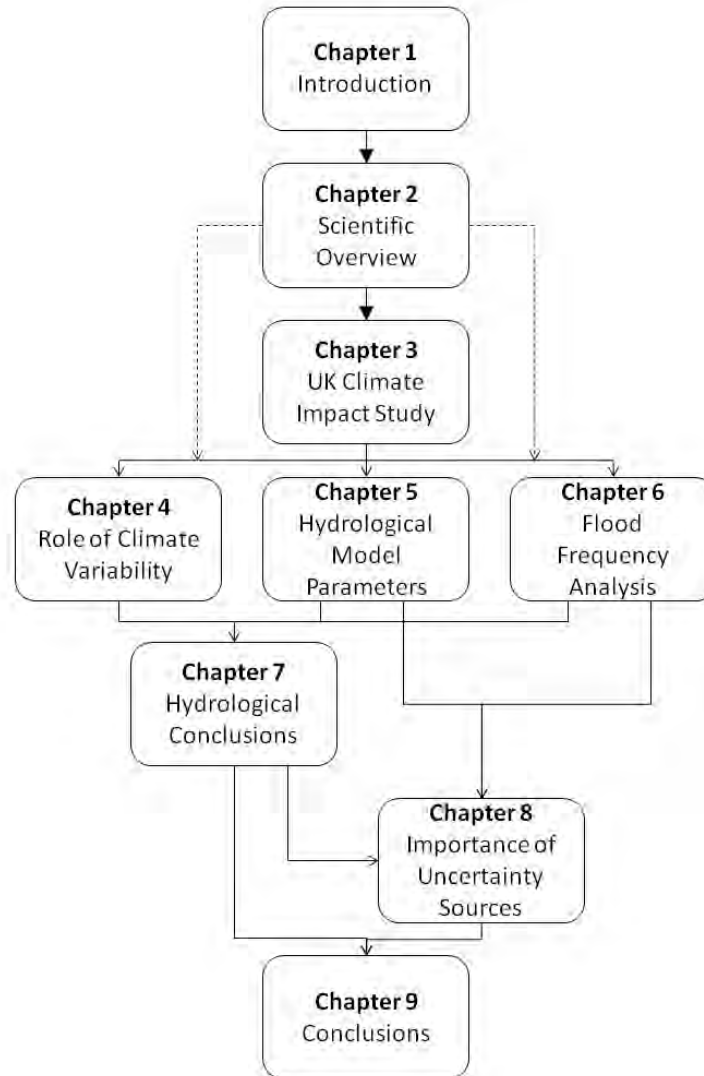
Figure 1.2 Schematic of thesis structure.

Chapter 4 investigates the role of the climate variability in climate change impact studies and a new resampling methodology is developed to quantify plausible ranges of GCM precipitation variability. In Chapter 5 the role of hydrological model parameter uncertainty is investigated; firstly by creating multiple model parameter sets; and secondly by identifying how the model parameters are sensitive to climate change. Chapter 6 identifies the role of flood frequency analysis and its associated uncertainty when calculating changes in future flooding magnitudes. A number of hydrological conclusions are identified in Chapters 4-6,

which are summarised with further examples in Chapter 7. The research in Chapters 4-7 all contribute to research objective one outlined previously. The remaining research objectives are addressed in Chapter 8, which draws together the work from the previous chapters to identify the relative importance of each uncertainty component; and places future uncertainties in the context of present day flood estimation uncertainty. The thesis concludes in Chapter 9 with the main conclusions, scientific contributions and suggestions for future work.

The next chapter presents a literature review to identify the specific research gaps that need to be addressed to fulfil the research aims of this thesis.

CHAPTER 2
Scientific Overview

2.1 Introduction

The chapter presents a literature review on the assessment of the impact of climate change on fluvial flooding. This provides the scientific context for the research in this thesis, identifying research gaps which require investigation. The literature review is structured in the order of the 'top down' climate change impact study framework as identified in Chapter 1. Each aspect of the impact study framework is addressed in this review including emissions scenarios (section 2.2), climate modelling (section 2.3), downscaling (section 2.4), hydrological modelling (section 2.5) and flood frequency estimation (section 2.7). The review finishes with an overview of the current state of probabilistic impact assessments and uncertainty (section 2.7).

From this literature review a number of research gaps are identified and discussed in section 2.8, which provides the outline for the research in this thesis. The chapter concludes with a summary providing an overview of the chapter.

2.2 Emissions Scenarios

Climate change science has evolved to understand the anthropogenic influence on the Earth's climate, in particular the climate response as a result of increased greenhouse gas emissions. In the early stages of climate change research, most future projections were based on theoretical experiments through the doubling of CO_2 emissions. However with increasing focus on the potential impacts of climate change on natural systems, emissions scenarios have evolved so they can be linked to a number of future socio-economic story lines (or

'pathways'). This sections aims to provide a brief overview of the assumptions behind creating different emissions scenarios, followed by a review of how emissions scenarios contribute to the uncertainty in hydrological impact studies.

2.2.1 Emissions Scenario Development

Emissions scenarios provide the foundation for formulating future projections of climate under altered external forcings. The establishment of common emissions scenarios was essential for all climate models and the resulting impact studies to be assessed to the same benchmark. The main factors which dictate the formulation of common emissions scenarios are population, economics, political action and global energy resources (Moss et al., 2010). In the IPCC first assessment report (FAR - IPCC, 1990), four emissions scenarios were established which all used the same population and economic growth assumptions, with energy supply the main variation between scenarios. The energy assumptions varied from the use of reduced carbon fuel to a full conversion to nuclear and renewable energies. Due to the limitations of the first common emissions scenarios (i.e. considering only population and economics), and following real world political changes resulting from the Montreal protocol, a revised set of emissions scenarios were developed (IS92 Scenarios - IPCC, 1992). The revised emissions scenarios included changes in population growth and economic developments along with energy supply changes and hypothesised globally accepted emissions sanctions. The interaction of the different components of each emission scenario describes a distinct story of the global socio-economic development through the 21st century. An increased scientific understanding of greenhouse gases and their interaction with the climate as well as changing demands from scientists led to a revised set of emissions scenarios in 2000 (SRES Scenarios - IPCC, 2000).

The SRES scenarios were used in the IPCC third (TAR) and fourth (AR4) assessment reports; a summary of the greenhouse gas emissions for each scenario is provided in Figure 2.1 (left). The different pathway of each emissions scenario demonstrates the varying assumptions that lie behind each of the individual scenarios. The SRES scenarios have been used for 10 years, allowing for the early 21st century emissions estimates to be compared with observed emissions. Raupach et al (2007) found that the observed CO_2 concentrations for 2000-2005 lay at the high end of the most extreme SRES scenario (Figure 2.2 - Left). An update to the findings of Raupach et al (2007) provided by the Global Carbon Project further demonstrates that current global emissions are high relative to the SRES estimates (Figure 2.2 - Right).
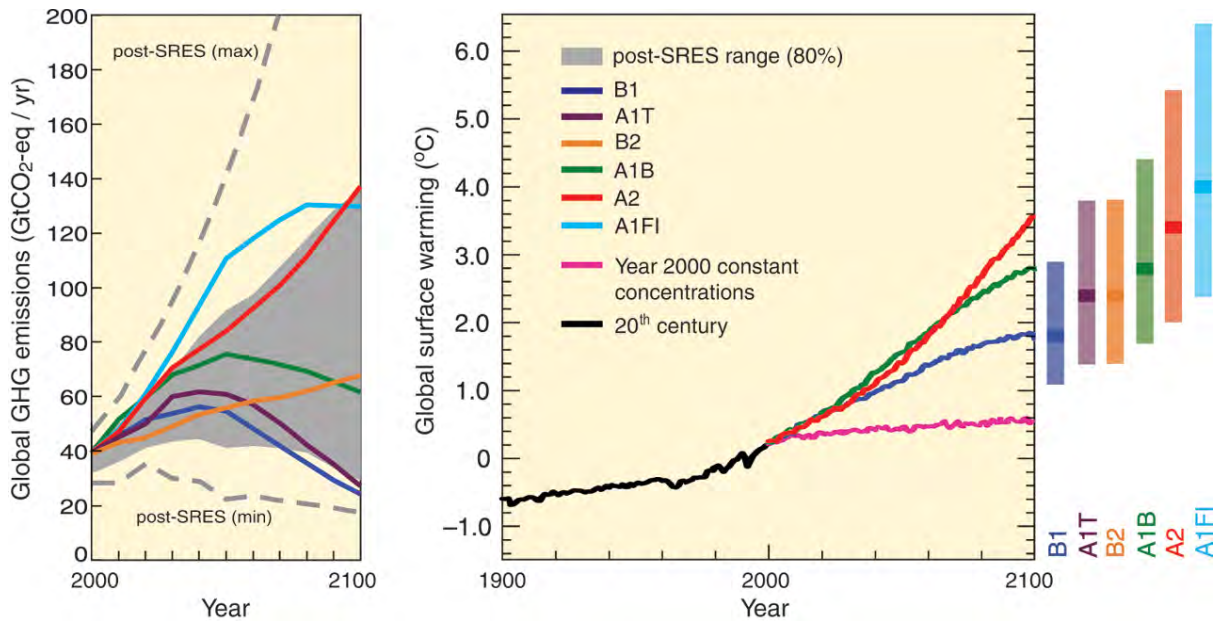
Figure 2.1 Emissions scenarios used in IPCC AR4. Left – Global GHG emissions through the 21st century under different emissions scenarios. Right – Global mean surface warming in response to each emissions scenario, with the full range displayed by bars on far right (Figure SPM5 - IPCC, 2007).

The different SRES emissions scenarios result in a wide range of global surface warming to be projected by climate models by the end of the 21st century (Figure 2.1- right); however in the nearer term (i.e. 2020s-2030s) their effect is reduced, resulting from the lag in the climate response to a change in the forcing (Schneider and Mastrandrea, 2005). The full range of surface warming response at the end of the 21st century spans from a minimum increase of 1.4 °C for SRESB1 to a maximum increase of 6.4 °C for SRESA1F1. This range in response shows the uncertainty between the different emissions scenarios, in turn highlighting that each scenario provides a projection based on a storyline describing a plausible future rather than a prediction.

To reflect the under-estimation of the SRES scenarios compared with early 21st century observations and to incorporate the latest scientific knowledge a new set of emissions scenarios, termed "representative concentration pathways" (RCPs) (Moss et al., 2008, van Vuuren et al., 2011) have been developed for use in the IPCC fifth assessment report. These will be the fourth set of common emissions scenarios, each set providing a demonstration of how climate science has evolved over time.
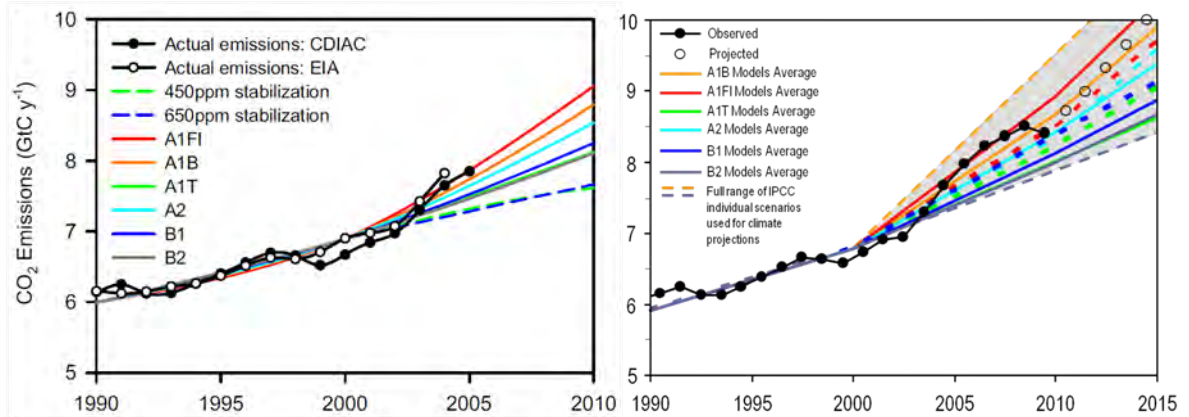
Figure 2.2 Comparisons of SRES emissions scenarios with observed emissions. Left: Figure taken from Rapauch et al (2007), Right: Updated from Raupach et al. 2007, PNAS; Data: Gregg Marland, Thomas Boden-CDIAC 2010; International Monetary Fund 2010: Global Carbon Project.

2.2.2 Emissions Scenarios in Impact Studies

The previous section demonstrated that the assumptions behind each emissions scenario, in particular the variation in the magnitude and pace of change of greenhouse gas concentrations in the atmosphere, have a strong influence on future projections of temperature. Given that climate models simulate the entire climate system response to the changes in emission, it is likely that other natural systems will also be influenced by the different emissions scenarios. This section outlines the role of the emissions scenarios within the hydrological climate change impact study framework.

In the previous section the temperature response to different emissions scenarios was shown to be small in the near term but increasingly variable at more distant time horizons. The same is found for precipitation projections with an increasing importance of the emission pathway over time, although small in comparison to climate model uncertainties (Hawkins and Sutton, 2011). The manner in which the emissions uncertainty in precipitation projections propagates through to hydrological impacts also varies depending on the time horizon. Typically the difference between emissions scenarios becomes most notable at the end of the 21st century (Arnell, 2003a, Prudhomme et al., 2003). However even by the 2080s the range between different emissions scenarios is found to be small in magnitude, varying between 5-10% for changes in mean flows (Nobrega et al., 2011, Xu et al., 2011) and 10%-20% for changes in flood peaks (Kay et al., 2009).

One common characteristic is for the SRES emissions scenarios to be associated with consistent relative temperature changes to one another, which led the UK climate impacts

programme (UKCIP) to tag the SRES B1, B2, A2 and A1F1 emissions scenarios as Low, Medium-Low, Medium-High and High respectively. The magnitude of the hydrological impact resulting from the UKCIP emissions scenarios has been shown to conform to the naming convention, with high emissions displaying the greatest flow changes (Arnell, 2004, Cameron, 2006).

> **2.2.3 Emissions Scenario Summary Box**
>
> Emissions scenarios are an important component in developing climate change projections. They describe the greenhouse gas emissions for a particular story line of how society may behave throughout the 21st century, using assumptions based on population growth, economic growth, power utilisation and international coordination. A number of different emissions scenario sets have been developed in the last two decades, reflecting how climate science and understanding have evolved. When different emissions scenarios have been considered in hydrological impact assessments their influence has been shown to be greatest towards the end of the 21st century (i.e. 2080s). However their role compared with other sources of uncertainty, such as variations between different climate models, has been shown to be small. Despite the smaller role of emissions scenarios in climate change impact studies, it is important to consider a number of emissions scenarios to provide a broad context for any climate change impacts. However it is important to recognise that emissions scenarios are not predictions, thus no one scenario can be considered more or less likely than any other.

2.3 Climate Modelling

The main tool used for understanding climate change and providing future projections of climate are global climate models. Climate models are computer simulated representations of the Earth's atmosphere and oceans. The models are designed from the fundamental laws of physics (e.g. conservation of mass and momentum), resolving the physical processes across a gridded representation of the Earth. Given the complex nature of the atmosphere and oceans even the most sophisticated climate model provides a simplified version of reality, due in part to computational limitations and an incomplete understanding of the physical systems. These limitations and simplifications introduce a degree of uncertainty in any climate projections. The contributions to the uncertainty in climate model projections can be partitioned into three main sources (Hawkins and Sutton, 2009). These uncertainty sources relate to model structure, model parameterisation and internal model variability. Each of the different sources

of climate model uncertainty are presented in this section, followed by a discussion of the contributions of climate model uncertainty within the climate change impact study framework.

2.3.1 Climate Model Uncertainty

In the IPCC AR4 report, a total of 23 GCMs developed by 18 research groups were used to assess the potential impact of climate change (Meehl et al., 2007). The climate models were all developed to simulate the Earth's climate under different atmospheric forcing scenarios, and all models are constrained to the same physical laws of science. However the manner in which the physical processes are translated from the real world into numerical code and simulation are all slightly different, leading to structural differences between models. The main differences between climate models include the representation of the gridded Earth, with the resolution and position of the grid (both horizontally and vertically) varying between models. Furthermore each model includes slightly different physical mechanisms and feedbacks with a varying degree of complexity as to how well integrated they may be within a model (e.g. sea ice, vegetation). The combinations of these factors lead each climate model to provide a slightly different 'answer' of how the climate is characterised. The effect of the model differences on simulating precipitation can be seen in Figure 2.3. In addition to the differences between each climate model, it is also important to acknowledge that many of the models share common components. It is therefore important to understand the similarities and differences of the climate models for use in an impact study.
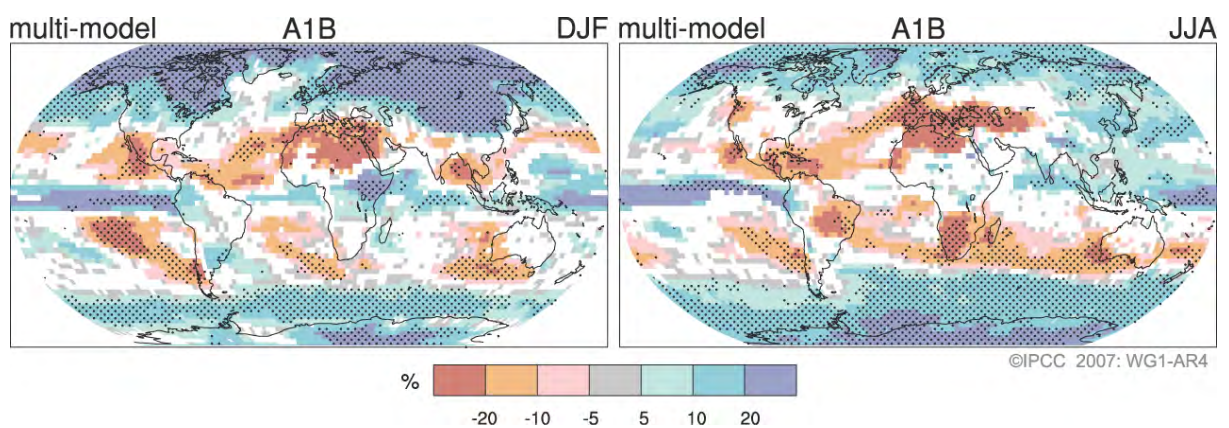
Figure 2.3 Figure and Caption from IPCC AR4. Relative changes in precipitation (in percent) for the period 2090–2099, relative to 1980–1999. Values are multi-model averages based on the SRES A1B scenario for December to February (left) and June to August (right). White areas are where less than 66% of the models agree in the sign of the change and stippled areas are where more than 90% of the models agree in the sign of the change.

In a given model there are a number of components which contribute uncertainty to the model outputs. Due to the coarse scale grid spacing of a climate model (e.g. 2-5 degrees latitude and longitude) a number of physical processes cannot be explicitly represented, and are in included as parameters instead (Murphy et al., 2004). Model parameterisation is common to all climate models, with each adopting different parameters according to their requirements. With any form of parameterisation there is uncertainty as to the acceptable value (and physical relation) of a given parameter. Typically each parameter has an acceptable range, meaning that different combinations of acceptable parameters can create different results. This has been addressed through implementing climate model perturbed physics ensembles (PPE) (Murphy et al., 2004, Stainforth et al., 2005). These ensembles are made up of multiple runs of a single climate model with the model parameter values varying between each ensemble run. Stainforth et al (2005) found that the spread of results from the PPE was greater for precipitation compared with temperature. The PPE experiment focussed on modifying parameters known to influence precipitation and cloud formation, such as convection or cloud to rain conversion. However, the degree to which the model parameter uncertainty influences the spatial and temporal variability of precipitation has implications for the direct use of precipitation from climate models.

The final component of uncertainty relating to climate modelling is from the impact of climate variability. A climate model is designed to reproduce the long term characteristics of climate under a given set of conditions. If a GCM was run multiple times with the same structure and parameters, it would create a different realisation of climate in each model run (Kendon et al., 2008, Deser et al., 2010). The difference between each model run is a result of climate variability, which causes deviations around the mean climate. A control period GCM run for the 20th century uses the observed emissions from the 20C3M emissions scenario, the climate variability within the model means that the individual years will vary from observations yet the long term mean climates will be similar. The magnitude and influence of climate variability differs between variables, with precipitation typically found to be more variable than temperature (Raisanen, 2001). This is confirmed by Deser et al (2010) who demonstrated that a significant change in temperature could be detected in a single model realisation of climate, whereas to detect a trend of similar significance in precipitation, 6-30 (depending on the region) precipitation realisations were required. This suggests that using a single model realisation of climate may not be representative of the overall projection, particularly for precipitation, where multiple realisations are required to separate the climate

variability and climate change signals. However the degree to which climate variability can be included in climate change impact studies is typically limited by there being few multiple model realisations available. One method suggested to overcome this is to resample the outputs from GCMs to improve the knowledge base from which to perform analysis (Raisanen and Ruokolainen, 2006, Ruokolainen and Raisanen, 2007).

The relative contributions of climate model structural uncertainties and climate model variability have been shown to vary between time horizons (Hawkins and Sutton, 2011, Yip et al., 2011). Figure 2.4 shows the relative contributions of climate model structure, variability and emissions scenario uncertainty to climate model precipitation projections. For European precipitation (Figure 2.4 - Right) climate model internal variability is dominant in the nearer term while climate model structure is shown to become more important at longer lead times. The choice of emissions scenario (as discussed in the previous section) is shown to be less important before the 2050s and is small thereafter for European precipitation. For temperature the role of climate variability is found to be smaller, while the emissions scenarios become more important (Hawkins and Sutton, 2009).
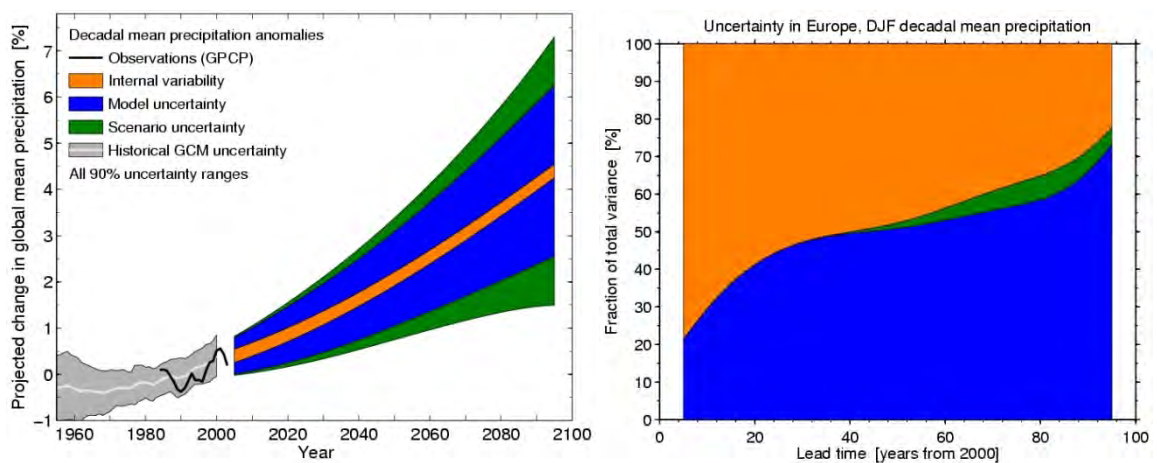
Figure 2.4 Relative contributions of uncertainty sources for global precipitation anomalies (left). Fractional sources of uncertainty for European winter precipitation (right) (Hawkins and Sutton, 2011).

2.3.2 Climate Models in Impact Studies

The uncertainty associated with GCMs and their outputs has significant implications for climate change impact studies, as GCMs are the main resource used for constructing climate change scenario inputs. Initially many climate impact studies used the outputs from a single or few GCMs (Arnell, 1999, Cameron et al., 2000), where the choice was primarily influenced by the availability of data. Through using just a single or few climate models, the

impact study is limited in the range of climate model uncertainty it can explore. It is recognised that a large number of climate models should be used in impact studies to assess the structural difference between the GCMs (Prudhomme et al., 2003, Kay et al., 2009). Through using multiple models, the choice of GCM has been identified as contributing the largest uncertainty within the impact study framework (Salathe et al., 2007, Vidal and Wade, 2008). Traditionally GCMs are all assumed to be equally likely and to all provide plausible representations of the climate; the appropriateness of this assumption is beginning to be questioned (Tebaldi and Knutti, 2007, Knutti et al., 2010). An alternative to an assumption of equal likelihood is to apply weightings to projections according to a user defined criterion. For example Wilby and Harris (2006) weighted each projection according to their bias compared with observations in reproducing summer effective rainfall. One of the challenges of weighting a climate model projection based on such a comparison is the risk of 'getting the right answer for the wrong reasons'. A model may have a number of internal inadequacies leading to simulation errors which are ignored if the output is similar to observations for a given time and location. A more robust approach may be to assess each model's ability to reproduce key processes which influence its outputs (Weigel et al., 2010). Models that are known to perform poorly on these key processes can then be eliminated, with the remaining models given equal weighting (Weigel et al., 2010). The difficulty with implementing this approach lies with the availability of data to assess how key processes are reproduced. Impact scientists traditionally have limited access to GCM outputs to make these informed decisions.

Despite being identified as a key uncertainty in climate modelling, there are few examples on the propagation of climate model parameter uncertainty through to the impact response (e.g. on hydrology) due to the limited number of perturbed physics ensemble runs. The computational expenditure required to generate perturbed physics ensembles is often given as the main limiting factor. This issue was overcome by Stainforth et al (2005) who established climateprediction.net to encourage the global public to utilise their home computers for running climate models. These perturbed physics ensemble runs were used by New et al (2007) to analyse the climate change impact on the water resources of the Thames basin. Future changes in river flows were found to adopt a wide range with the largest range of uncertainty at the highest flow quantiles.

> **2.3.3 Climate Model Summary Box**
>
> Climate models are the primary tool used for constructing inputs for climate change impact studies. Due to the complex nature of the physical world, GCMs provide a simplified version of reality which introduces a number of uncertainties deriving from model structure assumptions, model parameterisation and model internal climate variability. As a result of these inherent uncertainties climate models contribute the largest source of uncertainty within the climate change impact study framework. To address the role of climate model structure it is important to utilise as many different climate models as possible to capture the full spread of model variability within a climate change impact study. Including the role of climate model parameterisation and internal climate variability within a climate change impact study is more challenging due to the limited availability of data but has been shown to be of importance when propagated through to the hydrological impact study.

2.4 Downscaling

Modelling the impacts of climate change on flooding requires climatological data at the catchment scale, typically tens of km in the UK. Furthermore in flood modelling applications data is required for at least a daily time step due to the typical response time of a flood event in the UK. These impact modelling requirements are in contrast to the climate model outputs which are grid-averaged over several degrees of longitude and latitude, and often only available at monthly time steps due to computational storage demands. To overcome the spatial and temporal differences in scale between climate models and hydrological impact models, downscaling methods are used. There are broadly two distinct groups of downscaling methods. The first is dynamical downscaling where a higher resolution regional climate model (RCM) is nested within a GCM. The second group consists of statistical methods, typically devising relationships between (larger scale) GCM outputs and (finer scale) observed data. The research into downscaling methods and techniques is extensive, with many techniques developed and an endless number of comparative studies. As a number of comprehensive downscaling reviews have already been undertaken (Xu, 1999, Fowler et al., 2007), the aim of this section is to highlight a number of key points relevant to this thesis. It covers the main downscaling techniques and their limitations for both dynamical (section 2.4.1) and statistical (section 2.4.2) methods, followed by an overview of selected comparative studies (section 2.4.3).

2.4.1 Dynamical Downscaling

The limitation imposed by global scale GCMs on the scale and accuracy of climate change impact studies was recognised early in the development of climate change science (Giorgi and Mearns, 1991). One approach to addressing this issue is to develop higher resolution regional climate models with boundary conditions driven by a coarser scale GCM. This idea, initially coined as limited area modelling (LAM), developed from methods used in weather forecasting applications (Giorgi, 1990). The theory behind using a higher resolution model is that processes (i.e. convection) and features (i.e. topography) can be better represented at the regional scale, while they are lost at the coarser GCM scale.

There are many known issues surrounding regional climate modelling (full review in Giorgi and Mearns, 1999), one primary factor when linking GCMs and RCMs is the concept of "garbage in, garbage out" (Giorgi and Mearns, 1991). An RCM inherits its boundary conditions from a driving GCM, and although it then runs freely, it is strongly influenced by the errors or biases from the GCM inputs (Noguer et al., 1998, Rummukainen et al., 2001). In the model inter-comparison project PRUDENCE, the uncertainty resulting from uncertain boundary conditions was found to be greater than the uncertainty between different RCMs nested within the same GCM, particularly for temperature (Déqué et al., 2007).

The climate model uncertainties highlighted in section 2.3 also play a role in RCM projections. Similarly to GCMs, RCMs include different processes and feedbacks, resulting in a range of differing model structures (Jacob et al., 2007). The differences between RCMs is highlighted by another inter-comparison project, ENSEMBLES, where Christensen et al (2010) present results from 13 different RCMs forced using observed reference boundary conditions. Models showed both warm/cool and dry/wet biases across much of Europe, with wide inconsistencies across different models. Due to the differences between RCM outputs weightings were applied to favour better performing models (assessed relative to observations), however the weightings were shown to have little influence on the ensemble of model projections (Christensen et al., 2010). Owing to the combined effect of boundary condition uncertainty and RCM uncertainty, multiple GCM and RCM combinations must be used, however issues with model access and high computational demands mean only a limited number of projections of this nature exist (e.g. NARCCAP, ENSEMBLES).

A number of studies have analysed RCM simulations of extreme precipitation, which is particularly important for flood impact studies. Findings have varied from a good

reproduction of spatial patterns with systematic magnitude biases (Frei et al., 2006) to inconsistent spatial patterns with both positive and negative biases (Fowler et al., 2005a). It is clear that despite the finer resolution of RCMs compared with GCMs the issues of model scale compared to the hydrological impact remains. This is particularly significant for precipitation, where RCM output is area-averaged and thus not directly comparable with finer averaged or point observational records (Durman et al., 2001, Fowler et al., 2005a). This has implications for the use of RCM outputs in hydrological impact studies as catchment averages are typically required which are smaller than, and not overlaid by, RCM grids.

The majority of hydrological impact studies operate at spatial scales where the use of direct RCM data has been shown to be inappropriate due to its area-averaged nature (Hay et al., 2002). The solution suggested by Hay et al (2002) and many others (Wood et al., 2004, Engen-Skaugen, 2007, Fowler and Kilsby, 2007) is to use a bias correction on RCM outputs to improve the magnitude of precipitation totals relative to the observations at a finer-averaged scale. In Hay et al (2002) the RCM precipitation distribution was magnitude corrected using the distribution of observation based precipitation data. An average monthly bias correction was applied to RCM outputs by Fowler & Kilsby (2007) when simulating mean river flows; simple bias-corrected RCM outputs were shown to perform well when compared with observed mean flows. The implementation of the bias correction methodology typically relies on the observational data to correct RCM outputs for the same reference period of record. For climate change studies the same bias is assumed to be constant through time and applied to all future periods (Kay et al., 2006, Fowler and Kilsby, 2007). The assumption of a stationary bias within a regional climate model has been shown to be questionable, with modelled temperature and precipitation biases found to depend on modelled temperature (Christensen et al., 2008). This suggests that in a future warmer climate the required bias correction may be larger than the bias correction in the period of observation.

2.4.2 Statistical Downscaling

Statistical downscaling is a broad term used to refer to many different methods for analysing GCM or RCM outputs for the purpose of altering their temporal or spatial scale. Included in this review under the statistical downscaling title are change factors, weather generators, transfer relational methods, and weather typing methods.

The simplest use of climate model outputs is the change factor method (Arnell and Reynard, 1996, Hay et al., 2000, Prudhomme et al., 2002, Hay and Clark, 2003, Haylock et al., 2006, Anandhi et al., 2011). Change factors describe the changes in the future climate within a model from a baseline reference period. Change factors define the 30 year mean change in climate, typically comparing the 1961-1990 reference period and a thirty year future time slice i.e 2071-2100. The change factors are then used to perturb an observed variable record either in an additive (e.g. temperature) or multiplicative (e.g. precipitation) method. Change factors are limited by only allowing changes in the mean, and in turn minima and maxima, of a climate variable (Diaz-Nieto and Wilby, 2005). The future variability of the climate variable is therefore assumed to be unchanged, with an identical sequence of day to day weather. Attempts to address changes in variability have been adopted, Arnell (2003b) altered the year to year variability of monthly precipitation by rescaling the observed anomalies. This method only changes the year to year variability, with the sub-monthly rainfall distribution maintained. To include sub-monthly variability Prudhomme et al (2002) adopted two alternative methods. Firstly by including extra rain days in the observed time series, and secondly by applying the change factors to the three largest rainfall events each month, creating enhanced storms. The different methods provide a range of impacts, however there is little empirical evidence to support how to implement such changes.

Typically change factors are single values for each month and variable. An alternative approach is to have a scaled change factor each month (Anandhi et al., 2011), where a change factor is calculated for different percentiles of the variables monthly distribution. For example the scaled change factors are calculated for the 10th-20th percentiles of the model precipitation and then applied to the same percentiles in the observed record. This allows for the changes in the future variance of precipitation to be accounted for. The limitation here, similar to the use of RCM derived precipitation outlined in section 2.4.1, is that grid-averaged climate model output fails to reproduce observed precipitation distributions. Although the scaled change factors allow for changing the precipitation variance, they are informed by climate models which do not reproduce physically realistic variance, and hence might not be plausible scenarios.

The outlined limitations of change factors are often acknowledged, yet they are still widely used in climate change impact studies due to their ease of application and the lack of evidence based alternative. The most recent climate change scenarios for the UK, UKCP09 (Murphy et

al., 2009), are available in the form of change factors. An alternative to using the change factors directly with observations is to use them in conjunction with a weather generator.

Weather generators are stochastic models which produce artificial climate time series. They have been developed to simulate many different climate variables, however most attention is paid to precipitation as it is the most naturally varying climate variable (Srikanthan and McMahon, 2001). Due to the high temporal variability in precipitation compared with other less varying climate variables (e.g. temperature), precipitation time series are typically generated first with the other climate variables then generated to be temporally and spatially auto-correlated with the precipitation (Kilsby et al., 2007). The generation of precipitation is typically a two stage process consisting of generating the sequences of wet and dry days, followed by creating precipitation magnitudes (Wilks, 1998). Often weather generators are valid for single sites, hence producing spatially independent time series. This might be an issue in hydrological impact studies, as the spatial variability in rainfall is important for flood generating mechanisms.

An extension to the traditional use of a single site weather generator is to produce correlated multi-site precipitation scenarios in combination with relational downscaling methods linking larger scale atmospheric variables with local scale climate (Wilby et al., 2003). Relational downscaling methods use large scale climate indices as predictors which are linked to local scale weather and climate. In their simplest form relational methods can be described as climate analogues where a climate series is constructed through matching large scale variables in GCMs against observations and extracting the observed local scale variable (Zorita and von Storch, 1999). In their more complex form, relational methods seek to establish regression relationships which link a number of atmospheric predictors (i.e. sea level pressure, humidity and geopotential heights) to create local scale temperature and precipitation time series (Wilby et al., 1999, Zorita and von Storch, 1999). The main limitation behind relational methods is an assumption of stationarity. In both the analogue method and regressions based methods the relationships between the large scale atmospheric variables and local scale climate are established for the baseline climate with their relationship assumed to be constant under future climate projections. An alternative to deriving direct statistical relationships is to use weather classification schemes to group the atmospheric conditions (Conway and Jones, 1998, Bardossy et al., 2002). In contrast to the regression based downscaling methods, weather classification schemes provide a physical

basis for their relationships (Conway and Jones, 1998). However limitations exist for their application to GCM outputs as the local scale climate variable (i.e. temperature or precipitation) are not well re-produced compared with observations. To overcome this, weather pattern methods have also been used to condition multi site weather generator methods (Fowler et al., 2005b), which create local scale climate time series based on GCM weather patterns.

2.4.3 Downscaling Comparative Studies

The previous sections have outlined a number of different approaches which have been developed to create local climate scenarios from larger scale model outputs, either dynamically (section 2.4.1) or using one of a number of statistical methods (section 2.4.2). This section aims to provide an overview of some of the studies that have undertaken a comparison of the different downscaling methods. The typical framework for a comparative study is to apply a number of different downscaling methods to the same region and model outputs to assess which provides the best performance compared with the observed climate.

Change factors have been compared with statistical downscaling techniques in a number of hydrological impact studies (Hay et al., 2000, Diaz-Nieto and Wilby, 2005, Chen et al., 2011). Diaz-Nieto and Wilby (2005) note that statistical techniques provide the opportunity to provide ensemble estimates through multiple repeat analysis (assuming there is a stochastic component) but these repeats are in turn computationally more intensive than deriving change factors. A further issue raised is a pre-assumed knowledge in choosing predictor variables which may (or may not) relate to the region of interest. Chen et al (2011) issue a caution over the use of change factors when looking beyond seasonal changes, due to the day to day variance of a variable remaining unchanged.

Comparisons of a number of statistical methods and dynamical methods (with and without bias correction) are increasingly common (Haylock et al., 2006, Hay and Clark, 2003, Wood et al., 2004, Chen et al., 2011). The overall theme which encompasses all of these studies is that all downscaling approaches can provide a good method for translating GCM scale data to the local scale. The factors which influence the appropriateness of the different methods include the study location, data availability and the impact of interest. In general temperature displays less variability between methods than precipitation (Chen et al., 2011), and statistical methods may provide more consistency than dynamical methods (Hay and Clark, 2003). The

conclusions drawn by nearly all downscaling comparison studies are that no single method provides an optimum solution and a number of different methods should be considered.

2.4.4 Downscaling Summary Box

This section has outlined the main methods for downscaling GCM outputs to the local catchment scale. Dynamical downscaling using an RCM can be undertaken to increase the resolution of GCM simulations but is strongly influenced by errors in the boundary GCM. Furthermore despite the finer scale of RCMs they remain too coarse for some impact scales requiring their use in conjunction with statistical downscaling methods. A number of statistical downscaling methods exists each with their known limitations. The appropriateness of different methods is linked to the region of interest, the data availability and the impact under investigation. Downscaling method comparison studies typically conclude that a number of downscaling methods should be used in a climate change impact study, while no single method has been identified as an optimum solution.

2.5 Hydrological Modelling

In the climate change impact study framework, the hydrological model requires an input from a catchment scale climate projection typically obtained using the downscaling methods outlined in the previous section. The hydrological model transforms the projected changes in climate into changes in catchment hydrology and the resulting river flows. The focus in this thesis is on continuous flow simulation over longer record lengths, as opposed to singular event based modelling. Hydrological systems have processes which occur at a wide range of scales that are often difficult to observe as most are underground. These factors have shaped a number of different ideologies behind hydrological model development which are discussed in section 2.5.1. From this discussion it becomes clear that there are a number of simplifications in hydrological models, which require parameters to be included in models to represent physical processes and interactions. An overview of the role of model parameterisation is provided in section 2.5.2. This section closes with a summary of the overall implications of hydrological modelling uncertainty in the impact study framework.

2.5.1 Hydrological Model Structure

When modelling hydrology for the sole purpose of rainfall-runoff transformation, many of the complex physical processes and interactions within a catchment do not need to be represented in a model (Jakeman and Hornberger, 1993). The two components essential to every

hydrological model are runoff production (i.e. not all precipitation is stored in the catchment) and runoff routing (i.e. runoff is made up of quick flow and slow flow) (Beven, 2001). In developing hydrological models with these components there are broadly two ideologies; lumped conceptual modelling or distributed modelling. A full history of how hydrological modelling has evolved to form these ideologies is provided by Todini (2007), this review briefly summarises the main concepts, with their key differences identified.

The concept of a lumped model is that the catchment is viewed as a single unit, with processes and variables averaged across the catchment. This conceptualisation aims to simplify physical process representation, where processes and interaction are controlled through a series of empirical equations whose values and calculations are controlled through a parameterised model structure. A large number of lumped conceptual models exist with the main difference being the runoff generation component. Runoff generation can be controlled, but is not limited to, using a probability distribution of storage (PDM - Moore, 2007), linked to local topography (TOPMODEL - Beven, 1997), calculated as a precipitation loss function (IHACRES - Jakeman et al., 1990) or based on a water balance model (CATCHMOD - Environment Agency, 2005). Once runoff has been generated it is typically routed between a quick flow route and a base (slow) flow route (representing the delay due to slower moisture movement in the soil and storage in the ground), which may be estimated from a physical characteristic such as a catchment's base flow index (BFI) or parameterised and then calibrated. The main limitation of lumped conceptual models is that through simplifying a catchment to a single unit it is difficult to simulate larger catchments, due in part to the greater spatial variability in topography, soils, land use and precipitation (Beven, 2001).

To incorporate a greater heterogeneity across a catchment semi-distributed models have been developed. In such models a catchment is split into a number of sub-basins, each of which is simulated individually, with the output of each sub-basin routed through a main channel (e.g. HBV (Lindstrom et al., 1997), ARNO (Todini, 1996), CLASSIC (Crooks and Naden, 2007)). The main benefit of semi-distributed models are their use in larger heterogeneous catchments, or for analysing sub-catchment changes such as land use (Ghavidelfar et al., 2011). If rainfall-runoff transformation is all that is of interest, the extra complexity of semi-distributed modelling may not be required (Ajami et al., 2004).

Fully distributed modelling is the next advance from semi-distributed modelling. A catchment is typically divided into cells, similarly to semi-distributed models but at a finer regular grid,

and flow routing occurs as an iterative time step process between grid cells. The main difference for distributed models is that there is a reduced (or no) calibration process; the model is physically based without fitting it to catchment data. Distributed models have been developed for more complex hydrological regions where calibration based models are not suited (e.g the SHE model (Abbott et al., 1986) is applied in Denmark due to the importance of groundwater). Alternatively distributed models have been developed for river flow simulation in ungauged catchments for flood forecasting applications (TOPKAPI - Liu et al., 2005, G2G - Bell et al., 2007).

A number of comparison studies between the different modelling ideologies have been made, although this may not be appropriate given the different design applications of each model type. However for rainfall-runoff applications lumped conceptual models have been shown to provide the best performance in simulating observed river flow time series (Reed et al., 2004, Cole and Moore, 2008). These findings support Jakeman and Hornberger's (1993) assertion that for rainfall-runoff modelling, reducing complexity is favourable.

Although three main ideologies exist for the construction of hydrological models, within each ideology a number of different methods exist for constructing a model. This is most notable for lumped conceptual models, where the simplification of process representation has led to different model formulations. Perrin et al (2001) showed that increasing the number of model parameters allowed a model to perform well during calibration but produces poor results outside of the calibration period. They suggest that a model often becomes over parameterised to compensate for a poor model structure. In contrast, other studies have found no connection between the number of parameters and model performance (Lee et al., 2005, Bastola et al., 2011). Model comparisons across different catchment types found no single model is preferable for a given catchment type (Perrin et al., 2001, Lee et al., 2005).

It is widely acknowledged that different hydrological models provide different results and performance; the primary limiting factor in assessing these differences is having access to different models. Each institution, university or consultancy, typically develop their own hydrological model and rely on this for their impact modelling. Although access to different models can often be granted, the differing input requirements and interfaces between models create difficulties for undertaking such a comparison procedure.

2.5.2 Model Parameters

The previous section outlined the main concepts surrounding hydrological model development and choice. The common components to all hydrological models are the parameters which control or represent physical processes in both time and space within a model. The values which parameters adopt are typically derived through training a hydrological model using observed meteorological data to reproduce an observed river gauge record (Boyle et al., 2000). A number of issues arise from hydrological model parameter estimation, particularly with respect to lumped conceptual models which are discussed in this section.

Calibration of model parameters traditionally seeks to find an optimum solution, defined by a performance measure, for reproducing an observed flow record. Due to the reduced complexity of lumped hydrological models the problem of equifinality arises (Beven and Binley, 1992, Beven, 2006). Equifinality is the situation whereby no single optimum solution for a model exists; instead a number of different parameter combinations exists which each produce an equally acceptable model performance. In response to the issue of equifinality particular focus has been paid to examine model and parameter sensitivity during calibration.

A number of simple approaches are suggested to addressing the issue of equifinality. The calibration of a hydrological model on a jackknifed observed time series (i.e. systematically removing a single year at a time from the observed record) has been shown to generate flood quantile magnitudes that deviate by ±5% (Kay et al., 2009). Alternatively a perturbation (e.g. ±10%) can be applied to already calibrated model parameters which leads to small variations (0%-15%) in monthly river flows (Arnell, 2011). Both of these parameter sensitivity methods test the reliability in the range of the fitted values, but fail to explore the full feasible parameter space (i.e. model parameters could adopt opposite ranges to cancel each other). They are therefore best viewed as methods for identifying catchment and parameter sensitivity, but fail to address the full problem of equifinality.

In order to explore the full range of the parameter space, from which a parameter may take its value, Monte Carlo analysis has been adopted as accepted practice. Monte Carlo analysis helps to address the equifinality problem through allowing all parameters to co-vary, often resulting in the cancellation of errors between parameters. This was highlighted by Uhlenbrook et al (1999) who demonstrated that plausible parameter sets could take values from a wide range of individual values. Some parameters were found to adopt smaller

plausible ranges, thus being more sensitive to calibration and having better identifiability. Other studies have used Monte Carlo analysis in a similar manner to address the equifinality problem (Wilby, 2005, Steele-Dunne et al., 2008).

An extension of the Monte Carlo method is the Generalized Likelihood Uncertainty Estimation (GLUE) method, first presented by Beven and Binley (1992). GLUE is underpinned by an informal Bayesian methodology where a prior distribution, which is typically uniform unless there is expert knowledge of a catchment and model (Beven and Freer, 2001), is sampled using Monte Carlo analysis to produce multiple sets of model parameters. The parameter sets are used to simulate catchment flows with their simulation assessed by a user defined likelihood measure (goodness-of-fit). The model parameter sets are given weightings based on their likelihood measure, with the final model simulation weighted according to each parameter set weighting. The choice of likelihood measure is noted as being subjective (Beven and Binley, 1992) and can influence the calibration results (Beven and Freer, 2001, Cloke et al., 2010). Due to the informal subjectivity of defining a likelihood measure which rejects non-behavioural models and weights the final results, GLUE has come under closer scrutiny and some criticism (Mantovan and Todini, 2006, Stedinger et al., 2008). The main criticism is that a likelihood measure must be chosen which accurately reflects the model errors in relation to the statistical distribution of the data. This issue has prompted an extensive debate with a long exchange of papers (Mantovan and Todini, 2006, Beven et al., 2007, Mantovan et al., 2007, Beven et al., 2008). The choice of a likelihood measure is common to all calibration procedures, highlighting the degree of subjectivity in all model calibration. Despite these ongoing debates over the GLUE method it is still widely used. Bastola et al (2011) found the use of GLUE added value to hydrological simulations of present and future river flows by avoiding the use of an inappropriate model.

An alternative extension of a Monte Carlo based analysis approach is Dynamic Identifiability Analysis (DYNIA-Wagener et al., 2003). DYNIA provides an approach to identify which parameters in a hydrological model are most identifiable (i.e. there is a clear range for acceptable parameter values), and under which hydrological conditions (e.g. wet or dry period) this identifiability occurs. The DYNIA method has demonstrated that simulated high flow periods do not always have a direct connection with a single model parameter in a lumped hydrological model, making their calibration more difficult (Cullmann and Wriedt, 2008). Furthermore due to the non-physical nature of parameters in reduced conceptual

models, parameter identifiability may have no physical connection to the simulated flow series (Abebe et al., 2010). One of the main issues that DYNIA raises is that parameter values may vary depending on hydrological conditions they are calibrated against. This is particularly important from a climate change perspective as it suggests that model parameters cannot be assumed to be stationary through time.

The rationale for parameter non-stationarity is that the parameter sets are calibrated to a specific hydrological regime but may no longer be valid if that regime changes. The hydrological regime change could be a result of changes in climatology (e.g. climate change) or catchment alterations (e.g. land use). This issue of parameter stability in the context of non-stationary hydrological regimes has been addressed by a number of studies (Niel et al., 2003, Wilby, 2005, Vaze et al., 2010, Merz et al., 2011). The method typically adopted is to split the observed river flow series into shorter record windows, performing a model calibration across each window, followed by a validation of the parameter sets on all other windows. Niel et al (2003) found the stability of parameters to be independent from the stationarity of the climatology of the period of calibration. However the dependence on the window of calibration was found to be important by Wilby (2005), where parameters calibrated from dry years performed poorly when validated against wet years whereas calibration of parameters in wet periods performed well in dry periods. In contrast to this, high flow periods are shown by Merz et al (2011) to offer the lowest parameter stability which has been corroborated in other studies (Vaze et al., 2010). Merz et al (2011) suggest that mean and low flows are more stable through time, with high flow periods rarer, making the model calibration most sensitive to high flows. The stability of parameters has so far been discussed in the context of shifting windows in the observed record. Wilby (2005) extended this analysis to future changes in flow in relation to the period of calibration. In some instances the uncertainty due to the calibration period was found to be of the same order of magnitude as the uncertainty from future emissions scenarios.

2.5.3 Hydrological Modelling Summary Box

This section has outlined the main sources of uncertainty that surround the hydrological modelling component of an impact study. Due to the physical simplifications and conceptualisations in the modelling process a number of different models exist, from lumped to fully distributed models, with the performance varying between different models and across different catchments. Although multi-model analysis is important to consider, access to models can prove limiting to this process, leading many studies to use a single hydrological model. Lumped conceptual models are considered beneficial when the rainfall-runoff relationship is the primary interest. In the UK the majority of hydrological impacts are assessed using conceptual hydrological models. However the main uncertainty resulting from lumped conceptual models is the parameterisation process which requires calibration of model parameters. Because of the simplification of hydrological processes by lumped conceptual models through a set of parameters the problem of equifinality arises, meaning that a model's parameter space must be extensively explored to provide multiple equally performing parameter sets. Lastly the stability of parameters in a predictive capacity outside of a calibration period should be considered, particularly when moving between periods of differing hydrological regime.

2.6 Flood Frequency Estimation

Flood events by their rare nature are difficult to characterise. Each catchment has its own flood peak history, with the size and impact of an event specific to that catchment. From a planning perspective simply knowing the size of flood events that have previously occurred is not the only important information, as understanding the likelihood that an event of the same size or bigger may occur again is critical. To meet this requirement flood events are typically expressed as T-year floods, where T is the return period describing the average number of years between events of a similar magnitude or greater. This section provides an overview of the different approaches that have been adopted to estimate flood return periods (section 2.6.1) followed by a discussion in section 2.6.2 of the uncertainties associated with the process.

2.6.1 Flood Frequency Estimation Methods

The calculation of the T-year flood event for a catchment requires the statistical analysis of the river flow time series. A river spends only a small proportion of time in a flood state with flood flows for a typical UK catchment lasting for only a few days at a time. In order to focus

solely on the flood periods of a river flow series a sampling procedure is undertaken to extract the largest flood events. There are two methods for this sampling; annual maxima data (AM) (Institute of Hydrology, 1999) where the largest flood event is extracted each year, or a peaks over threshold method (POT) (Bayliss and Jones, 1993) where a number of peaks are extracted according to a certain threshold. The AM technique is widely used as each event has a clearly defined occurrence, however POT sampling may be favourable as it provides more information from the river flow series (Beguería, 2005). In AM sampling the 2nd or 3rd ranked flood events in a year may be larger than the annual maxima in another year but would be ignored.

The next step in calculating a return period quantile is to associate a frequency to each event relative to each other event in the flood sample, based on its ranked position with respect to the overall flood peak population (Rao and Hamed, 2000). This frequency is then typically transformed to be expressed as a return period. Both AM and POT sampling provide a flood peak population which is a sample of the extreme distribution tail of the total flow population. To estimate the relationship between a flood magnitude and return period from the flood peak population an extreme value distribution needs to be fitted against the data; the model distribution which is used depends on the flow sampling strategy. The flood estimation handbook (FEH – Institute of Hydrology (1999)) recommends the use of a Generalised Logistic (GL) distribution for use with AM sampling or a Generalised Pareto (GP) distribution for POT sampled data. However it is important to note that although the GL and GP distributions are recommended for the UK, a wide range of statistical distributions exist (see Kidson and Richards (2005) for summary of distributions) which are recommended for use in other countries (e.g. USA: log-Pearson type 3, China: lognormal, and previously in UK: generalised extreme value (Singh and Strupczewski, 2002)). Whichever distribution is selected, the fitting of a statistical distribution removes the variability of the flood peak sample and allows for extrapolation/interpolation of the data.

The estimation of a flood magnitude for a given return period from a river flow series depends on a number of assumptions made in deriving flood return period quantiles, hence leading to a degree of uncertainty about any estimate. The following section will cover these uncertainties and discuss the current methods that are implemented to address these uncertainties.

2.6.2 Flood Frequency Estimation Uncertainty

The assumptions underpinning flood frequency analysis can influence the overall outcome leading to a large uncertainty in a flood estimate (Rosbjerg and Madsen, 1995). A full discussion of uncertainty can be found in either Kidson and Richards (2005) or Merz and Thieken (2005) with a summary provided here. The sources of uncertainty in flood frequency relate to measurement error of observations, plotting position formula, flood peak sampling, flood frequency distribution, the statistical distributions parameter estimation, and overall sample uncertainty (i.e. record length). Typically assumptions are made about each of these sources of uncertainty and included in the final flood estimate, however attempts have been made to separate the different sources (Merz and Thieken, 2005). Perhaps the greatest source of uncertainty is the choice of flood frequency distribution (Rosbjerg and Madsen, 1995, Kidson and Richards, 2005), where models may adequately reproduce the observed flood peaks but act very differently when extrapolated beyond the population. This extrapolation is often necessary due to frequency analysis being undertaken on relatively short records. By separating the uncertainty sources Merz and Thieken (2005) demonstrate that increasing the length of flow record does not generally alter the value of a flood estimate; it improves the confidence of that estimate and reduces its range of uncertainty.

To overcome the issue due to short (or sometime absent) flow records, regional flood frequency analysis is recommended (Institute of Hydrology, 1999). Regional frequency analysis exploits the flood frequency data from other catchments displaying similar properties and flood responses to the catchment of interest (Kjeldsen and Jones, 2009). This extends the knowledge base on which to calculate flood return periods, thus providing a more robust estimate. Although this provides a more robust estimate it does not explicitly calculate the associated uncertainty. Kjeldsen and Jones (2006) included uncertainty measures in regional frequency analysis through calculating sample variances for the GL distribution (Kjeldsen and Jones, 2004) which indicated that regional frequency analysis did decrease the flood estimate uncertainty compared with a single site analysis.

An alternative method to quantify the uncertainty associated with flood frequency estimation is the use of continuous simulation (Cameron et al., 1999, Lamb, 1999, Lamb and Kay, 2004). Continuous simulation uses a hydrological model to produce a continuous flow record (as opposed to an event based simulation) which can be used to extract flood return periods as outlined in section 2.6.1. One of the main benefits to this methodology is the application of

multiple stochastically generated precipitation datasets allowing for an assessment of the natural variability beyond the observed period of record (Cameron et al., 1999). This allows for any flood return period estimates to have a reduced range of uncertainty due to the extended knowledge. In the absence of records the method may be useful in producing flood estimates for ungauged catchments (Lamb and Kay, 2004), although it has been shown that hydrological simulation is not always comparable to observations due to the role of estimating hydrological model parameters (Lamb, 1999).

2.6.3 Flood Frequency Estimation and Climate Change

Unlike the wide spread research and guidance for baseline flood estimation, there are few studies which provide guidance for flood frequency estimation in a future climate. One of the main complications behind this is the role of stationarity. Flood frequency analysis is typically underpinned by an assumed stationarity of the flood peak series, so that frequency can be expressed as a return period (Villarini et al., 2009). However in the future where the climate is expected to change, such assumptions may no longer be valid (Olsen et al., 1998, Milly et al., 2008). This is particularly important for applications of regional flood frequency analysis where relationships between catchments calculated for present day may no longer be the same in the future.

Due to the complexity in deriving statistical methods to account for non-stationarity, traditionally climate change impact studies have applied the baseline flood frequency analysis methods outlined previously to future river flow series. The future river flow series may be derived from change factor perturbed time series (Reynard et al., 2001, Prudhomme et al., 2002, Prudhomme et al., 2003), RCM model time series (Dankers and Feyen, 2008, Dankers and Feyen, 2009, Kay et al., 2009, Kay and Jones, 2011) or continuous stochastic precipitation modelling (Cameron et al., 2000, Cameron, 2006). Notable in many of these studies is the absence of any formal quantification of the uncertainty associated with the calculated flood quantiles. Kay et al (2009) quantify the flood frequency uncertainty through a seasonal bootstrap resampling method and demonstrate that it is large in comparison with a number of sources of uncertainty within the climate change impact modelling framework. An alternative resampling approach is to use a stochastic rainfall model in combination with climate change scenarios to generate a large number of rainfall time series for use in continuous simulation (Cameron et al., 2000, Cameron, 2006).

2.6.4 Flood Frequency Estimation Summary Box

Flood frequency estimation is integral in calculating design standard return period flood quantiles. A number of statistical methods exist for deriving flood estimates although a POT sampling is recommended to maximise the information from the flow series, which in turn leads to a recommendation of using a GP distribution to model flood peaks. Current methods for accounting for the uncertainties associated with estimating flood magnitude return periods are not easily applicable to a changing climate, due to questions of non-stationarity, leading many studies to investigate the potential changes in future flood frequency estimates without considering uncertainty. However, flood frequency uncertainty has been shown to be large, especially for higher return periods.

2.7 Probabilistic Assessments of Change with Uncertainty

So far in this chapter the different components of the climate change impact study framework have been identified and discussed in the context of a common theme of uncertainty. Each component contributes a degree of uncertainty throughout the framework. This section outlines the current manner in which these different uncertainties are combined in impact analysis (section 2.7.1). This is followed in section 2.7.2 with a discussion of probabilistic impact assessments, their requirement, and current approaches.

2.7.1 Combining Uncertainties

Global climate models have been identified as one of the largest sources of uncertainty within the climate change impact study framework (see section 2.3), and a number of studies have developed methods to quantify the different components that contribute to the total range of GCM uncertainty (New and Hulme, 2000, Visser et al., 2000, Knutti et al., 2003). This focus implicitly suggests that GCM uncertainty is the most significant to address, resulting in a somewhat 'constrained' approach to quantifying uncertainty in impact studies. This can still be seen in a number of recent studies which claim to quantify uncertainty (Nobrega et al., 2011, Xu et al., 2011) where a number of different GCMs and often emissions scenarios are incorporated in an impact study with no consideration of other uncertainty sources.

The majority of hydrological climate change impact studies rely on a multi-GCM/emission scenario approach whilst incorporating uncertainty relating to the impact hydrological model. The GLUE and Monte Carlo methodologies in particularly have been widely applied to hydrological models to sample the hydrological model parameter uncertainties in

combination with the climate model and emissions scenarios (Cameron et al., 1999, Cameron et al., 2000, Steele-Dunne et al., 2008, Cloke et al., 2010). While this is becoming a well established framework for assessing uncertainties in hydrological impacts, this approach is limited in the range of uncertainty it explores and places a large emphasis on the contribution of hydrological model parameter uncertainty which is thought to be small (Kay et al., 2009). Furthermore there is often no attempt to attribute the impact distribution to the different sources of uncertainty, instead providing an end impact distribution in a black-box format.

The contributions of the different uncertainty sources are comprehensibly considered by Kay et al (2009), however each component is analysed independently making a relative comparison between each component difficult. In a top-down climate change impact study framework an assumption that the uncertainties are independent is difficult to justify, given that each source cascades into the next. For a full assessment of the relative scales of uncertainty each source must be considered simultaneously. Quantifying the relative uncertainty contributions should aid in the development of probabilistic scenarios which are discussed in the following section.

2.7.2 Probabilistic Assessments

The recognition that many different uncertainties are associated with climate change impact studies has shifted impact studies from a deterministic perspective towards probabilistic approaches; as suggested for hydrological applications by Wilby and Harris (2006) and New et al (2007). The overall framework in both cases is to quantify the uncertainty relative to each component of the climate change impact study to create a final distribution of impact with associated probabilities. In any case a number of assumptions will be made by the impact scientist (e.g. Wilby and Harris (2006) apply weights to each GCM) which will influence the final impact distribution. Despite requiring user assumptions, developing probabilistic scenarios provides the advantage of expressing a prediction with its uncertainty in a single result. In the UK the creation of probabilistic assessments is now aided by the latest climate projections from the UK climate impacts programme, the UKCP09 scenarios (Murphy et al., 2009). The creation of these scenarios places the onus on impact scientists to utilise them and further develop probabilistic assessment methods.

The move towards probabilistic assessments is not without its draw backs. The main issue is how to make adaptation decisions from probabilistic information (Hall, 2007) and whether these decisions are actually an improvement compared with previous methods (Dessai and

Hulme, 2004). As highlighted by Hall (2007), probabilistic scenarios may not sample the full range of uncertainties, while the probabilities they provide are not probabilities of predictions (i.e. they are not likelihoods) but probabilities based on our current knowledge (Beven, 2011). Therefore any decision based on probabilistic scenarios may be more scientifically robust, but no more (or less) right (or wrong). This is part of the difficulty in the presentation and in turn the interpretation of probabilistic information (Hulme et al., 2009).

> **2.7.3 Probabilistic Assessments of Change with Uncertainty Summary Box**
>
> Current climate change impact studies are often limited in their inclusion of uncertainty, focussing on the uncertainty from emissions scenarios and GCMs. To fully explore uncertainty in climate change impact studies, the uncertainty of each component of the climate change impact study should be considered simultaneously (instead of independently). Characterising the uncertainty in this manner aids in the creation of probabilistic assessments which help to provide a robust context for decisions. However, it is important to note that future probabilistic projections do not represent a likelihood of future occurrence but probabilities based on our current understanding of uncertainty.

2.8 Research Gaps

This literature review has provided an overview and background to the current state of climate change impact studies on flooding with particular reference to the different sources of uncertainty which contribute within the 'top down' impact study framework. Following this review a number of research gaps have been identified:

- Climate variability is an important component of climate model projections which has not been widely included in impact studies; typically due to the lack of multiple realisations of climate model outputs.
- The concept of equifinality can lead to a number of equally acceptable hydrological model parameters. Methods such as GLUE or Monte Carlo simulations have been widely applied but rarely in the context of flooding.
- Hydrological parameters have been shown to display a range of responses outside the period of calibration, however their specific sensitivity to climate changes has not been demonstrated.
- Flood frequency analysis is a highly uncertain procedure, the uncertainties of which have often been over looked in previous impact studies. Methods which quantify its

- magnitude of uncertainty in the baseline might not have direct applicability to the future due to questions over stationarity.

- Both climate model and emissions uncertainties have been shown to vary depending on the time horizon of interest. It is not currently known how this response propagates through to the impact study and how the impact study uncertainties contribute in relation to this.

- One of the biggest challenges remains in how to quantify and make use of uncertainties. One suggestion is to incorporate uncertainties within probabilistic frameworks, however a key question remains over how to make uncertainty meaningful.

These specific research gaps will form the basis for the research in this thesis, which is structured around the research objectives as outlined in Chapter 1.

2.9 Chapter Summary

This chapter has provided an overview and critical review of the science and literature within the 'top down' climate change impact study framework in the context of flooding. Emission scenarios were discussed in section 2.2 and were shown to play an important role in defining the impacts of climate change, in particular towards the end of the 21st century.

The emissions scenarios are used to force global climate models (as outlined in section 2.3) which contribute the largest source of uncertainty in climate change impact studies. Global climate models outputs are influenced by the model structure, model parameters and internal climate variability. The differences in model structure is the most widely addressed issue with both parameter uncertainties and climate variability receiving less attention due to data and computational limitations.

GCMs simulate the atmosphere and oceans at a coarse resolution, typically 100's of km's, leading to a spatial and temporal scale mismatch between global climate models and hydrological processes and subsequent impacts. This has led to a large focus on downscaling techniques to bridge these differences in scale as discussed in section 2.4. These include the use of dynamical RCM techniques which have been shown to have deficiencies in direct application to hydrological impacts, often requiring the need for correction of RCM outputs or statistical downscaling. The statistical downscaling techniques range from the simplest change factor method to more complicated regression based techniques. There is no

consensus over the best or most applicable downscaling methods leading to numerous comparison studies concluding that a number of techniques should be considered.

The downscaled climate variables are used as input to a hydrological model (section 2.5). In general models of lower complexity are shown to be preferred, although due to their simplicity the issue of equifinality surrounds the model structure and parameters. To address this issue a number of methods have been applied to generate multiple acceptable parameter sets. The model parameters have been shown to have different levels of transferability between different time periods during the model calibration and validation process, suggesting that their validity in a changing climate may vary. There have been few studies which investigate how the hydrological calibration and in turn model parameters should be approached in a flood frequency context.

There are a number of methods which exist for undertaking flood frequency analysis (section 2.6); the use of peak-over-threshold sampling is often recommended as it provides a greater wealth of information on the flood series. This in turn leads to the use of a Generalised Pareto distribution for modelling flood return period quantiles. Due to the statistical nature of flood frequency analysis there are a number of uncertainties associated with any flood return period estimate. A number of methods exist for accounting for this uncertainty during the baseline period, however due to issues of non-stationarity they are difficult to apply in a climate change context.

As highlighted in section 2.7 each of the components in the climate change impact study framework contributes to the overall uncertainty in the impact response to climate change. It is important to quantify all the different sources of uncertainty simultaneously so as to account for their inter-dependence and relationships. Through quantifying the various stages of uncertainty it is possible to create probabilistic climate change impact assessments to express the projection and uncertainty in a single distribution.

From this review a number of research gaps have been identified (section 2.8) which form the basis for the research objectives of this thesis as outlined in Chapter 1. The next chapter outlines the main methods used in this thesis to undertake a climate change impact assessment on UK flooding.

CHAPTER 3

Tools for Assessing the Impact of Climate Change on UK Flooding

3.1 Introduction

The 'top down' climate change impact study framework is a widely used approach, however it is often used with little acknowledgement of uncertainty. The focus of the research in this thesis is to investigate the role of uncertainty in each component of the 'top down' framework. This chapter outlines the main tools and methods which are used in this thesis. Details are presented here on the elements of the climate change impact study which are common across all chapters. Extra detail is provided in each chapter where necessary.

To tackle the research aims of this thesis, the impact of climate change is considered across a suite of case study catchments which are presented in section 3.2. The impact model, PDM rainfall-runoff model, is described in section 3.3. PDM simulated river flows are analysed using the flood frequency analysis methods in section 0. Lastly the data sources used to construct climate changes scenarios along with a description of how they are used can be found in section 3.5.

3.2 Case Study Catchments
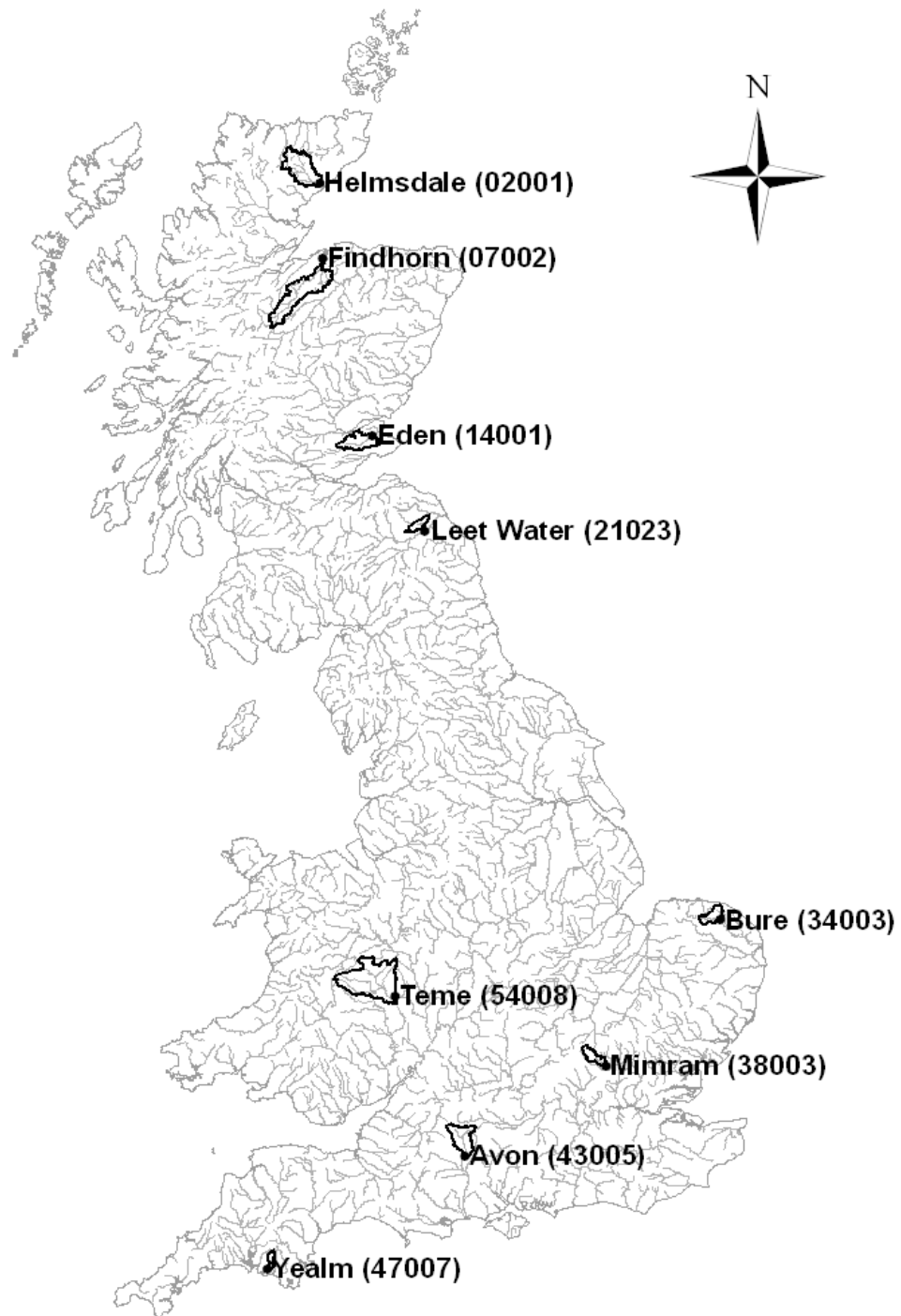
Figure 3.1 UK river network map with the nine case study catchment outlines highlighted. © NERC (CEH). Contains Ordnance Survey data © Crown copyright and database right 2011.

The research in this thesis will be undertaken on a suite of UK catchments. Their locations and catchment boundaries in the context of the UK river network can be seen in Figure 3.1.

There is a North-South divide between the catchment locations allowing for different climatological and geological conditions to be considered. The catchments in the South East (Bure (34004), Avon (43005) and Mimram (38003)) are all permeable catchments with an underlying chalk geology leading to a greater dominance of the contribution of baseflow to overall river flow. Three catchments have a greater dependence on quick flow surface runoff, leading to a flashier storm response (Findhorn (07002), Helmsdale (02001) and Leet Water (21023)). The Findhorn (07002) and Helmsdale (02001) are upland catchments in Scotland with some snow fall in winter, which are predominantly underlain by bedrock, leading to a rapid flow response to precipitation represented by a base flow index (BFI) of 0.47 and 0.41 respectively. The Leet Water (21023) catchment is a lower lying Scottish catchment characterised by boulder clay, it has the lowest BFI of all nine catchments (0.34). The remaining catchments (Eden (14001), Yealm (47007) and Teme (54008)) have more mixed response. The Eden (14001) is another low lying catchment in Scotland with a mixed geology and contains some arable farming activities. The Yealm (47007) catchment drains southern Dartmoor and despite a mid level BFI (0.56), can display a rapid response to precipitation. The Teme (54008) catchment lies on the border of England and Wales containing some high relief, mixed with lower lying valleys. All nine catchments are predominantly rural with little influence of urban areas, in particular there are no abstraction requirements. This simplifies the hydrological analysis and simulation of the catchments through reducing the number of external influences on the catchments.

The nine catchments have been used in a previous study (Reynard et al., 2010) which sought to regionalise the hydrological response to climate change across the UK. The study applied the same systematic changes to the precipitation and potential evaporation inputs across all the catchments to identify how sensitive their flood regimes are to climate change. The changes in flood response were found to be highly non-linear, varying significantly between different catchments. In total nine different flood response types were identified with each of the catchments used here belonging to an individual response type (Table 3.1). The response types vary from a dampened response, where flood changes are proportionately smaller to precipitation changes, to an enhanced/sensitive response where the flood response is greater than the change in precipitation. Through using the nine response type catchments a wide range of the UK's hydrological sensitivity to climate change can be explored.

Table 3.1 Catchment details of the nine case study catchments. Base flow index (BFI) is the proportion of runoff resulting from baseflow and quickflow. Response types have been classified by Reynard et al (2010) and characterise the hydrological response of a catchment to a change in its inputs.

NRFA Gauge	Catchment and Station	Area (km^2)	Data Coverage	BFI	Response Type
07002	Findhorn at Forres	781.9	1961-2001	0.40	Dampened-Extreme
02001	Helmsdale at Kilphedair	551.4	1975-2001	0.47	Dampened-High
14001	Eden at Kemback	307.4	1967-2001	0.63	Dampened-Low
47007	Yealm at Puslinch	54.9	1963-2001	0.56	Neutral
34003	Bure at Ingworth	164.7	1961-2001	0.83	Mixed
54008	Teme at Tenbury	1134.4	1961-2001	0.56	Enhanced-Low
21023	Leet Water at Coldstream	113.0	1970-2001	0.34	Enhanced-Medium
43005	Avon at Amesbury	323.7	1965-2001	0.91	Enhanced-High
38003	Mimram at Panshanger Park	133.9	1961-2001	0.93	Sensitive

Daily river flow records and catchment precipitation are provided by the national river flow archive (NRFA). Record lengths range from a maximum of 40 years for four catchments to a minimum of 26 years for the Helmsdale (02001). Catchment precipitation is derived from UK Met Office rain gauge records. Potential evaporation for each catchment is provided by the UK Meteorological Office Rainfall and Evapotranspiration Calculation System (MORECS by Thompson et al., 1981, Hough and Jones, 1997). The MORECS data is in the form of monthly totals across a 40 km x 40 km UK grid. To create a daily evaporation time series to correspond with the river flow and precipitation records, the monthly total is assumed to be equally distributed across each day of a month.

3.3 Impact Model – Hydrological Simulation

In Chapter 2 conceptual hydrological models with reduced complexity were identified as being suitable for rainfall-runoff simulation. The main benefits of conceptual models are their lower data requirements, computational efficiency and, in the case of lumped models, their applicability to small catchments. In this thesis all case study catchments have an area less than 1200 km^2, a relatively small size, and thus are suitable for simulation using a lumped conceptual model. One lumped conceptual model which has been widely used in climate change impact studies is the probability distributed moisture model (PDM) (Prudhomme et al., 2003, Kay et al., 2009, Arnell, 2011). This section provides a description of the PDM hydrological model and its calibration.

3.3.1 Probability Distributed Moisture Model

The probability distributed moisture model is a lumped conceptual rainfall-runoff model that represents catchment hydrological process through a sequence of mathematical steps; a complete description is provided by Moore (2007) with a conceptualisation in Figure 3.2.
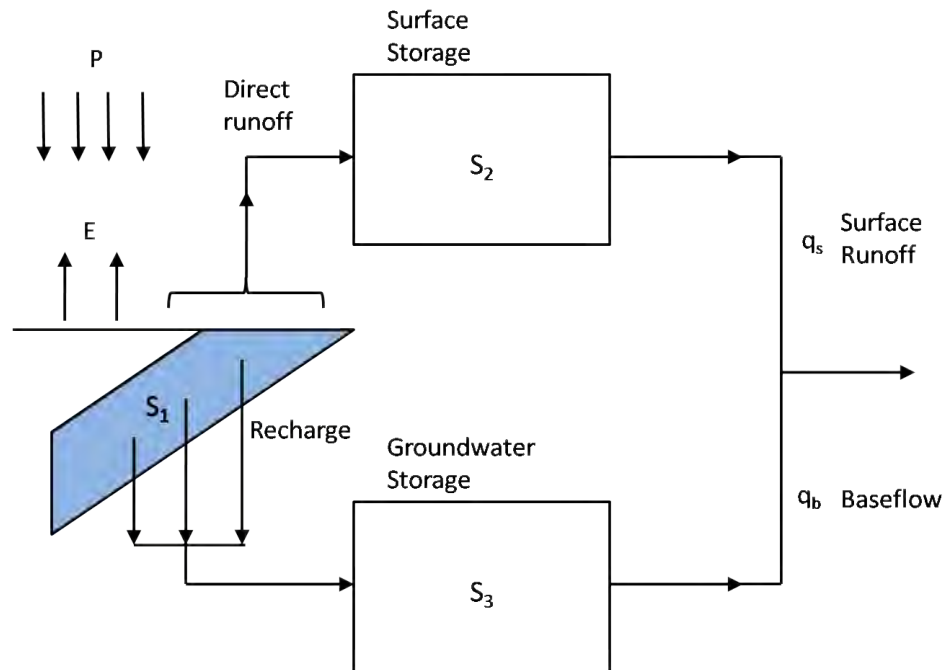
Figure 3.2 Conceptual outline of the probability distributed moisture model (PDM). Figure is re-drawn from Moore (2007).

The PDM model requires time series inputs of precipitation and potential evaporation at either the hourly or daily time step; in this thesis the catchments are all simulated at a daily time step (as outlined in section 3.2). The transformation of precipitation into direct runoff is based on a saturation excess process, which is defined by a storage capacity. The storage capacity concept includes physical properties such as canopy extent, surface properties and soil characteristics which are defined by two parameters controlling the minimum (C_{min}) and maximum (C_{max}) storage capacity within the catchment. A Pareto distribution is used to describe the distribution of the storage capacity across a catchment, with the distribution shape (b) altered to reflect different proportions of deep or shallow stores. If the storage capacity at a point is exceeded, direct runoff occurs, otherwise water remains in storage with losses to evaporation (b_e). Both the direct runoff and the recharge component proceed to a further storage element to represent surface storage and groundwater storage. The surface storage (K_1) and groundwater storage (K_b) components act as a delay in the system to

represent different catchment characteristics. The catchment river flow output combines the discharges from the surface and groundwater stores.

In this thesis a slightly altered version of PDM is used where runoff initially only occurs via the saturation excess route meaning there is no baseflow recharge from the probability distributed storage capacity (parameters with description in Table 3.2). In this alternative setup the direct runoff is partitioned with a proportion (α) directed to a fast routing store and the rest (1-α) directed to a slow routing store. These stores are equivalent to the surface and groundwater stores in the traditional model structure. The value of α is estimated using soils data and is set to 1-BFIHOST, where BFIHOST is the baseflow index (BFI) of a catchment estimated using HOST (Boorman et al., 1995) soils data (Institute of Hydrology, 1999). The rationale for the altered PDM model is to reduce the number of parameters that are calibrated through simulation. The more parameters that are calibrated the greater the potential for equifinality (Beven, 2006).

Table 3.2 Overview of PDM model parameters used in this thesis with a description of each parameters function and their method of estimation.

Parameter	Description	Estimation
f_c	Rainfall multiplicative factor	Set to 1
b_e	Exponent in actual to potential evaporation formula	Set Regionally
C_{min}	Minimum depth of moisture storage	Set to 0
C_{max}	Maximum depth of moisture storage	Calibrated
b	Exponent in Pareto distribution of storage capacity	Set Regionally
α	Surface/Baseflow routing partition	Set by BFIHOST
K_1	Time constant of surface storage	Calibrated
K_b	Time constant of baseflow storage	Calibrated

3.3.2 Snowmelt Modelling

One limitation of the PDM model is that it does not contain a snowmelt component. On the whole UK hydrology is not strongly influenced by snow processes however in northern regions at higher altitudes snowfall plays a more significant role in the characteristics of precipitation, which in turn can influence the timing of flow peaks. This is particularly important with respect to climate change as temperature changes may significantly alter the timing of snowmelt and in turn alter a catchment's hydrological regime (although temperature changes are not considered in this thesis). To simulate the influence of snowfall and storage

in a catchment a snowmelt module is implemented as a pre-processor to the catchment precipitation time series. A brief description of the snowmelt module is given here, while full details are in Bell and Moore (1999).

The snowmelt module requires inputs of a temperature time series and catchment elevation information. Precipitation falls as snow if the temperature drops below 1^oC, and enters into a snow pack store. The snow pack has two storage components, a 'wet' store for rain falling on snow and a 'dry' store for direct snowfall. Snowmelt from the snow store occurs at a constant rate for every degree in temperature above 0^oC and is then incorporated into the catchment rainfall via either a fast or slow storage outlet. The snowmelt module described is a conceptual design, when implemented it is used as a pre-processer to the precipitation time series for input into PDM. If snowfall occurs a lag in the precipitation is introduced, with the lagged precipitation re-distributed over time according to the modelled snowmelt.

Table 3.3 Overview of parameters used in the snowmelt module.

Parameter	Description	Value
T_{snow}	Snowfall threshold	$1\ ^o$C
T_m	Snowmelt threshold	$0\ ^o$C
T_{drel}	Drainage release threshold	$0\ ^o$C
α	Lapse rate	$0.0059\ ^o$Cm^{-1}
$mfac$	Snowmelt rate	6.0 mm/day/^{o}C
k_{1s}	Lower outlet storage constant	0.5 day^{-1}
k_{2s}	Upper outlet storage constant	0.9 day^{-1}
s_c	Maximum liquid content as fraction of total	0.18
$rgfac$	Correction factor for rainfall falling as snow	1.1

3.3.3 Hydrological Calibration and Performance

The nine catchments were calibrated previously with full details provided in Crooks et al (2010). The PDM model has eight parameters, five of which were set for each catchment prior to calibration. The precipitation factor parameter (f_c), typically used in flood forecasting to account for inaccurate precipitation data, was set to a constant of 1 in all catchments except the Avon (43005). b_e and b were set as a constant by geographical region, with catchments in the south allocated a slightly higher evaporation rate (higher b_e) and a greater proportion of deeper storage capacities to shallower storage capacities (lower b). The minimum catchment

storage (C_{min}) was assumed to be 0 across all catchments with the flow partitioning parameter (α) estimated from HOST soils data. The remaining three parameters (C_{max}, K_1 and K_b) were calibrated using a Monte Carlo sweep approach.

Table 3.4 Model metrics comparing the PDM simulated flows with the observed gauge record for the full period of calibration. The Nash Sutcliffe criterion compares the variance of model errors with the variance of the observations.

NRFA Gauge	Nash Sutcliffe 1-Day	Nash Sutcliffe 30-Day	Volume Error (%)
Findhorn (07002)	0.37	0.81	-6.0
Helmsdale (02001)	0.50	0.89	1.8
Eden (14001)	0.67	0.96	1.3
Yealm (47007)	0.69	0.97	-3.8
Bure (34003)	0.53	0.62	-2.9
Teme (54008)	0.74	0.96	-2.0
Leet Water (21023)	0.47	0.85	8.2
Avon (43005)	0.87	0.91	3.7
Mimram (38003)	0.69	0.72	-6.9

The Monte Carlo calibration method involves randomly varying a parameter within a pre-defined range with its resulting model performance compared with an objective metric. The objective metrics used were the Nash Sutcliffe criterion (Nash and Sutcliffe, 1970) at the daily (NS_{daily}) and 30-day (NS_{30}) time step and the flow volume error (V_{err}). The NS_{daily} criterion describes the fraction of variance in the PDM simulated flow series that is accounted for in the observed flow series used for calibration by comparing the daily flow values of each series; a value of 1 indicates a perfect model fit. The main limitation of the NS_{daily} criterion is that it does not account for any small lag between the simulated and observed record. To account for this the NS_{30} is used to analyse the same flow relationship over a 30 day period to smooth out any daily lag differences. The V_{err} metric describes the water balance within the PDM simulation, with an error close to 0 indicating there are no significant simulated river flow gains or losses compared with the observations. In the Monte Carlo analysis each of the three parameters were assessed sequentially from C_{max}, K_1 and then K_b. C_{max} was calibrated first and then fixed at a set value for the calibration of K_1, with both C_{max} and K_1 fixed for then calibrating K_b. The process is then repeated for each parameter individually in a second sweep with the other two parameters fixed at their current best

estimates. The final calibration of K_1 is performed with reference to the observed and simulated flood frequency curves with a final expert subjective decision on the K_1 value. This fine tuning towards the flood frequency curve is not quantifiable using objective metrics and is therefore not represented in the metrics for the final catchment calibrations (Table 3.4).

3.4 Impact Analysis - Flood Frequency Estimation

In a planning context, fluvial flooding is typically described using flood peak magnitudes associated with an expected frequency of exceedance, expressed as a return period in years. The purpose of a return period is to provide a probability of an event occurring over a given time scale. The larger the magnitude of a flood event, the higher the associated return period and the lower the probability of exceedance. A return period is not necessarily an expected value, it is a likelihood to reflect the risk of occurrence based on the current record. The calculation of return periods associated with flood peak magnitudes is a statistical procedure, with the outcome dependent on the observational record from a given gauging station.

As identified in Chapter 2 a river is in a flood state for only a short period of time in comparison to its overall record and statistical analysis requires a sub-sample representing the flood peak population. This flood information is obtained using either an annual maximum (AM) or peaks-over-threshold (POT) sampling method. POT sampling is preferable to AM as it provides an extended data population from the same length of record, as AM sampling may only extract a single event from a year which was particularly flood rich (i.e. there may have been two to three individual flood events which are greater than maxima events in drier years). Commonly POT flood events are extracted for an average of three peaks a year (POT3), providing three times as much information on the flow record compared with the annual maxima from the same series. When using a POT sampling approach the recommended statistical distribution is the Generalised Pareto (GP) distribution fitted against the POT data to estimate flood magnitudes at a given return period (Institute of Hydrology, 1999). Flood frequency analysis using POT3 sampling with a GP flood frequency estimation procedure has previously been widely used in UK climate change flood impact assessments (Reynard et al., 2001, Prudhomme et al., 2003, Kay et al., 2009, Prudhomme et al., 2010).

3.4.1 Flood Frequency Calculation

Each catchment flow series is subjected to a POT3 sampling procedure to provide a flow peak population. The GP distribution is then fitted against the extracted POT3 flow peak population, where the GP distribution is defined as:

$$Q(F) = \varepsilon + \frac{\alpha}{k}\{1 - (1 - F)^k\}$$

Equation 3.1

Where *F* is the probability of non-exceedance and is related to the T year return period by:

$$T = \frac{1}{1 - F}$$

Equation 3.2

The GP distribution (Equation 3.1) is a three parameter extreme value distribution used for modelling the tail of a distribution. The three parameters describe the distribution's shape(k), scale(α) and location(ε) and are estimated from the POT3 data. The parameter estimation procedure is undertaken using probability weighted moments (PWM - Greenwood et al., 1979, Hosking and Wallis, 1987), which are transformed to describe the linear transformation of the moments (L-moments) of the fitted GP distribution and observed POT3 distribution. The POT3 data and fitted flood frequency curve are typically displayed using a plotting position formula which assigns each POT3 event a given return period based on the POT3 events relative size within the total POT3 population (Figure 3.3). In this thesis a flood magnitude for a given return period is denoted as *T*RP, where *T* is the return period in years (e.g. 50RP is the flood magnitude associated with the 50 year return period).
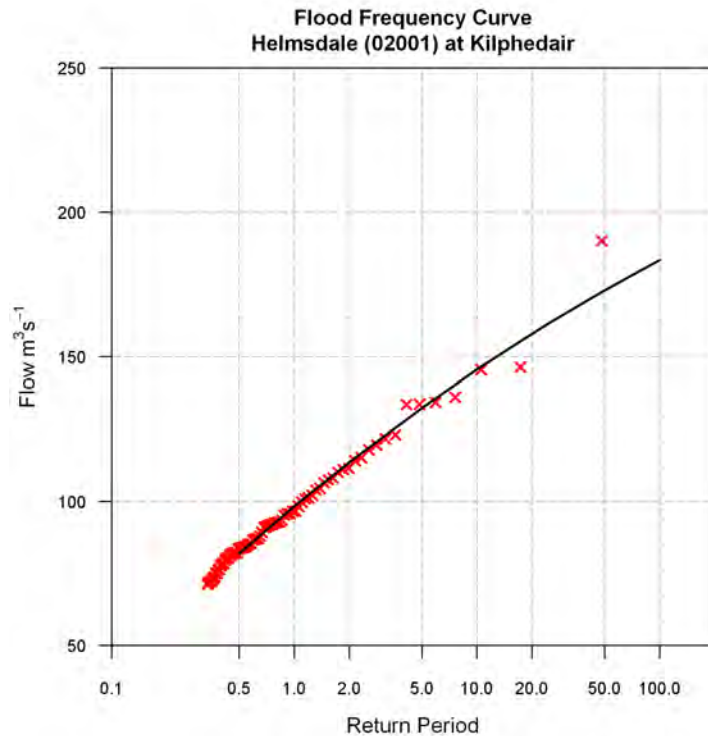
Figure 3.3 Fitted flood frequency curve with POT3 population data for the Helsmdale (02001) catchment. The POT3 data and flood frequency curve are transformed to have associated return periods using Gringorten plotting positions (Gringorten, 1963).

3.4.2 Catchment Flood Frequency Curves

The flood frequency curves for all nine catchments are shown in Figure 3.4 derived from observed flow records (red) and from a flow series simulated by PDM for the same period of record (blue). The nine catchments each display different flood regime characteristics, as described by the shape of the flood frequency curve. The flood regimes can be broadly described by two categories; firstly flood frequency curves that are unbounded, found in the Findhorn (07002), Bure (34003) and Leet Water (21023) catchments. In these catchments the increase in flood quantile magnitudes becomes proportionally larger as the return period increases. This suggests that the magnitude of the largest flood event that could occur in a catchment is not constrained by the catchment properties. The second flood characteristic are flood frequency curves that are bounded above, found in the remaining six catchments. In this flood regime, as the length of return period increases, flood events increase in magnitude but at a decreasing proportionate rate. Therefore as a return period increases in size the magnitude of the flood events tends towards a maximum value.
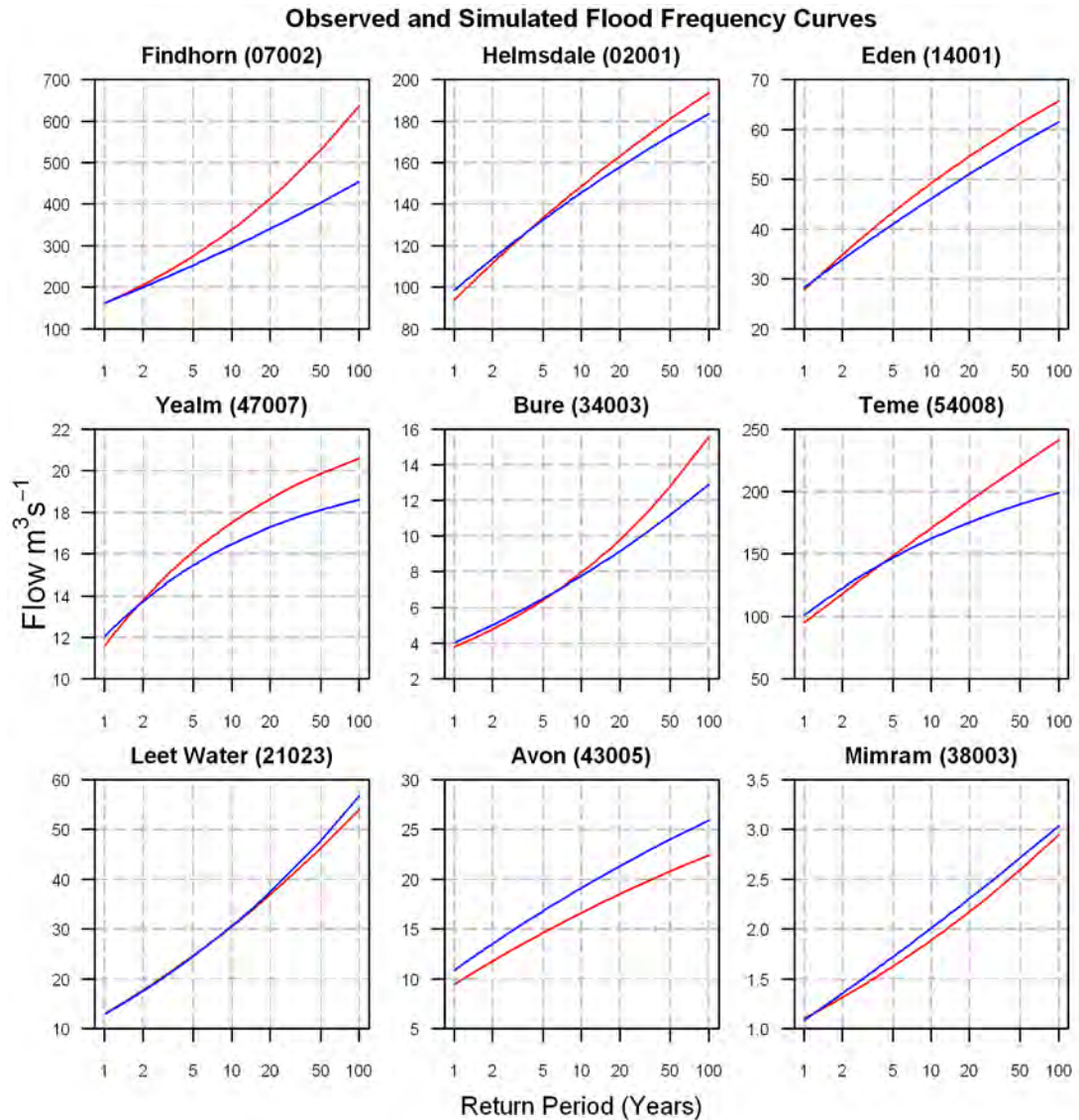
Figure 3.4 Observed (red) and PDM simulated (blue) flood frequency curves for the nine case study catchments.

A catchment growth curve is a standardised flood frequency curve allowing for the comparison of flood regime behaviour between catchments where flood magnitudes differ. The growth curve is standardised by expressing the flood frequency curve as a ratio relative to the Q_{med}, where the Q_{med} is approximated as the two year return period flood quantile (2RP). The two categories of flood behaviour are highlighted by calculating the growth curves for each catchment (Figure 3.5). The three catchments with unbounded growth curves (Findhorn (07002), Leet Water (21023) and Bure (34003)) have contrasting flow regimes as described by their BFI. The Findhorn and Leet Water have a low BFI, characterising a rapid rainfall-runoff response, whereas the Bure has a high BFI, indicating a slow hydrological response. The areas of the catchments are also very different ranging from 113 km^2 (Leet

Water) to 782 km² (Bure). This suggests that a catchment's growth curve is primarily influenced by the flood peak record rather than a definable catchment characteristic.
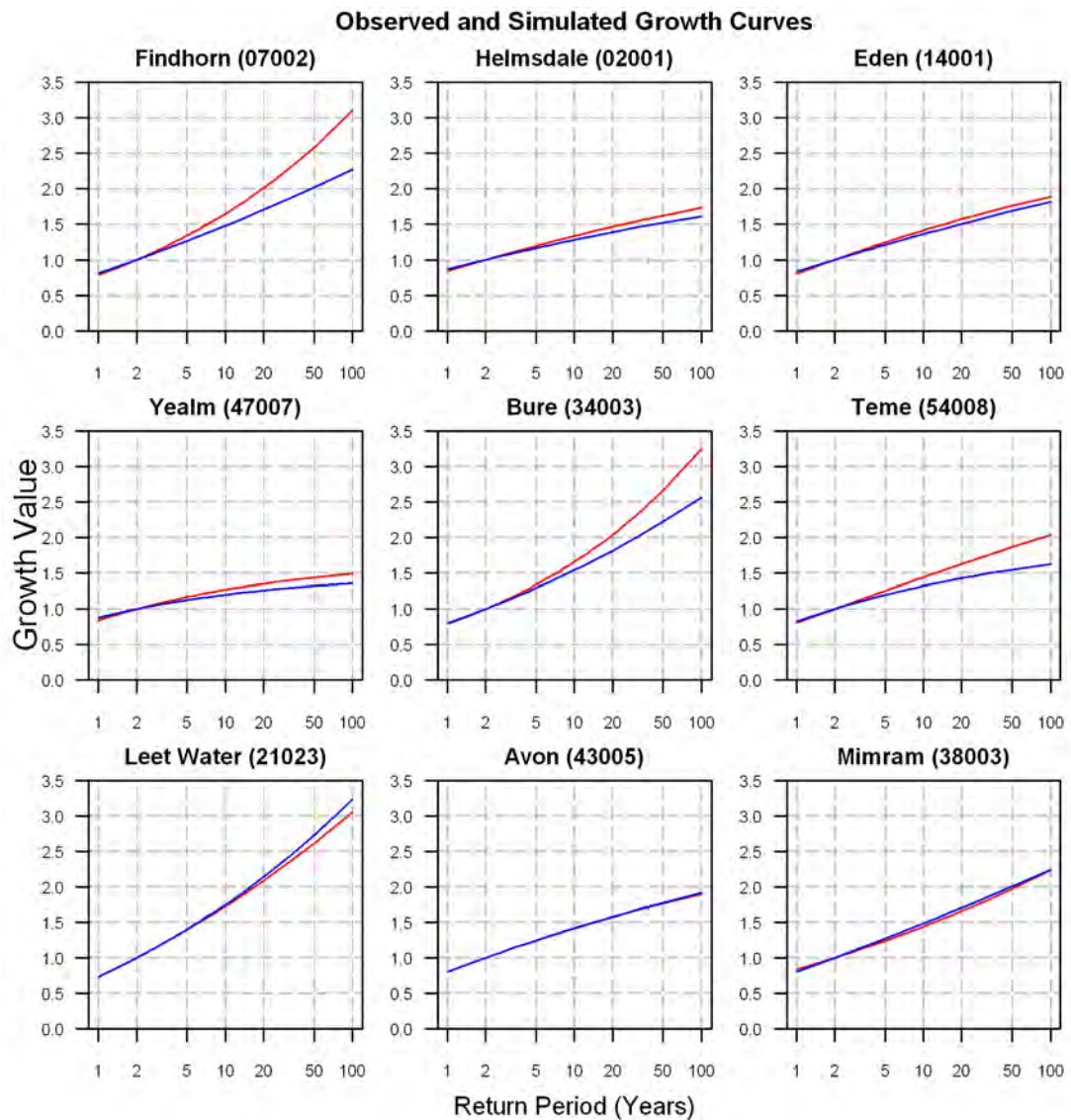
Figure 3.5 Observed (red) and PDM simulated (blue) growth curves for the nine case study catchments. Growth curves standardise a flood frequency curve using the Q$_{med}$ (approximately 2RP), allowing for a comparison of flood behaviour between catchments. All graphs are scaled to the same y-axis.

The ability of the PDM to reproduce the catchment flood regimes can be assessed through the comparison of the observed and simulated flood frequency curves and growth curves. The importance of the combined assessment of the flood frequency curves and growth curves when analysing hydrological model performance is highlighted in the Avon (43005) catchment where the flood regime characteristics are well reproduced, with near identical growth curves (Figure 3.5), however flood magnitudes are consistently over estimated (Figure 3.4). On the whole the PDM simulations provide a good representation of the catchment flood

regimes as described by the catchment growth curves (Figure 3.5). However the flood magnitudes at the higher return periods are underestimated in several catchments, most significantly in the Findhorn (07002), Bure (34003) and Teme (54008) catchments (Figure 3.4). In light of this it is important to consider that the flood frequency curves extrapolate information beyond the observed flow records at the higher return periods, with the estimated flood magnitudes at the 50RP and 100RP increasingly sensitive to extrapolation.

3.5 Climate Change Scenarios

In a 'top-down' climate change impact study framework future climate projections from climate models are generally used to construct climate scenarios for input to the impact model. Climate models are based on the fundamental laws of physics, where the processes and feedbacks within the atmosphere and ocean are resolved over a conceptually gridded Earth. Simulations from both global and regional climate models (GCM and RCM respectively) are computationally intensive in both the time they take to run and the volume of data they produce. Due to the human and computational resource demands that are involved with developing and running a climate model, only a small number of institutions worldwide have developed climate models. It is not traditionally the impact scientist who runs the climate model, instead they rely on the availability of GCM or RCM data to construct scenarios. For UK impact studies there are two main climate modelling resources, CMIP3 and UKCP09, from which climate change scenarios can be constructed for an impact study.

3.5.1 CMIP3

The coordinated efforts of the IPCC to bring together the latest climate change research in its assessment reports instigated the process towards a better coordination and consensus in climate change research. The coupled model inter-comparison project (CMIP) was established to bring this consensus to the modelling activities of the different institutions developing climate models. It set forth guidelines outlining which simulations all institutions would undertake, along with how and where the outputs from the model simulations would be made available. The third stage of the coupled model inter-comparison project (CMIP3 - Meehl et al., 2007) brought together the modelling activities which contributed towards the IPCC AR4. The data are freely available to download for academic purposes from the IPCC data distribution centre with a full list of the available models and outputs provided in Meehl et al (2007).

Table 3.5 Information on CMIP3 climate models used in this thesis. All data and information obtained from the IPCC data distribution centre (www.ipcc-ddc.org).

Modelling Group	GCM	Atmospheric Resolution		Oceanic Resolution	
		Latitude	Longitude	Latitude	Longitude
NCAR	CCSM3	1.40	1.40	1.125	0.27
CCCma	CGCM3.1	3.75	3.75	1.80	1.80
CNRM	CM3	2.80	2.80	0.50-2.00	2.00
MPI	ECHAM5	1.90	1.90	1.50	1.50
CSIRO	MK3.0	1.90	1.90	0.84	1.88
GFDL	CM2.0	2.00	2.50	1.00	1.000
GFDL	CM2.1	2.00	2.50	1.00	1.00
GISS	ER	3.00	4.00	3.00	4.00
UKMO	HadCM3	2.75	3.75	1.25	1.25
INM	CM3.0	4.00	5.00	2.00	2.50
IPSL	CM4	2.50	3.75	2.00	2.00
NIES	MIROC3.2	2.80	2.80	0.50-1.40	1.40
MRI	CGCM2.3.2	2.80	2.80	2.00	2.50

The climate models used in this thesis were selected based on the common availability of data for two emissions scenarios. The first emissions scenario is the 20C3M which represents the 20th century based on observed external forcings. The second scenario used is the SRESB1 emissions scenario which represents a conservative scenario of future greenhouse gas emissions throughout the 21st century. Thirteen climate models provide runs based on these two emissions scenarios (Table 3.5). They cover a wide range of spatial resolutions with the finest NCAR-CCSM3 of the order of 1.40^{o}, while the coarsest is GISS-ER at $4.00^{o}/5.00^{o}$.

3.5.2 UKCP09

The latest climate projections for the UK, UKCP09, are provided by the Met Office Hadley Centre as part the UK climate impacts project (UKCIP). A full comprehensive description of the climate projections can be found in Murphy et al (2009), the main aspects of the scenarios are outlined here.

UKCP09 is the first concerted effort to include the known uncertainties associated with climate change and climate modelling in future climate change projections for end users. The projections are constructed using the Hadley Centre GCM and RCM to provide climate

simulations at 25km resolution across the UK. 21st century simulations were undertaken using low, medium and high emissions scenarios. Climate model structure uncertainty is accounted for through incorporating the projections from twelve CMIP3 climate models in addition to the UK Hadley centre models HadCM3 and HadRM3. Climate model parameter uncertainty is addressed through the use of perturbed physics ensembles of the HadCM3/HadRM3 models to identify the full range of parameter space which a climate model's parameters may lie in, along with its corresponding impact on the climate simulations. Lastly the natural variability within a climate model is accounted for through model ensemble runs using the same model setups. Through exploring this wide range of uncertainties, future projections of climate show a range of possible projections. The range of all the simulations creates a sample space, which was then sampled to statistically generate future climate projections.

The climate projections are available as climate change factors, describing the mean change in climate for a future 30 year period relative to the baseline climate of 1961-1990. The statistical procedure used to create the climate change factor projections results in an ensemble of 10,000 probabilistic climate change scenarios across a 25km UK grid for each decade in the 21st century (2020-2080). The climate change factors can be used directly (as applied in this thesis and discussed in the next section) or in combination with a weather generator.

3.5.3 Application of Climate Change Factors

In this thesis climate change scenarios from the CMIP3 models and UKCP09 are applied using the change factor methodology, applied to precipitation only. Precipitation is the principle mechanism for flood occurrence and variability, with changes in temperature shown to have a small impact on flood magnitude changes in climate change impact studies (Prudhomme et al., 2010). Each climate change factor scenario consists of twelve monthly percentage changes describing the mean change in a 30 year future period compared with a 30 year baseline period. The baseline reference period which is typically used in impact studies is 1961-1990 and is also used here. In the example of precipitation, the precipitation change factor scenario is applied to the observed catchment precipitation in a multiplicative manner. The values in the observed record are perturbed by their corresponding monthly percentage change in the change factor scenario. This is repeated for each month of the year to create a new precipitation time series representative of the future time period of interest. The main limitations of applying the change factors to the observational record include

maintaining the day to day sequencing of the observed record as well as an assumption that the observed variance remains unchanged. A full discussion of their limitations is outlined in Chapter 2. The new perturbed time series can then be used as the precipitation input to PDM similarly to the baseline time series in section 3.3. The impact of climate change is assessed through analysing the difference between the baseline PDM simulation and the future perturbation driven PDM simulation.

3.6 Chapter Summary

This chapter has outlined the tools and methods that are used throughout this thesis in assessing the impact of climate change on UK flooding. Nine UK catchments have been selected which cover a wide geographical distribution and physical characteristics, for which the changes in flood characteristics have previously been shown to display a different sensitivity to climate change. The catchments are simulated using the PDM lumped conceptual rainfall-runoff model, with the resulting river flow outputs transformed to return period flood quantiles using a POT3 sampling procedure with a fitted GP distribution. Climate change scenarios are in the form of monthly change factors taken from the CMIP3 model archive or UKCP09. The climate change factors are used to perturb the observed catchment precipitation to create a new precipitation time series representative of the future which can used as input to PDM.

The methods and tools outlined in this chapter are used in the rest of this thesis with extra details provided where necessary. The next chapter addresses the first research question of the role of climate variability in climate change impact studies.

CHAPTER 4
Role of Climate Variability

4.1 Introduction

The aim of this chapter is to understand the role of climate variability when undertaking a climate change impact study on flood flows, particularly when calculating changes derived from a future climate relative to a baseline reference period. There are a number of key research goals which contribute to this chapter:

- Understand the importance of the temporal averaging period when constructing climate change impact studies.
- Develop a new resampling methodology which extends the range of climate variability produced by climate models to allow for a broader inclusion of climate variability in impact studies.
- Investigate whether there is any evidence for climate variability to change in its pattern or magnitude in the future.

An overview of climate variability in the UK and current methods for assessing climate variability is given in section 4.2. The importance of the temporal averaging period when calculating changes is shown in section 4.3. Section 4.4 introduces a new resampling methodology for creating climate change scenarios which account for climate variability (Ledbetter et al., 2012). This resampling method is then used to investigate whether precipitation variability may change in the future (section 4.5). The resampling methodology creates an ensemble of scenarios which are compared with the UKCP09 probabilistic scenarios in section 4.6. The chapter finishes with a discussion and conclusions (section 4.7), followed by a chapter summary (section 4.8).

4.2 Climate Variability - Background

Climate refers to the long-term average atmospheric conditions which a specific region experiences. The UK has a temperate maritime climate with typically mild and wet winters and cool summers. This can be established from long term averages of climatological data. However the same data also tells us that we experience departures from the average conditions with sequences of warmer (cooler) or dryer (wetter) conditions between months, years and decades. This variation of the climate over time is climate variability, caused by the natural processes in the atmosphere and oceans. The climate of the UK is influenced by a number of competing processes which result in the large variability in climate (Woollings, 2010). The climate variability is predominantly influenced by the North Atlantic Oscillation (NAO) (Hurrell, 1995, Hurrell et al., 2001) along with the Atlantic Meridional Overturning Circulation (MOC) (Marshall et al., 2001). The NAO phases characterise strengthening (weakening) westerly winds leading to an increase (decrease) in precipitation over the UK (Fowler and Kilsby, 2002) at time-scales from years to decades. The MOC describes the heat and salinity transports within the North Atlantic with fluctuations over decadal time scales (Latif et al., 2006). The interaction of the NAO and MOC lead to climate variability at a number of different time scales. Current climate models recreate these large scale processes of the climate but some physical processes and mechanisms influencing climate variability (i.e. jet stream variations, blocking) are known to be inadequately reproduced in global climate models (Parker et al., 2007, Woollings, 2010). This leads to two issues relating to climate models and climate variability when undertaking a climate change impact study. Firstly, how to account for the fact that climate model output may not fully recreate the variability of the observed climate? Secondly, the climate variability that is produced in one climate model realisation may have been different in another realisation from the same model. With very few multiple runs available for a given climate model setup, impact studies are limited in the range of climate variability they can explore.

One method suggested for accounting for climate variability with a limited number of climate model realisations is to apply a resampling technique to GCM outputs (Raisanen and Ruokolainen, 2006, Ruokolainen and Raisanen, 2007, Kendon et al., 2008, Prudhomme et al., 2010). Raisanen and Ruokolainen (2006) identify a baseline period and future period of interest (e.g. 1971-2000 & 2011-2020) and calculate the multi model mean change between the two periods. GCM outputs are then analysed to identify matching pairs of periods that provide the same change as the period of interest (e.g.1906-1935 & 1991-2000 or 2051-2080

& 2086-2095). The methodology generates, from an initial 21 GCM realisations, a total of 420 resampled realisations. The results demonstrate that the resampling technique increased the range of possible climatic changes, particularly with respect to a greater probability of precipitation decreases. This is particularly important to the analysis of future flooding as it demonstrates that through using the standard GCM outputs alone, the range of precipitation projections may be underestimating the range of changes which is only identified through resampling the GCM outputs. An alternative resampling method is presented by Prudhomme et al (2010) where every 20 year averaging period in an extended baseline window (e.g. 1951-2000) is compared to every 20 year averaging period for a future window (e.g. 2071-2100). Their results demonstrate that the direction of change in future precipitation can be dependent on the averaging period and its mode of climate variability. The resampling examples outlined in this section assume that the climate model realisation contains an adequate representation of climate variability, which can be sampled through choosing different averaging periods. In the technique developed by Raisanen and Ruokolainen (2006) it is assumed that the multi model mean change from the baseline and future provides a 'correct' change from which to generate resamples. As highlighted previously, climate models are known to inadequately simulate key processes and features which generate climate variability. A resampling methodology which allows for sequences of variability beyond those produced by a climate model would allow for a broader characterisation of the role of climate variability in climate change impact studies.

4.3 Climate Variability and Climate Change

The impact of climate change typically refers to a change in the mean climate from a baseline period of reference compared with a period in the future of the same length. However the manner in which the mean climate is defined can influence any calculated climate change. This section analyses the outputs from HadCM3 run under SRESB1 for a grid cell centred on longitude 0.00 and latitude 52.50. Figure 4.1 shows the annual precipitation totals from the transient HadCM3 projection with a 10, 30 and 50 year moving average calculated from the values. The 10 year moving average (orange) shows considerable variability with sometimes large variations over a short space of time (i.e. 1930-1940). Using such a short period to average the climate would lead to significant variations in calculated changes which are dependent on the time period chosen and its phase of climate variability. To avoid misrepresenting the influence of climate variability the World Meteorological Organization (WMO) recommends a period of 30 years to define an average climatological period (Carter,

2007). The 30 year average (Figure 4.1 – red line) removes a large amount of the variability that is present in the 10 year average, yet maintains more variability and hence more information on the time period compared with a 50 year average (blue). This confirms that a 30 year climatological reference period provides a robust approach to summarising the climate without placing too great an influence on the climate variability.
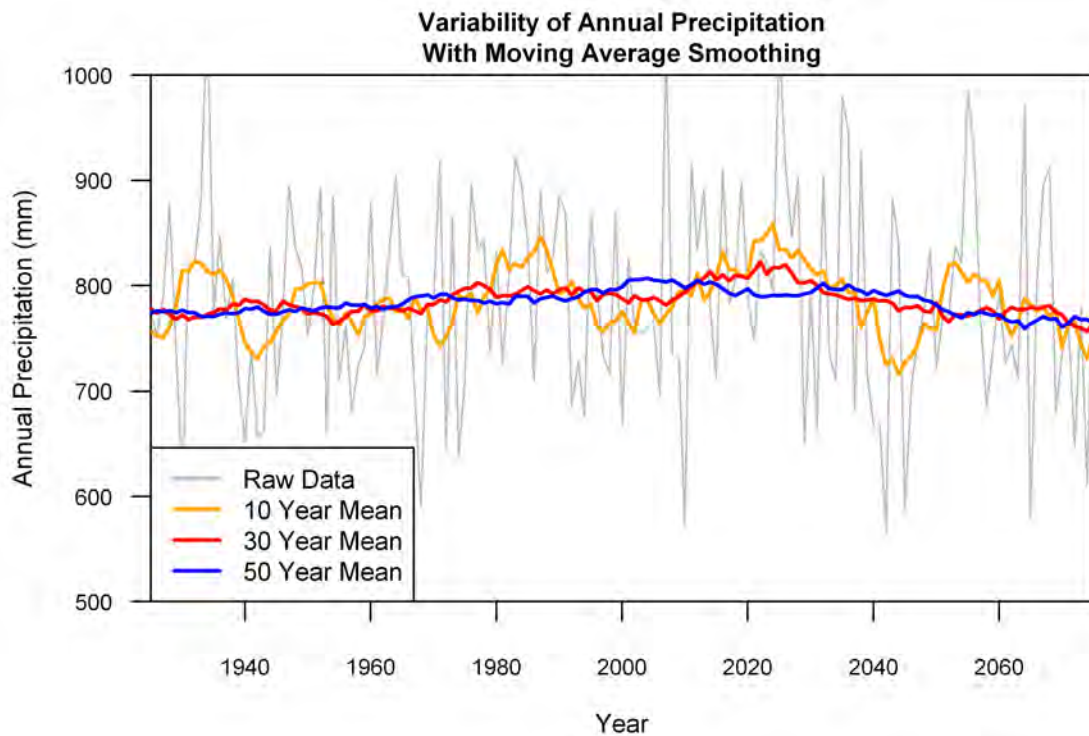
Figure 4.1 Precipitation time series (grey) with 10 year (orange), 30 year (red) and 50 year (blue) moving average calculated for annual precipitation totals.

It is important to recognise that the period chosen for averaging a climate variable still plays an important role when defining a change in climate. Although the 30 year average is less variable than the 10 year average, there remains a degree of variability from one 30 year period to the next (Hulme and New, 1997, Ruokolainen and Raisanen, 2007). To demonstrate the influence this has on calculating climate change factors, each 30 year precipitation average in the transient projection is expressed as a percentage change relative to three different baseline periods; 1950-1979, 1955-1984 and 1960-1989 (Figure 4.2). The temporal structure of the changes is the same for each reference period, it is the magnitude and in some cases the direction of change which varies. For example the transient projection shows an upward trend in precipitation in the early 21st century with a declining trend after 20-30 years. Using a reference period of 1960-1989 a negative change in precipitation occurs during the

2030s, while with 1950-1979 as the reference a negative change is not apparent until the 2050s. This is an important factor to consider when undertaking a climate change impact study, particularly with respect to using climate change factors.
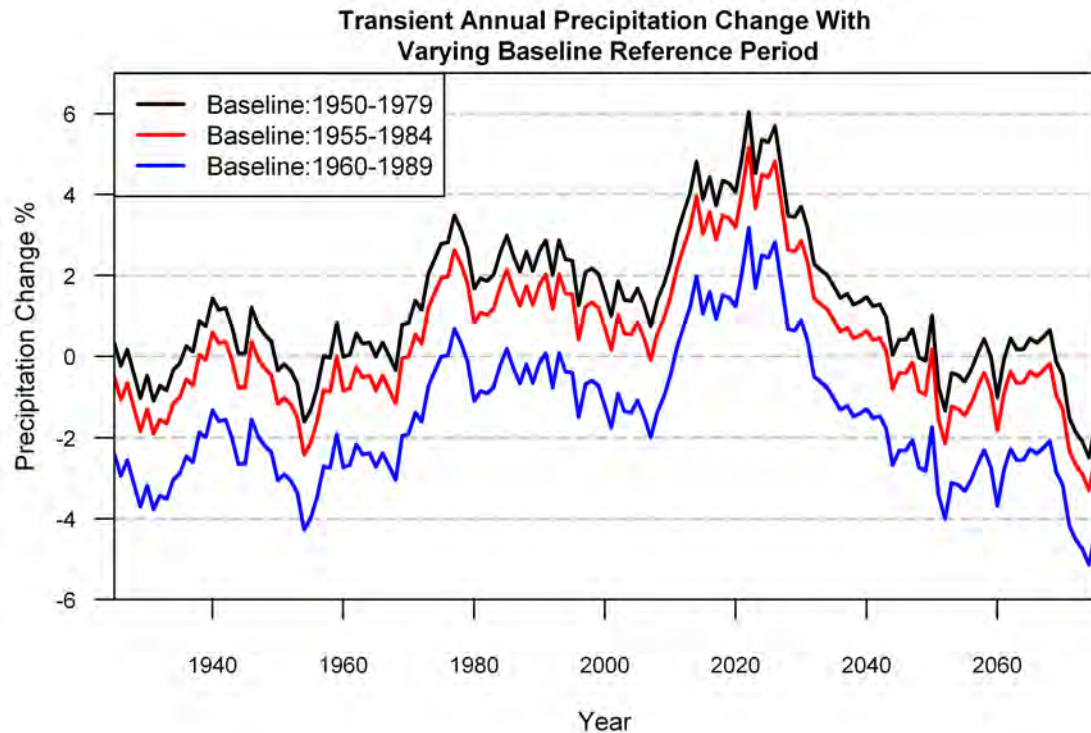
Figure 4.2 Change in annual precipitation averaged over a 30 year time period. Precipitation change is calculated relative to three different baseline periods.

As outlined in Chapter 3 the typical baseline reference period used to define climate change factors is 1961-1990. The precipitation change factors from the transient time series for 2071-2100 relative to 1961-1990 are shown in Figure 4.3 (left), with a clear seasonal cycle of winter increases and summer decreases in precipitation. The importance of the baseline reference period is demonstrated by using every consecutive 30 year period between 1950 and 2000 to define the baseline, and calculating the corresponding precipitation change factors for the 2080s (Figure 4.3-right). The same seasonal cycle of change is maintained, however the magnitude of change varies by at least 10% each month through using a different baseline period. The reference period of 1961-1990 is at the tail end of changes in February and August, while in April the direction of change may be reversed depending on the choice of baseline period. This issue is accentuated further if the uncertain choice of future period is also considered. The 2080s is typically defined by 2071-2100; the use of 2070-2099 would be equally valid and provide slightly different climate changes (not shown).
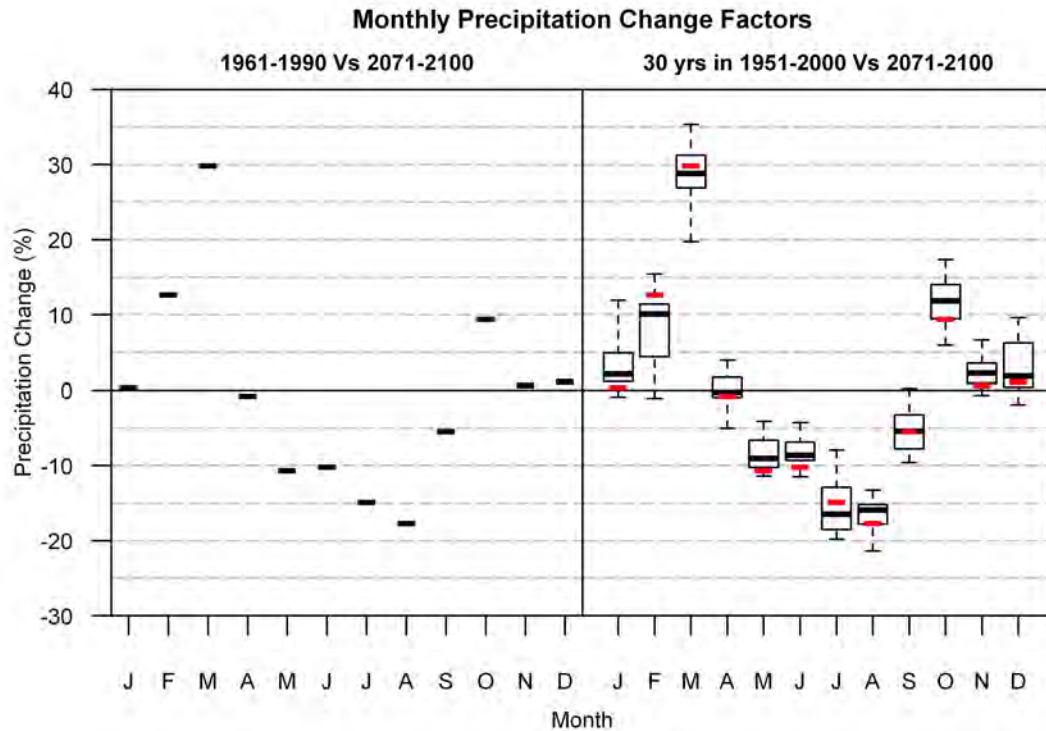
Figure 4.3 Climate change factors for the 2071-2100 relative to 1961-1990 (left) and every consecutive 30 year period from 1951-2000 (right). Boxplots show the median (bold), the inter-quartile range (box) and the full range of data (whiskers). Red dashes are the points from the left panel overlaid on the boxplots.

The role of climate variability is especially significant with respect to using climate model outputs to construct climate scenarios. As a climate model is not a forecasting or hindcasting tool, the time period of 1961-1990 in the model 'world' does not necessarily relate directly to the observed world of 1961-1990 as it may be in a different phase of variability (Kendon et al., 2008). A climate model is initialised by running it freely to establish an equilibrium climate with no changes to its external forcings (i.e. a pre-industrial world). Once the equilibrium climate is established, the model is forced with observed 20th century emissions to provide a 20th century simulation of climate, from which impact scientists typically extract the 1961-1990 time series. This 20th century simulation is initialised from an arbitrary end point of the equilibrium climate which may not have any relation to the observed climate at the start of the 20th century. The model period of 1961-1990 (or any other 30 year period i.e. 2070-2100) will vary between every climate model realisation, thus making its individual selection somewhat arbitrary. To establish a robust climate dataset a large number of model realisations would be required to create an ensemble from which to calculate climate averages and changes. Due to computational constraints there are few multi-realisation climate scenarios available, often limiting the inclusion of climate variability within an impact study.

The next section outlines a simple resampling methodology which creates multiple realisations of climate from a single climate model realisation, allowing for the explicit inclusion of climate variability within an impact study.

4.4 Resampling Climate Variability

The aim of the resampling procedure is to change the sequencing and repetition of values in a climate time series originally produced by a climate model. While the procedure does not generate events that are not simulated by the climate model, through modifying the sequencing and frequency of events in the original time series a new climate realisation is created. Given that the model simulation and resampled realisation contain mostly the same information, it is assumed they are both equally valid representations of the climate. However, the manner in which a variable can be resampled is dependent on its temporal structure.

4.4.1 Resampling Methodology

The simulated precipitation time series of monthly totals is split into two sets of thirty year sub-series for a baseline (1961-1990) and a future period (2070-2099). These time series will form the basis for the resampling process, each being resampled independently. To create a new baseline time series the 1961-1990 time series is split into twelve monthly groups. A new thirty year time series is generated by randomly selecting a value from its corresponding monthly group and placing it in the new time series. The method samples with replacement so the value is returned back to its group for reselection. For example the same January value could occur thirty times in a thirty year time series, although this is unlikely to happen. The process is repeated until a new thirty year time series is constructed. The same procedure is then repeated for the future period of 2070-2099. A key assumption made in this resampling strategy is that precipitation can be treated as independent from month to month; this is tested in the following section.

4.4.2 UK Precipitation Temporal Structure

Understanding the temporal properties of precipitation is a critical step to inform the resampling procedure. The analysis is undertaken for all observed catchment precipitation along with every considered GCM (Table 3.5) and grid cell covering the UK, the results shown here are only for the Eden catchment and a HadCM3 grid cell covering northern UK.

Autocorrelation is the measure of correlation between time series observations at different temporal spacing, and is applied to the precipitation time series of monthly totals (Figure 4.4-top) with each month correlated with the following 23 months (i.e. two years). The initial autocorrelation results (not shown) display an oscillating seasonal cycle, due to winter precipitation being oppositely correlated with summer precipitation. The time series is de-trended by removing the time series monthly means from each monthly value, therefore removing the seasonal cycle and leaving the autocorrelation of monthly anomalies. The correlogram of monthly anomalies shows that there is no significant correlation of precipitation from one month to another (Figure 4.4-bottom).
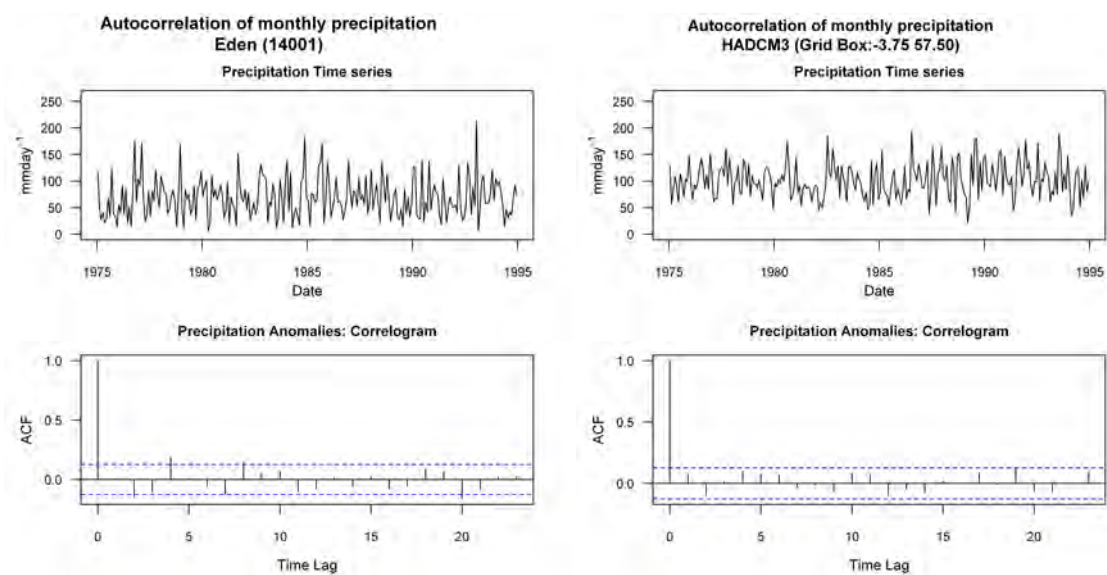
Figure 4.4 Monthly precipitation totals for the Eden catchment observations (top-left) and simulated by HadCM3 for the same location (top-right) with their autocorrelation coefficient and correlogram's (bottom) of corresponding anomalies. Correlogram has 95% confidence limits (dashed lines) at $\pm 2/\sqrt{N}$, where N is the number of observations.

The autocorrelation test informs us that there is no regularly occurring cycle within the precipitation structure, but this does not provide information on the possibility of any intermittent persistence of either a wet or dry period. It is therefore important to identify if there is persistence of high, medium or low magnitudes of precipitation occurrences. A further test is conducted by separating the time series into twelve monthly groups. Each monthly group is then further divided into five categories of equal size according to the magnitude of each precipitation value, category one being the lowest 20% of values and category five being the highest 20% of values. Each precipitation value in the time series is then assigned the value of its associated magnitude category (Figure 4.5-top), resulting in a

time series of integers. A new persistence time series is generated where a month is assigned a value of 1 if it is followed by a month of the same magnitude category (direct persistence), 0.5 if a category is ±1 (lateral persistence) or 0 if there is no persistence (Figure 4.5-bottom). As precipitation magnitudes were split into five groups, a perfect random process would generate a persistence between months in 20% of cases. The nine observed catchment precipitation time series display a persistence ranging from 19% (Eden) to 24% (Leet Water) (Table 4.1), while no persistence occurs in monthly precipitation between 39% (Helmsdale) and 49 % (Eden and Avon) of the time. The GCM analysis (Table 4.2) shows a similar pattern of occurrences with a slightly extended range, with persistence occurring from a minimum of 13% to a maximum of 26%. The sequence and persistence analysis show no evidence of persistence through time, suggesting that month to month precipitation occurrences can be described as a random process. The results across observations and GCM derived values display a range from 15% to 25% indicating a predominantly random process. This analysis does not account for long term persistence from features such as the NAO but provides evidence for a lack of month to month persistence which is integral to the resampling methodology.
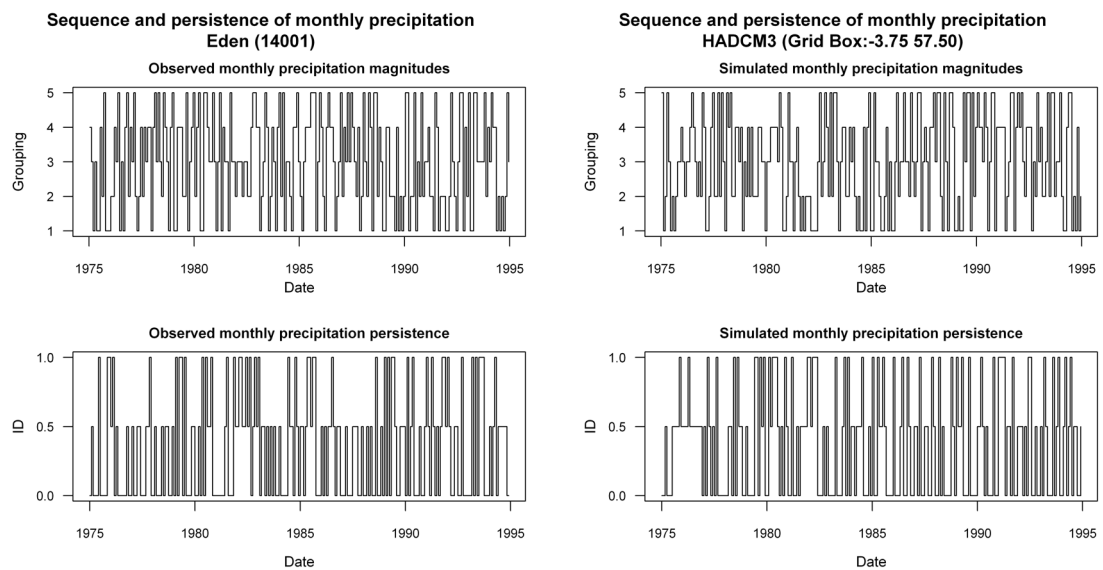
Figure 4.5 Sequencing of persistence in precipitation magnitudes. Magnitude groups of monthly precipitation for the Eden catchment (top-left) and HadCM3 (top-right), 1 being the lowest 20% and 5 the highest 20% of precipitation magnitudes. Sequencing of categories (bottom) with 1 representing sequencing of months of the same magnitude category, 0.5 is a month followed by ± 1 category, 0 indicates no sequencing.

The autocorrelation test and the analysis of sequencing and persistence of events demonstrate that precipitation can be considered independent between months across the UK. This property of month-to-month independence can therefore be exploited within the planned resampling methodology.

Table 4.1 Summary of catchment observed monthly precipitation persistence.

Catchment	No Persistence %	Lateral Persistence %	Direct Persistence %
Findhorn (07002)	42.08	34.17	23.75
Helmsdale (02001)	39.17	41.25	19.58
Eden (14001)	48.75	32.08	19.17
Yealm (47007)	47.08	31.67	21.25
Bure (34003)	47.92	28.75	23.33
Teme (54008)	45.42	34.58	20.00
Leet Water (21023)	48.33	27.50	24.17
Avon (43005)	48.75	30.83	20.42
Mimram (38003)	45.42	30.83	23.75

Table 4.2 Summary of GCM derived monthly precipitation persistence. Analysis of every UK grid cell for each GCM with the minimum and maximum UK grid cell values presented.

GCM	No Persistence %		Lateral Persistence %		Direct Persistence %	
	Min	Max	Min	Max	Min	Max
CCSM3	39.58	52.50	25.42	40.00	15.00	26.25
CGCM3.1	46.25	49.58	28.75	36.67	16.25	22.50
CNRM-CM3	45.83	50.83	27.92	35.00	19.17	22.50
CSIRO-MK3.0	43.75	52.92	26.67	38.75	15.00	23.75
ECHAM5	46.67	56.67	26.25	35.42	13.33	22.92
GFDL-CM2.0	43.75	48.75	27.50	36.25	18.75	23.75
GFDL-CM2.1	38.33	48.33	28.33	38.33	15.42	25.00
GISS-ER	44.58	49.58	31.67	36.67	18.33	22.92
HadCM3	41.25	50.83	28.33	40.00	14.58	22.92
INM-CM3.0	42.50	49.17	32.92	36.25	14.58	22.08
IPSL-CM4	41.25	49.17	29.58	34.58	18.75	24.17
MIROC3.2	45.00	46.25	31.67	34.58	20.00	23.33
MRI-CGCM2	41.25	48.75	27.50	37.50	21.25	25.00

4.4.3 Resampling UK Precipitation Variability

Climate variability has been identified as an important factor to consider within the impact study framework; however it has been acknowledged that current climate models do not adequately reproduce some of the mechanisms fundamental to simulating the UK climate. This section uses the resampling methodology to explore whether GCM precipitation variability is similar to the observed precipitation variability in the UK.

The resampling procedure allows for an unlimited number of new climate realisations to be created. For 13 GCMs and every grid cell in the UK region, 1000 new precipitation realisations were created through resampling the GCM period of 1961-1990. The resampling was undertaken at the monthly time step as outlined previously, with replacement (i.e. the same monthly value can be resampled more than once). For each GCM grid cell the mean of each of the 1000 time series is calculated and expressed as a percentage departure relative to the original GCM 1961-1990 time series mean. The standard deviation of the 1000 time series mean departures is then used to characterise the magnitude of precipitation variability for that grid cell. The results for the 13 GCMs are shown in Figure 4.6.

The results for each GCM display a different magnitude of precipitation variability. The GCM which produces the lowest level of variability is CNRM-CM3, while MRI-CGCM2 has the greatest variability. From the magnitudes of precipitation variability between GCMs in Figure 4.6 there is no evidence to connect GCM grid cell resolution and the magnitude of variability. Climate models with comparable resolution display large differences in precipitation variability (e.g. ECHAM5 vs CCSM3 or CNRM-CM3 vs HadCM3). The precipitation variability produced through the resampling procedure is dependent on the original GCM realisations, indicating that some GCMs have a simulated climate inherently more or less variable than others. This variation between the GCM climates is likely to be a result of their different process representation and structure. This emphasises the need to consider a number of different GCMs in any impact analysis in order to sample a wide range of different simulated climates.
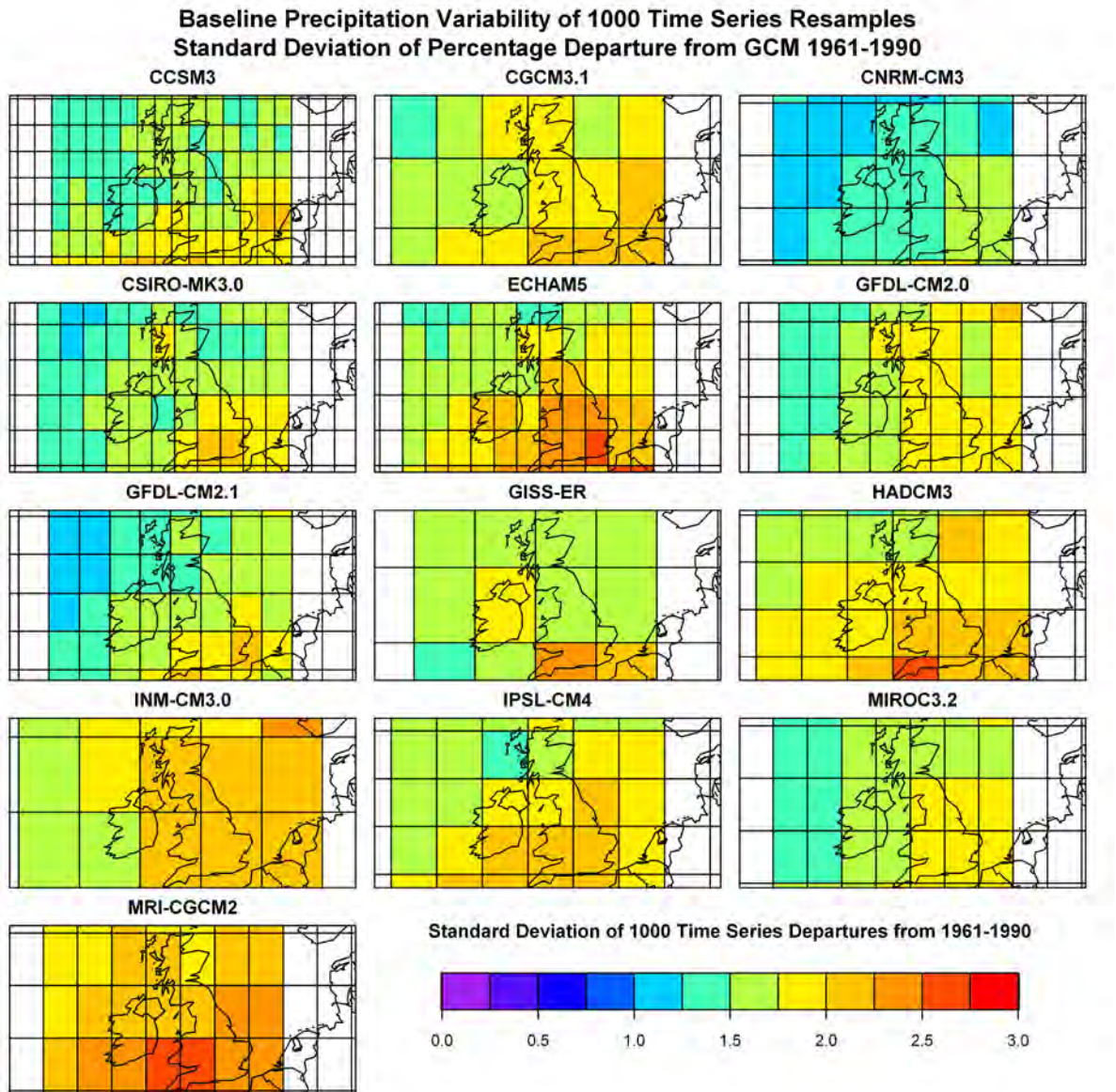
Figure 4.6 Resampled GCM precipitation variability. Time series means from 1000 precipitation resamples for each GCM grid cell are expressed as a percentage departure from the GCM 1961-1990 time series mean. The standard deviation of the 1000 time series departures describes the variability for a given GCM grid cell.

Geographically there is an overall pattern across all the models for higher precipitation variability across the south and east of the UK and lower precipitation variability in the north and west of the region. While this spatial pattern is consistent across all models there is a noticeable difference in its detail and magnitudes between models. There is no evidence for a difference in the precipitation variability between land or ocean grid cells.

The next stage of analysis is to compare the GCM produced precipitation variability to the variability of the observed climate. The ENSEMBLES gridded observational dataset (E-Obs)

is used for the comparison, which has a resolution of 0.5^o x 0.5^o for land regions only (Haylock et al., 2008). The same resampling procedure is undertaken for the E-Obs precipitation data with 1000 resampled time series created for each grid cell. Due to the differences in resolution between the E-Obs grid and the larger scale GCM data a re-gridding process is required to enable comparison. It is important to note that the larger GCM resolution may have averaged over a degree of variability which may be lost prior to this comparison. Due to the limited geographical distribution of the E-Obs data (i.e. land cells only) the GCM data is re-gridded to the 0.5^o x 0.5^o grid of the E-Obs data. This was undertaken using bi-linear interpolation to interpolate the larger scale data to the finer scale. The resulting re-gridded GCM data allows an easier comparison of the GCM precipitation variability (re-gridded from Figure 4.6) with the resampled E-Obs realisations. The E-Obs precipitation variability measure is subtracted from the GCM climate variability measure for the same 0.5^o x 0.5^o grid cell with the results presented in Figure 4.7.

There is a clear underestimation of precipitation variability in the re-gridded GCMs compared to E-Obs. Each GCM displays a different bias compared to E-Obs, which is linked to its own magnitude of precipitation variability. CNRM-CM3 displays the lowest level of precipitation variability and in turn displays the greatest negative bias. Similarly MRI-CGCM2 has the highest precipitation variability and displays the smallest bias to E-Obs; and in some western regions it shows marginally greater precipitation variability. Overall the GCMs do not produce the same precipitation variability compared with the observational data. This is similar to the findings by Ruokolainen and Raisanen (2007) who compared the variability of climate model precipitation from an alternative resampling methodology with the variability of gridded observations.
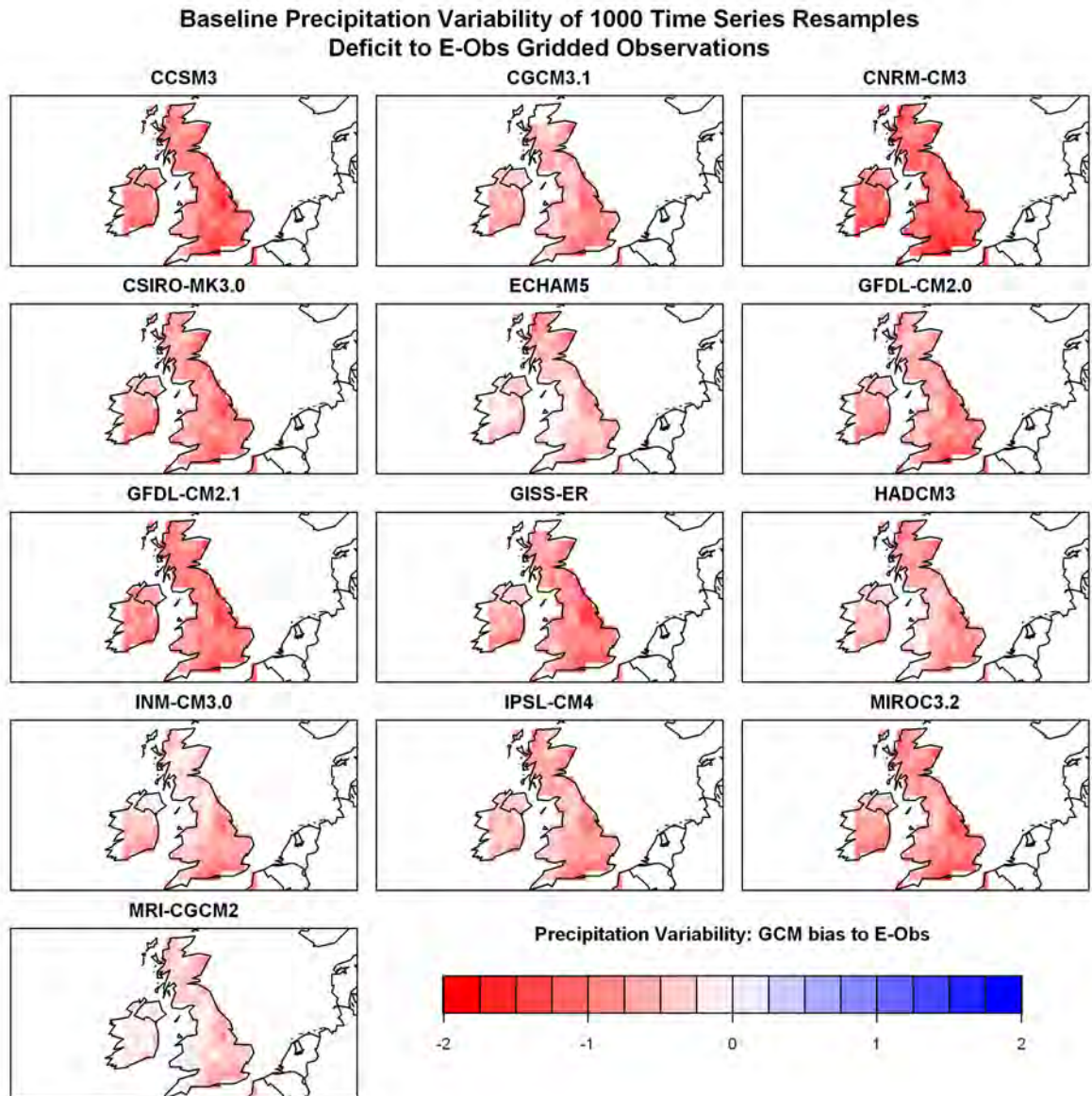
Figure 4.7 Comparison of GCM precipitation variability to observed E-Obs variability. All GCM data are re-gridded to the 0.5^o grid of E-Obs. Maps display the bias of each GCMs precipitation variability to variability of the E-Obs gridded observations.

The bias in precipitation variability does not show any strong spatial pattern, suggesting a systematic bias rather than a more complex error. Note also that the re-gridding of the GCM would not have corrected for the larger spatial resolution of the original GCM precipitation variability. However the fact that CCSM3 (highest resolution GCM) does not have the smallest bias to the E-Obs observations suggests that GCM resolution is not the only factor linked to the simulation of precipitation variability.

The analysis in this section has demonstrated that the spatial patterns of precipitation variability are relatively well produced by CMIP3 GCMs, however the range of precipitation variability varies significantly between each GCM and is low compared with that of observations. This suggests that climate models underestimate the precipitation variability of climate, perhaps linked to their inability to simulate key climatological processes. However this influences the magnitude of variability rather than its geographical distribution. The results highlight the limitations of using climate model precipitation outputs directly due to their underestimation compared with observations.

This section has outlined the use of the resampling methodology for assessing climate model precipitation simulation of an observed period. To extend the resampling methodology further it needs to be incorporated within the climate change impact study framework. This allows for the impact of climate variability to be explicitly included in a climate change impact assessment.

4.4.4 Number of Resampled Time Series

In section 4.4.3 the resampling process was repeated 1000 times to create 1000 new realisations of precipitation time series. In a climate change impact study this number of resamples might be difficult to deal with, as climate change factors calculated from 1000 baseline realisations and 1000 future realisations would result in 1,000,000 change factor scenarios (comparing all baseline and future combinations). When generating climate change factors from resampled climate time series the question of how many resampled time series are necessary to capture the full range of climate variability arises. The resampling procedure allows for the creation of an unlimited number of realisations so that impact studies are no longer limited to a few model realisations; however this may have practical consequences for impact applications that are computationally intensive. Therefore the number of new baseline and future time series created needs to be a compromise between practical but efficient climate change impact modelling whilst ensuring that the final distribution of climate change impacts represents the influence of climate variability. Considering too few time series could potentially skew a final distribution, while too many time series would increase the computational effort for little gain.

The resampling methodology is first tested for precipitation from one GCM, HadCM3, using 10, 20, 30, 40, 50 and 60 baseline and future resamples resulting in 100, 400, 900, 1600, 2500 and 3600 precipitation change factor ensembles (relative difference between all baseline and

future combinations). The distribution of the January precipitation change factor is presented in Figure 4.8 (top), showing an increase in range as the ensemble size increases. Smaller ensemble sizes (size increasing from left to right) have a more variable distribution of precipitation change, whilst larger ensembles create a more normally distributed precipitation change.

The resampling process is repeated for each resample size 100 times to evaluate the variability in the ensemble distribution of changes. These 100 distributions have been summarised using the median, 5th and 95th percentiles of the precipitation changes (Figure 4.8-middle). There is convergence of each percentiles distribution as the ensemble size increases (Figure 4.8-middle and bottom). This indicates that using a larger number of resamples provides a more consistent distribution of change which is independent from the number of resampled realisations used. Using a 60 resample set (i.e. an ensemble of 3600 change factors) would therefore provide the most robust solution, however both 40 and 50 resample sets provide relatively similar distributions. There may be a compromise solution where using 40 or 50 resamples provides a similar distribution to 60 resamples, thus reducing the resulting computational load.
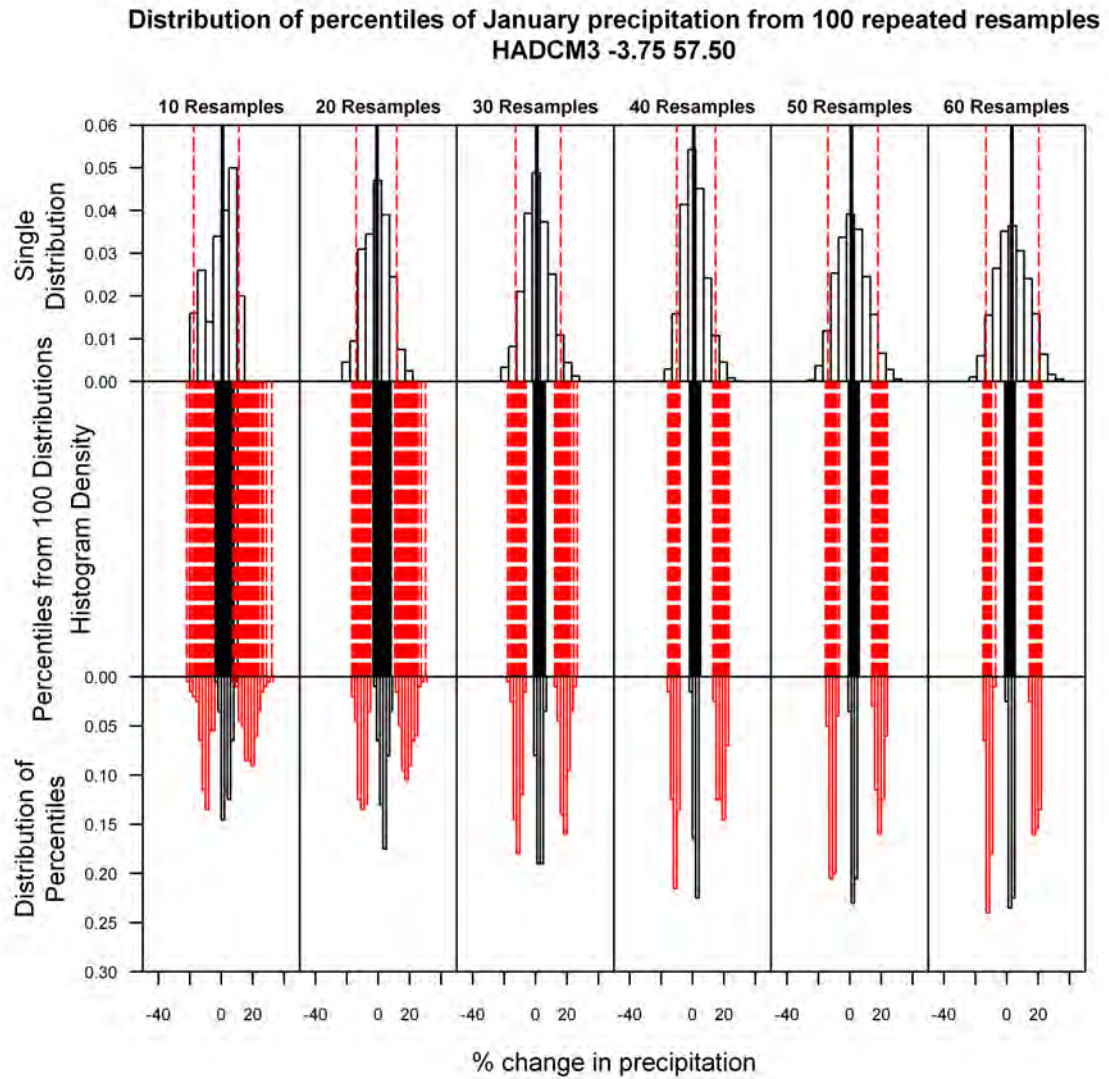
Figure 4.8 Distribution of January precipitation change factor from HadCM3 for different resample sizes from left to right (top) with the median in bold and 5th and 95th percentiles in dashed. The resampling process is repeated 100 times with the median, 5th and 95th for each of the 100 distributions plotted for the different resample sizes (middle). The distribution across the median, 5th and 95th for each different number of resamples is then calculated (bottom).
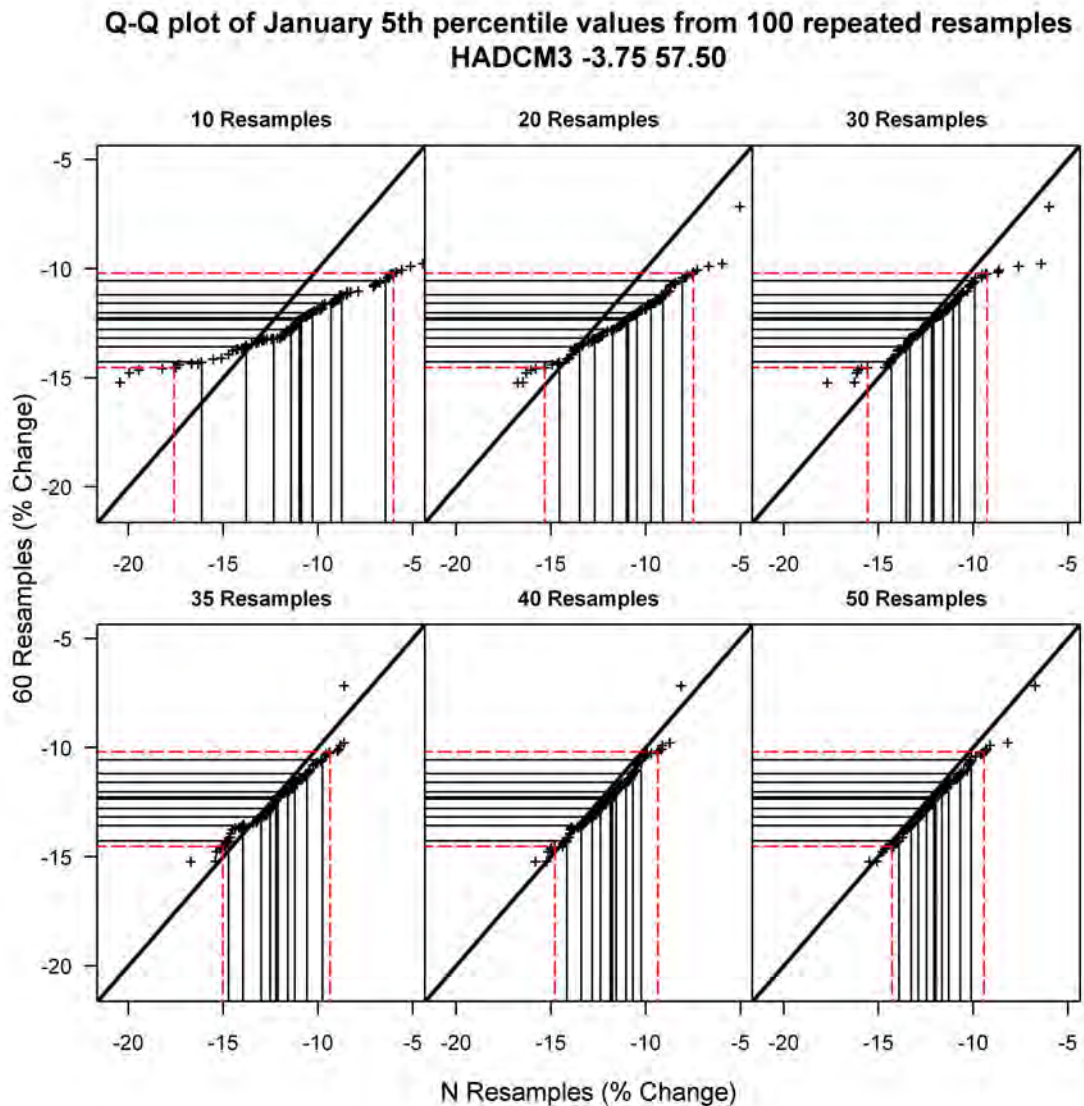
Figure 4.9 Quantile-Quantile plot for HadCM3 comparing the distribution of the 5th percentile of 100 ensembles of precipitation change from repeated resampling. Y-axis is a 60 resample ensemble and x-axis is 10, 20, 30, 35, 40, and 50 resample ensembles from left to right. Dashed lines are 5th and 95th percentiles of precipitation change distributions, with lines at 10% increments (median in bold). As distributions become similar they adopt a line similar to x=y. The transition from 35 to 40 resamples shows this trend.

An ensemble containing the combination of 60 resamples for both baseline and future provides the most consistent distribution (Figure 4.8) and is taken as reference. Q-Q plots (Figure 4.9) compare the distribution of the percentiles for each ensemble size (i.e 10, 20, 30, 40 & 50 resamples) with the reference ensemble size (60 resamples) and highlight when increasing the number of resamples adds little benefit to the distribution of precipitation changes. This occurs from 40 resamples onwards for HadCM3, with a close to one to one fit indicating the distribution from 40 resamples is similar to that produced by 60 resamples (Figure 4.9).

The same assessment was repeated for three additional GCMs (CNRM-CM3, IPSL-CM4 and MRI-CGCM2) at a range of grid cells and for different months. Both IPSL-CM4 and MRI-CGCM2 displayed similar results to HadCM3 with an acceptable minimum resample number of 40, while CNRM-CM3 displayed a lower variability with 30 resamples proving an adequate resample number. This highlights the difference in variability between GCMs, CNRM-CM3 has a lower precipitation variability compared with the other GCMs (Figure 4.6). MRI-CGCM2 was shown to have the greatest precipitation variability in section 4.4.3, suggesting that the remaining GCMs should not require more than 40 resamples to capture their variability. For a practical application and to avoid placing more or less weight on any GCM, a resample number of 40 baseline and future realisations is hence deemed sufficient to accurately represent the change factors across the different months, locations and GCMs in the UK.

4.4.5 Precipitation Change Factors

For each case study catchment and each GCM the resampling methodology described above is applied. The GCM simulation for the baseline under the 20C3M emissions scenario is used to provide a time series of 1961-1990. The period from 2070-2099 is extracted from a future time series simulated using the SRESB1 emissions scenario. Each of these 30 year time series are resampled at the monthly time step with replacement, repeated 40 times for both baseline and future time periods generating an ensemble of 1600 precipitation change factors for each GCM in the 2080s. This section presents the precipitation change factors for the Eden catchment, but similar patterns were found across all catchments.

The resampling methodology is initially applied to just a single GCM, HadCM3. The climate change signal from HadCM3 has a distinct seasonal precipitation cycle, with projected increases in precipitation between October and April followed by a decrease in precipitation across the summer months (Figure 4.10, left). Incorporating precipitation variability, by resampling a single model realisation, results in a range of possible future changes each month. The largest range, describing the largest variability in precipitation change (larger box and whiskers, Figure 4.10, right), occurs in the spring months with summer months showing the least variability in precipitation change. The seasonal cycle is maintained after resampling although in some months there is uncertainty in the direction of change. For example the median value of change for May is close to 0, indicating that climate variability could lead to either an increase or decrease in precipitation in the 2080s.

HADCM3: Precipitation Monthly Change Factors
Eden (14001) at Kemback: 2080s SRESB1
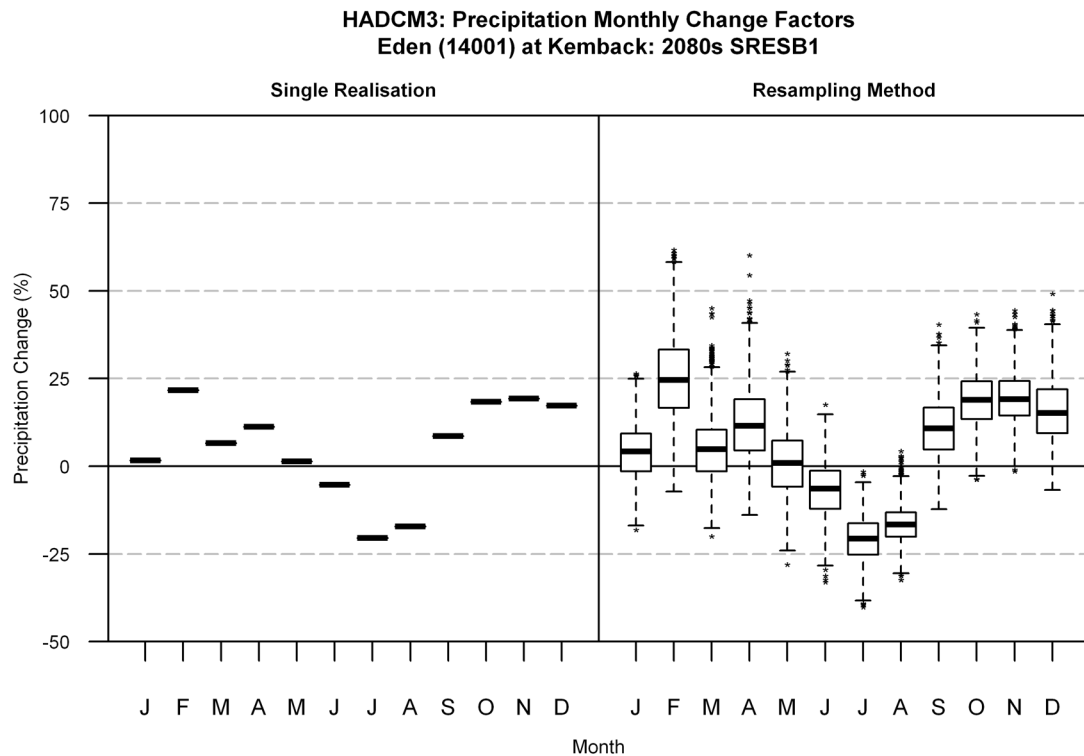
Figure 4.10 Precipitation change factors from HadCM3 for the Eden catchment. Comparison between using a single realisation (left) and the resampling methodology (right). Boxplot whiskers indicate the full data range, the box shows the quartile range with the median in bold.

The resampling is repeated for the twelve other GCMs with all thirteen GCMs combined with equal weighting to form a single climate change distribution of precipitation change factors. The multi-GCM distribution displays a range of future changes each month (Figure 4.11, right), larger than that of a single GCM (Figure 4.10, right). The multi-GCM median precipitation change has a modest seasonal cycle with higher increases in winter/spring, whilst median summer changes indicate no change. This is a weakened cycle compared with the results from just using HadCM3 (Figure 4.10). This indicates that the seasonal structure of precipitation changes given by other GCMs is different in its timing or its strength of cycle (and different to HadCM3). This is confirmed by comparing the single realisation precipitation change factors from each GCM (Figure 4.11, left). The greatest consensus of change is in autumn/winter months between September and December (Figure 4.11-Right), although the full range of variability in precipitation changes in these months could still lie between -25% and 50% thus displaying a large range of uncertainty.
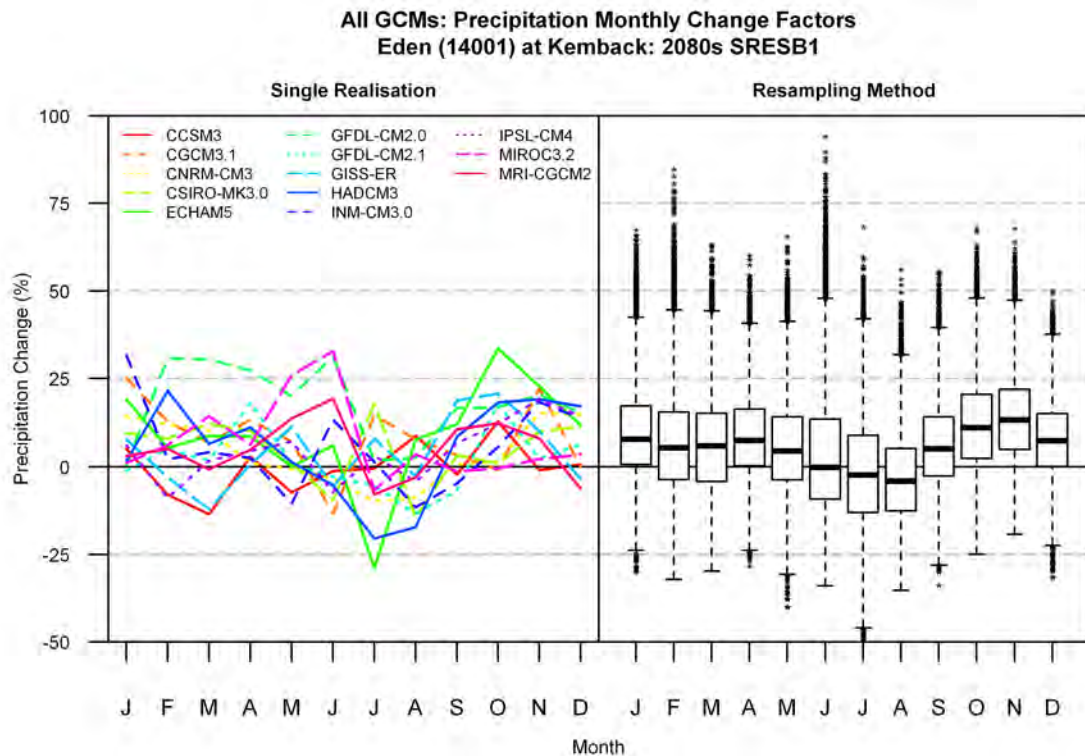
Figure 4.11 Precipitation change factors from all GCMs for the Eden catchment. Comparison between using a single realisation from 13 GCM (left) and resampling the 13 GCMs to provide 20800 scenarios (right). Boxplot whiskers indicate the full data range, the box shows the quartile range with the median in bold.

Across all nine catchments similar precipitation change factor scenarios were created covering a wide range of precipitation changes (Figure 4.12). The most notable variation between the catchments is a stronger seasonal cycle in southern UK, caused by greater summer decreases in precipitation. This strong seasonal cycle is influenced by five (CNRM-CM3, ECHAM5, GFDL-CM2.0, GFDL-CM2.1, and HadCM3) of the thirteen GCMs which all display an enhanced decrease in summer precipitation. In northern UK the seasonal cycle is only present in two GCMs (CNRM-CM3 and HadCM3) resulting in a combined change factor ensemble with a weaker seasonal cycle.

The resampling methodology has been demonstrated as being capable of creating precipitation change factors which sample a wide range of climate variability. Each GCM has been shown to have a unique temporal structure of precipitation change with differing magnitudes of variability. The combined multi-GCM ensemble indicates uncertainty in the direction of change in precipitation for each month across all catchment locations. The next section uses the multi-GCM ensemble of resampled change factors to test the sensitivity of mean river flows to precipitation change and variability.
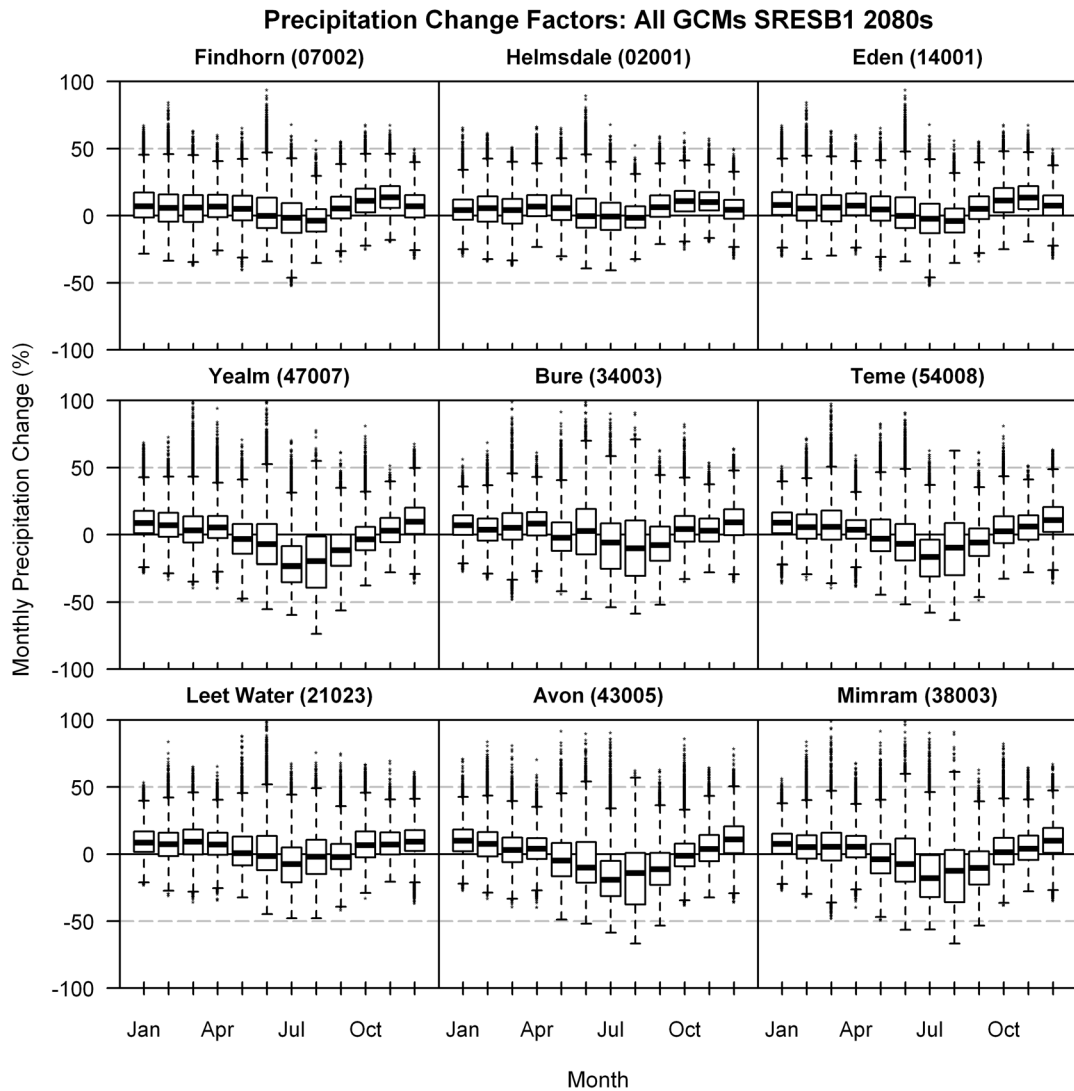
Figure 4.12 Precipitation change factors from ensemble of 13 resampled GCMs for the nine case study catchments in the 2080s.

4.4.6 Sensitivity of Mean River Flows to Precipitation Changes

The multi-GCM ensemble of resampled precipitation change factors derived for each catchment in section 4.4.5 are used to perturb the observed catchment precipitation to generate new daily precipitation time series (as outlined in Chapter 3) representative of the 2080s under an SRESB1 emissions scenario. The perturbed precipitation time series are used as input to the PDM hydrological model which results in 20,800 (13 x 40 x 40) river flow time series for each catchment. This section describes the analysis of the sensitivity of mean annual flow change in the Eden and Mimram catchments, and the mean monthly flow changes across all catchments.

Mean annual flow changes are shown in Figure 4.13 for the Eden (top) and Mimram (bottom) catchments. The left panel shows the flow change calculated from each GCMs original realisation, the middle panel is the flow change from each GCMs 1600 resampled change factors, while the right panel is a histogram of the multi-GCM ensemble of 20,800 flow changes.

The multi-GCM ensemble of mean annual flow change in the Eden catchment (Figure 4.13-top right) displays a median increase of 10%. The distribution is near normal with a long tail towards larger flow increases, it has a 5th-95th percentile range of 30%. In contrast the Mimram catchment (Figure 4.13-bottom right) has a median annual flow change close to a 0% with a total 5th-95th percentile range of ~60%, nearly double the range of the Eden.

The change from each GCM resampled individually (Figure 4.13-middle) displays a fairly consistent signal in the Eden, with increases up to 20%. The positive tail which is present in the combined ensemble (Figure 4.13-top right) is associated with a single outlying GCM (GFDL-CM2.0). In the Mimram catchment the flow changes between different GCMs display a much greater variability (Figure 4.13-bottom middle). The variability between the GCMs is linked to the stronger seasonality of precipitation change identified in section 4.4.5, with larger annual flow decreases associated with the GCMs which display a greater decrease in summer precipitation. By comparing the flow changes from the same GCMs between the Mimram and Eden, it is clear that the range of changes in the Mimram is much greater. This suggests that the Mimram catchment enhances the changes in precipitation compared with the Eden catchment and is therefore hydrologically more sensitive to precipitation changes.
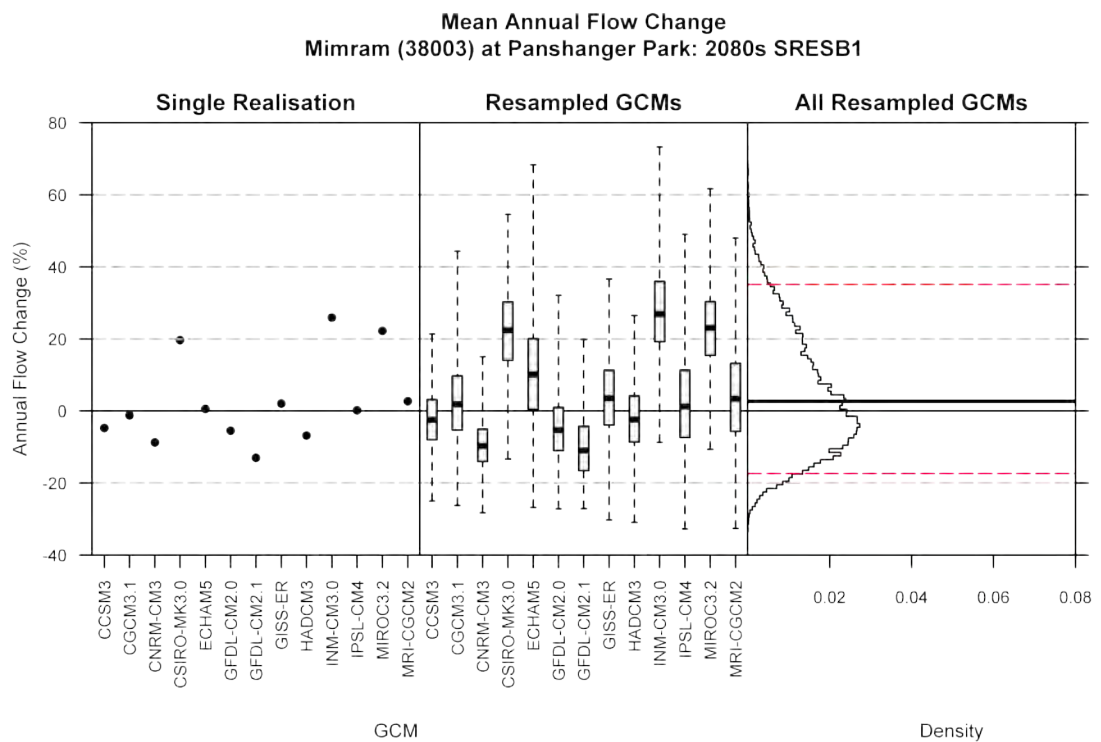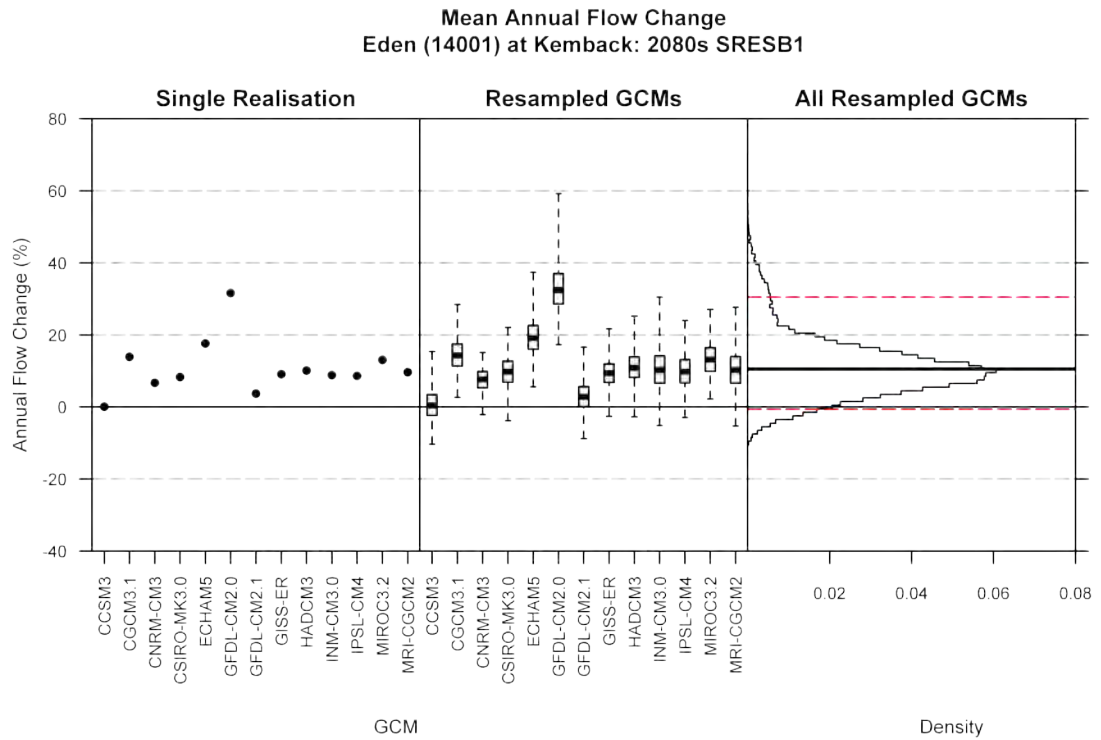
Figure 4.13 Simulated mean annual flow change in the Eden catchment (top) and Mimram catchment (bottom) in the 2080s using precipitation climate change factors derived from 13 CMIP3 GCMs. Changes are derived for each GCM from a single realisation (points-left), resampled realisations (boxplots-middle) and combined in a single distribution (histogram right). The histogram median is shown with the bold line and the 5th and 95th percentiles in dashed lines.
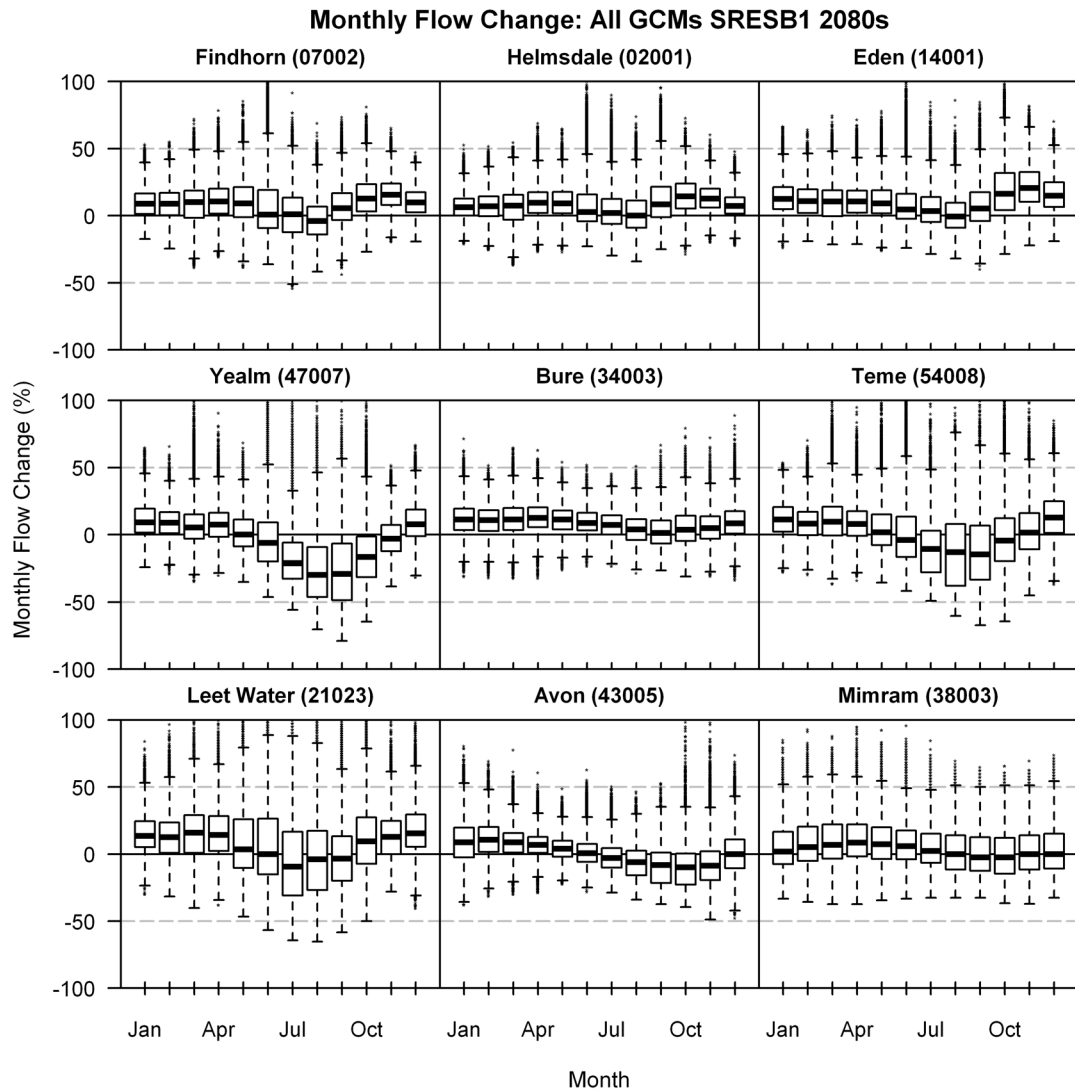
Figure 4.14 Monthly flow changes combining changes from 13 GCMs for the nine catchments in the 2080s.

The mean monthly flow changes from the multi-GCM ensemble for the nine catchments are displayed in Figure 4.14. Precipitation change and variability leads to a large range of monthly flow changes in each catchment. There is no discernible geographical pattern in the monthly flow changes, in contrast to the strength of seasonality indentified in the precipitation changes (Figure 4.12). The dominant control on a catchment's response to changes in precipitation is the physical characteristics of each catchment. The three base flow dominated catchments (Bure, Avon and Mimram) display low levels of seasonal variation. This is in contrast to the strong seasonality of the precipitation changes for these catchments. The Leet Water catchment, which has the lowest BFI of 0.34, displays a strong seasonality of flow changes. This strength of seasonality is not displayed by the other Scottish catchments

(Findhorn, Helmsdale and Eden) which all have a similar response with positive median flow changes in all months except summer where there is no overall median change in flow. The Yealm and Teme catchments have the greatest seasonal cycle of monthly flow changes, influenced by the stronger seasonality in the southern UK precipitation change factors.

It is clear that the catchment properties dictate the catchment response to the precipitation changes. The baseflow catchments are all in southern UK which has a strong seasonality in precipitation changes, but this seasonality is dampened in the flow response. The catchment properties buffer the flow response to the variable precipitation changes. In contrast the Leet Water displays a seasonal cycle which is enhanced in comparison to the precipitation changes, in this example the precipitation changes are therefore amplified in the catchment response. The remaining catchments display flow changes which are of a similar pattern and structure to the precipitation changes.

4.4.7 Sensitivity of Flood Quantiles to Precipitation Changes

For each catchment the 20,800 river flow series derived from the multi-GCM ensemble of resampled precipitation change factors are analysed using a GP distribution with POT3 sampling (section 0) to calculate changes in flood return period quantiles in the 2080s. The sensitivity of the flood regime in each catchment to changes in the magnitude and variability of precipitation is shown in Figure 4.15 for a range of return periods.

The majority of changes in flood quantiles indicate an increase in flood magnitudes in all catchments. There is evidence that flood magnitudes at larger return periods may increase by a greater proportion compared to smaller return period events in the Helmsdale, Yealm, Teme and Mimram. The remaining catchments display relatively uniform magnitude changes across all return periods with the exception of the Bure, which shows the greatest increases at smaller return periods. Typically the larger return period floods show the greatest range of future changes across all catchments, while smaller return periods typically display the smallest range of changes. The Bure, Avon and Mimram catchments provide the exception to this, where the range of changes are uniform across all return periods.
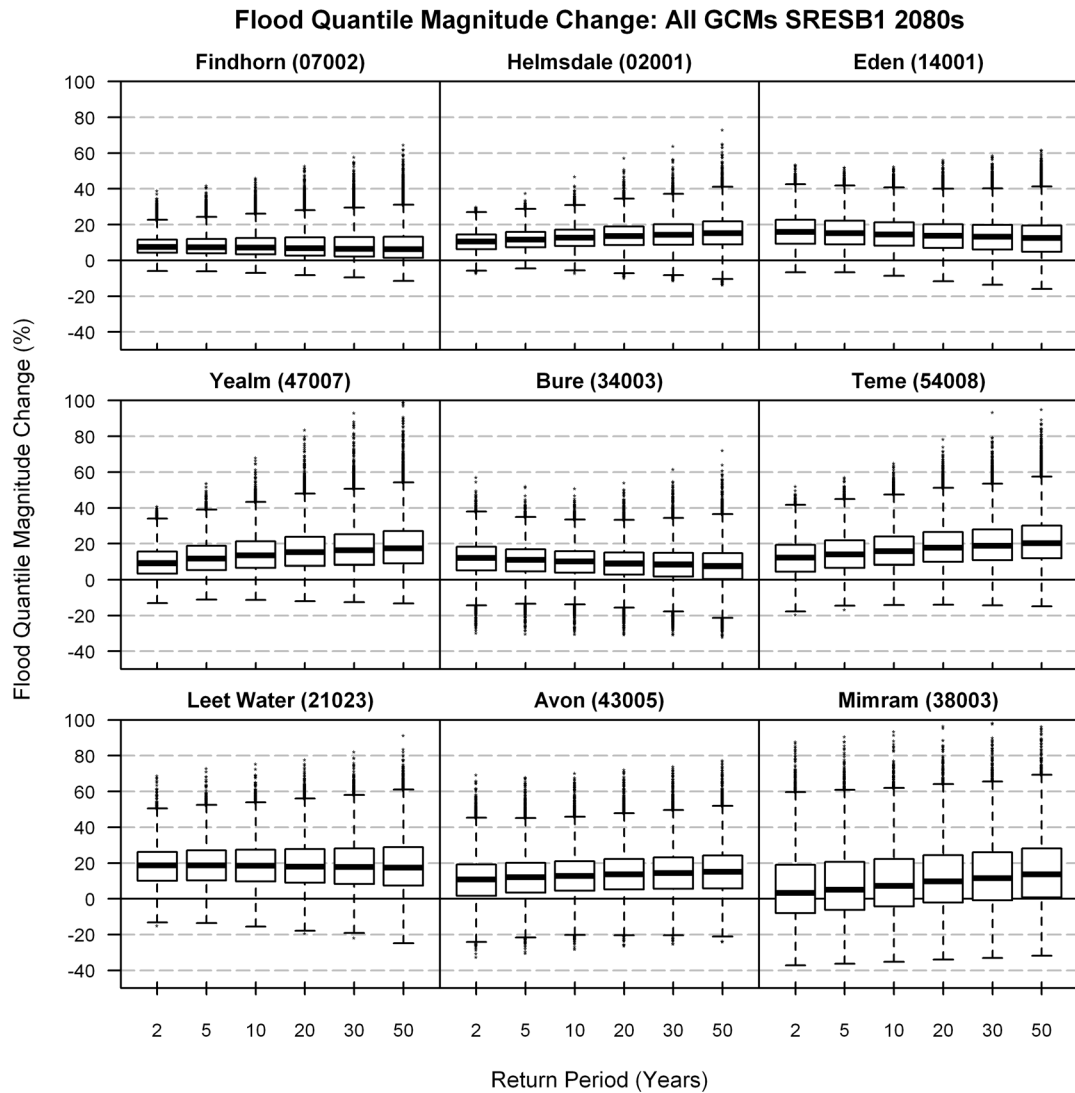
Figure 4.15 Flood return period quantile changes combining changes from 13 GCMs for the nine catchments in the 2080s

The distribution of changes in 20RP flood from the resampled multi-GCM ensemble allows for a more advanced analysis of the flood response across the nine catchments (Figure 4.16). Nearly all catchments display an increase in the 20RP flood for 95% of the distribution with the exception of the Mimram catchment which has the most sensitive flood response (largest 5th-95th percentile range). The distributions of change in flood quantile magnitudes for each catchment are mostly near-normal, although there is a degree of variability at the tails of some catchments. For example, the Findhorn catchment has a greater skew towards the lower distribution indicating a greater consensus of results in this region. This skew could be the result of variations in the mean change of each GCM (i.e. an outlying GCM) or non-linear response of the catchment.
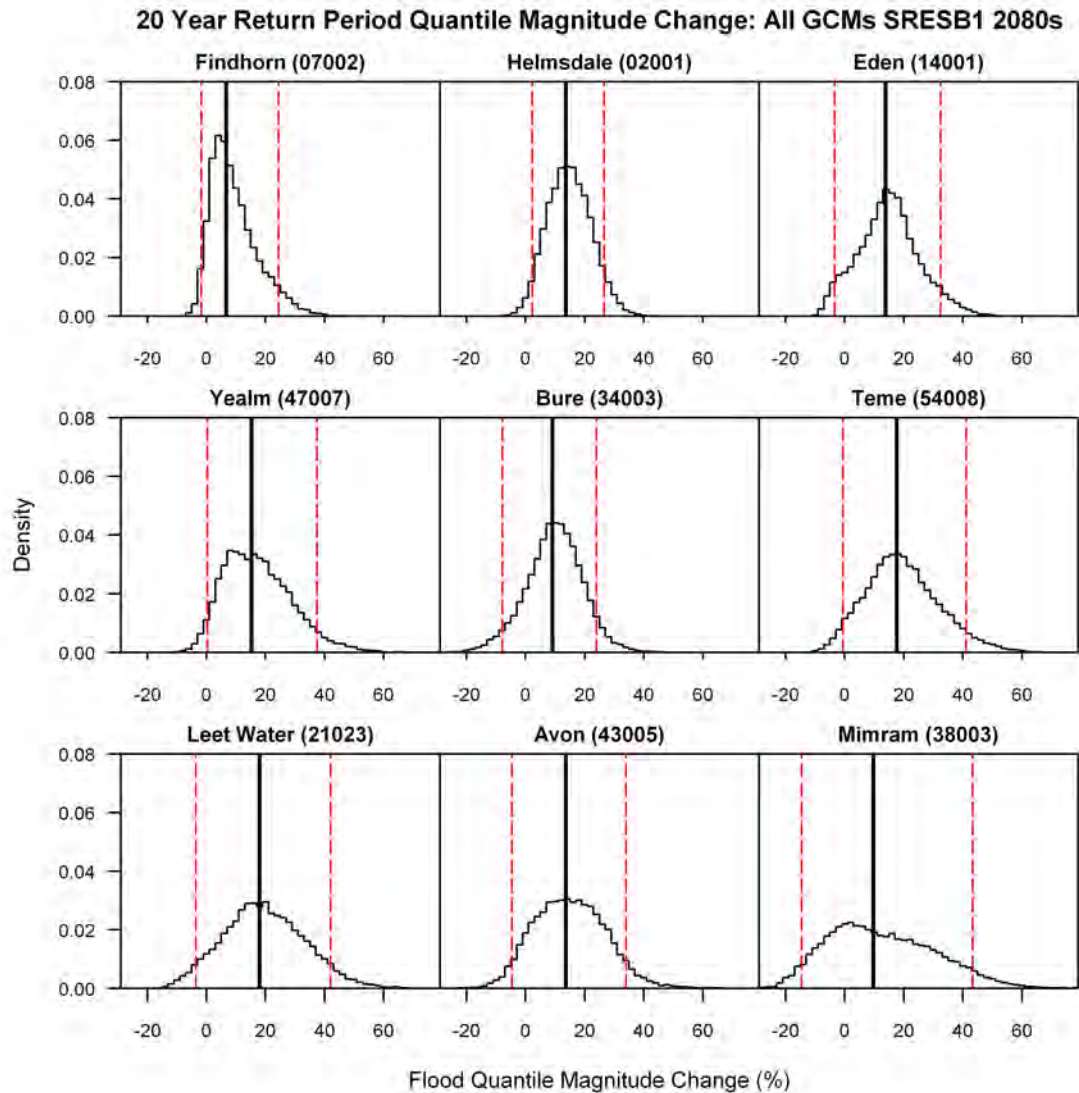
Figure 4.16 Distribution of the change in the 20 year return period flood quantile in the 2080s from the 13 resampled GCMs for the nine catchments. The median is shown with the bold line and the 5th and 95th percentiles in dashed lines.

The range of catchment flood quantile changes does not show the same connection to catchment properties as the mean flow changes. The structure of change across the different return periods (Figure 4.15) and the shape and range of change in the 20RP distribution (Figure 4.16) appear to be independent from the catchment properties. The sensitivity of each catchment response is however associated with the catchment types (section 3.2) identified by Prudhomme et al (2010).

4.5 Changing Climate Variability?

This chapter has so far highlighted the importance of understanding and incorporating climate variability in climate change impact studies, with specific focus on the role of precipitation variability. The aim of this section is to analyse whether projections of future precipitation are more or less variable than the simulated baseline precipitation. This is undertaken using the resampling methodology to separate the competing signals of climate change and climate variability.

4.5.1 Changing Variability Methodology

A single climate realisation from a GCM can be interpreted as a climatological mean plus a single scenario of climatic variability. The resampling methodology presented in this chapter can be used to separate the climatological mean from the variability. This was demonstrated for baseline precipitation in section 4.4.3, where the original model realisation was used as a reference period to calculate the departure of 1000 resampled baseline time series means. The same method can be applied to the future resampled time series, using the original GCM 2070-2099 time series as a reference. This results in two populations of anomalies around the mean climate, one population describing the baseline variability (as in section 4.4.3) and the other describing the future variability. This analysis is initially undertaken for 1000 future climate resamples in each GCM grid cell for comparison with the previous baseline analysis. However to reduce the number of PDM iterations in the analysis, the variability is also calculated for 40 baseline and future resamples which are created in section 4.4.5. The full 1000 deviations are used in the first part of section 4.5.2 for the analysis of UK wide variability, while the 40 deviations are used thereafter for the analysis of the catchment response to changing climate variability.

4.5.2 Changing UK Precipitation Variability

In section 4.4.3 each GCM baseline time series was shown to have a different degree of internal variability, with an overall pattern of greater variability in the south of the UK. The same analysis is repeated for the future time period of 2070-2099 with similar results found (not shown). To assess a change in variability, the values of precipitation variability (the standard deviation of 1000 percentage departures from a reference period) for the future are then expressed as a percentage difference compared with the baseline variability. Figure 4.17 displays the change in the variability between the baseline and future on an interpolated 0.5°

grid. The interpolation was undertaken bi-linearly to smooth out the local cell to cell variations of precipitation variability change.
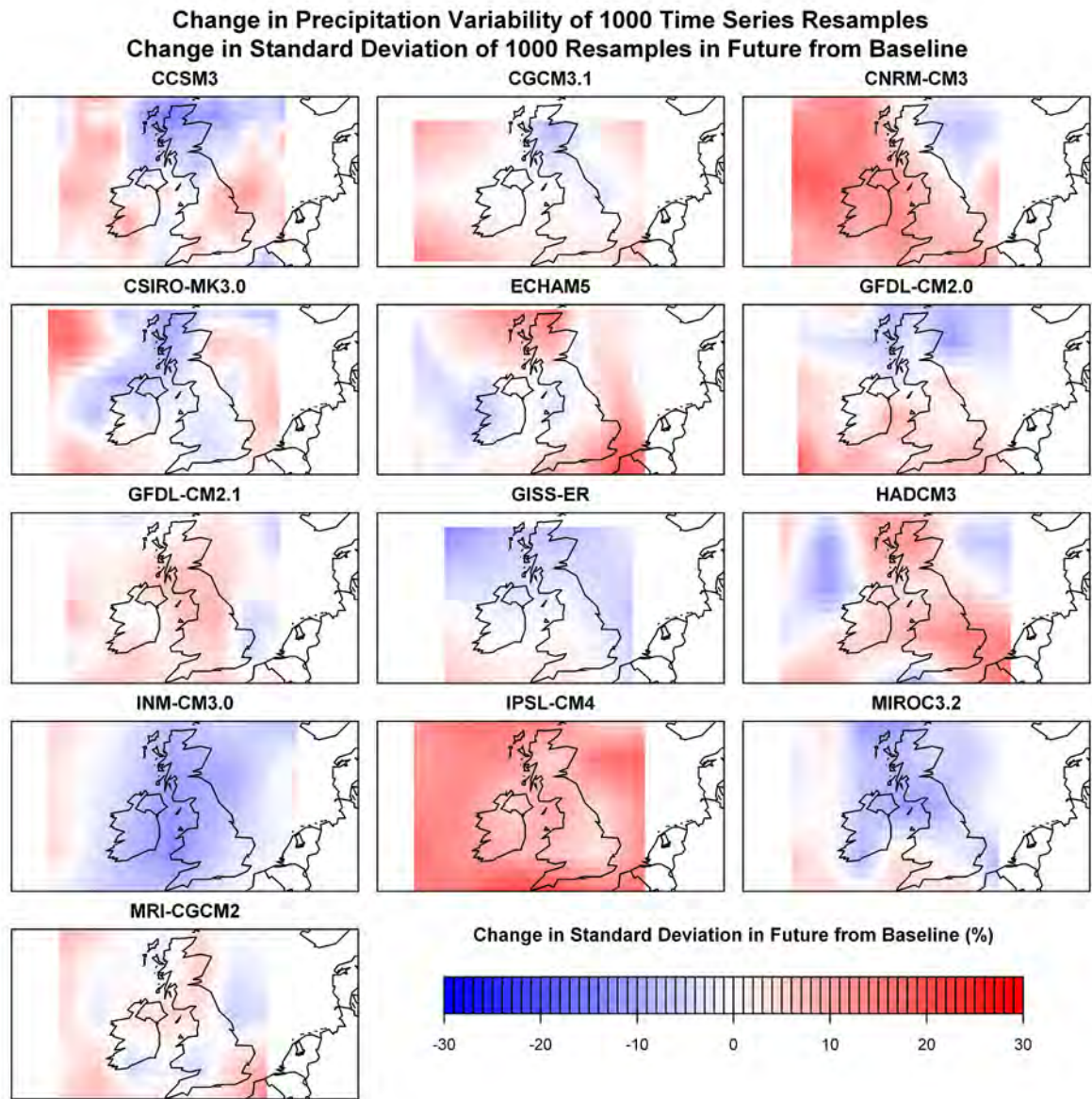
Figure 4.17 Percentage change in precipitation variability as described by the percentage difference in standard deviation of 1000 baseline (1961-1990) time series means compared with standard deviation of 1000 future (2070-2099) time series means. Original GCM data is re-gridded to 0.5^o x 0.5^o grid to smooth grid cell to grid cell variability.

Each GCM displays a different pattern of precipitation variability change although there is a consistent pattern of increasing variability in the south and a decreasing variability in the north across several GCMs (CCSMS, CGCM3.1, CNRM-CM3, CSIRO, GFDL-CM2.0). A spatially uniform increase in variability is shown by IPSL-CM4, with near spatially uniform decreases displayed by INM-CM3.0 and MIROC3.2. The GCMs with a magnitude of

precipitation variability closest to the E-Obs observations in Figure 4.7 (ECHAM5, IPSL-CM4 and MRI-CGCM2) display contrasting patterns of precipitation variability change. From Figure 4.17 there is no clear indication of a consistent signal of change in precipitation variability in the future due to the variations in the projections given by each GCM.

The precipitation variability of the 40 baseline and future GCM resamples for each catchment location are shown in Figure 4.18. Each GCMs inherent precipitation variability is again highlighted with low variability GCMs (CNRM-CM3, GFDL-CM2.1) clustering towards the bottom left corner (Figure 4.18-Left). Each GCM displays a different pattern of variability change, although there is a weak overall pattern towards a more variable future. This pattern is accentuated by ECHAM5 and if this GCM were excluded the overall pattern would be weakened. There is a north-south divide in the magnitude of precipitation variability (Figure 4.18-Right), with catchments in the north (Helmsdale (02001), Findhorn (07002), Eden (14001) and Leet Water (21023)) associated with a lower overall precipitation variability than those in the south, but there is no similar pattern for changes in precipitation variability.
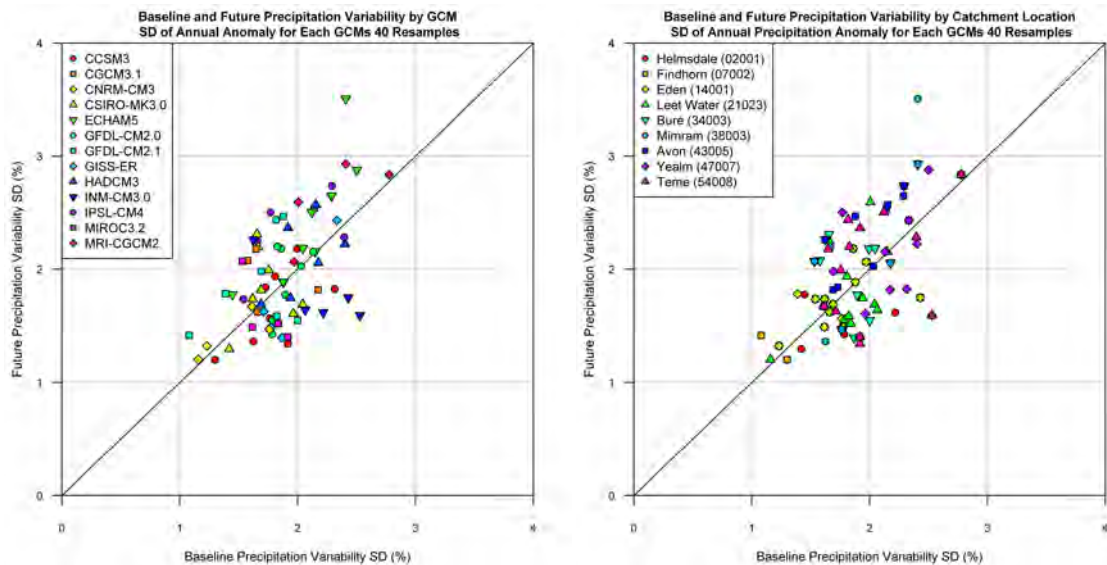
Figure 4.18 Precipitation variability of baseline (x-axis) and future (y-axis) from 40 resamples. Points are coloured according to GCM (left) and catchment location (right).

4.5.3 Changing Variability in Flood Quantiles

The monthly deviations for 40 baseline and future precipitation resamples are used to perturb the observed precipitation record similarly to climate change factors. This method creates 40 precipitation time series perturbed by the magnitude of baseline variability and 40 time series perturbed by the magnitude of future variability. The generated precipitation time series are

input to the PDM model, with 20RP values calculated from the resulting flow series to produce two distributions of flood values, one associated with the baseline precipitation variability and one associated with the future precipitation variability.

The variation in the 20RP resulting from the baseline and future precipitation variability is shown in Figure 4.19, with the standard deviation of the 20RP values from each 40 resample used to characterise the flood variability. 20RP values display an increase in variability in the future, shown by a greater proportion of increases in standard deviation. The clustering of flood variability by catchment in Figure 4.19 (right) suggests that the catchment properties are the dominant factor in translating precipitation variability to flood variability. The catchment clustering corresponds to the catchment response types in section 3.2, with the greatest level of 20RP variability associated with the most sensitive catchment, the Mimram. Furthermore there is a reduced clustering of GCMs compared with the precipitation variability (Figure 4.18-left); this can be seen in Figure 4.19 (left) where the GCM with the lowest precipitation variability, CNRM-CM3 (yellow diamonds), no longer shows the same degree of clustering as for precipitation due to the influence of each catchments properties. Within each catchment the role of GCM precipitation variability is still important, for example CNRM-CM3 generally provides the lowest variability in the 20RP flood for all catchments.
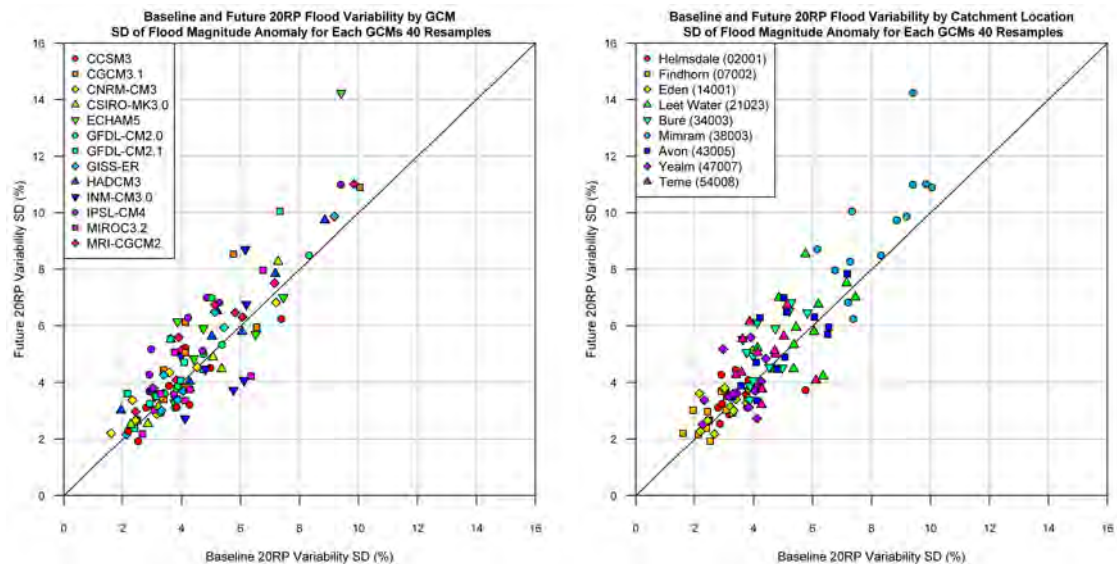
Figure 4.19 20RP variability of baseline (x-axis) and future (y-axis) from 40 resamples. Points are coloured according to GCM (left) and catchment location (right).

The propagation of precipitation variability (derived in section 4.5.2) through to the 20RP flood variability demonstrates the non-linearity in hydrological systems. Whereas the magnitude of the variability in precipitation is strongly linked to each GCM, the magnitude of variability in the flood response is mostly influenced by the catchment. Furthermore the pattern towards a greater future variability is considerably stronger in the 20RP response compared to the precipitation pattern, suggesting that the flood response may be sensitive to small variations in precipitation.

4.6 Resampling Comparison with UKCP09

The resampling methodology developed in this chapter provides a fast and simple approach to developing multi-model ensembles of climate change factors. This section compares the resampled multi-model ensembles (RMME) from the resampling methodology with the UK Climate Impacts Programme's probabilistic scenarios outlined in section 3.5.2, UKCP09.

There are a number of differences between the two sets of scenarios which should be considered before presenting the analysis. The RMME scenarios include thirteen equally weighted GCMs while UKCP09 includes eleven GCMs with a degree of weighting applied to each GCM. Despite the inclusion of eleven GCMs the UKCP09 scenarios are predominantly constructed using the Hadley Centre GCM (HadCM3) and RCM (HadRM3). The UKCP09 scenarios are at a 25km resolution compared with the range of degree scale resolutions of the 13 GCMs used in the RMME scenarios. Lastly the RMME scenarios explore the range of climate variability provided by a single GCM realisation, whereas UKCP09 includes the uncertainty from the GCM parameters as well as that of climate variability.

4.6.1 Change Factor Comparison

Both sets of precipitation change factor scenarios display a wide range of precipitation changes across all months. A comparison of the median precipitation changes for the north of the UK (Figure 4.20-Top) displays a contrasting strength of seasonality, with a stronger seasonality of change for UKCP09 compared to RMME. However the range of precipitation changes each month are of a comparable magnitude, suggesting that while the mean change of UKCP09 is not reproduced by RMME, the magnitude of precipitation variability is. In southern UK (Figure 4.20-Bottom) the seasonality of the precipitation changes is similar between UKCP09 and RMME. The ranges each month are also of a similar magnitude,

although UKCP09 displays a greater range during summer months. It is clear that the seasonal cycle is present in both methods in the south but only UKCP09 in the north.
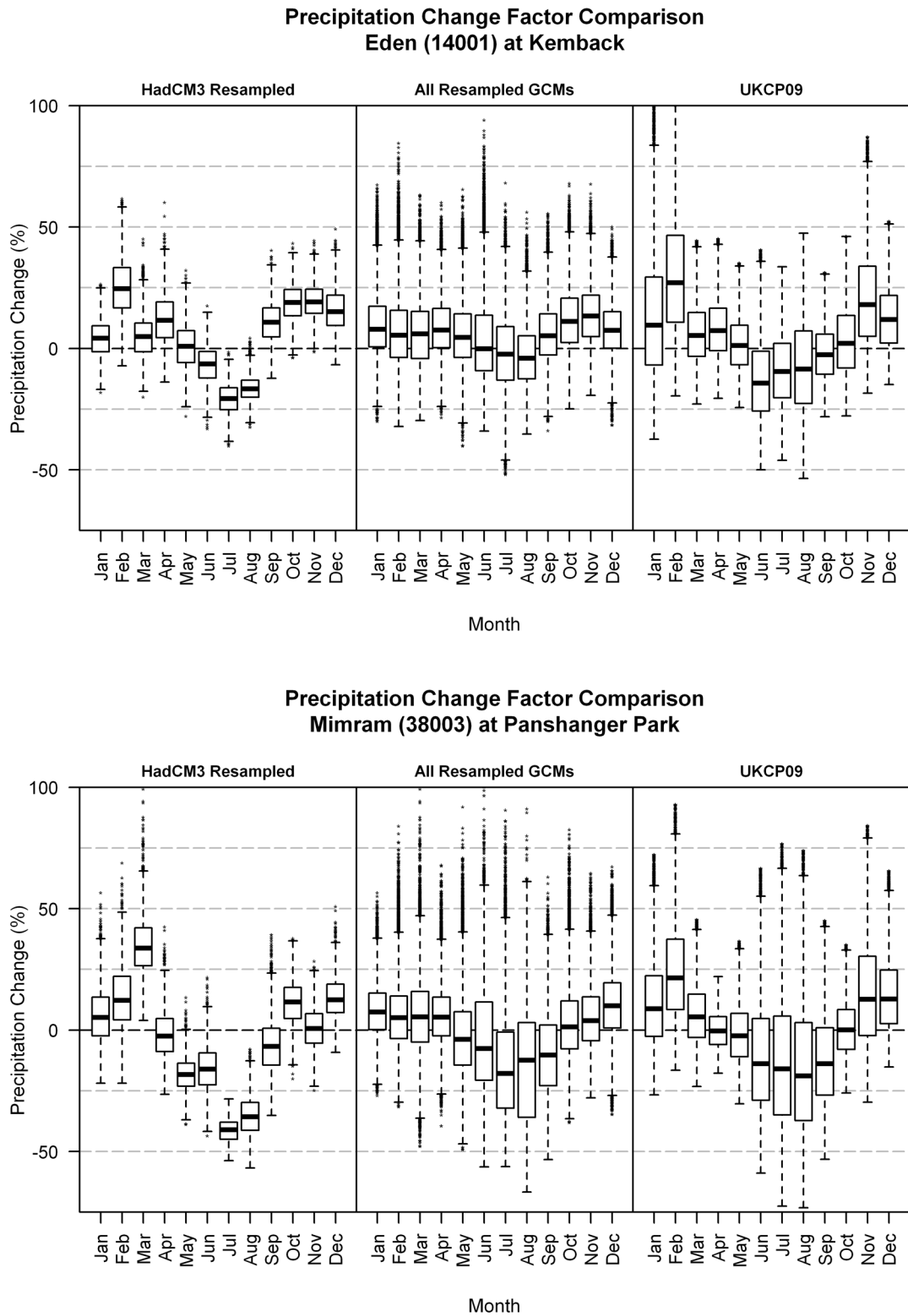
Figure 4.20 Monthly precipitation change factors from the resampled HadCM3 (left), all resampled GCMs (RMME) (middle) and UKCP09 (right) for the Eden (top) and Mimram (bottom) catchments.

One hypothesis could be that the seasonality of the UKCP09 precipitation scenarios is linked to the strong seasonality contained in the underlying HadCM3 GCM. Whereas for RMME in the northern scenarios, only two GCMs display a strong seasonal cycle (i.e. resulting in a overall weaker seasonal cycle), in the south six GCMs have a strong seasonality. This explains the north-south variation in the seasonal cycle of precipitation in the RMME scenarios. It may also suggest that the model weightings applied in UKCP09 influence the manner in which the seasonality of precipitation changes is created.

4.6.2 20RP Flood Comparison

In contrast to the precipitation changes, where UKCP09 and RMME produce similar ranges of change, the UKCP09 20RP changes display a much greater range compared with the 20RP changes from RMME (Figure 4.21). The difference varies between catchments; some display minor deviations (Findhorn, Teme), while others have very different response (Yealm, Avon). The greatest differences occur at the 95th percentile of 20RP changes with UKCP09 projecting significantly larger increases in flood magnitudes compared with RMME. At the 5th percentile, which typically describes small decreases in the 20RP, both UKCP09 and the RMME indicate similar magnitude changes in flood peaks across all catchments.

The boxplots in Figure 4.20 do not show the individual monthly precipitation change factor sets from UKCP09 and RMME. For the individual change factor sets there is large difference in the month to month variability of the UKCP09 change factors compared to RMME, which typically maintains the seasonal structure of precipitation changes in each GCM. This greater variability in the UKCP09 scenarios may result in an increased range of potential changes in the 20RP flood. This provides further evidence that the catchments flood response may be sensitive to small variations in the precipitation changes as identified in section 4.5.3.
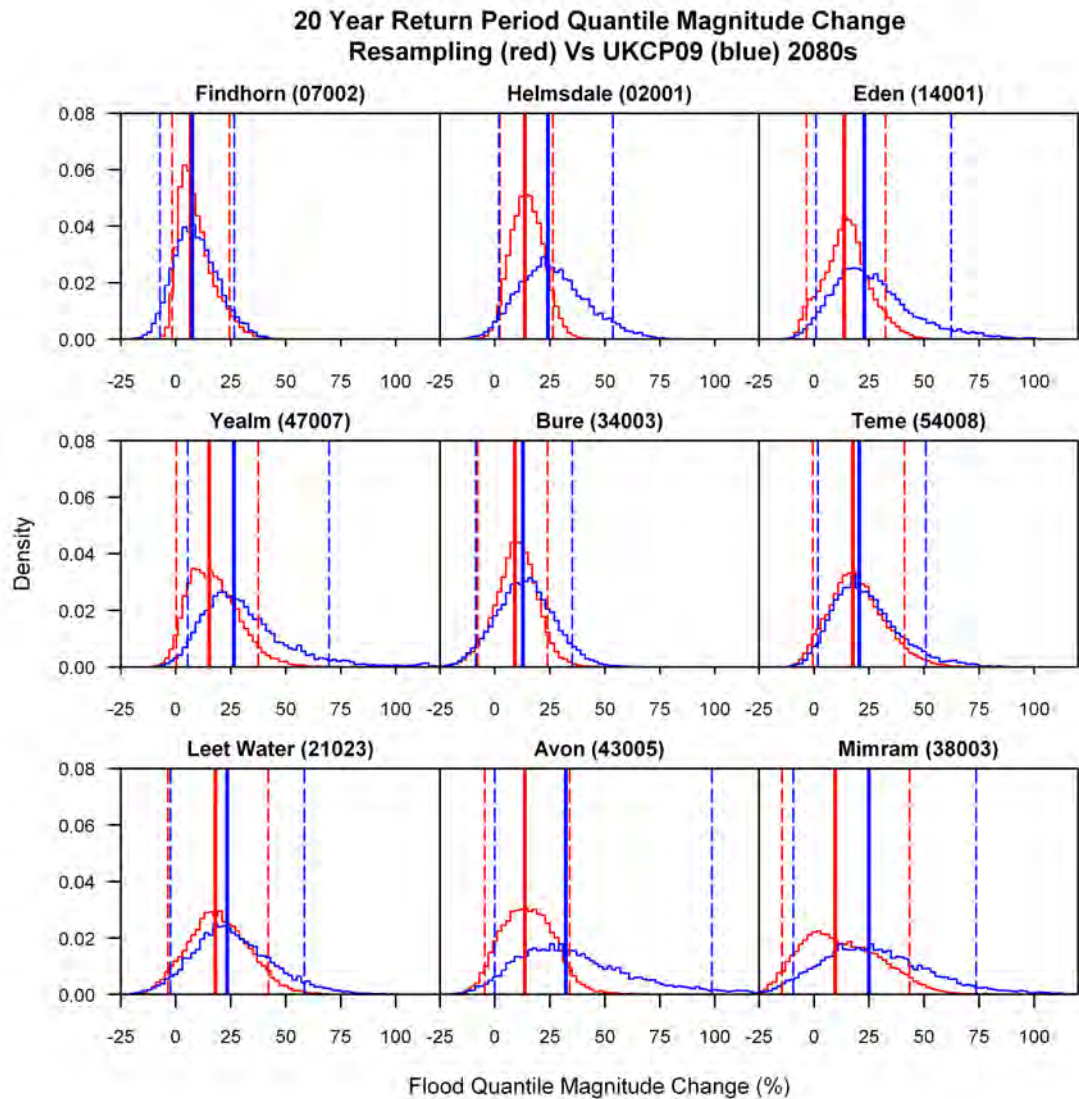
Figure 4.21 Comparison of the change in the 20RP flood in the nine catchments from applying the resampling methodology (RMME) to 13 GCMs (red) and using UKCP09 (blue) change factors. Dashed lines are for the 5th and 95th percentiles with the median in bold.

4.7 Discussion and Conclusions

Climate variability has been shown to play an important role when creating climate change scenarios. Section 4.3 demonstrates the importance of precipitation variability within the climate change signal, whereby climate variability could change the overall direction of a calculated climate changes. From this it is clear that using a single or small number of climate projections may lead to the misrepresentation of climate change combined with climate variability. Typically the inclusion of climate variability is limited through the availability of only a few GCM model realisations. To overcome this issue a simple resampling

methodology has been developed which creates ensembles of climate change scenarios from a single GCM realisation.

One of the main assumptions in how the resampling methodology has been implemented here is the independence of monthly precipitation, as identified for the UK. In different climatic regions this assumption may not be valid. For instance in a monsoon climate once the monsoon starts, it could not be stopped and then restarted again. As well as the influence of location, analysing a different climate variable could require a different resampling strategy (e.g. temperature). The methodology provides the opportunity to account for these factors as well as incorporating multiple variables through altering the resampling strategy. The temporal time step of the resampling is dictated by the highest temporal level of correlation for all the considered variables. For example, if including both precipitation and temperature simultaneously, the resampling of both variables may be undertaken for seasonal blocks due to the stronger month to month correlation of temperature compared with precipitation. In light of this the resampling methodology allows for multivariate, spatially coherent and temporally coherent scenarios to be created through applying the same resampling procedure simultaneously to all variables and locations of interest.

The resampling methodology can be applied to any number of GCMs and used individually or combined in a multi GCM ensemble (as performed here). The importance of using a large number of GCMs is demonstrated as each GCM has been shown to have a different spatial distribution of climatic (precipitation) variability as well as differing magnitudes of variability. Despite the variations between each GCM there is a pattern across the GCMs for a greater precipitation variability in the south of the UK compared with the north for simulations of the baseline climate (1961-1990). For the future time horizon a similar spatial pattern of precipitation variability remains while there is no clear indication of any magnitude change or spatial pattern change in precipitation variability in the future.

The resampling methodology in this chapter is shown to be a powerful, efficient tool in quickly developing multi-model ensemble projections based on climate variability, when no multi-ensemble probabilistic projections are available. Through a comparison with the full probabilistic UKCP09 projections the resampling methodology is shown to create precipitation changes which lie within the plausible range of UKCP09. Despite the similar range of precipitation changes, UKCP09 provides a greater range of changes in future flood magnitudes compared with the RMME. Due to the greater range of precipitation and flood

magnitude changes provided, the UKCP09 climate change projections are used in the rest of this thesis. This provides the advantage of reducing the number of climate scenarios that need to be considered, 10,000 as opposed to 20,800, while exploring a wider range of potential climate change impacts.

4.8 Chapter Summary

This chapter has explored the role of climate (and in particular precipitation) variability in climate change impact studies on flood flows. Climate variability is particularly important when expressing future changes relative to a baseline period where the magnitude or direction of change may vary depending on the magnitude of climate variability. To address the issue of climate variability when only a few climate model realisations are available, a simple resampling methodology has been developed. The methodology involves the resampling of GCM precipitation at the monthly time step to create 40 baseline and 40 future resampled time series. The use of 40 baseline and future resamples provides a robust compromise in creating 1600 precipitation change factors. The resampling methodology has been applied to the precipitation outputs from 13 GCMs, creating 20,800 change factor scenarios, and applied to nine UK catchments.

The GCM derived precipitation variability was shown to vary across the UK, with a greater (lesser) variability shown in the south (north) of the UK. The resampling increased the range of potential changes in precipitation each month whilst maintaining each GCM's seasonality. The impact on flood quantiles was typically for an increase in flood magnitudes in each catchment at all return periods although in a minority of cases climate variability may lead to small decreases. The methodology was used to identify whether a future climate may have more or less variable monthly precipitation than at present. Each GCM displayed a very different pattern with no clear signal of a change in precipitation variability, however the response in terms of change in the 20RP flood did show signs of becoming more variable in the future.

The role of the catchment properties was found to be important in propagating precipitation changes to river flow changes. In the case of mean flows the non-linear transformation of precipitation changes was found to be associated with a catchments physical properties (i.e. BFI). For flood flows the catchment response types were shown to have the greatest connection with the catchment flood response.

The RMME scenarios from the resampling methodology were then compared with the UKCP09 probabilistic climate change scenarios. The range of precipitation change factors were shown to be similar for both ensembles although UKCP09 displayed a stronger seasonal cycle in precipitation change, particularly in northern UK. The derived 20RP changes typically have a larger range when UKCP09 scenarios are used, compared with the RMME scenarios. As a result the UKCP09 scenarios are used during the rest of this thesis to explore the greatest possible range of future flood projections.

The following chapter addresses the next component in the impact study framework, hydrological modelling, the role of the model calibration and model parameters and how the model parameters influence a catchment's flood response to climate change.

CHAPTER 5

Hydrological Model Parameter Uncertainty

5.1 Introduction

In the previous chapter hydrological simulation was undertaken using single parameter sets for each catchment which were calibrated as described in Chapter 3. Using model parameters sets in this way assumes that the single model setup is 'correct' and does not take into account the uncertainty surrounding model calibration and parameterisation; described in part as equifinality (Beven, 2006). Further to this, the same model parameter sets were used for the baseline and future simulation periods, underpinned by an assumption of parameter stationarity. This is a widely used assumption in hydrological applications due to the lack of an evidence based alternative, however this assumption of parameter stationarity may not be valid for all catchments (Niel et al., 2003). The primary aim of this chapter is to identify whether the use of a given set of hydrological model parameters in a climate change impact study influences the magnitude of change for a given flood return period quantile. In light of this there are two stages in this chapter which contribute towards the primary aim; firstly to produce a number of model parameter sets which are considered equally valid, and secondly to identify how these parameter sets cause sensitivity in the flood response to different climate change scenarios. The development of an automatic calibration procedure for flood simulation is described in section 5.2, with the sensitivity of the parameters to climate change tested in section 5.3. The chapter closes with a discussion (section 5.4) and summary (section 5.5).

5.2 Automatic Model Calibration for Flooding

5.2.1 Monte Carlo Simulation

Monte Carlo simulation is a widely used technique to sample within the range of a defined uncertainty space. For hydrological modelling applications this involves randomly selecting parameter values from within a defined parameter range to create multiple model parameter sets. The hydrological simulation of each parameter set is assessed using an objective function describing its performance. The method is beneficial in a hydrological calibration context as it allows for certain parameters to display a range of identifiability (Uhlenbrook et al., 1999, Wilby, 2005), which describes the values of a given parameter which are shown to offer good hydrological simulation for a given catchment. The Monte Carlo procedure requires the sample space to be defined by the user for each parameter (i.e. the minimum and maximum parameter values to search between); the parameters which are used in the Monte Carlo analysis are outlined in the following paragraph.

The PDM version used so far and outlined in section 3.3 has nine parameters, three of which (C_{max}, K_1, and K_b) were originally calibrated by hydrological simulation, while the remaining six were estimated or set at fixed values (by expert judgement or empirically). In this method the b parameter (controlling catchment storage distribution) was fixed as a regional estimate; however by fixing the b parameter, the value of the calibrated C_{max} parameter (defining the maximum storage depth) is constrained to a small range due to parameter interdependence in PDM. The b_e parameter (describing the ratio of actual to potential evaporation) is also set at a regional value but is known to be sensitive in some catchments (i.e. the Mimram catchment (Crooks et al., 2010)), in which case a fixed value may constrain model simulation. Therefore to fully explore the issue of equifinality in this automatic calibration the b and b_e parameters are included in the Monte Carlo simulations as well as the three other previously calibrated parameters; C_{max}, K_1, and K_b. The routing partition parameter α is fixed at the previous estimated value, using BFI HOST, due to the physical reasoning in its estimation. The f_c and C_{min} parameters are again fixed at 1 and 0 respectively as they can be treated as constants.

The Monte Carlo parameter sampling is undertaken for all five parameters simultaneously, allowing their values to co-vary. The sample ranges are the same for each catchment and are pre-defined for each parameter based on plausible ranges which are assumed to be uniformly distributed. The simultaneous sampling is repeated 10,000 times for each catchment with all 10,000 generated parameter sets used to drive PDM for the period of observational record.

The resulting flow time series are analysed using three objective metrics, NS_{daily}, NS_{30day} and V_{err} (as outlined in section 3.3), which describe the performance of a given parameter set compared to the observed flow time series.
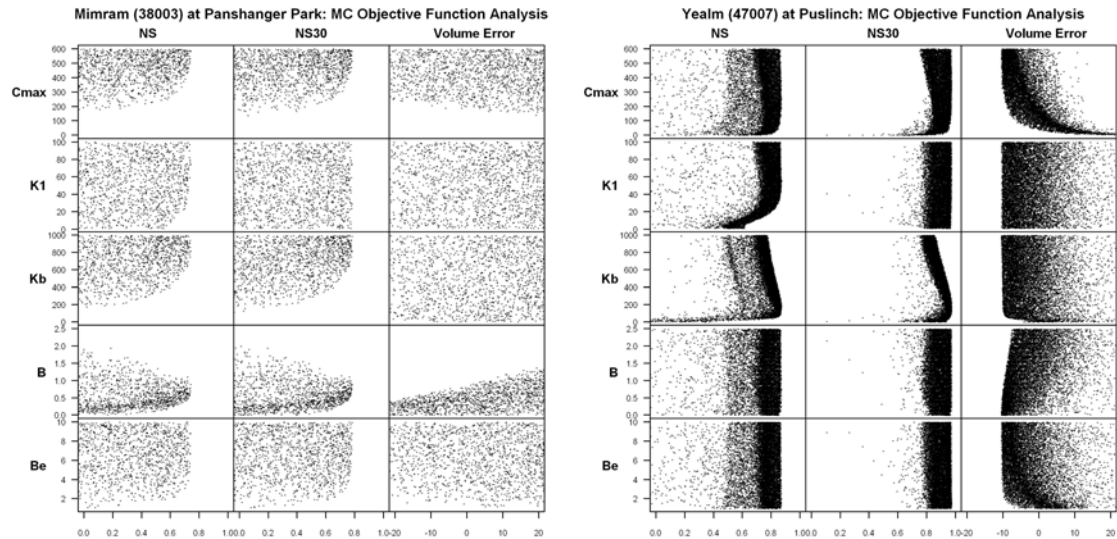
Figure 5.1 PDM Monte Carlo parameter simulation for the Mimram (left) and Yealm (right). Cross comparison of five varied parameters (y-axis) and three objective functions (x-axis). Note that x-axes limits are clipped to NS values > 0 and V_{err} values ± 20%.

The results vary between catchments but can be broadly generalised between catchments with higher and lower BFIs, described herein using the Mimram (higher BFI) and Yealm (lower BFI) catchments (Figure 5.1). The Mimram displays a low overall proportion of parameter sets which provide good objective function values. This can be seen in Figure 5.1 by the lower density of points in the parameter plots compared with the Yealm (note the clipped axes to 'reasonable' objective function values). The Mimram displays good identifiability for minimum values of C_{max} and K_b reflecting the need for higher values of storage and baseflow routing which confirm the baseflow dominant nature of the catchment. This is also reflected in the values of b which obtain their best values of NS_{daily} and NS_{30day} as b tends towards 0.5 (i.e. a higher proportion of deep to shallow stores). The K_1 and b_e parameters do not display strong identifiability based on the objective metrics used here (i.e. the best model performance can be obtained from a wide range of parameter values). This makes physical sense for the K_1 parameter in baseflow catchments due to the low quickflow contribution to flow simulation (as dictated by α). Notably b_e values less than 2 have a lower NS_{daily} and NS_{30day} compared with values greater than 2, which indicates a high actual evaporation rate is required. The Yealm catchment has a high proportion of parameter sets which provide good

objective metrics, with dense areas of the plots in Figure 5.1 (right). C_{max}, K_1 and K_b all show a degree of identifiability when compared with V_{err}, NS_{daily} and NS_{30day} respectively, although good objective metric values can be obtained by wide ranges of parameter values. The b and b_e parameters do not show any particular relationship with the objective metrics.

The results in the Yealm and Mimram highlight that by comparing a given parameter with each objective metric different relationships exist between them (e.g. V_{err} can describe the performance of C_{max} but not K_1). The strength and manner of these relationships vary between catchments so it is therefore important to include a number of different metrics to aid in model calibration due to the inter-relationship between different parameters and metrics. The Monte Carlo simulations have provided a number of good model simulations for each catchment as assessed by the different metrics independently. However the independent analysis of each metric means a parameter set may provide a good NS_{daily}, but a poor V_{err}. Assessing which parameter sets are deemed to be acceptable across all three metrics is less straight forward and is discussed in the next section.

5.2.2 Multi-Objective Selection

An acceptable parameter set is typically determined using a user selected metric to conform to an objective function (i.e. Nash Sutcliffe $\rightarrow$ 1, Volume Error $\rightarrow$ 0). If the aim is to calibrate the model to obtain a single set of parameters the accepted parameters will be the parameter set which provides the best values of objective functions (typically with an added user judgement). If there are more than one or two objective functions, deciding which parameter sets are better than others becomes increasingly difficult to define. This can lead to each objective function being used independently as has been applied in the calibrated PDM used so far in this thesis, where each calibrated parameter is assessed against a different objective function (section 3.3.3). To obtain a number of acceptable parameter sets through Monte Carlo simulation the objective functions cannot be assessed independently. An alternative would be to set a threshold value for each objective function (e.g. $NS_{daily} > 0.5$, $V_{err} < \pm5\%$) and select all parameter sets that reach these defined thresholds. However such thresholds are subjective to the user and their values would vary significantly between catchments (see Table 3.4 for variations between calibrated catchment objective function). Furthermore prior analysis and knowledge of each catchment would be required which is not desirable or in some cases possible in an automatic calibration procedure. To overcome this, the multiple objective functions need to be self selecting. This problem of multi-objective

selection has been addressed in the field of multi-objective optimisation whereby a computational algorithm is used to find an optimum solution to multiple objective functions. In the example of hydrological modelling, the algorithm would alter the model parameters to obtain the best possible values of NS and V_{err}. Such techniques have been successfully used for hydrological model calibration (Shafii and De Smedt, 2009, Zhang et al., 2010); however the aim here is to obtain a number of acceptable parameter sets rather than a single optimum solution. The derivation of a single solution would contradict the issue of equifinality being addressed. The requirement here is to use the self-selection component of the computational algorithm, prior to the optimisation process to obtain a number of self selecting parameter sets.

The non-dominated sorting technique (Deb et al., 2002) for multi-objective selection prior to an optimisation procedure is applied here. Non-dominated sorting allows the best performing Monte Carlo simulations, assessed using NS_{daily}, NS_{30day} and V_{err}, to be naturally sorted in ranks. Ranks are assigned through a domination test, where one simulation is dominant over another simulation if it outperforms it based on at least one of the three objective functions, while the remaining two objective functions must be of at least equal performance. Initially all 10,000 Monte Carlo simulations are compared with one another; the simulations which are not dominated by any other simulation are assigned a rank of 1 and removed from the population. The ranking process is repeated for the remaining simulations with the next non-dominated solutions assigned a rank of 2 and removed from the population, with the process repeated until all simulations have been assigned a rank. Example results are shown in Figure 5.2 for NS_{daily} and V_{err} in the Yealm catchment. Results can be seen to cluster at the greatest NS_{daily} values which correspond to V_{err} close to 0. To select a number of acceptable parameter sets from within these results the non-dominated rank associated with a minimum of 50 parameter sets are selected (i.e. at least the top 0.5%).

Example of Non-Dominated Sorting in the Yealm (47007) Catchment

● Rank 1 □ Rank 2 ◇ Rank 3 ▲ Rank 4 ▼ Rank 5
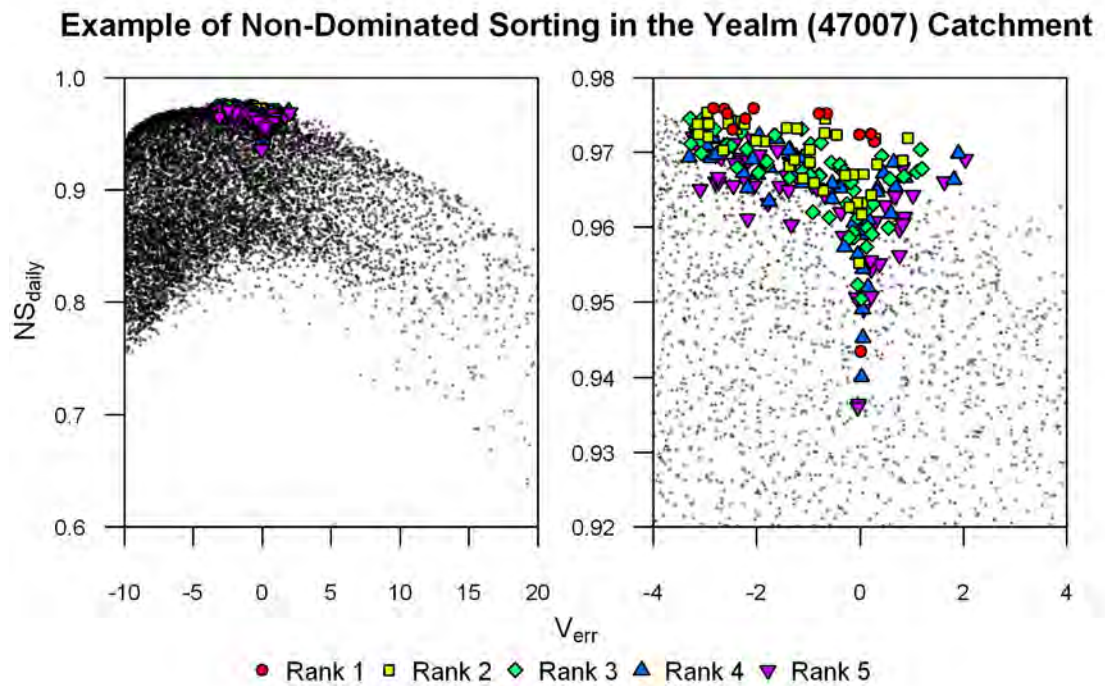
Figure 5.2 Non-Dominated sorting in the Yealm catchment. The values of V_{err} (x-axis) and NS_{daily} (y-axis) are highlighted with respect to the total population (left) and local values (right).

Table 5.1 Non-dominated sorting results for all catchments.

NRFA Gauge	Non-Dominated Rank	No of Parameter Sets
Findhorn (07002)	2	87
Helmsdale (02001)	2	58
Eden (14001)	3	64
Yealm (47007)	3	104
Bure (34003)	3	58
Teme (54008)	3	69
Leet Water (21023)	3	53
Avon (43005)	3	71
Mimram (38003)	4	51

The non-dominated sorting provides a different number of acceptable parameter sets in each catchment with an associated non-dominating rank (Table 5.1). The non-dominated rank in each catchment indicates the degree of sensitivity of that catchment to the Monte Carlo model calibration procedure. For catchments with a low rank (e.g. the Findhorn and Helmsdale) it is easier to find an acceptable parameter set compared with the catchments with a higher rank

(e.g. the Mimram). The Mimram displays the greatest sensitivity to the Monte Carlo sampling with 51 parameter sets provided at rank 4, corroborating with the low density of points for the Mimram in Figure 5.1.

The accepted parameter sets are overlaid over the total sample population in Figure 5.3 for the Mimram and Yealm catchments. The Yealm catchment (right) displays good identifiability for the K_b parameter and limited identifiability for the K_1 parameter. The b and C_{max} parameter both display broad accepted ranges, likely due to their interdependence, where a high value of C_{max} can be counteracted with a low value of b and vice versa. This situation is more likely to occur in catchments with a lower BFI due to the decreased importance (and hence lower identifiability) of catchment storage components in model simulation. In contrast to the Yealm, the Mimram catchment has good identifiability of b, C_{max} and K_b which reflect the baseflow nature of the catchment. The K_1 parameter has a wide range of acceptable values, due to its reduced importance, caused by only a limited proportion of runoff being routed through the quick flow store as dictated by the fixed α parameter.
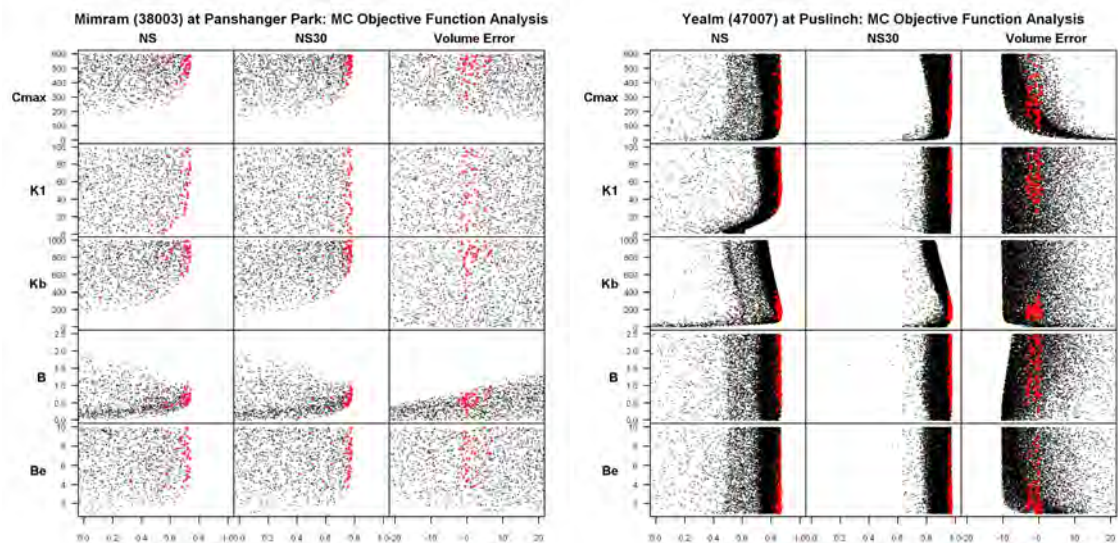
Figure 5.3 PDM Monte Carlo parameter simulation for the Mimram (left) and Yealm (right). Cross comparison of five varied parameters (y-axis) and three objective functions (x-axis). Accepted parameter sets are overlaid as red points. Note that x-axes limits are clipped to NS values > 0 and V_{err} values ± 20%.

Objective functions provide an initial performance measure of hydrological simulation; however they should not be solely relied on without consideration of the direct hydrological model outputs. The mean monthly flows for the full 10,000 Monte Carlo simulations (left) and for those selected by the non-dominated sorting (right) for the Mimram and Yealm

catchments are shown in Figure 5.4. The accepted parameter sets (right panels) provide a good simulation of mean monthly flows compared with the observations (red points) demonstrating that the non-dominated sorting provides a suitable method for selecting acceptable parameter sets from the full 10,000 Monte Carlo simulations (left panels).
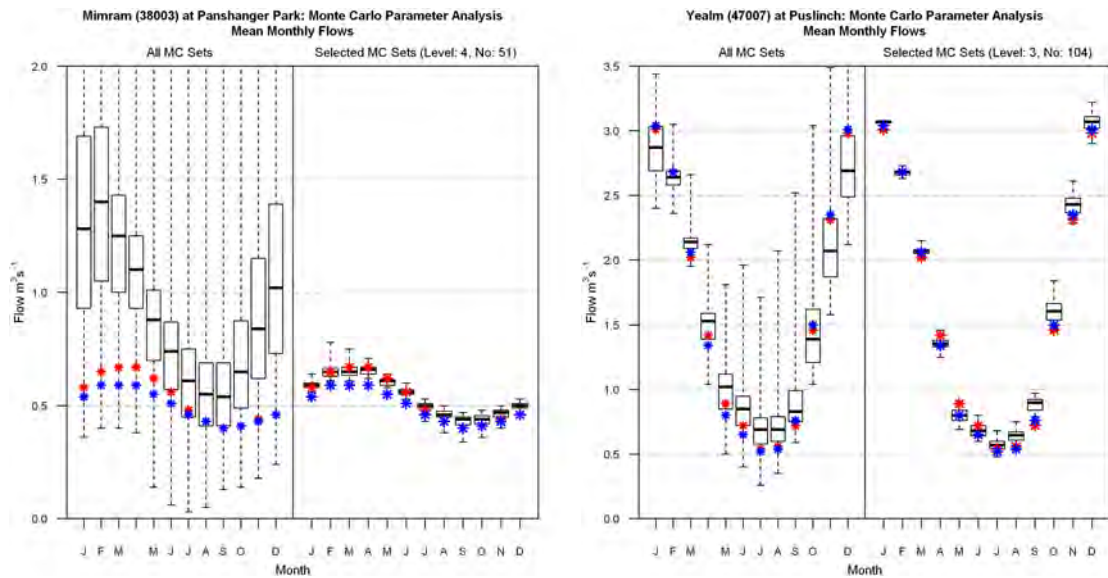
Figure 5.4 Mean flows from 10,000 Monte Carlo parameter simulations (left panel) compared with mean flows from non-dominated accepted parameter sets (right panel) for the Mimram catchment (left plot) and the Yealm catchment (right plot). Red points display observations and blue points display original PDM calibrated parameters (from section 3.3.3).

The flood magnitude values (Figure 5.5) display a different range of behaviour compared to the mean flow results. In the Mimram (left figure) the acceptable flood values (right panel) over estimate the flood return period magnitudes compared with the observations (red points). The full 10,000 Monte Carlo simulations (left panel) display a stronger trend for over estimation, suggesting that the majority of parameter sets are causing the model to output too much water at high flows. Conversely the Yealm (right figure) systematically underestimates the flood magnitudes for the accepted parameter sets (right panel) compared with the observations. Note that for the Yealm, the full 10,000 Monte Carlo parameter sets (left panel) contain solutions with a similar magnitude to the observations but these are not selected in the non-dominated sorting as at least one of the objective functions is not fulfilled.
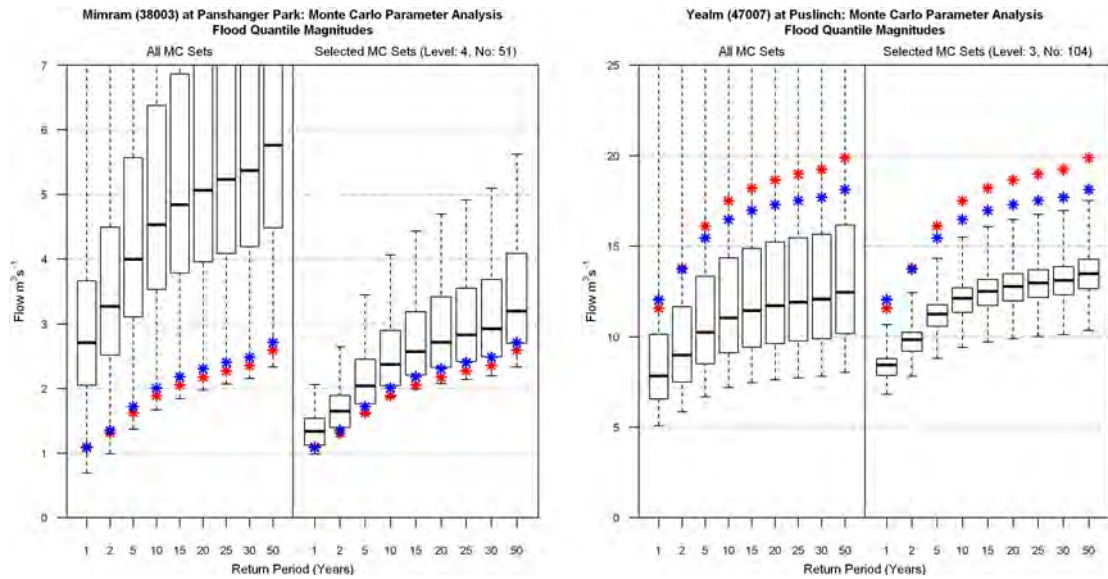
Figure 5.5 Flood quantile magnitudes from 10,000 Monte Carlo parameter simulations (left panel) compared with flood quantile magnitudes from non-dominated accepted parameter sets (right panel) for the Mimram catchment (left plot) and the Yealm catchment (right plot). Red points display observations and blue points display current PDM calibrated parameters (from section 3.3.3).

When using the non-dominated automatic calibration procedure across all nine catchments, the Mimram is the only case where flood magnitudes are over estimated compared with observations. All remaining catchments, with the exception of the Avon, display an under-estimation of simulated flood quantiles similar to that of the Yealm. In the Avon catchment, simulated flood quantiles are of a similar magnitude as observations. The systematic under-performance of the accepted Monte Carlo simulations compared with the observations for flood flows, despite good simulation of means flows, may be a result of how the objective functions are defined. In particular, the three functions used so far do not explicitly account for the model performance with respect to flood flows, hence the selection of parameter sets does not specifically search for a good reproduction of flood magnitudes. The next section proposes a new metric which provides a measure of model performance directly from the catchment flood frequency curve to improve its representation in the calibration procedure.

5.2.3 Flood Frequency Metric

The automatic calibration methodology presented so far has shown good applicability to mean flows due to the defined objective functions (NS and V_{err}); however flood frequency curves in most catchments are poorly simulated compared with observations. The full range of the 10,000 Monte Carlo simulations includes simulations which reproduce the observed catchment flood frequency curve. These are currently not selected as acceptable during the

non-dominated sorting procedure, potentially due to two competing issues. Firstly the objective functions for these solutions are not 'acceptable' and the river flow series on the whole, as opposed to just the flood frequency curve, is poorly reproduced. While secondly the objective functions may not adequately describe the hydrological behaviour relevant to the flood frequency curve. To address the latter of these issues a new criterion is proposed which accounts for the flood frequency curve to be included during the calibration procedure.

Previous studies, such as Lamb (1999), have adopted a criterion adapted to flood applications based on the model simulation of the POT3 series. In their study only two years of data are used, with the POT3 criterion therefore based on the model simulation of only six flow peaks which could risk over-calibrating the model to a small number of peaks. To avoid such an issue it is possible to use information from the flood frequency curve directly rather than relying explicitly on a small number of peaks. The main features of the flood frequency curve which are important to recreate during model simulation are its overall mean location and the steepness of its slope. The flood frequency curve mean is described by the GP location parameter (u), while its slope is best represented by the growth curve values to remove any bias in its mean value (see section 3.4.2). A ratio of the GP location parameter and the 20RP growth value provides an overall quantitative description of the flood frequency curve (Equation 5.1).

$$FF = \frac{GP_u}{20RP_{growth}}$$

<div align="right">**Equation 5.1**</div>

To create a model simulation metric the flood frequency curve descriptor is calculated for both the original observational record and the PDM simulation with their combined ratio (Equation 5.2) providing a description of the PDM simulation compared with the observations.

$$FF_{metric} = \frac{FF_{OBS}}{FF_{SIM}}$$

<div align="right">**Equation 5.2**</div>

The objective function of the FF_{metric} is to reach a value of 1 where observed and simulated flood frequency curves provide the same value. This metric is included with NS_{daily}, NS_{30day} and V_{err} to provide four criteria for the non-dominated multi objective selection.
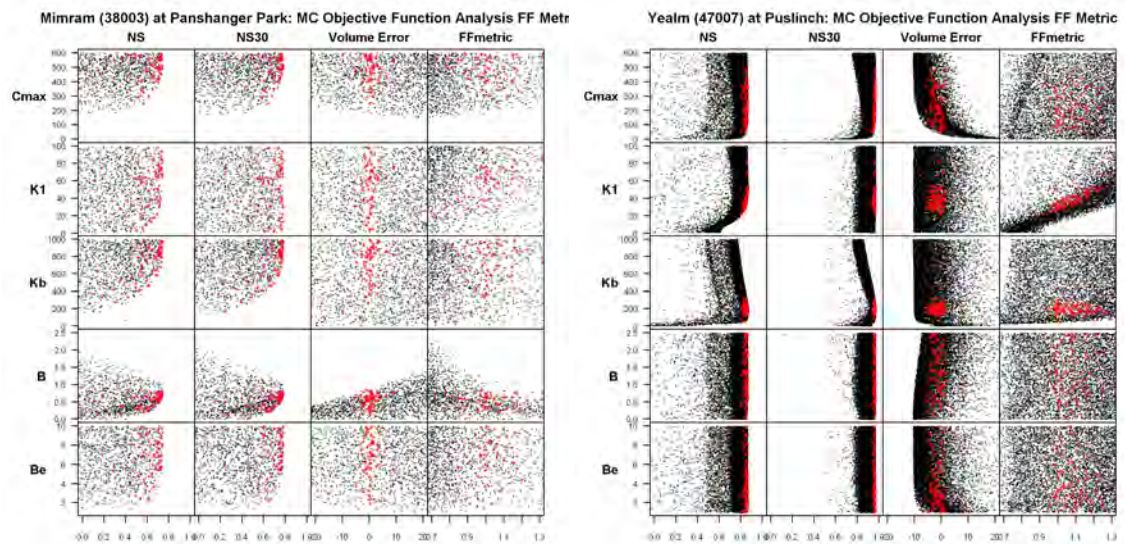
Figure 5.6 Same as for Figure 5.3 with the added objective function for the flood frequency metric. The difference between this figure and Figure 5.3 shows the influence of the FF$_{metric}$.

The result on the identifiability of catchment parameters when including the FF$_{metric}$ varies by catchment type. The quickflow catchments, as demonstrated by the Yealm catchment (Figure 5.6-right), show a strong relationship between the FF$_{metric}$ and the K_1 parameter with a reduced K_1 range adopted by the acceptable parameter sets. The K_1 parameter controls the time delay in the quickflow routing which has a clear direct control on the flood characteristics of a quickflow catchment. In the baseflow dominated catchments, for example the Mimram (Figure 5.6-left), the FF$_{metric}$ does not provide any improved identifiability in the catchment parameters. This has two important implications; firstly it highlights the more complex interaction of processes which control flooding in baseflow catchments. Catchment antecedent conditions are important in generating the flood events which are controlled over longer periods of time by the interaction of different model components (i.e. storage distribution, routing delays, and evaporation). Secondly given that no PDM model parameter displays identifiability with the FF$_{metric}$, the parameter ranges associated with the baseflow catchments may be difficult to constrain further in a flood frequency application. The baseflow catchment antecedent conditions are mostly controlled by the C_{max}, b and b_e parameters which have been shown to have a strong inter-dependence and cancellation of errors. In baseflow catchments it may be necessary to fix one or more of these parameters to constrain the ranges of the other parameters to improve model simulation.
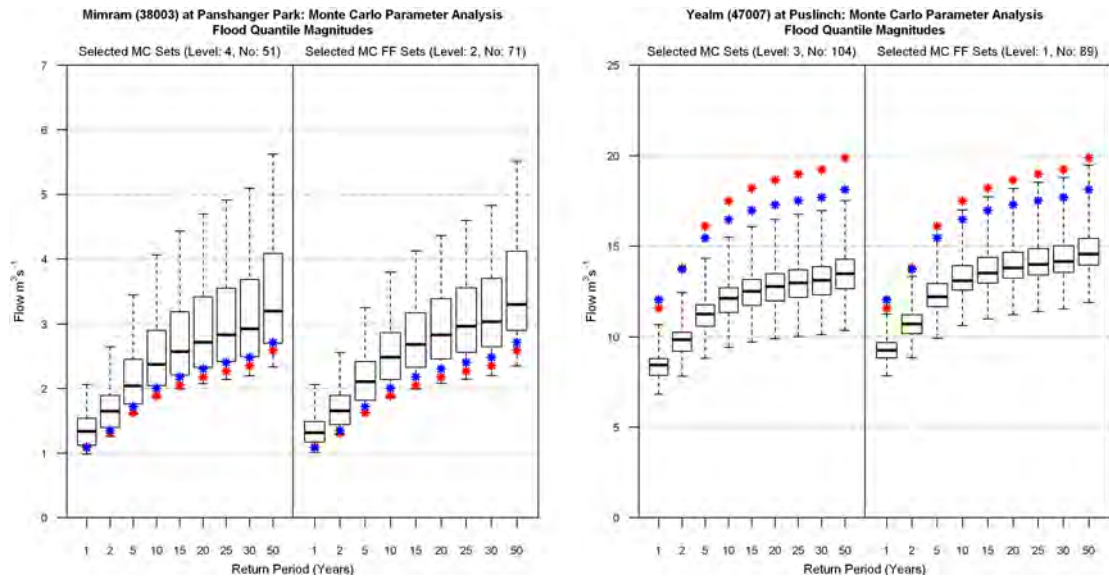
Figure 5.7 Comparison of the accepted flood magnitude values from the non-dominated selection based on three objective functions (left panel-as in Figure 5.5 right panel) and based on four with the inclusion of the FF$_{metric}$ (right panel) for the Mimram (left plot) and Yealm (right plot) catchments.

The lack of improvement in identifiability of catchment parameters in the Mimram is reflected in the associated flood quantile magnitudes (Figure 5.7-left). The acceptable simulated flood quantiles (right panel) are nearly identical with the inclusion of the FF$_{metric}$ compared with the simulated flood quantiles selected without the FF$_{metric}$ (left panel) in section 5.2.3. In the Yealm catchment, which displays improved identifiability of the K_1 parameter (Figure 5.7-right), there is an overall increase in the magnitude of the flood quantiles with the inclusion of the FF$_{metric}$ (right panel) compared with previously (left panel). Despite this magnitude increase in accepted flood quantiles, the majority of acceptable simulations still under estimate the flood quantile magnitudes compared with the observations.

Including the FF$_{metric}$ increases the magnitudes of accepted flood quantiles in quickflow catchments although overall flood quantile magnitudes remain too low compared with observations, while in baseflow catchments the FF$_{metric}$ is shown to have little influence. To improve the calibration procedure the sensitivity of different combinations of parameters and objective functions are tested in the next section.

5.2.4 Combinations of Parameters and Objectives

This section aims to explore a number of different calibration setups to identify the sensitivity of the currently proposed calibration procedure to the parameters and objective functions that are included. The number of parameters that are allowed to co-vary in the Monte Carlo simulation are altered along with changing the combinations of the objective metrics used to extract acceptable parameter sets.
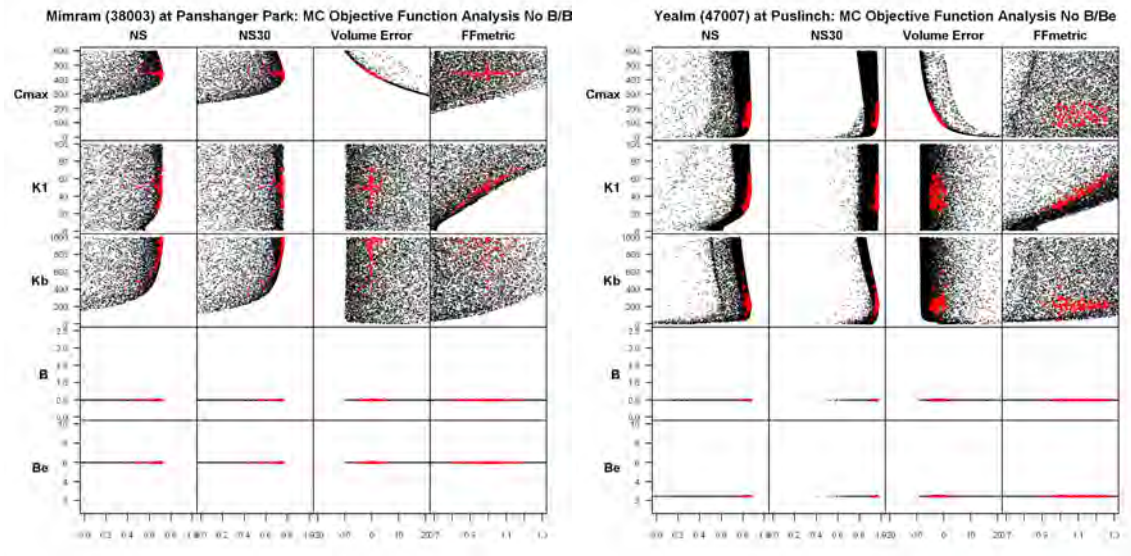
Figure 5.8 PDM Monte Carlo parameter simulation for the Mimram (left) and Yealm (right). Cross comparison of three varied parameters (y-axis) and three objective functions (x-axis). Red points denote accepted parameter sets.

The previous section identified that the flood frequency curves for the baseflow catchments display no direct connection to a specific PDM model parameter. Therefore the identifiability of the model parameters may only be improved by reducing the number of parameters that are allowed to co-vary. To test this, the b and b_e parameters are fixed at their original values from Chapter 3, with only C_{max}, K_1 and K_b allowed to vary in the Monte Carlo simulation. Through fixing the b parameter the range of acceptable C_{max} parameter values is constrained (Figure 5.8-Top). This relationship is most notable when assessed using V_{err} where it is clear that with a fixed value of b, the C_{max} parameter has a defined impact on the volume of water stored in the modelled system. In the Mimram the range of accepted parameters is reduced for the three varied parameters (Figure 5.8-Left) compared with allowing all five parameters to co-vary (Figure 5.6-Left). The magnitude of the flood quantiles (not shown) is improved relative to observations. In the Yealm catchment the result is for the range of the C_{max} parameter to be better constrained while K_1 and K_b display similar accepted ranges to when

all five parameters are varied. The resulting flood quantiles (not shown) display decreases in their magnitude, suggesting a poorer model performance with a fixed b and b_e. In catchments which display poor identifiability of acceptable model parameters, reducing the number of parameters that are varied in the Monte-Carlo simulation can increase the identifiability of the remaining model parameters.

The parameter sets accepted in the non-dominated sorting procedure are dependent on the objective metrics used, as demonstrated in a number of catchments through the inclusion of the FF_{metric}. To test the influence of the different objective metrics the non-dominated sorting procedure is applied whilst excluding different combinations of metrics.

The V_{err} metric may not be representative of the catchment water balance as it assumes that the precipitation record and flow record are without error. Any small biases in either record would lead to a biased V_{err} criterion; therefore reducing the error towards zero may not be possible or may make poorly defined models appear acceptable. The omission of the V_{err} criterion leads to accepted parameter sets which generate a greater range of flood magnitude values; however the overall distribution mean is maintained at a similar magnitude to when V_{err} is included.

NS_{daily} is most applicable in hydrological forecasting applications, whereas here the long term hydrological characteristics are of most interest. The omission of the NS_{daily} criteria is perhaps the best justified in this model calibration procedure given that the day to day catchment flow simulation is not of most interest. The omission of the NS_{daily} criteria has little discernible influence on the accepted flood quantile magnitudes in the majority of catchments with only two catchments displaying small flood magnitude increases.

The calibration procedure is sensitive to the choice of objective metric although in most cases the impact is small. The V_{err} metric has the greatest influence in constraining the accepted flood quantile ranges; however due to the importance of simulating the catchment water balance it cannot be excluded. The main limitation of the V_{err} metric is that in the non-dominated sorting procedure equal weighting is applied to values about zero (i.e. ±5% are considered the same). Analysis prior to calibration to understand any errors in observed records could allow for a better implemented V_{err}.

The inter-dependencies and relationships between model parameters and the model performance metrics vary from catchment to catchment making any automatic calibration

procedure difficult to implement. The method presented in this section using Monte Carlo simulations in combination with a non-dominated multi objective selection process has shown good applicability to mean flows but overall difficulties in the context of flood frequency estimation. The inclusion of a flood frequency metric generally improved the calibration process, but the majority of catchments are still associated with model parameter sets which underestimate flood quantile magnitudes. This may be due to the difficulties in accurately reproducing flood peaks by simulation with a lumped hydrological model, or errors in the input/output data used for hydrological simulation and evaluation. Despite these limitations a range of parameter sets have been generated for each catchment with accepted errors. The next section tests whether the choice of the parameter set selected in a climate change impact analysis influences the magnitude of change for a given flood return period quantile.

5.3 Hydrological Model Parameters in Climate Change Impact Studies

Typically in climate change impact studies, hydrological parameters are kept constant between the baseline and future time periods. Firstly, this assumption is deemed to be valid as the calibrated model parameters describe a catchment's hydrological processes which are assumed not to change with climate. Secondly the assumption is adopted as there is very little alternative given the absence of a future flow record to match the calibration demands of reduced complexity hydrological models. This section aims to address how this assumption influences the calculated changes in flood quantile magnitudes through a sensitivity based approach.

The previous section highlighted some difficulties in developing an automatic calibration procedure for the PDM model for flood frequency estimation. Although the calibration method is acceptable for mean flow analysis, a number of catchments demonstrated a significant under simulation of flood quantile magnitudes. The impact of this under simulation when calculating flood changes in response to precipitation changes is assessed in this section. A minimum of 50 parameter sets are generated for the nine catchments using the Monte Carlo methodology presented in the previous chapter. The C_{max}, K_1 and K_b parameters are varied in the Mimram and Bure catchments with the non-dominated sorting undertaken using NS_{daily}, NS_{30day} and V_{err}. The remaining seven catchments also include b and b_e in the Monte Carlo simulation with the FF_{metric} included in the non-dominated sorting. Due to the acknowledged 'under-simulation' in this methodology, parameter sets are also created using a perturbation method as follows. The calibrated parameter set for each catchment from

Chapter 3 are perturbed by ±20% with 50 new parameter sets generated in each catchment through uniformly sampling the perturbed parameter range independently for C_{max}, K_1, K_b, b and b_e.

To understand the influence of parameter uncertainty to potential climate change a sensitivity approach is adopted here to allow comparisons between catchments by applying the same synthetic precipitation changes to each catchment. Furthermore to avoid mixing each catchment's baseline climate seasonality with the seasonality of a synthetic precipitation scenario no seasonal changes in precipitation are considered in the sensitivity testing. Uniform monthly changes of -50%, +50% and +100% are used to perturb catchment precipitation which is in turn used as input to PDM using the multiple different parameter sets. The resulting changes in the simulated flood quantiles in the Mimram and Yealm catchments are shown in section 5.3.1 for the Monte Carlo parameter sets and section 5.3.2 for the perturbation derived parameter sets.

5.3.1 Sensitivity of Flood Change to Monte Carlo Parameters

The largest increases in precipitation generate the largest range of uncertainty in flood changes for Monte Carlo parameter sets. In the Mimram catchment the range of uncertainty across all flood return periods resulting from a 100% increase in precipitation varies between 300% and 600% depending on the parameter set (Figure 5.9-top left). The greatest range of uncertainty is at the smaller return periods, with the range decreasing as the return period increases. A similar trend occurs for a 50% increase in precipitation although the magnitudes and range of changes are smaller. For a uniform decrease in precipitation of -50% the uncertainty range for flood changes across the different parameter sets is small in comparison to the ranges resulting from precipitation increases. Similarly to the Mimram, the Yealm catchment also displays the greatest range of flood quantile changes for the largest change in precipitation (Figure 5.9- top right). The range across all return periods varies between increases of 125% and 175% in flood quantile changes, in response to a 100% uniform increase in precipitation. The range of uncertainty in the flood quantile change to the same uniform precipitation change is smaller in the Yealm compared with the Mimram. In contrast to the Mimram the range of changes for the different return periods is fairly uniform.

Across all catchments each parameter set causes a different flood sensitivity to change which is enhanced as the uniform precipitation change increases in magnitude. The sensitivity of the PDM parameters to decreases in precipitation is small. The sensitivity ranges of the

parameters between catchments can be linked to the catchment sensitivity types identified by Prudhomme et al (2010) and discussed in section 3.2. Generally as the catchment response type increases in sensitivity the range of sensitivity in the catchment parameters increases.
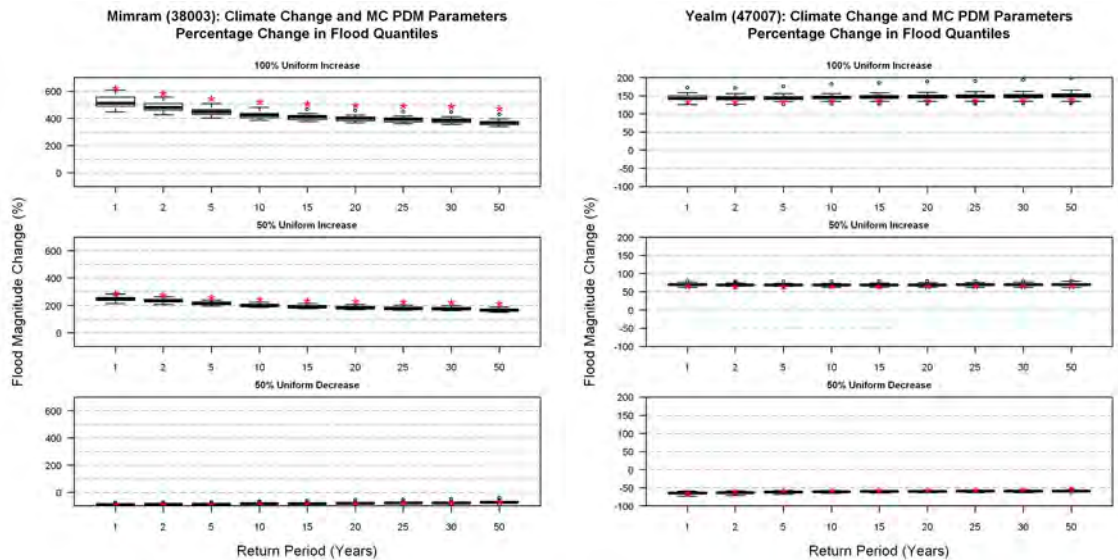
Figure 5.9 Percentage change in flood frequency magnitudes in the Mimram (left) and Yealm (right) catchments for accepted Monte Carlo parameter sets. Flood quantile changes in response to uniform monthly precipitation changes of -50% (bottom), +50% (middle) and +100% (top). Changes for the single parameters sets from section 3.3.3 are in red points.

In Figure 5.9 the red points represent the flood change for the currently calibrated PDM parameter set. The under-performance in simulating flood quantile magnitudes from the automatic calibration procedure in section 5.2 has a varied influence on the flood changes. In the Mimram the current model calibration generates flood quantile changes lying within the range of Monte Carlo parameter sets, except for the largest precipitation change of 100% where there is a systematic underestimation of flood changes when using automatically calibrated parameter sets. In the Yealm the current calibration lies in the range of the Monte Carlo parameter sets for all scenarios. This suggests that simulation errors due to poor parameter sets are of a similar magnitude for the baseline and future periods, hence resulting in similar flood quantile changes from all parameter sets. The exception is when precipitation increases are very large (here a 100% uniform increase in precipitation; however such a very extreme scenario is not projected by any current climate models).
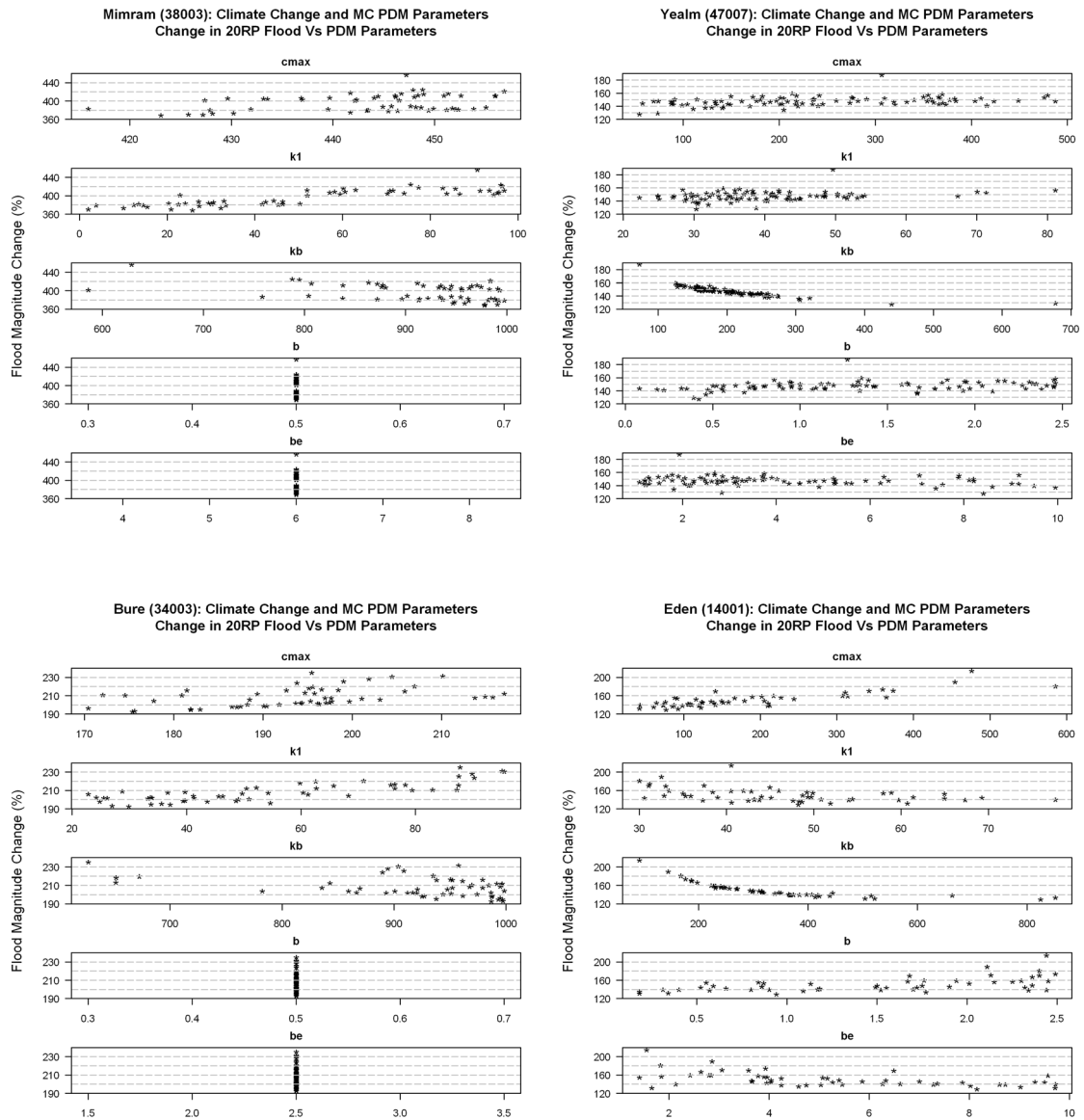
Figure 5.10 PDM Monte Carlo parameter sensitivity of the 20RP change to a +100% uniform increase in precipitation for the Mimram (top left), Yealm (top right), Bure (bottom left) and Eden (bottom right) catchments.

Although the uncertainty in flood changes is relatively small between parameter sets, it is important to identify if any relationships exist between individual model parameters and flood quantile changes. Figure 5.10 displays the change in the 20RP in response to a 100% increase in precipitation compared with the associated PDM parameter values for four catchments. There are two relationships of note; firstly in baseflow catchments (Figure 5.10-top left and bottom left) the larger changes in the 20RP are associated with larger values of the K_1 parameter. Secondly; the quickflow catchments (Figure 5.10-top right and bottom right) display the largest changes in 20RP associated with smallest values of K_b. In both cases this

implies a relationship between the time constant of the secondary model routing (K_1 or K_b as dictated by the α parameter) and the magnitude change of the flood quantile. This suggests that the time constant for the modelled secondary routing contributes a degree of non-stationarity when simulating changes in flood peak. One explanation for this might be that in the baseflow catchments the majority of runoff is partitioned to baseflow and as a result there is an increased lag between precipitation input and river flow output. The remaining flow is routed as quickflow with its time delay controlled by the K_1 parameter. A higher value of K_1 increases the lag between precipitation input and river flow response leading to a greater potential for the interaction between the baseflow and quickflow routed components. In the quickflow catchment example the reverse situation occurs where the minority flow component is controlled by the K_b parameter. A low value of K_b causes a shorter lag time leading to quicker potential interaction between the two runoff routing components. An increase in precipitation to the model leads to a greater volume of water being directed through both quick and slow routes, with a greater potential for a interaction between the two routes. This leads to an enhanced flood peak and hence a greater change in the 20RP.

5.3.2 Sensitivity of Flood Change to Perturbed Parameters

The range of uncertainty from Monte Carlo parameter sets tested in the previous section may be largely due to the inadequacy of the automatic calibration procedure and in turn could lead to unrealistic conclusions. To verify the results from the previous section, perturbed PDM parameter sets were generated through randomly sampling 50 new parameter sets from a ±20% range around the currently calibrated parameter sets in Chapter 3. The perturbed parameter sets only explore the uncertainty of the best calibration as opposed to the full parameter space, resulting in parameter sets which may be a better representation of the catchment processes and properties. The uncertainty resulting from the perturbed parameter sets is tested in the same manner as the Monte Carlo parameter sets in the previous section; using uniform monthly precipitation changes of -50%, +50% and +100%. The results of this sensitivity analysis on catchment flood quantiles are shown in Figure 5.11.

The range of uncertainty in the flood peak change in the Mimram catchment (Figure 5.11-left) due to model parameter uncertainty increases with larger precipitation changes. The uncertainty in the flood peak change is greatest for smaller return periods compared with larger return periods. In contrast, the uncertainty in the flood quantile change in the Yealm catchment (Figure 5.11-right) has a very low sensitivity to the parameter perturbations. The

range of changes is fairly uniform across all return periods and precipitation changes; only at the largest return periods under a 100% precipitation increase does the range start to increase. The magnitude change across the different return periods is also uniform.
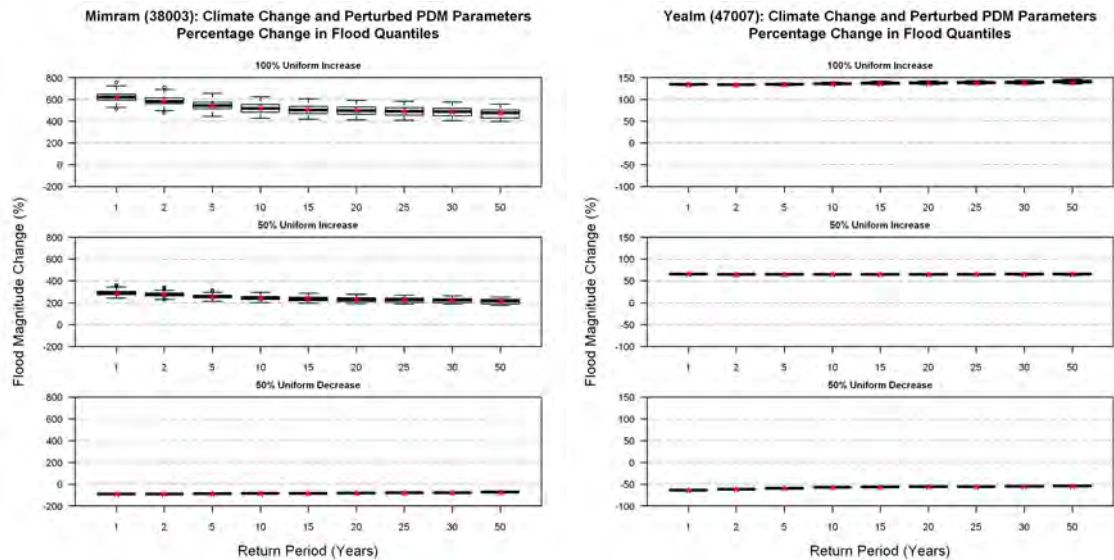
Figure 5.11 Percentage change in flood frequency magnitudes in the Mimram (left) and Yealm (right) catchments for 20% perturbed parameter sets. Flood quantile changes in response to uniform monthly precipitation changes of -50% (bottom), +50% (middle) and +100% (top). Changes for the single parameters sets from section 3.3.3 are in red points.

The relationship between each perturbed parameter set and the resulting change in the 20RP in response to a 100% increase in catchment precipitation is shown in Figure 5.12. The secondary routing relationship identified in section 5.3.1 remains evident in the quickflow catchments (Yealm and Eden), however this is no longer the case in the baseflow catchments (Mimram and Bure). This is because the range of the K_1 parameter is smaller for the perturbed parameter sets compared with the Monte Carlo K_1 parameter range in the baseflow catchments. Conversely the C_{max} parameter has a larger range in the perturbed parameter sets compared with the Monte Carlo sets for the baseflow catchments (left), which displays a positive relationship between an increasing C_{max} leading to greater change in 20RP. A larger value of C_{max} increases the maximum catchment storage. In the calibration period this may result in a high proportion of precipitation input remaining in storage; however when the precipitation is increased by 100% the store is filled faster, in turn generating runoff quicker and thus producing an enhanced flood peak.
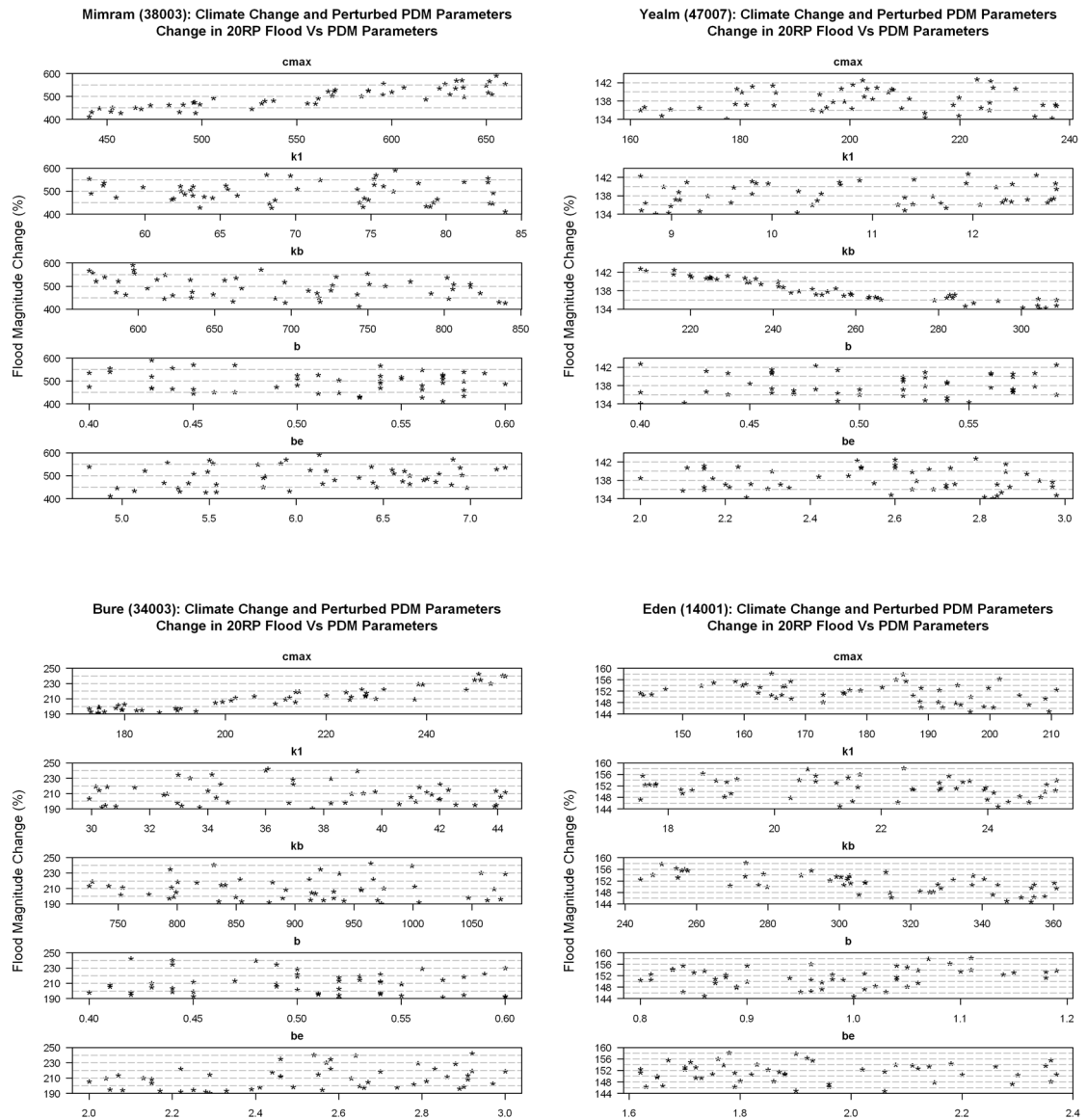
Figure 5.12 PDM perturbed parameter sensitivity of the 20RP change to a +100% uniform increase in precipitation for the Mimram (top left), Yealm (top right), Bure (bottom left) and Eden (bottom right) catchments.

5.3.3 Comparison of Parameter Methods

The perturbed PDM parameters from section 5.3.2 display a different behaviour compared with the Monte Carlo parameters in section 5.3.1. In the Mimram the range and magnitude of flood quantile changes resulting from the perturbed parameters is greater than that of the Monte Carlo parameters, particularly for the largest precipitation increase. The Monte Carlo parameters underestimate the change compared with the original calibrated parameter set (Figure 5.9-left, red points), whereas the perturbed parameters form a distribution around the current calibration (Figure 5.11-left). The Monte Carlo parameters for the Mimram have a

smaller range compared with the perturbed parameters, suggesting that the perturbed parameters, based on the original calibrated parameters, result in a higher sensitivity of flood quantile changes.

In the Yealm catchment the perturbed parameters display a reduced range of uncertainty in flood quantile changes (Figure 5.11-right) compared with the Monte Carlo parameters (Figure 5.9-right). The magnitude of changes for both parameter sets are similar and closely match the original calibrated values (red points). The small range of changes from the perturbed parameters indicate a low sensitivity of the currently calibrated parameters to climate inputs. It also reflects the smaller parameter space which the perturbed parameters occupy compared with the Monte Carlo parameters in the Yealm. The similar magnitudes of change for both parameter methods, despite occupying varied parameter spaces, demonstrate that the catchment is less sensitive to parameterisation and calibration. Acceptable parameter sets are easier to attain for the Yealm compared to the Mimram.

5.4 Discussion and Conclusions

The primary aim of this chapter was to understand how hydrological model parameter uncertainty influences the magnitude of change for a given flood return period quantile. To achieve this aim two stages were undertaken; firstly multiple parameter sets were generated for each catchment, and secondly the influence of model parameter uncertainty in climate change impact studies was analysed.

The Monte Carlo calibration procedure highlights the importance of understanding the role of selecting objective functions which reflect model parameter performance. Often subjective thresholds are defined for objective functions dictating an acceptable model performance. The choice of a subjective threshold differs between catchments due to the complexity of the hydrological processes, as well as possible errors in input or output data. To avoid any subjective decision the non-dominated sorting method was implemented to naturally select the best performing Monte Carlo simulations based on the NS_{daily}, NS_{30day} and V_{err} objective functions. These three objective functions do not provide information on the simulation of the catchment flood frequency curve which required the development of a new function, FF_{metric}, based on the simulated flood frequency curve shape and magnitude. The FF_{metric} improves the calibration in quickflow catchments but not for baseflow catchments. The inclusion of the FF_{metric} raises two issues; firstly in baseflow catchments there is no direct connection between any PDM parameter and the flood frequency curve making the calibration of the model for

flood purposes difficult. The simulation of the flood regime behaviour in baseflow catchments relies on a more complex interaction of model components compared with quickflow catchments (which are typically controlled by the K_1 parameter). The identifiability of baseflow catchment parameters is improved by fixing some parameters as constants. Secondly does the inclusion of such specific measures such as the FF_{metric} attempt to over calibrate the model? In its application here the FF_{metric} is used in conjunction with three other objective functions so that no single objective is relied on or given preference. Previous examples (Lamb, 1999) have used a similar flood criteria independently, at which point the parameter and model performance is being gauged on only a small number of peak flow events.

Despite the inclusion of the FF_{metric} the accepted Monte Carlo parameter sets in the majority of catchments under simulate the magnitude of the flood peaks. The main cause of this is the implementation of the V_{err} criteria with the non-dominated sorting. The objective function of the V_{err} is to achieve a value of zero which assumes there are no biases in either the precipitation or flow records. An equal weighting was given to V_{err} values of the same magnitude but contrasting sign (i.e. $\pm10\%$), but it could be argued that a model performing to a V_{err} of $+10\%$ is very different from a performance of -10%, thus an equal weighting is not appropriate and it is likely that one provides a better reproduction of the flood peaks. In the application here the remaining objective functions are relied upon to distinguish the two equally likely V_{err} simulations which may not always be possible in the non-dominated sorting procedure. When the V_{err} criterion is removed from the process the range of accepted flood quantiles increased uniformly in both directions. If either the positive ($+10\%$) or negative (-10%) V_{err} could be discriminated against instead of being equally valid, the range of flood quantiles would likely to be reduced by half leaving the best performing simulations.

A sensitivity approach is implemented to identify the role of model parameter uncertainty in defining climate change impacts. Uniform precipitation changes of -50%, $+50\%$ and $+100\%$ are applied to catchment precipitation and simulated using multiple PDM parameter sets. The different PDM parameters are shown to generate different flood quantile changes for the same change in precipitation. Larger values of the C_{max} parameter can lead to larger changes in flood quantiles. This is a result of the catchment storage capacity being reached quicker in a wetter period than the calibration period with increased runoff generated over a shorter time period and hence an accentuated change in flood peak. The role of C_{max} is most important in

baseflow catchments where larger stores are required to reduce runoff, whereas in quickflow catchments C_{max} has a lower value to generate a greater proportion of quickflow runoff.

A second relationship is identified between the magnitude change in the catchment flood quantiles and the secondary-routing parameter. A value of the secondary routing parameter (K_b in baseflow and K_1 in quickflow) which is larger (smaller) will produce a greater change in the flow quantile of baseflow (quickflow) catchments. It is hypothesised that an increase in precipitation leads to the primary and secondary routing having a greater potential for interaction when both routes are combined as river flow which occurs in a non-linear manner as the volume of water in both routes increases.

5.5 Chapter Summary

This chapter has sought to explore the influence of hydrological model parameter uncertainty in climate change impact studies. The sensitivity of flood quantile changes to specific model parameters was tested through generating multiple equally valid parameters sets. The method of parameter generation was based on Monte Carlo parameter simulations with model objective metrics assessed simultaneously using the non-dominated sorting procedure. Flood quantiles were found to be under-simulated in most catchments which led to the creation of a new objective function (FF_{metric}) which compares the observed and simulated flood frequency and growth curves. The inclusion of the FF_{metric} improved the magnitude of the flood quantiles in quickflow catchments but had no influence in the baseflow catchments. This was a result of the poor identifiability of any PDM parameter with the flood frequency curves in baseflow catchments due to the more complex processes in generating flood events, in particular the role of antecedent conditions.

The model parameters obtained from the Monte Carlo procedure as well as a second technique using a perturbed parameter method were subjected to sensitivity tests to assess the parameter influence on the sensitivity of flood quantile changes to precipitation changes. The uncertainty from the model parameters varied significantly between catchments and as precipitation changes became increasingly large. The C_{max} parameter, controlling the maximum catchment storage, was found to have a positive relationship with the 20RP change. This is a result of catchment storage capacity being reached sooner with increased precipitation, increasing runoff and thus accentuating the relative change to the calibration period. The secondary routing storage parameter (K_1 or K_b as dictated by a catchments α parameter) was also found to influence the magnitude changes in flood quantiles.

The PDM model parameters have been shown to be sensitive to increases in precipitation. The degree of sensitivity varies between catchments and precipitation scenarios but is influenced by the C_{max} and secondary routing parameter (K_1 or K_b). The sensitivity tests applied here were extreme precipitation scenarios; the application of climate model derived scenarios, which are less extreme, may produce lower parameter sensitivity.

This chapter has highlighted the importance of hydrological model parameter uncertainty which will be discussed in combination with other uncertainty sources in Chapter 8. The next chapter addresses the uncertainty of estimating flood quantiles which in the previous chapter and this chapter have been discussed as absolute values with no uncertainty.

CHAPTER 6

Flood Frequency Analysis Uncertainty

6.1 Introduction

So far in this thesis the uncertainty associated with the impact of climate change on the T-year flood quantile has been discussed with an assumption that the calculated flood quantiles are certain. However in Chapter 2 it was identified that there is a large degree of uncertainty associated with estimating flood quantiles using flood frequency analysis. The aim of this chapter is to quantify the uncertainty associated with flood frequency analysis.

A background to the current methods for flood frequency uncertainty is provided in section 6.2, followed by an analysis on quantifying flood frequency uncertainty in section 6.3. A conceptual issue that arises relating to the use of climate change factors in flood impact studies is discussed in section 6.4 and a method to account for the flood frequency uncertainty in the climate change impact study framework is presented in section 6.5. The chapter concludes with the discussion and conclusions (section 6.6) from this work followed by an overall summary (section 6.7).

6.2 Flood Frequency Background

In the context of present day climate (assuming stationarity) the uncertainty for a given flood frequency method is typically included in one of two ways in the UK. The first approach is to use pooling group analysis, whereby catchments that display similar flood characteristics to the catchment of interest (but are not necessarily geographically close) are used to extend the knowledge base to perform flood frequency analysis (Institute of Hydrology, 1999, Kjeldsen and Jones, 2009). In a climate change impact study river flows from each catchment used in

the pooling group analysis would need to be simulated for a future climate. However changes in climate vary between locations, hence introducing a possible non-uniformity in the climate change signal imposed on the different catchments. The possible variation in climate changes may result in different hydrological responses between catchment, leading to non-stationarity in the pooling group statistics. When using UKCP09 change factor projections there is no spatial coherence between grid cells, meaning that the same scenarios cannot be applied consistently across all catchments. These limitations would require the pooling group methodology to be substantially altered for climate change impact studies.

The second widely used method is to use continuous hydrological simulation in conjunction with a weather generator or resampled observations to provide multiple (or long) precipitation time series to provide better informed flood quantile estimates (Cameron et al., 2000, Cameron, 2006, Kay et al., 2009). The examples of continuous simulation have previously been applied using a small number of climate change scenarios (e.g. 6 UKCIP02 scenarios (Cameron, 2006)). If probabilistic projections are considered, using multiple precipitation realisations for each projection may become computationally intensive. For example the 10,000 UKCP09 scenarios would each need to be run with a minimum of 100 weather generations (Kilsby et al., 2007), leading to 1,000,000 simulations for a single emissions scenario and time horizon in a given catchment, which might be difficult in practice. The existence of a computationally efficient method for incorporating flood frequency analysis uncertainty would therefore encourage flood frequency uncertainty to be more widely considered in climate change impact studies on flooding.

6.3 Flood Frequency Estimation and Uncertainty

6.3.1 Calculating Flood Frequency Curves

Using the flood frequency estimation methods outlined in section 0, flood frequency curves for the study catchments are calculated for PDM simulated river flows for the baseline period and each of the 10,000 future river flows series derived from the UKCP09 change factors; the example for the Helmsdale catchment is shown in Figure 6.1. The resulting flood frequency curves from UKCP09 derived changes display a wide range as a result of climate change alone, without accounting for the flood frequency uncertainty associated with the estimation of each flood frequency curve.
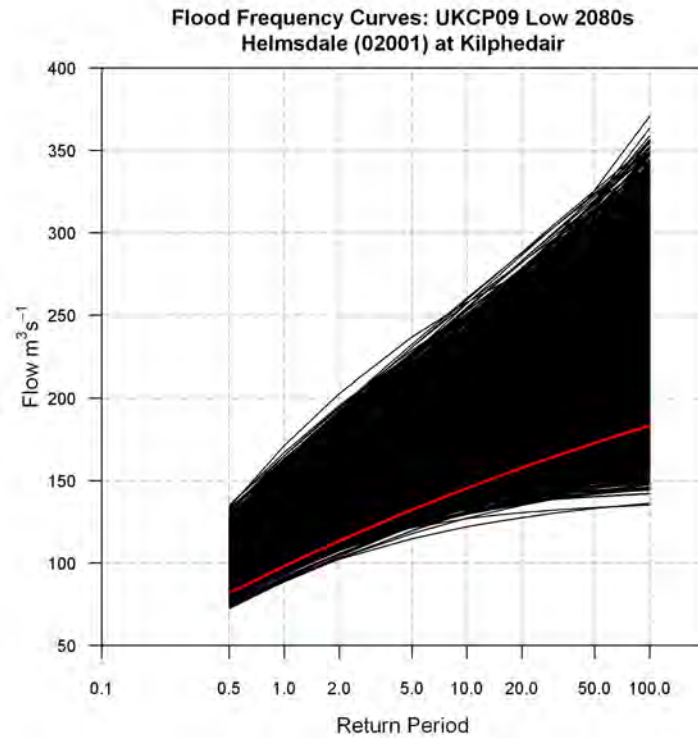
Figure 6.1 Flood frequency curves from the Helmsdale for the simulated baseline (red) and 10,000 UKCP09 precipitation change factors for the 2080s under a low emissions scenario (black).

6.3.2 Flood Frequency Estimation Uncertainty

Due to the statistical nature of flood frequency estimation certain limitations arise. The primary limiting factor is the length of available record. Even in the UK, with a well established river gauging network, typical daily river flow record lengths are in the order of 30-40 years. However in a planning context events associated with return periods beyond the length of flow record are often discussed, leading to flood quantile estimation from an extrapolation (sometimes large) of the fitted flood frequency distribution beyond the recorded flow peak population. The second conceptual limitation is that even for a well established flow record where flood frequency distribution extrapolation is not required beyond the observed peaks, there is only one realisation of the flood peak distribution within a catchment with no comparable population to test the fitted distribution. If the same catchment had experienced a different cycle of natural variability, the observed flow series would not have been the same, thus producing a slightly different population to fit a flood frequency distribution.

Table 6.1 Standard error in percent of the baseline flood quantile estimate for 5, 20 and 50 year return period events.

NRFA Gauge	Standard Error of Estimate for Baseline (%)		
	5 Year	20 Year	50 Year
Findhorn (07002)	6.26	14.62	23.72
Helmsdale (02001)	3.95	8.11	12.14
Findhorn (14001)	4.90	10.25	15.55
Yealm (47007)	3.01	5.57	7.66
Bure (34003)	6.99	17.40	29.30
Teme (54008)	4.47	8.57	12.19
Leet Water (21023)	8.95	23.02	39.50
Avon (43005)	5.49	11.31	16.97
Mimram (38003)	6.28	14.29	22.84

To account for the uncertainty associated with the fitted GP distribution a standard error of estimate (SE, Equation 6.1) can be calculated from the GP parameters (Rao and Hamed, 2000) (Table 6.1).

$$SE = \sqrt{\left(\frac{dx}{d\alpha}\right)^2 var(\alpha) + \left(\frac{dx}{dk}\right)^2 var(k) + 2\left(\frac{dx}{d\alpha}\right)\left(\frac{dx}{dk}\right) cov(\alpha, k)}$$

Equation 6.1

Where:

$$var(\hat{\alpha}) = \frac{\alpha^2}{N} \frac{(7 + 18k + 11k^2 + 2k^3)}{(1 + 2k)(3 + 2k)}$$

Equation 6.2

$$var(\hat{k}) = \frac{1}{N} \frac{(1 + k)(2 + k)^2(1 + k + 2k^2)}{(1 + 2k)(3 + 2k)}$$

Equation 6.3

$$cov(\hat{\alpha}, \hat{k}) = \frac{\alpha}{N} \frac{(2 + k)(2 + 6k + 7k^2 + 2k^3)}{(1 + 2k)(3 + 2k)}$$

Equation 6.4

$$\frac{dx}{d\alpha} = \frac{1}{k}[1 - (\lambda T)^{-k}]$$

<div align="right">**Equation 6.5**</div>

$$\frac{dx}{dk} = \frac{-\alpha}{k^2}[1 - (\lambda T)^{-k}] + \frac{\alpha}{k}(\lambda T)^{-1}\log(\lambda T)$$

<div align="right">**Equation 6.6**</div>

Where λ is the average number of peaks per year; in the case of POT3 sampling $\lambda = 3$.

The SE accounts for the uncertainty associated with the shape (k) and scale (α) parameters of the GP distribution which have greater significance, in comparison to the location (ε) parameter, when calculating flood frequency curves. This is highlighted in Figure 6.2 (left), where a large number of POT3 events define the location (ε) of the flood frequency curve, whereas only seven (it could be argued only one) POT3 peaks have greatest influence on the scale and shape of the flood frequency curve. The SE estimate can be interpreted as an estimate of the standard deviation of the flood frequency distribution, with the distribution mean approximated as the original calculated flood frequency curve. These approximations of the mean and standard deviation of the flood frequency distribution allow the calculation of confidence intervals, assuming a normal distribution, about the fitted flood frequency curve (Figure 6.2-Right). A higher confidence is associated with flood quantiles of smaller return periods due to there being a greater likelihood of the observed flow series being representative of these quantile estimates. Conversely the lowest confidence is associated with the higher return period quantile estimates, where the fitted distribution is dependent on just a few observed events (Figure 6.2). This is the case for all catchments (Table 6.1) although the magnitude of SE varies between catchments as it depends on the slope of the flood frequency curve. Flood frequency curves that are bounded above (the slope (k) is greater than 0) have a lower SE than curves that are unbounded (k less than 0). The relationship between the magnitude of SE and flood frequency curve slope can be seen by comparing the growth curves of the 9 catchments in Figure 3.5. The three catchments with the largest SE (Findhorn, Leet Water and Bure) display a very different growth curve compared with the other catchments.
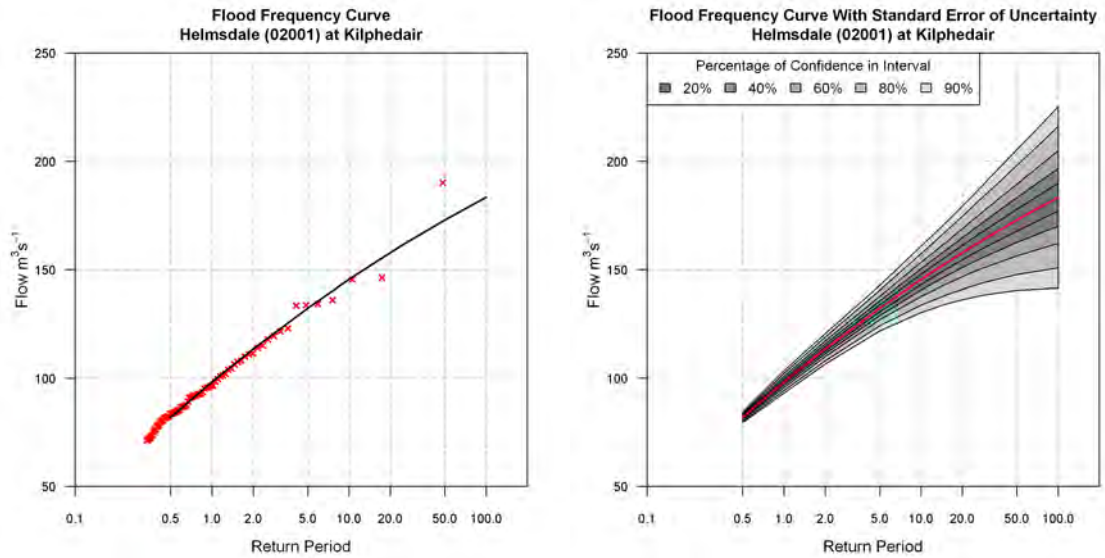
Figure 6.2 Flood frequency curves from the Helmsdale (02001) at Kilphedair. Left – Flood frequency curve with POT3 population it is fitted against. Right – Flood frequency curve with confidence intervals calculated using standard error estimate.

6.3.3 Calculating a Change in Flood Frequency

Future climate change impacts are typically expressed as the percentage change from a baseline reference period estimate. However, as seen from calculating the SE associated with flood frequency analysis, the baseline flood frequency curve and flood quantile estimate are uncertain. As the same methodology is applied to flood frequency analysis for both baseline and future time horizons, uncertainty is also likely to exist for any future flood quantile estimate. This means that estimating a change between the baseline and future flood quantiles is not quite as straightforward compared with when no flood frequency analysis uncertainty is accounted for.
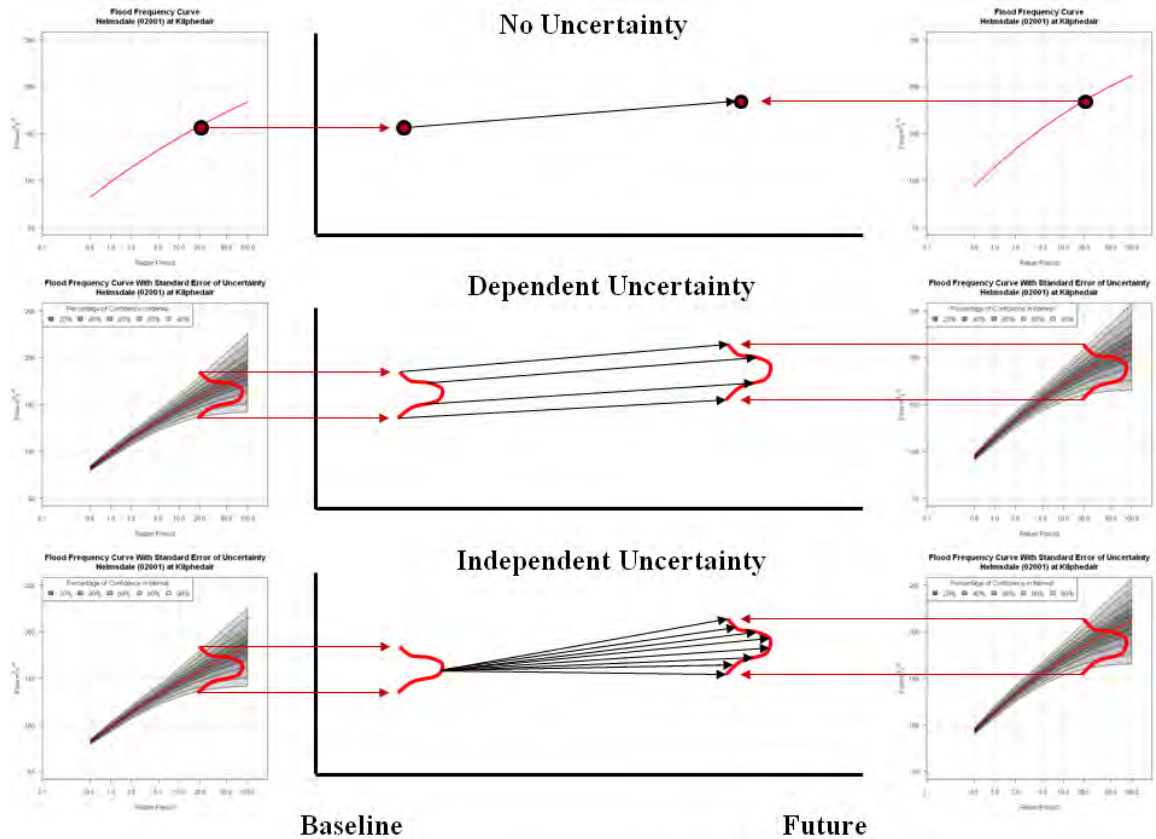
Figure 6.3 Visualisation of how inclusion of uncertainty influences how to calculate climate change in the 20RP for a single climate projection from the UKCP09 10,000. Top panel: Description of change from one baseline to one future considering no uncertainty. Middle Panel: Dependent uncertainty change from baseline uncertainty distribution to future uncertainty distribution. Bottom Panel: Independent uncertainty change from baseline uncertainty distribution to future uncertainty distribution.

As an example, consider the 20RP for a single future projection compared with the 20RP for the baseline. When no flood frequency uncertainty is considered, the impact of climate change is simply the percentage difference between the two 20RP's (Figure 6.3 - Top). In this instance the baseline and future are considered to be independent from one another, given they are many decades apart. However in this study monthly precipitation change factors have been used to perturb an observed precipitation record, hence both baseline and future flood estimates are derived from the same underlying precipitation time series. With the inclusion of normally distributed confidence intervals about both the baseline 20RP and the future 20RP the climate change can be considered in two ways:

1. **Dependent Change**. Changes may only occur in a linear manner from baseline to future (Figure 6.3 - Middle). The 5th percentile of the baseline flood quantile distribution is transformed to the 5th percentile of the future flood quantile

distribution; similarly the 50th percentile baseline estimate will become the 50th percentile future estimate. This results in a change in a given flood quantile between paired percentiles in the baseline and future distributions. The change between baseline and future are dependent on one another when uncertainty is included around the 20RP.

2. **Independent Change**. Changes may occur from any percentile of the baseline flood quantile to any percentile of the future flood quantile (Figure 6.3 – Bottom). i.e. the 5th percentile of the baseline may become any of the 1st-99th percentiles of the future. This results in a change in a given flood quantile which can be calculated from any combination of percentiles from the baseline and future distributions. The change between baseline and future is independent of one another, any baseline 20RP and future 20RP can co-occur.

6.4 Role of Baseline Precipitation and Monthly Change Factors

Understanding the influence that the underlying baseline precipitation time series has in defining both the baseline and future flood quantiles is integral to identifying whether flood frequency uncertainty propagates dependently or independently. The aim of this section is to analyse how important the observed precipitation record is for defining future flood quantiles when precipitation change factors are used through the perturbation method.

6.4.1 POT3 Analysis

Climate change factors are applied by perturbing an observed precipitation time series on a monthly time scale according to a corresponding monthly precipitation change factor (i.e. Jan+10%, Feb+30% etc). Due to the application of precipitation change factors at the monthly time scale, sub-monthly variance in precipitation is unaltered. This means that a long period of wet days in the observed record is maintained in the same temporal position in the future, with the magnitude each day perturbed according to the change factor value. Given that flood events in the UK are typically associated with sequences of wet days or a single exceptional precipitation event, the question of how the precipitation change factors interact with the observed precipitation record is important.
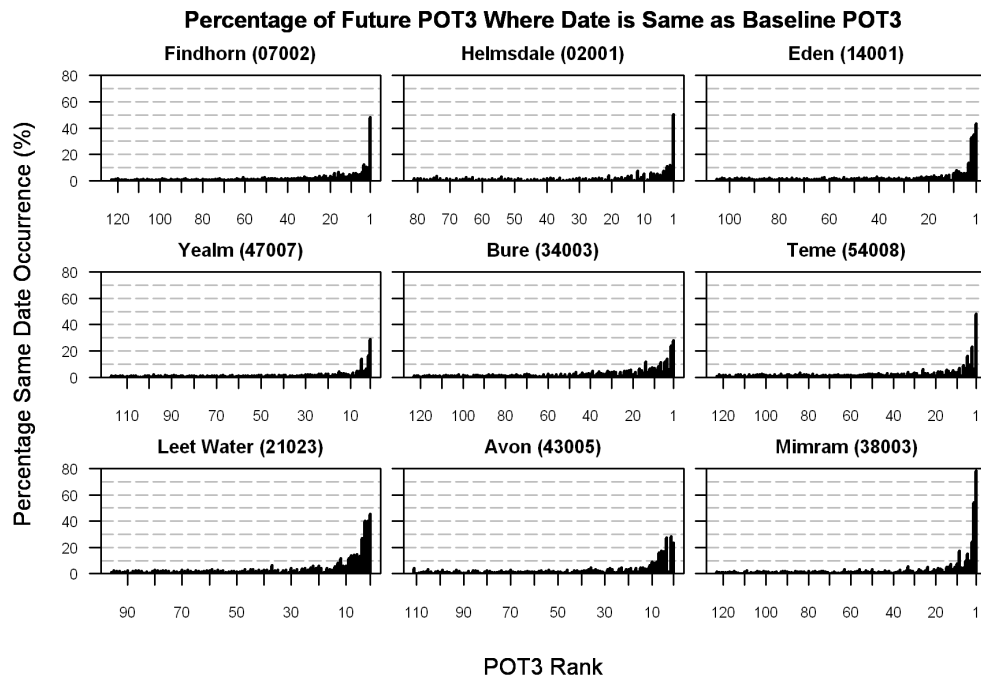
Figure 6.4 POT3 flow events ordered in size (i.e. Rank 1 = largest event), with the percentage of the 10,000 future climate projections that simulate a POT3 rank event to occur on the same day of simulation as the baseline POT3 event of the same rank.

The interaction between the observed precipitation and the precipitation change factors is analysed by comparing the number of time steps from the beginning of the simulation of a given POT3 ranked event (i.e. the rank 1 POT3 event) in the baseline and in the future. The hypothesis is that when the POT3 event occurs on the same simulation time step in the baseline and future, it is the same precipitation event in the observed precipitation record that has generated both baseline and future flood events. Figure 6.4 displays the percentage of the 10,000 UKCP09 derived flow series where the simulation time step for a given POT3 rank is identical to the time step of the same POT3 rank in the baseline.

In the Helmsdale catchment the rank 1 POT3 event (i.e. largest observed flow peak) occurred on 06/10/1993, day 6853 of the baseline hydrological simulation. Of the 10,000 perturbed future climate time series, 50% generate a river flow time series where the rank 1 POT3 event also occurs on day 6853 of the simulation (Figure 6.4– Middle/Top). In the most extreme example, the Mimram catchment, the timing of the rank 1 POT3 is maintained in 80% of the future time series and the rank 2 event is maintained by 50% of the future scenarios. The Mimram is a chalky catchment with a high base flow index (0.93), where the rank 1 and 2 POT3 flood events are preceded by long periods of precipitation in the observed record which are clearly difficult to disrupt, no matter which change factor set is applied. This suggests that

the future perturbed precipitation, which defines the future POT3 events, maintains a degree of memory from the original baseline precipitation which is then propagated through to the resulting future flood record. Across the nine study catchments the percentage of future scenarios which maintain the same baseline and future POT3 timing is greatest for the largest POT3 ranks (> rank 10) and less important at lower POT3 ranked events. This suggests that the largest POT3 events in the future record are often pre-defined by the baseline precipitation time series. This has important implications in the context of flood frequency estimation, where the fitting of a flood frequency curve is most sensitive to the largest POT3 events (Figure 6.2 - Left).

6.4.2 Catchment Precipitation Resampling

The importance of the baseline precipitation in defining future flood events is tested further in this section through a boot-strap resampling method. The observed precipitation is resampled at a monthly time step to create 100 new realisations of precipitation time series for each catchment. A single set of 12 monthly change factors is applied to each of the 100 baseline time series realisations to derive 100 future precipitation time series realisations. This creates 100 pairs of precipitation (1 baseline and 1 future) where the differences between the baseline and future are a result of the set of change factors applied. PDM hydrological simulation is undertaken for the 100 baseline and future precipitation time series, with 20RP values calculated from the simulated river flow series. This analysis is repeated using different sets of precipitation change factors, providing 100 baseline and future pairs of 20RP values for each set of change factors. The results from nine precipitation change factors applied in the Helmsdale catchment are shown in Figure 6.5, describing the relationship between the 100 baseline and 100 future 20RP magnitudes.
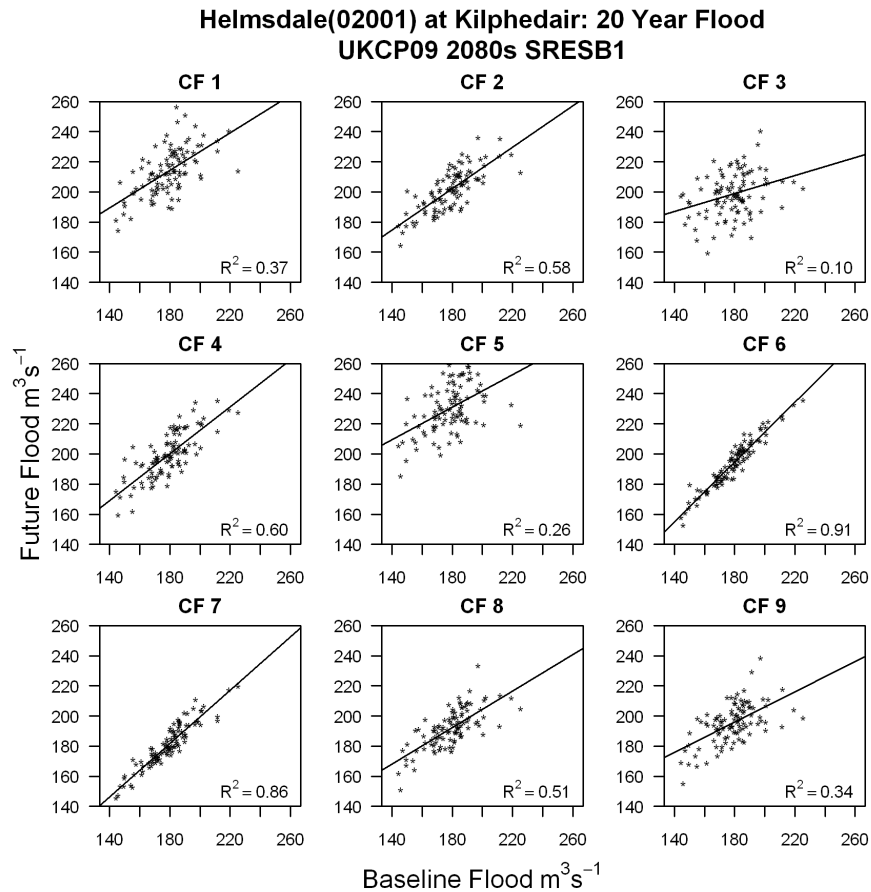
Figure 6.5 Sensitivity of flood frequency analysis to catchment precipitation. Analysis of 20RP for the baseline (x-axis) and future (y-axis). Each plot corresponds to a different precipitation change factor set, with each point a different precipitation realisation. R^2 values are calculated for a linear regression between baseline and future flood quantiles.

The relationship between the baseline 20RP and future 20RP is quantified using a linear regression analysis. The R^2 coefficient, describing the strength of linear relationship, summarises how closely the magnitude of the future 20RP is associated with the magnitude of their corresponding baseline 20RP pair. An R^2 values close to 1 describes that the future 20RP is linearly dependent on the baseline 20RP, whereas an R^2 value close to 0 describes that the future 20RP is not linked to the baseline 20RP.

The result for the Helmsdale (Figure 6.5) displays a range of R^2 coefficients from a minimum of 0.10 to a maximum of 0.91. This suggests that in some instances the magnitude of the future 20RP is highly dependent on the magnitude of the baseline 20RP (R^2=0.91) and in other instances the future 20RP is independent from any baseline 20RP. A similar conclusion emerges across the remaining eight catchments (not shown).

The strength of the relationship between the baseline 20RP and future 20RP is influenced by the seasonality of the precipitation causing the POT3 events and the seasonality of the monthly precipitation change factors. For example, if the precipitation driving the flood peaks occurs in January, and in turn the precipitation change factors have the greatest increase in January, the baseline POT3 distribution will be maintained in the future scenario. In contrast if the precipitation driving the occurrence of flood peaks events occurs across several months (i.e. October-March), the future POT3 distribution is then more influenced by the timing and magnitude of the precipitation change factors.

Applying monthly change factors directly to observed precipitation using a perturbation method can lead to future flood quantile estimates that are a directly linked to the observed record. The occurrence and strength of this linkage is dictated by the timing and magnitude of the observed precipitation causing the catchment flood peaks and the precipitation change factors. This is a clear limitation of the use of change factors for future flood impact analysis. Alternatively a weather generator could be used to create a new daily precipitation time series for each of the 10,000 change factor sets. In this case, the differences between the 10,000 projections would be a mix of the climate change signal (change factors) combined with the climate variability (weather generator), requiring the inclusion of multiple weather generator realisations. To understand both climate change and climate variability each of 10,000 climate change factor sets would require multiple weather generator realisations, which as discussed in section 6.2 could present a computational burden. In light of this the use of the change factor perturbation method is continued in this thesis; with the full quantification of flood frequency uncertainty.

6.5 Climate Change and Flood Frequency Uncertainty

The previous section has shown that baseline and future flood quantile estimates may be both dependent and independent from one another. This property can be exploited in defining the method used to incorporate flood frequency uncertainty between the baseline and different futures. Changes in the 5RP, 20RP and 50RP are estimated in two ways: 1) Assuming that baseline and future flood frequency uncertainty is dependent (referred to as 'dependent uncertainty'); 2) Assuming that baseline and future flood frequency uncertainty is independent (referred to as 'independent uncertainty'). The results of these two methods are compared with the context of including no flood frequency uncertainty in calculated flood quantile changes (referred to as 'no uncertainty').

6.5.1 Dependent Uncertainty

Figure 6.6, Figure 6.7 and Figure 6.8 show the changes in the 5RP, 20RP and 50RP respectively incorporating a 'dependent uncertainty' for each of the UKCP09 change factors (blue histograms-front), compared with the assumption of 'no uncertainty' (grey histograms-back). Changes in the 5RP (Figure 6.6) assuming a 'dependent uncertainty' are very similar to changes assuming 'no uncertainty', as shown by the similar 5th, 50th and 95th percentiles (referred to in this chapter from here as $p5$, $p50$ and $p95$) of 5RP distributions of change. One exception is the Avon where the $p95$ is 20% smaller when a 'dependent uncertainty' is assumed compared with 'no uncertainty' (the blue dashed line are to the left of grey dashed line). For changes in the 20RP (Figure 6.7) a similar pattern emerges with the majority of catchments showing similar distributions of flood quantile changes for both 'no uncertainty' and 'dependent uncertainty'. The $p95$ of the 20RP changes is smaller for a 'dependent uncertainty' compared with 'no uncertainty' in the Avon, Yealm and Mimram catchments. This pattern is stronger for the 50RP (Figure 6.8) with reductions in the greatest change ($p95$) compared with 'no uncertainty' in seven catchments. The $p50$ also displays reductions, although proportionately smaller compared with the $p95$, for three catchments. The 'dependent uncertainty' $p5$ remains similar compared with the 'no uncertainty' $p5$ across all catchments.

The results for all three return periods suggest that the largest potential changes (defined by each distribution $p95$) are smaller when a 'dependent uncertainty' is assumed compared with 'no uncertainty'. This is a consequence of the largest changes in a flood quantile magnitude being caused through very large simulated future flood events. Given the size of these large flood events in relation to the length of record, their magnitude is typically associated with a large SE and hence a larger range of uncertainty. This large SE increases the range of values across the greatest flood quantile changes, which in turn places a greater confidence on the smaller flood quantile changes, resulting in a reduced $p95$ compared with 'no uncertainty' (a broader discussion of this issue is provided in section 8.2.2). Overall the assumption of a 'dependent uncertainty' leads to small decreases in the range of future flood quantile changes compared with the 'no uncertainty' assumption. Therefore incorporating the dependent flood frequency uncertainty ('dependent uncertainty') in the analysis provides little extra information from assuming no uncertainty.
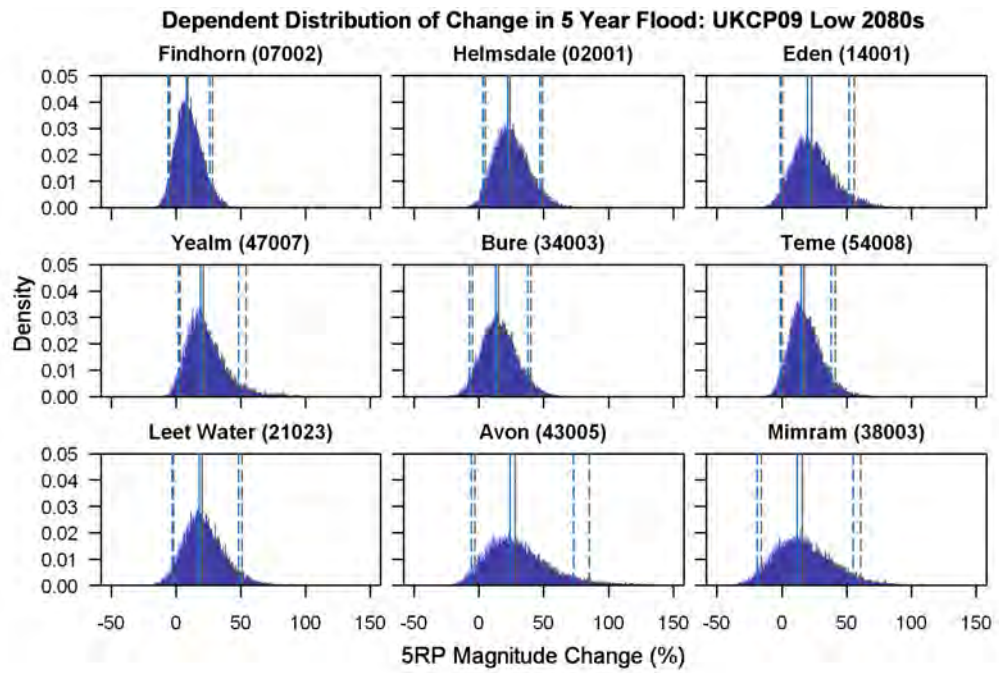
Figure 6.6 Change in 5 year return period flood quantile for the 2080s under a low emissions scenario. The UKCP09 changes assuming no flood frequency uncertainty are plotted in dark grey (back). Results assuming a dependent flood frequency uncertainty are overlaid in blue. Dashed lines show the 5th and 95th percentiles with the median in bold.
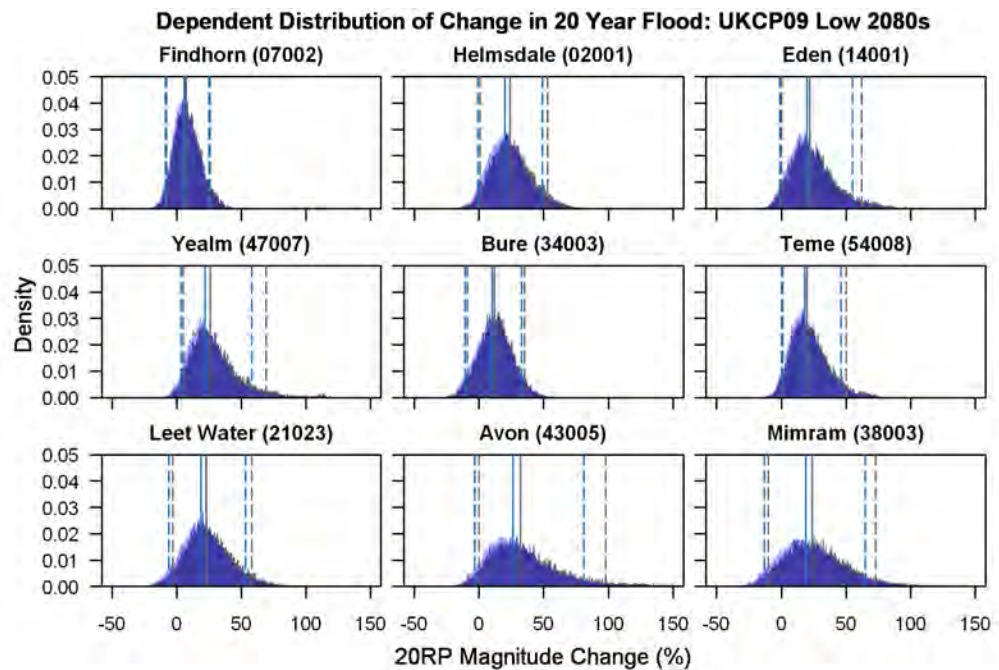
Figure 6.7 Change in 20 year return period flood quantile for the 2080s under a low emissions scenario. The UKCP09 changes assuming no flood frequency uncertainty are plotted in dark grey (back). Results assuming a dependent flood frequency uncertainty are overlaid in blue. Dashed lines show the 5th and 95th percentiles with the median in bold.
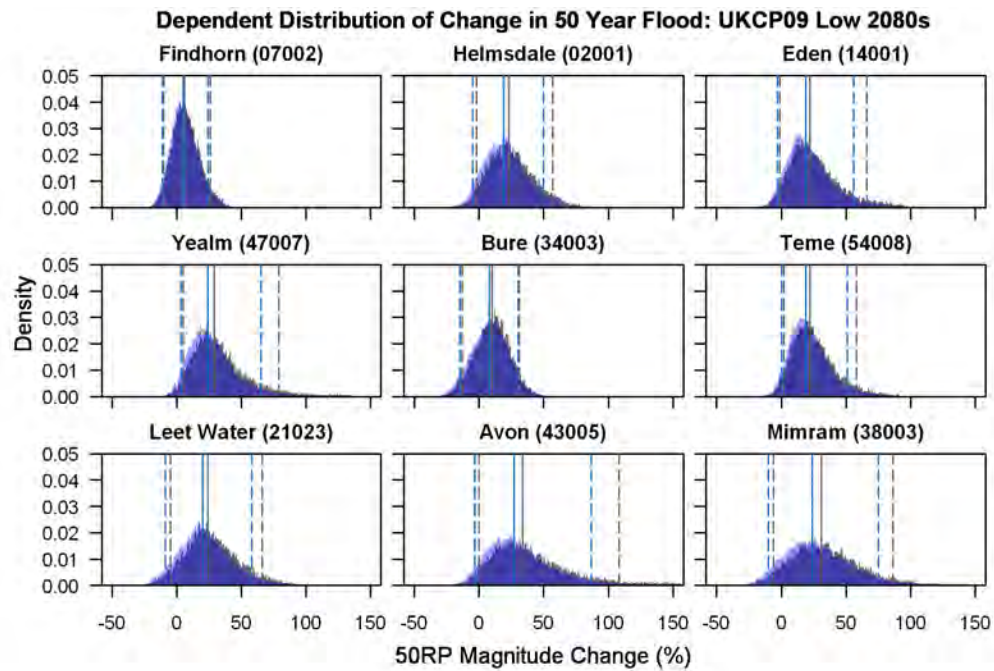
Figure 6.8 Change in 50 year return period flood quantile for the 2080s under a low emissions scenario. The UKCP09 changes assuming no flood frequency uncertainty are plotted in dark grey (back). Results assuming a dependent flood frequency uncertainty are overlaid in blue. Dashed lines show the 5th and 95th percentiles with the median in bold.

6.5.2 Independent Uncertainty

Figure 6.9, Figure 6.10, and Figure 6.11 show the changes in the 5RP, 20RP and 50RP respectively assuming an 'independent uncertainty' for each of the UKCP09 change factors (red histograms-front), compared with the assumption of 'no uncertainty' (grey histograms-back). 'Independent uncertainty' does not alter the range of future flood quantile changes compared with 'no uncertainty' for the 5RP (Figure 6.9), except for small variations in the $p5$ and $p95$ in a few catchments. For the 20RP (Figure 6.10) the 'independent uncertainty' has a greater influence on the distribution of flood quantile changes in three catchments (Findhorn , Bure and Leet Water) with a larger range in 20RP changes compared with 'no uncertainty'. The remaining six catchments display smaller decreases in the $p5$, while the $p50$ and $p95$ remain relatively unchanged compared to 'no uncertainty'. At the largest return period considered, 50RP (Figure 6.11), the distribution of flood quantile changes assuming an 'independent uncertainty' is nearly double the range from just climate change alone ('no uncertainty') in the Findhorn, Bure and Leet Water. In the other six catchments the influence of an 'independent uncertainty' is small and generally associated with small decreases in the $p5$. The increased likelihood of a flood quantile decrease is a consequence of an independent

uncertainty increasing the likelihood that the baseline flood quantile is larger than the future flood quantile when the SE is included. For example, the 50th percentile baseline has a lower magnitude than the 50th percentile future (comparison of 50th percentiles is equivalent to 'no uncertainty'); however assuming an 'independent uncertainty' compares all percentile combinations, for instance the 90th percentile baseline may have a greater magnitude than the 50th percentile future.

For some catchments, 'independent uncertainty' is much larger than 'no uncertainty' suggesting that flood frequency uncertainty analysis must be incorporated in a climate change impact study to provide a robust assessment of the change in future flood quantiles. However for six catchments this is not the case. The next sections investigates how to identify for which catchments and return periods the flood frequency uncertainty analysis must be included for a robust assessment of the climate change impacts on flooding.
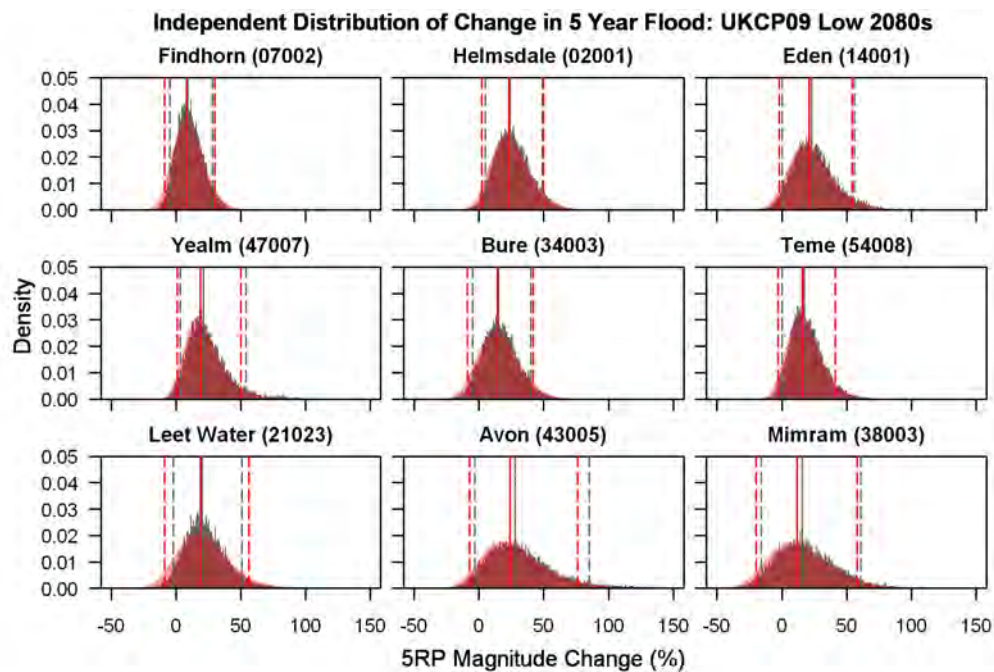
Figure 6.9 Change in 5 year return period flood quantile for the 2080s under a low emissions scenario. The UKCP09 changes assuming no flood frequency uncertainty are plotted in dark grey (back). Results assuming an independent flood frequency uncertainty are overlaid in red. Dashed lines show the 5th and 95th percentiles with the median in bold.
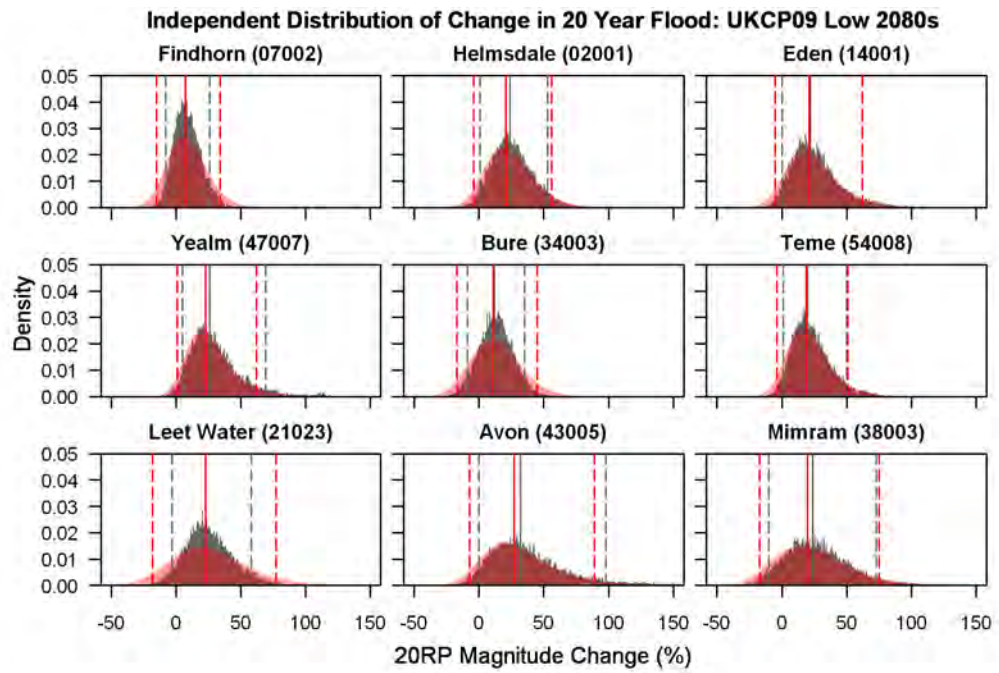
Figure 6.10 Change in 20 year return period flood quantile for the 2080s under a low emissions scenario. The UKCP09 changes assuming no flood frequency uncertainty are plotted in dark grey (back). Results assuming an independent flood frequency uncertainty are overlaid in red. Dashed lines show the 5th and 95th percentiles with the median in bold.
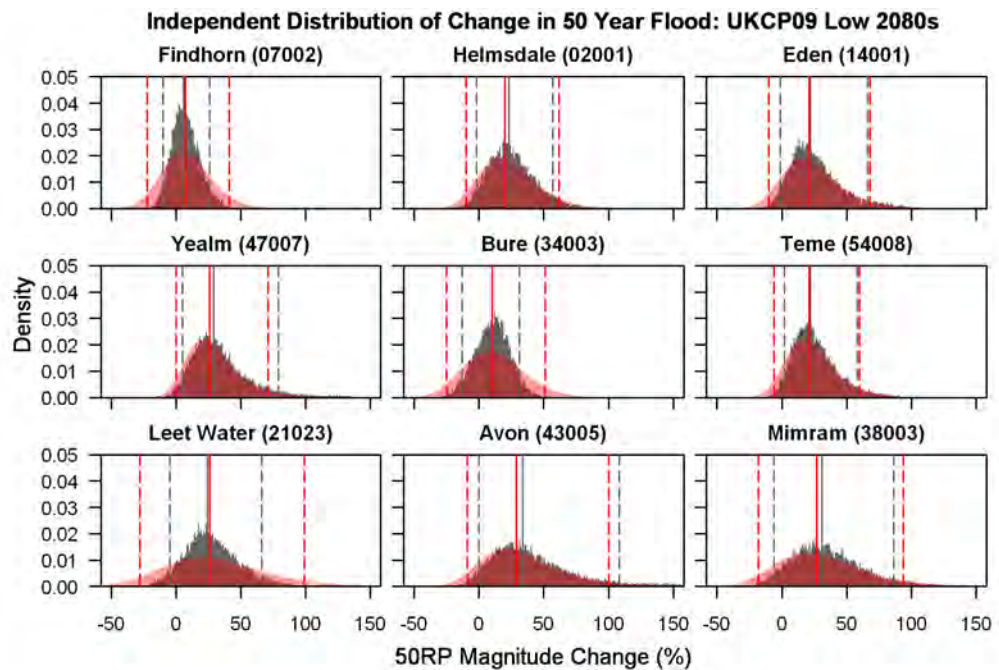
Figure 6.11 Change in 50 year return period flood quantile for the 2080s under a low emissions scenario. The UKCP09 changes assuming no flood frequency uncertainty are plotted in dark grey (back). Results assuming an independent flood frequency uncertainty are overlaid in red. Dashed lines show the 5th and 95th percentiles with the median in bold.

6.5.3 Predicting the Role of Uncertainty

The interaction between the precipitation change factor scenario and baseline precipitation was shown in section 6.4 to define the type of uncertainty (i.e. dependent or independent) that is most likely to occur when estimating changes in flood quantiles. This means that for the UKCP09 scenarios which include a range of precipitation change factor scenarios, it is likely that a combination of both dependent and independent uncertainty should occur. Given that considering a 'dependent uncertainty' results in changes in flood quantiles that are similar to an assumption of 'no uncertainty', the uncertainty in future flood quantile changes will be considered as 'independent uncertainty' to provide the most robust characterisation of uncertainty. The influence of the 'independent uncertainty' between baseline and future flood frequency quantile changes is controlled by two interacting factors. The first factor is the size of the baseline flood frequency uncertainty as measured by the magnitude of SE for a flood quantile of a given return period in a catchment, although from Table 6.1 it can be seen that this statistic alone does not dictate the role of flood frequency uncertainty. The Findhorn and Mimram have similar baseline standard errors across all three return periods, but the inclusion of the SE assuming 'independent uncertainty' has a larger influence on the distribution of future flood quantile changes in the Findhorn. The second influencing factor is the range of the climate change distribution prior to considering flood frequency uncertainty ('no uncertainty'). In the case of the Findhorn it has a much smaller range of future flood quantile changes from the impact of just the UKCP09 precipitation change factors compared with the Mimram. This suggests that the influence of assuming an 'independent uncertainty' for a given catchment and return period, relies on the size of the standard error of the baseline flood quantile estimate and the range of the distribution of future flood quantile changes with no uncertainty.

Assuming that the baseline flood quantile's standard error of estimate ($Base_{SE}$) is representative of the uncertainty for both baseline and future flood frequency analysis, and that the standard deviation of the distribution of future flood quantile changes resulting from multiple precipitation change scenarios (CC_{SD}) represents 'no uncertainty', a ratio of $Base_{SE}/CC_{SD}$ gives the relative importance of both factors. The ratios are shown in Table 6.2 for all catchments and three return periods. In the Findhorn, Bure and Leet Water the ratio exceeds 1 for the 20RP and 50RP. The ratio is significantly less than 1 for all other catchments for the 20RP and 50RP, and in all catchments for 5RP.

Table 6.2 Ratio of the standard error for baseline flood quantile estimate (Base$_{se}$) to the standard deviation of the 'no uncertainty' distribution (CC$_{sd}$) of future flood quantile changes without uncertainty ('no uncertainty'). Ratios > 1 indicate the uncertainty in the baseline flood estimate is greater than the distribution of climate change.

NRFA Gauge	Ratio Base$_{SE}$/CC$_{SD}$		
	5RP	20RP	50RP
Findhorn (07002)	0.62	1.43	2.23
Helmsdale (02001)	0.29	0.52	0.69
Eden (14001)	0.29	0.55	0.77
Yealm (47007)	0.18	0.28	0.33
Bure (34003)	0.51	1.32	2.19
Teme (54008)	0.35	0.57	0.70
Leet Water (21023)	0.56	1.25	1.88
Avon (43005)	0.20	0.37	0.51
Mimram (38003)	0.26	0.56	0.81

The efficiency of this metric to measure the influence of incorporating an 'independent uncertainty' when assessing flood quantile changes is evaluated using a linear regression analysis. The regression analysis uses Base$_{SE}$/CC$_{SD}$ as the predictor of the percentage difference in the range (*p*95-*p*5) of flood quantile changes assuming 'no uncertainty' and 'independent uncertainty'. The percentage difference is used as opposed to the absolute ranges to allow for comparison between catchments. The regression relationship is fitted for the 5RP, 20RP and 50RP floods across all nine catchments (Figure 6.12-Left). It shows a strong linear correlation and a good model fit with an R^2 value of 0.96 suggesting the ratio is an effective metric. The Findhorn, Leet Water and Bure cluster in two positions near Base$_{SE}$/CC$_{SD}$ values of 1.5 and 2.2 for the 20RP and 50RP floods respectively. All other catchments and return period values are clustered with a Base$_{SE}$/CC$_{SD}$ less than 1 where the difference in ranges is less than 20%. The regression relationship was then tested in a predictive manner for the 100RP flood (Figure 6.12-Right) with the results displaying a good fit compared with the regression line calculated from the smaller return period values. This analysis indicates that the magnitude of an 'independent uncertainty' relative to 'no uncertainty' can be quantified using the ratio Base$_{SE}$/CC$_{SD}$ as an indicator. However the difference in range between the 'independent uncertainty' and 'no uncertainty' cannot be directly applied to the 'no uncertainty' distribution due to the differences between

'independent uncertainty' and 'no uncertainty' being non-linear (i.e. the difference at the *p95* is larger than the difference at the *p5*).
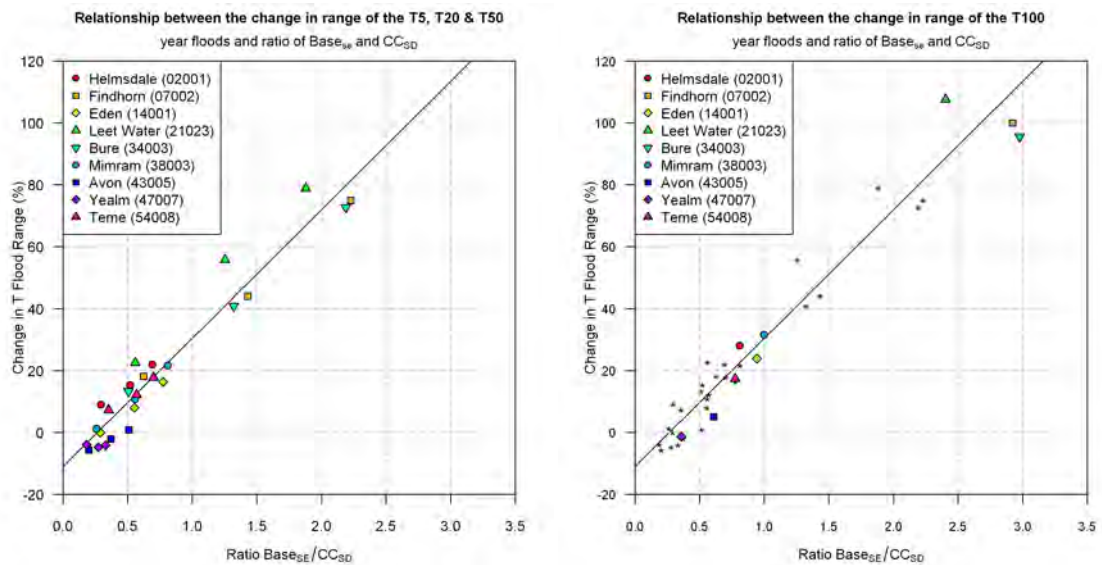
Figure 6.12 Regression relationship between Base$_{SE}$/CC$_{SD}$ and the percentage difference in the range of flood quantile changes assuming 'no uncertainty' and 'independent uncertainty'. Regression relationship is based on the 5RP, 20RP and 50RP year floods (left), with the relationship tested for 100RP (right). Black diagonal line is the regression model fit. Starred points on right panel are the coloured points from the left panel.

This section has demonstrated that the effect of including flood frequency analysis uncertainty has a degree of predictability by estimating the magnitude of its impact on the range of the distribution of future flood quantile change. The ratio can be used as an initial screening tool to identify in which catchments flood frequency uncertainty is important and should therefore be included in assuming an 'independent uncertainty'. This allows for the robust characterisation of flood frequency analysis uncertainty, but identifies when flood frequency uncertainty can be ignored if the information it contributes is of lesser importance compared to the uncertainty due to the climate projection alone.

6.6 Discussion and Conclusions

This chapter has sought to quantify the uncertainty associated with calculating the climate change impact on the T-year flood event using flood frequency analysis. The flood frequency uncertainty has been quantified using a standard error of estimate calculated from the GP distributions parameters for the baseline river flow series and future river flow series derived from 10,000 UKCP09 precipitation change factors. The magnitude of the standard error of

uncertainty is associated with the return period of interest (i.e. higher return periods have a larger standard error) with the SE magnitude dictated by the slope of the flood frequency curve. Curves with a slope less than 0 (unbounded) have a higher associated standard error compared with bounded flood frequency curves (slope > 0). The slope of the flood frequency curve is defined by the observed flood events more so than the catchment characteristic. The standard error can therefore not be generalised across categories of catchments and is specific to a catchment's observational record.

When using precipitation change factors the future perturbed precipitation time series maintains a degree of memory from the baseline precipitation, causing flood events to be generated at the same time step of both baseline and future hydrological simulations. Therefore the future flood quantiles and their associated uncertainty may in some cases be an artefact of the observational record (and in turn the decisions of the impact scientist) rather than the influence of climate change. Whether this is the case depends on the combined seasonality of the flood driving precipitation in the observational record and the seasonality of the precipitation change factors. This is a clear limitation of the use of climate change factors for the analysis of extremes such as flooding, however through characterising the flood frequency uncertainty this can be accounted for.

In light of this, when calculating changes in flood quantiles the flood frequency uncertainty for the baseline and future can be considered in two ways; dependently, so that the magnitude of the baseline and future flood quantiles are linearly linked, and independently, where any baseline flood percentile can result in any flood percentile of the future flood distribution. Assuming a dependent flood frequency uncertainty offers little additional information compared to the results with no uncertainty, suggesting it need not be considered in the impact analysis. Assuming an independent flood frequency uncertainty between baseline and future has little influence at the smallest return period (5RP), but at the largest return periods (20RP & 50RP) is shown to influence the range of future changes in three catchments. At the largest return period (50RP) the range of future flood quantile changes nearly doubles when an independent flood frequency uncertainty is assumed compared with considering no uncertainty. The month to month variability of each UKCP09 precipitation change factor means that different proportions of the 10,000 change factors are likely to be associated with either a 'dependent uncertainty' or 'independent uncertainty'. In this study all 10,000 change factor sets are assumed to have an 'independent uncertainty' to robustly capture the impact of

flood frequency analysis uncertainty. Alternatively, prior analysis of each change factor set could create a targeted approach of when to assume an 'independent uncertainty' or 'dependent uncertainty'. The results also highlight that flood frequency uncertainty must be considered in climate change impact studies of flooding, although not in all catchments.

The need to incorporate the independent flood frequency uncertainty can be indentified using the ratio of the baseline flood frequency uncertainty to the standard deviation of the climate change impact distribution (i.e. is the uncertainty associated with flood frequency estimation larger than that due to climate change uncertainty). There is a strong linear relationship between this ratio and the size of the distribution of the T-year flood change (in percent) when independent uncertainty is assumed, showing that the combined range of climate change and flood frequency uncertainty can be estimated. However the estimated range cannot be used as a substitute for a full uncertainty analysis as the difference between 'independent uncertainty' and 'no uncertainty' is non-linear. Further analysis, with a larger number of catchments, could allow for this non-linearity to be accounted for in the estimation process.

6.7 Chapter Summary

This chapter has quantified the uncertainty associated with calculating changes in T-year flood quantiles using flood frequency analysis. The uncertainty associated with a flood quantile estimate at a given return period was calculated using a standard error of estimate based on the GP distribution parameters. The size of the standard error was found to be linked to the slope of a catchment's flood frequency curve.

Precipitation change factors were shown to have a strong influence on the derivation of future flood quantiles meaning that the translation of flood frequency uncertainty from the baseline to the future was considered in two ways, either dependently or independently. A dependent flood frequency uncertainty was found to have little influence on the distribution of future flood quantile changes. Whereas assuming an independent flood frequency uncertainty was found to be important in three out of nine catchments at larger return periods (20RP and 50RP) but not at the smaller return period (5RP). In the remaining six catchments the uncertainty in flood frequency estimation was found to be of lesser importance.

The impact on the flood quantile distribution from assuming an independent flood frequency uncertainty was found to have a degree of predictability. This predictability was informed by

the size of the climate change distribution and the magnitude of a catchment's baseline flood estimate standard error. This allowed for the creation of a simple screening process to identify when it is important to include flood frequency analysis uncertainty prior to undertaking a full impact analysis.

This chapter and the preceding two chapters have raised a number of issues relating to climate change and flooding, including hydrological non-linearities, the importance and reliance on the observed precipitation record and the combined seasonality of climate change and flooding, which will all be discussed in greater detail in the next chapter.

CHAPTER 7

Hydrological Conclusions

7.1 Introduction

The previous chapters in this thesis have focussed on different sources of uncertainty which contribute to assessing the impact of climate change on flooding. The role of the different uncertainty sources have been shown to vary between the nine study catchments and are influenced by a number of factors. This chapter aims to highlight three hydrological factors which influence the assessment of the impacts of climate change on flooding; these include:

- The role of the observed flow record in flood frequency analysis.
- The non-linearity of a catchment's hydrological response to a change in the catchment climatological inputs.
- The combined but competing influence of the seasonality of a catchment's flow regime and the seasonality of climate change projection.

Each of these factors is presented in a different section of this chapter; the role of the observed record is presented in section 7.2, followed in section 7.3 by a discussion of hydrological non-linearities. Linking the combined influences of observed flood seasonality and climate change factor seasonality is the last hydrological conclusion discussed in section 7.4. The chapter finishes with a summary in section 7.5.

7.2 Role of the Observed Flow Record in Flood Frequency Analysis

In Chapter 6 the observed flow record was shown to be important when calculating flood return period quantiles because it defines the size of the error associated with a given quantile as well as the magnitude of the quantile itself. Furthermore when using precipitation change

factors in a climate change impact assessment the baseline precipitation record was shown in some cases to directly define the magnitude of future flood events due to a memory effect between baseline precipitation and change factor perturbed future precipitation. This section further explores the importance of the observed flow record by undertaking flood frequency analysis using different record lengths and averaging periods.

7.2.1 Flood Frequency with Varying Record Length and Averaging Period – Method

So far in this thesis flood frequency analysis has been undertaken using the maximum available record length (26-40 years depending on catchment) to utilise as much information as possible when estimating flood return period quantiles (Kidson and Richards, 2005). An alternative method is implemented here by moving a window of differing record length (2, 5, 10, 20 and 30 year record length) across the observed river flow record. For each window the flow series is sampled using POT3 analysis with a GP distribution as outlined in section 0, with a standard error (SE) of estimate calculated for each flood quantile (as outlined in section 6.3). The analysis is undertaken for the Findhorn, Mimram and Teme catchments which have the longest available records of 40 years from 1961-2001.

7.2.2 Flood Frequency with Varying Record Length and Averaging Period - Results

The results of undertaking flood frequency analysis using a moving window with varying record length for estimating the 50RP and associated SE are shown in Figure 7.1 for the Findhorn (top) and Mimram (bottom); for the Teme catchment analysis was undertaken for 5RP (Figure 7.2-left) and 50RP (Figure 7.2-right).

The 50RP results (top panels) for all three catchments show an increasing sensitivity of the magnitude of the flood quantile estimate as the record length decreases. For shorter record lengths (2-5 years) there are significant step changes in flood magnitude estimates as the record window moves caused by small or large POT events entering or exiting the period of record. The variability of the flood estimate decreases with longer record lengths where estimated flood quantiles tend towards similar magnitudes independent of the averaging period. Note that in practice, it is recommended not to estimate a return period that is greater in size than double the record length when undertaking flood frequency analysis (Institute of Hydrology, 1999).
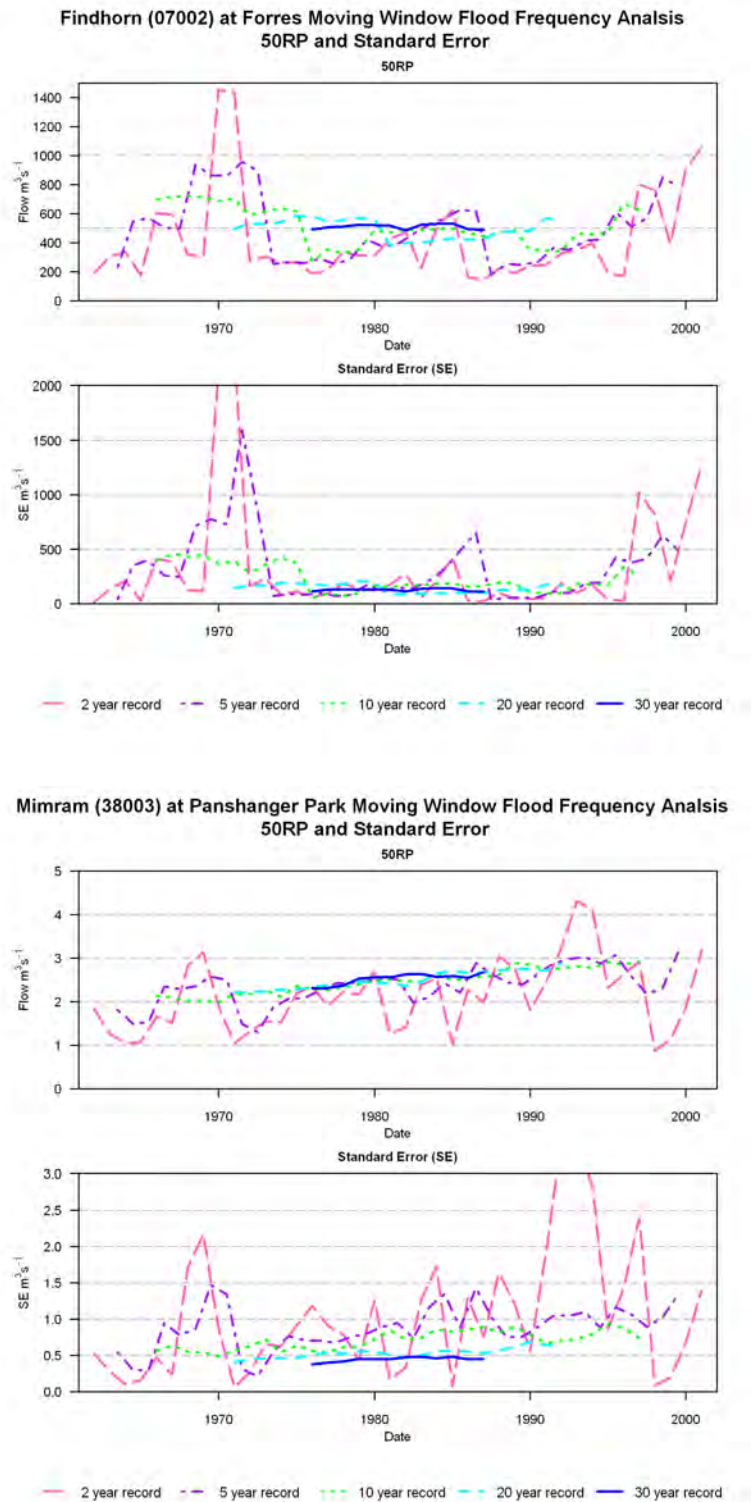
Figure 7.1 Assessment of the role of the observed flow record for flood frequency analysis in the Findhorn (top) and Mimram (bottom) catchments. Moving window analysis of the 50RP using a 2 year record (pink dashed), 5 year record (purple dot dash), 10 year record (green dotted), 20 year record (cyan long dash) and 30 year record (blue solid) shown in the top panel and the associated standard error of estimate (se) shown in the bottom panel.
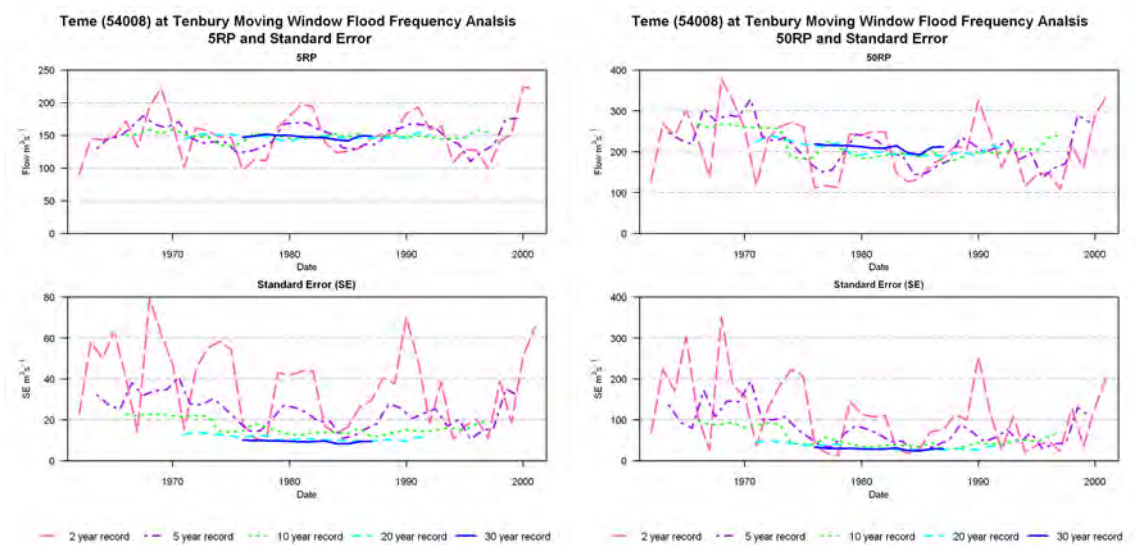
Figure 7.2 Flood frequency analysis using a moving window and varying record length to calculate the 5RP (left) and 50RP (right) in the Teme catchment. Description of graphs same as for Figure 7.1.

In the Findhorn catchment there is a greater variation in the 50RP value between the 20 and 30 year records compared with the other catchments. This variation is the result of a single extreme POT event which has a strong influence on the estimated flood quantile. In 1971 there is a large stepped increase in the 2 year and 5 year record lengths in response to this large POT event becoming part of the POT sample. Its influence in the 10 year record length can be seen in the late 1970s where a stepped decrease in 50RP magnitude occurs when the event is no longer included. The same effect, although smaller in magnitude, can be seen for the 20 and 30 year records in the early 1980s.

In the Mimram and Teme catchments the 50RP values are of consistent magnitude for the 10, 20 and 30 year record lengths. However, the standard error of estimate for each 50RP estimate can be seen to decrease in magnitude as the record length increases. In these instances increasing the length of record does not influence the magnitude of the 50RP estimate; the lower standard error indicates a greater confidence in the 50RP calculated from the longer record.

There is evidence in the 50RP estimates for the Teme and Mimram of longer term variations in the flood estimate, likely to be caused by natural variability in the climate. The 50RP in the Mimram catchment displays a gradually increasing magnitude over time. Using a 30 year record centred in the mid 1970s provides a 50RP 20% lower than for a 30 year record centred

in the mid 1980s. In the Teme catchment the 50RP has a 10% decrease in magnitude for 5 years in the 1980s in the 30 year record.

The 5RP and 50RP are both calculated for the Teme catchment with the 5RP displaying less variability in its estimated magnitude compared with the 50RP. The greater variability of the 50RP is due to its dependence on a small number of larger flood peaks when fitting a GP distribution. When fewer POT samples are used (i.e. from shorter record lengths) the GP distribution must be extrapolated beyond the observations for the 50RP estimate. This is not the case for the 5RP which has a greater number of observed POT events which are 'representative' of its return period compared with the number of POT events representative of the 50RP. This is demonstrated by the standard error for the 5RP having a much smaller magnitude compared with the 50RP, quantifying the difference in confidence of the POT events representing the return period estimate.

The observed flood record has been shown to play an important role when calculating flood return period quantiles. The influence of a single observed flood peak can significantly alter the magnitude of an estimated return period quantile, even with a record length of 20 years. The variation in a flood quantile estimate is greatest for larger return periods which are more sensitive to the fitting of an assumed flood frequency distribution; often due to an extrapolation of the distribution beyond the observed peaks.

The length of the observed record is also important, with longer records generating less variability in an estimated flood quantile. Although it is important to note that the length of record itself does not necessarily define the flood quantile magnitude; the 10, 20 and 30 year record lengths are shown to provide the same flood estimate in the Mimram and Teme. For these two catchments increasing the length of record does not alter the flood magnitude estimate, but it provides a greater confidence in the calculated value.

In these example case studies of flood frequency analysis a 20 year record length provides the minimum record length from which a consistent 50RP estimate can be made; although a degree of variability still occurs in some instances. Estimates from longer records will have an associated greater confidence as indicated by the lower standard error.

7.3 Non-Linearity of Hydrological Response

Catchment systems have been shown to have a non-linear response to changes in catchment precipitation inputs. This is shown in Chapter 4 where monthly precipitation changes are buffered when translated to monthly flow changes. Chapter 5 used a sensitivity based approach for analysing model parameter reponses to uniform precipitation increases; the 50RP change in response to a 100% uniform increase in precipitation ranged from 100%-400% across all nine catchments. Furthermore the nine case study catchments used in this thesis have been identified in a previous study as displaying a different hydrological response to a change in their inputs (Prudhomme et al., 2010). This section explores the non-linearity in a catchment's flood reponse by using the 10,000 UKCP09 precipitation change factors to derive changes in the 20RP for the 2080s in the Helmsdale and Teme catchments.

The 10,000 UKCP09 precipitation change factors are used to perturb the observed catchment precipitation which is input to the PDM model to create 10,000 new river flow series. Flood frequency analysis is then undertaken on each river flow series to derive changes in the 20RP relative to the baseline. The results are plotted in Figure 7.3 comparing the change in 20RP with the magnitude of its corresponding monthly change factor for the Helsmdale (top) and Teme (bottom). The 5th, 50th and 95th percentiles of each monthly change factor distribution are calculated with their associated 20RP change highlighted in red. The 5th, 50th and 95th percentiles of the changes in 20RP distribution are calculated with blue points marking the change factors which caused those 20RP changes. The aim of this analysis is to highlight the non-linear nature of a catchment's response to a given change.
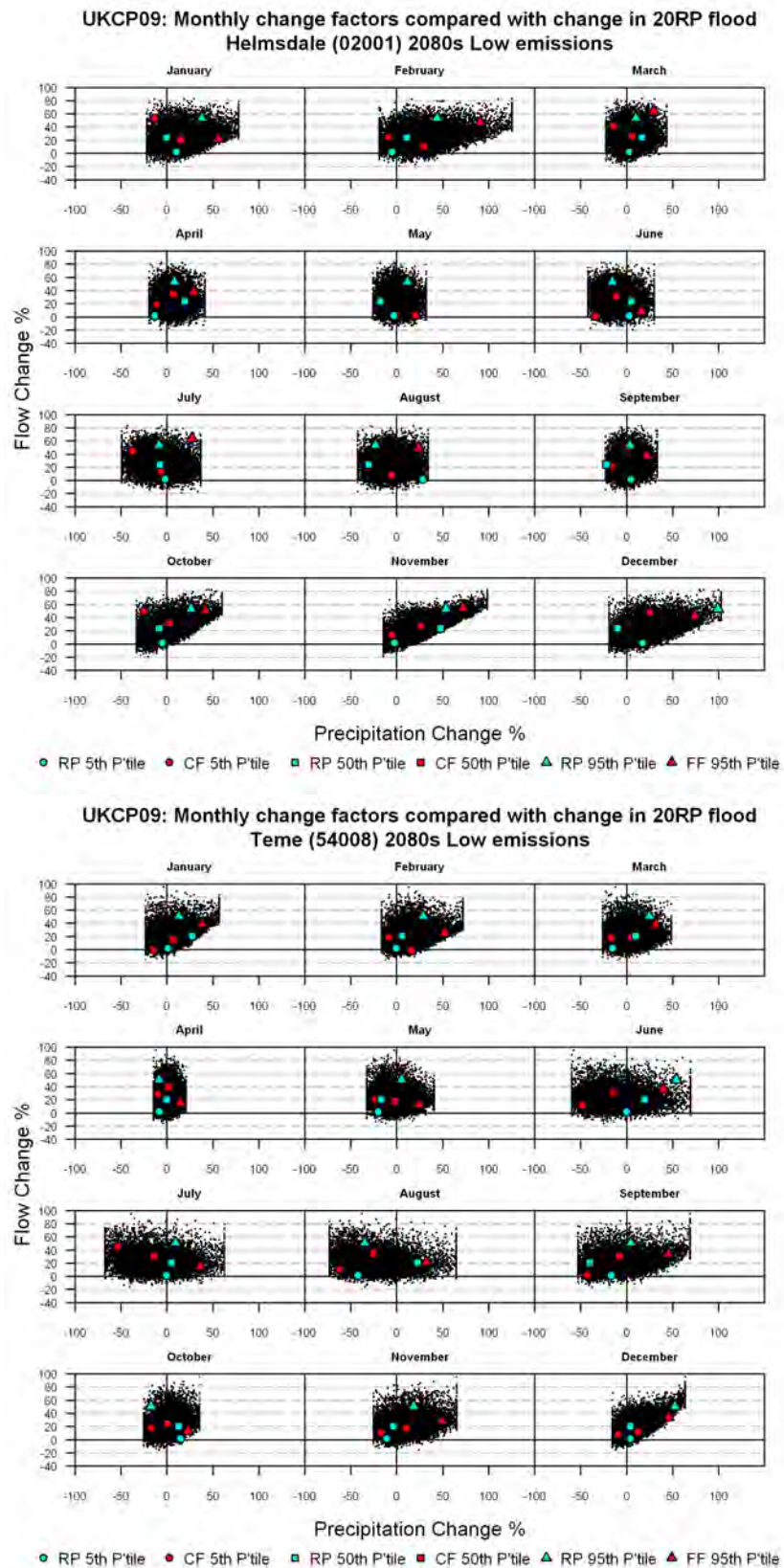
Figure 7.3 20RP change compared with monthly precipitation change factor for the Helmsdale (top) and Teme (bottom) catchments. Points derived for the 5th (circles), 50th (squares) and 95th percentile (triangles) of the 20RP distribution (blue) and precipitation change factor distribution (red) are highlighted.

In each catchment the change in 20RP displays a degree of relationship with different monthly precipitation change factors, where larger precipitation changes are associated with a minimum change in 20RP (i.e. for a given precipitation change the 20RP change is always greater than this threshold). For the Helmsdale catchment the changes in 20RP are associated with the change factors for October, November, December, January and Febuary; the relationship is strongest in November. In the Teme a similar relationships is found for the change in 20RP with November, December, January and February monthly change factors. However, although these months display a positive correlation with flood changes it is not possible to establish an empirical relationship between a flood change derived from a given precipitation change (work not shown). This is due to the inter-relationships between the different combinations of change factors each month, highlighted by the wide spread of flood changes.

The monthly change factors which produced the 95th percentile 20RP flood are shown as blue triangles. In the Helmsdale this is linked to large precipitation changes in November (+55%) and December (+100%). However, the same magnitude change in 20RP could be obtained with a precipitation change of -10% in November and -20% in December; this shows that changes in flood peaks do not only depend on changes in precipitation for specific months but on the precipitation changes over a combination of months. The converse relationship is also true where a large precipitation change does not necessarily lead to a large 20RP change. The red points represent the 95th percentile precipitation change factor for each month and their associated change in 20RP. In the Teme the 5th and 50th percentiles of December precipitation change are both associated with a 10% increase in 20RP, but the same magnitude of December precipitation change could result in flood changes ranging from -10% to +50%.

The results confirm that due to the non-linearity in the hydrological response, it is not possible to establish empirical relationships between monthly precipitation changes and their associated flood changes. This highlights the importance and necessity of undertaking hydrological impact studies through rainfall-runoff modelling. Furthermore this non-linear hydrological response highlights a challenging issue with the advent of probabilistic climate change scenarios (i.e. UKCP09). In the example of UKCP09, which provides 10,000 scenarios, there may be a desire to use a reduced number of scenarios for reasons of computational efficiency. Because of the non-linear flood response and the inter-relationships of monthly precipitation change factor response, care must be taken when sampling a reduced

number of projections. Analysis must be undertaken to ensure that the reduced sample of projections are representative of the full sample of catchment impact response as well as the input climate change information.

7.4 Influence of Seasonality of Climate Change on Flooding

The previous section has shown that the seasonality of precipitation change factors influences the magnitude change of flood quantiles (i.e. positive correlation between some monthly change factor and 20RP change). In Chapter 6 the combined seasonality of the flood events in the observed record and the future precipitation change factors were shown to lead to baseline and future flood changes which are dependent on one another. The hypothesised rationale in both these cases is that where large increases in a precipitation change factor occur in the same month as the precipitation causing the observed POT flood events, the sequence and timing of 'future' flood events is unchanged and simply increased in magnitude. In these instances the future flood frequency distribution is defined by the baseline flood distribution rather than the impacts of climate change alone which could potentially misrepresent the impact of future climatological changes. It is important to note that this hypothesis arises due to the use of change factors as opposed to alternative use of the future climate information (i.e. weather generators, RCMs).
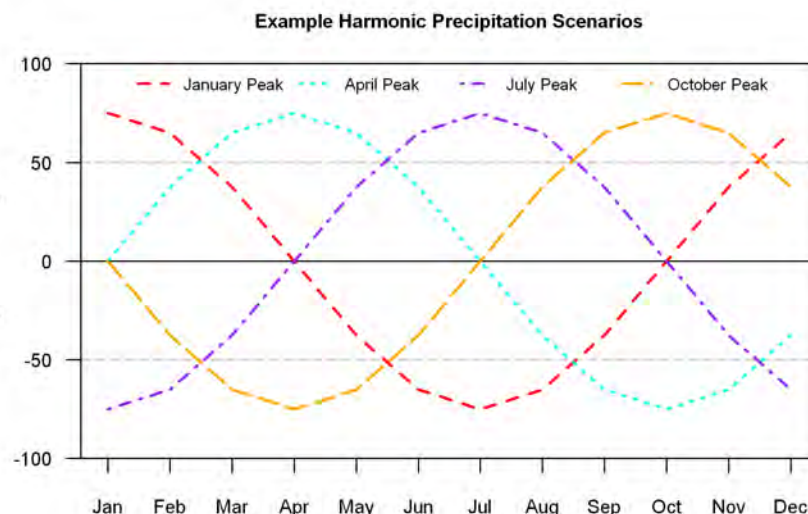
Figure 7.4 Precipitation change factors created using harmonic functions with a mean of 0 and amplitude of ±75%.

The hypothesis is tested here using artificially created monthly precipitation change factors derived using a harmonic function. A harmonic function is an oscillating function similar to a

sine or cosine curve created here with a phased fixed for each month of the year, with amplitude of ±75% about a mean change of zero (Figure 7.4). This creates 12 sensitivity change factor sets, with a maximum peak fixed for each month of the year. These harmonic change factors are used to perturb the observed precipitation similarly to the change factor method applied throughout this thesis. The changes in flood return period quantiles resulting from each monthly phase peak are shown in Figure 7.5 for the Yealm (top left), Leet Water (top right), Bure (bottom left) and Mimram (bottom right) catchments.

The Yealm catchment (top left) displays large changes for only the highest flood return periods for scenarios with a peak in precipitation change between March and August. When the peak in precipitation change occurs between November and January the flood changes become increasingly uniform across the different return periods. Notably the magnitude change of the largest return period quantiles display little variability across the different monthly phases. This is particularly significant in the example of a July harmonic precipitation peak which only has precipitation increases between May and September, resulting in a 90% increase in the 50RP. Between May and September in the observed record the three largest POT events have a rank of 9, 42 and 65 (i.e. a season typically of modest flood events). The flood response of the Yealm catchment has a large sensitivity to precipitation change to generate such a large flood increase from such modestly ranked baseline flood events. This sensitivity is a reflection of the catchments 'flashy' hydrological response to rainfall.

In the Leet Water catchment (top right) the largest return period floods display the greatest changes in precipitation that peak from September to November. However as the precipitation phase peak moves through the year the smaller return period changes increase in magnitude until in December near uniform changes occur in all months. When precipitation peaks in January onwards, the smaller return periods have changes of greater magnitude than the largest return periods. This is also the case in the Bure catchment; with the uniform flood increases occurring in October as opposed to December. In these two catchments the precipitation in the months prior to the month displaying uniform flood changes have the greatest influence over the largest flood peaks, whereas the precipitation in the months that occur after the uniform changes are more important for smaller flood peaks.
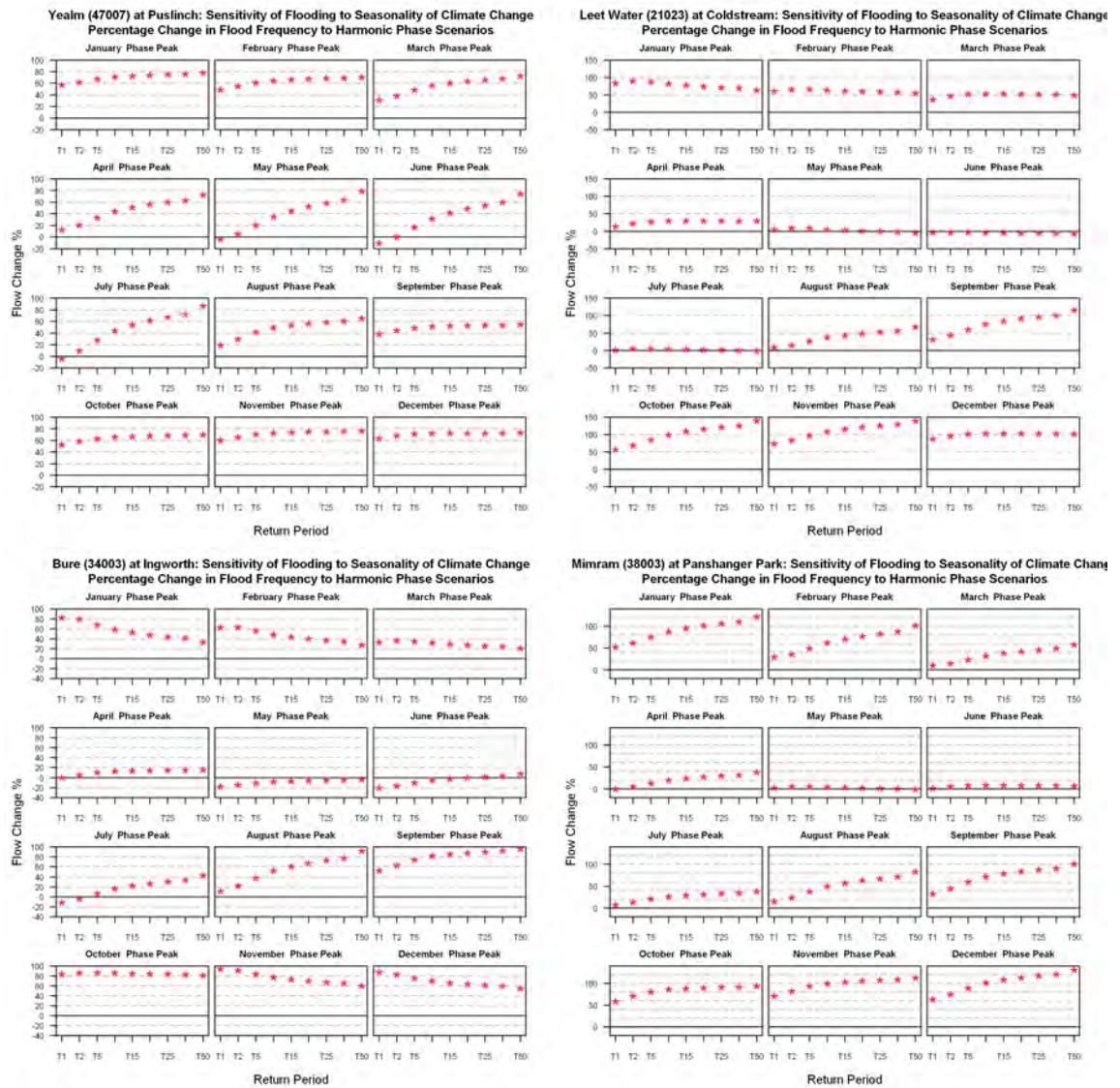
Figure 7.5 Percentage change in flood return periods for the Yealm (top left), Leet Water (top right), Bure (bottom left) and Mimram (bottom right) catchments in response to precipitation changes derived with a harmonic phase fixed at each month of the year (monthly panels).

There is a seasonal cycle in the magnitudes of flood quantile changes in the Mimram catchment (Figure 7.5-bottom right). The largest return period floods always display the largest changes in magnitude regardless of the seasonality of the precipitation change, with the greatest flood increases associated with a December precipitation peak. The precipitation scenarios which peak in May and June do not display a change in flood magnitude for any return periods. In the observational record the largest POT events (e.g. top 10 events) occur between February and April in the Mimram catchment. The largest flood changes occur with the December precipitation peak change, suggesting that December precipitation is important for establishing catchment antecedent conditions with a lagged flood response of 2-3 months.

A similar lagged response is found in the Bure catchment where the largest observed POT flows occur from November to April, however the greatest flood changes are associated with precipitation peaks in August, September and October. This lagged response is a feature of base flow dominated catchments where antecedent conditions are the most important control on the catchment flood response to rainfall.

This sensitivity analysis demonstrates the complex connection between changes in flooding in response to the varying seasonality of precipitation changes. The role of seasonality is different for each catchment, dependent on the seasonality of the baseline flood events and the catchment properties controlling antecedent conditions. Catchment properties are also influential with 'flashier' catchments having a flood sensitivity to precipitation changes in any month, whereas the flood changes in slower response base flow catchments are more dependent on the autumn/winter antecedent conditions. Further analysis was undertaken on the underlying future flow POT data (not shown). However establishing links between the seasonality of the POTs in relation to the seasonality of the precipitation changes was not possible. This is likely due to the way POT events are defined and extracted. In a future flow time series created by perturbed climate inputs an increase (decrease) in the number of POT events in a particular month can occur due to a decrease (increase) of events in a different month. For example there may be an increase in the number of December POT events due to a +30% increases in December precipitation; alternatively more POT events may occur in December due to a reduction in the number of POT events occurring in February independent from any links to December.

The combined interaction between the seasonality of precipitation change and the seasonality of the observed catchment flood regime has been shown to create different catchment responses and magnitudes of flood changes. This is due to the importance of the observed record when using climate change factors, with future flood changes dependent on the structure of the baseline flood regime and catchment properties.

7.5 Chapter Summary

This chapter has identified three main hydrological conclusions that can be drawn from this thesis; firstly the influence of the observed flood record in deriving flood return period estimates; secondly the non-linear response of hydrological systems to a change in catchment precipitation and lastly the inter-dependence between observed catchment flood seasonality

and the seasonality of precipitation changes when using a perturbation based impact study analysis.

The role of the observed flood record was demonstrated by undertaking flood frequency analysis using a shifting window with varying record lengths within the full observed record. The results demonstrated that a single flood event could have a significant influence on the flood estimates up to a record length of 20 years (up to the 50RP flood). In other examples flood estimates were found to be of similar magnitude calculated from a 10, 20 or 30 year record with a decreasing error at larger record lengths. These instances indicate a greater confidence in a flood estimate derived from a longer record length; although similar magnitude flood estimates can be obtained from shorter records just with less confidence.

The UKCP09 precipitation change factors were compared with their associated changes in the 20RP to highlight the non-linearities in hydrological systems. The inter-relationship between the monthly precipitation changes means that no direct empirical relationships can be established between a given monthly precipitation change and a resulting change in flood magnitudes. This shows the importance and necessity of hydrological modelling in impact assessments, and highlights that a wide combination of climate change scenarios need to be considered to undertake a robust impact assessment.

Lastly a sensitivity analysis was undertaken using harmonic function derived precipitation change scenarios. 12 scenarios were considered each with the maximum precipitation increase fixed for a different month of the year. The response in flood quantile changes varied between catchments depending on the seasonality of the precipitation scenario, again highlighting the non-linearities of different catchments and the catchment property controls on antecedent conditions. The magnitude and structure of the flood response in the catchments can be seen to vary depending on which month the precipitation peak occurs; however quantifying this effect is challenging due to the manner in which POTs are defined.

The next chapter draws together the different components of uncertainty in the 'top down' framework which have been presented in this thesis to identify the relative role and importance of each component when assessing the impact of climate change on UK flooding.

CHAPTER 8

Relative Importance of Uncertainty Sources

8.1 Introduction

This thesis has explored a number of sources of uncertainty which contribute to the assessment of the impact of climate change on flooding. So far each component of uncertainty has been treated independently for a single time period and emissions scenario. In this chapter the uncertainty associated with emissions scenarios, climate modelling, hydrological model parameters and flood frequency analysis are assessed in combination with one another across the 21st century. Through this assessment the relative scale and importance of the different sources of uncertainty can be analysed for temporal trends and variations between catchments which can in turn be placed in the context of baseline uncertainties. This chapter addresses the following research goals:

- Which sources of uncertainty are most important to consider and does this change over time and between different catchments?
- To what degree can future climate projections and their associated uncertainty be characterised by the range of uncertainty associated with the baseline period?

The experimental design describing the methods used for including the different uncertainty sources is in section 8.2. The relative scales of each component of uncertainty is addressed in section 8.3, and placed in the context of baseline uncertainty in section 8.4. The future climate projections are also assessed in comparison with a currently suggested adaptation allowance (section 8.4.4). The chapter finishes with the discussion, conclusions (section 8.5) and a summary (section 8.6).

8.2 Method for Combined Uncertainties Assessment

8.2.1 Experiment Design

The aim of this chapter is to estimate changes in flood quantile magnitude for all nine case study catchments simultaneously using different emissions scenarios, a range of climate model outputs, multiple hydrological parameter sets and include flood frequency analysis uncertainty.

The climate change scenarios used are the UKCP09 monthly precipitation change factors forced by low, medium and high emissions scenarios for the 2020s, 2030s, 2040s, 2050s, 2060s, 2070s and 2080s. Using the full UKCP09 ensemble of 10,000 precipitation change factors would present a large computational burden when combined with further uncertainty sources. Through sensitivity tests (not shown) which sampled the full 10,000 UKCP09 using varying ensemble sizes (i.e. 50, 100, 250, 500, 1000, 5000), 500 randomly sampled UKCP09 scenarios are found to provide an adequate representation of the full 10,000 for a given emissions scenario and time horizon. This compromise reduces the computational load resulting from the UKCP09 climate scenarios by 95%. The precipitation change factors are applied to the observed catchment precipitation series as previously outlined (section 3.5.3), creating 500 new precipitation time series for each time horizon and emission scenario.

Multiple hydrological parameter sets are derived using the parameter perturbation method outlined in Chapter 5. The perturbed parameter method is preferable to the Monte Carlo method from Chapter 5 as it provides an equal number of parameter sets for each catchment allowing for a fair comparison of parameter uncertainty across all catchments. A perturbation of ±20% is applied to the original calibrated PDM parameters with 50 new parameter sets randomly sampled from within the new ranges. Each of the newly created precipitation time series is simulated using all 50 PDM parameter sets leading to 25,000 (500 x 50) future daily river flow series for each time horizon and emission scenario. For seven time horizons and three emissions scenarios this results in 525,000 PDM simulated daily river flow series for each catchment. Each simulated river flow series is analysed for flood frequency using the POT3 sampling and GP distribution (section 0), with flood frequency estimation uncertainty quantified using a standard error (SE) of estimate (Chapter 6). Following the conclusions of Chapter 6 the flood frequency SE is treated as 'independent' between baseline and future to robustly capture the full range of flood frequency estimation uncertainty.

This experiment design produces a distribution of future changes for the 5RP, 20RP and 50RP flood quantiles for each time horizon and emissions scenario in a given catchment. The methods used to assess the relative contributions of the different uncertainty sources to the distribution of future change are outlined in the next section.

8.2.2 Separating the Influence of Different Uncertainty Sources

The influence of the uncertainty sources is separated using a sequential process where the impact of adding an uncertainty source is compared with the impact prior to its addition. In this structure there are three different levels of uncertainty components which are used for comparison in a 'top-down' framework; emissions scenarios and UKCP09 alone (referred to as UKCP), secondly a combination of emissions scenarios, UKCP09 and hydrological model parameters (referred to as UKCP-HP); and lastly emissions scenarios, UKCP09, hydrological model parameters and flood frequency estimation (referred to as UKCP-HP-FF). This sequential comparison is used to analyse the uncertainty contributions individually in sections 8.3.1, 8.3.2 and 8.3.3. The methods outlined below are used to analyse the combined uncertainty contributions in section 8.3.4 where different proportions of the impact distribution are attributed to individual uncertainty components.

Emissions and UKCP09 Uncertainty: Separating the uncertainty resulting from emissions scenarios and climate modelling has previously been performed using a baseline climate model realisation (Hawkins and Sutton, 2009, Hawkins and Sutton, 2011). UKCP09 does not provide such a baseline realisation; furthermore UKCP09 results in a distribution of changes rather than a single change from an individual climate model realisation. To separate the uncertainties for a given time horizon (i.e. 2020s) and flood return period (i.e. 50RP) the UKCP09 distributions of change for the three emissions scenarios are characterised by calculating the variance between the 5th and 95th percentiles for each emissions distribution. For each time horizon the smallest value of variance is used as reference and is assumed to represent the fraction of model uncertainty separate from emissions. The emissions scenario uncertainty is then calculated as the difference between the smallest and largest variances. These uncertainty values are expressed as fractional ratios for a given time horizon as:

$$ClimateModel_{U1} = \frac{EmissionsVar_{min}}{EmissionsVar_{max}}$$

Equation 8.1

155

$$Emissions_{U1} = 1 - ClimateModel_{U1}$$

Hydrological Model Parameter Uncertainty: For the UKCP and UKCP-HP distributions of flood changes the three emissions scenarios are combined resulting in a single distribution for both UKCP and UKCP-HP. The 5th to 95th percentile ranges of the UKCP and UKCP-HP single distributions are compared and expressed as a ratio to show the influence of incorporating hydrological model parameter uncertainty:

$$HydroParam_{U1} = 1 - \left(\frac{UKCP_{Q95} - UKCP_{Q5}}{UKCP\_HP_{Q95} - UKCP\_HP_{Q5}} \right)$$

The fractional ratios calculated for climate model and emissions scenarios uncertainty (calculated previously) are then scaled to match the UKCP fraction relative to the UKCP-HP fraction:

$$ClimateModel_{U2} = (1 - HydroParam_{U1}) \text{ x } ClimateModel_{U1}$$

$$Emissions_{U2} = (1 - HydroParam_{U1}) \text{ x } Emissions_{U1}$$

For example UKCP may represent 0.95 and UKCP-HP 0.05. The UKCP fraction may be formed from emissions of 0.6 and UKCP09 contributes 0.4, which are then scaled relative to 0.95 instead of 1. Therefore emissions = 0.57, UKCP09 = 0.38 and hydrological parameters = 0.05.

Flood Frequency Estimation Uncertainty: The methods for calculating the contribution of flood frequency estimation uncertainty are similar to those outlined for model parameter uncertainties, except with UKCP-HP-FF compared relative to UKCP-HP. The size of flood frequency uncertainty (for a given return period and time horizon) is described by:

$$RPn_{U1} = \left(\frac{UKCP\_HP_{Q95} - UKCP\_HP_{Q5}}{UKCP\_HP\_FF_{Q95} - UKCP\_HP\_FF_{Q5}} \right)$$

The UKCP and UKCP-HP uncertainty ratios are then scaled according to UK-HP-FF uncertainty so that:

$$HydroParam_{U2} = (1 - RPn_{U1}) \text{ x } HydroParam_{U1}$$

Equation 8.7

$$ClimateModel_{U3} = (1 - RPn_{U1}) \text{ x } ClimateModel_{U2}$$

Equation 8.8

$$Emissions_{U3} = (1 - RPn_{U1}) \text{ x } Emissions_{U2}$$

Equation 8.9

For example UKCP-HP may constitute 70% (i.e. fraction of 0.70) of the full range of UKCP-HP-FF. The previous fractions for emissions (0.57), UKCP09 (0.38) and hydrological parameters (0.05) are then scaled as a fraction 0.70. Resulting in emissions = 0.40, UKCP09 = 0.27, hydrological parameters = 0.04 and flood frequency = 0.30 (rounded to 2 d.p.).

Negative Contributions: Typically one would assume that including more components of uncertainty within the framework would result in an increase in the overall range of the impact distribution (in this example the change in a given flood quantile). This is not always the case, as demonstrated in Chapter 6 where in some instances the inclusion of flood frequency analysis uncertainty led to a reduction in the overall range of flood quantile changes. In the example of flood frequency uncertainty a reduction in the range of flood quantile changes occurs because there is a greater uncertainty associated with larger changes compared with smaller changes. This can be seen in Figure 8.1 with higher densities and in turn narrower distributions of uncertainty for smaller flood quantile changes and lower densities with wider distributions for larger flood quantile changes. When the individual distributions of uncertainty are combined this has the affect of placing less confidence on the value of the larger flood changes and greater confidence on the value of smaller flood changes. This leads to a change in the 5th and 95th percentiles of the distribution of flood quantile change which reduces the overall range of uncertainty when flood frequency uncertainty is considered. In the framework applied here, when the inclusion of an impact study component leads to a decrease in the range of flood changes, its fractional uncertainty contribution is considered to be a negative value. The total fraction of uncertainty is calculated as:

$$TotalUncertainty = Emissions_{U3} + ClimateModel_{U3} + HydroParam_{U2} + RPn_{U1}$$

Therefore where the sum of all fractional uncertainties equals one, the addition of each component of uncertainty increases the range of flood change. Where this is not the case, and a negative fraction occurs, one or more of the uncertainty sources leads to a reduction in the overall distribution of change. The absolute fractions of uncertainty will always be equal to one as described by:

$$|Emissions_{U3}| + |ClimateModel_{U3}| + |HydroParam_{U2}| + |RPn_{U1}| = 1$$
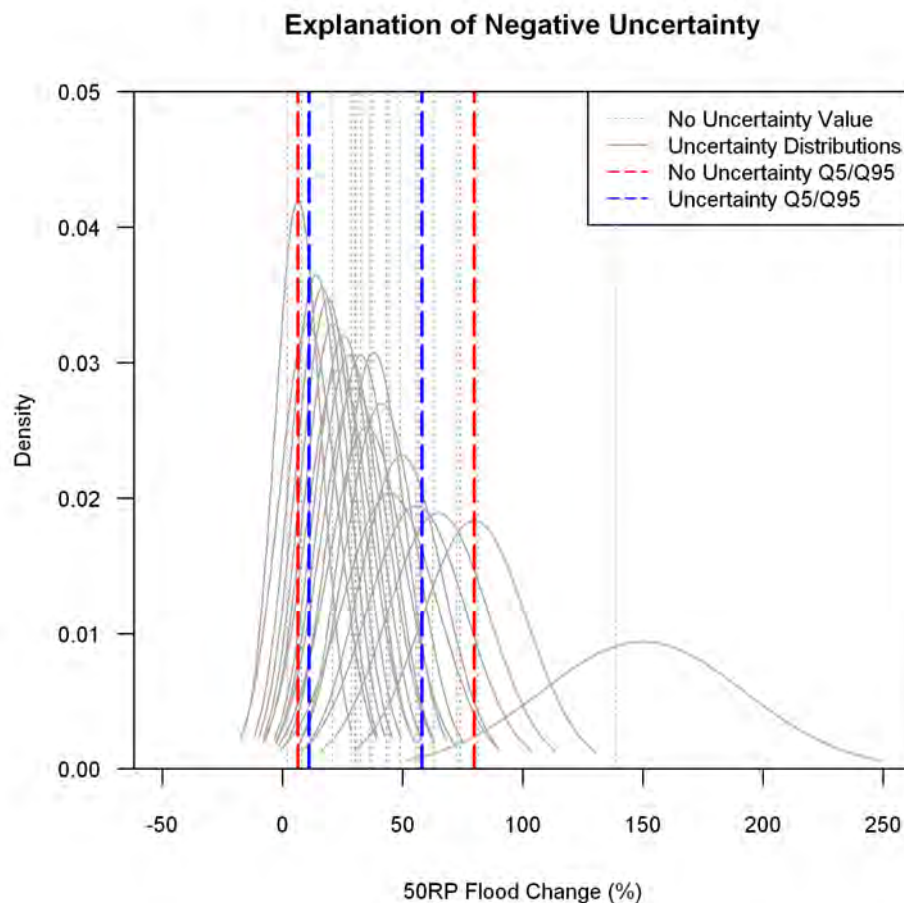
Figure 8.1 Explanation of negative uncertainty contribution. Grey dotted lines are 20 changes in the 50RP with their 5th and 95th percentile shown by the red dashes. Grey solid lines are distributions of uncertainty around each of the 20 50RP changes, with the 5th and 95th percentile all 20 distributions shown by the blue dashes.

8.3 Role of Different Uncertainty Sources

This section assesses the relative importance of the different components of uncertainty using the methods outlined in the previous section. Each of the uncertainty components is included simultaneously but their contribution to changes in future flooding are initially analysed separately as UKCP09 and emissions (section 8.3.1), hydrological model parameters (section 8.3.2) and flood frequency estimation (section 8.3.3). The relative size and importance of each uncertainty component are then analysed in combination with one another in section 8.3.4.

8.3.1 UKCP09 and Emissions Scenarios

The projected changes in 50RP from UKCP09 forced using low, medium and high emissions scenarios for the Helmsdale, Bure, Teme and Leet Water are shown in Figure 8.2 and Figure 8.3 for each decadal time horizon between 2020 and 2080.

The majority of projections for the Helmsdale catchment (Figure 8.2-top) display an overall increase in the 50RP across all time periods and emissions scenarios. The projections suggest a decrease in the 50RP at the 5th percentile for all emissions scenarios until the 2040s, with the 5th percentile for the low emissions scenario remaining negative until 2080. The range of changes from the three emissions scenarios is similar until 2040 and then increases for the medium and high scenarios at more distant time horizons. The influence of the emissions scenarios on flood changes is non-linear, with higher emissions at increasing time horizons displaying longer tails towards larger increases (i.e. 95th-50th percentile range is larger than 5th-50th percentile range as emissions and time increase).

The Bure catchment (Figure 8.2-bottom) has a large proportion of scenarios which project a decrease in the 50RP with the 5th percentiles remaining around -10% across all time horizons and emissions scenarios. The median change increases uniformly for each emissions scenario with low variability between time horizons. The 95th percentile remains relatively constant up until the 2070s where the high emission scenario projects increasingly larger changes. The 50RP changes in the Bure catchment are significantly dampened compared with the Helmsdale with smaller magnitude changes and much lower variability between the different emissions scenarios.

At the 5th percentile the Teme catchment (Figure 8.3-top) displays an increase in the 50RP for all time horizons and emissions scenarios. The differences between the three emissions

scenarios becomes greater from the 2040s onwards with a maximum increase in 50RP ranging from 50% (low) to 100% (high) by the 2080s. Similarly to the Helmsdale, the distribution of flood changes becomes increasingly skewed for increasing emissions scenario and time horizon, with large tails towards 50RP increases.

The Leet Water catchment (Figure 8.3-bottom) displays a small proportion of decreases in the 50RP up until the 2070s. The variations between the three emissions scenarios becomes apparent from the 2050s onwards, with the high emissions scenario displaying the greatest changes. The skew of the distribution of change also increases with time horizon and emissions scenario.

Each catchment displays a different response to the UKCP09 climate projections from the buffered changes in the Bure to the larger changes in the Helmsdale and Leet Water. A common trait found in all catchments is for the variation between the three emissions to be small at first with a clearer differentiation between scenarios occurring from the 2040s-2050s onwards. Moreover, changes for a given emission scenario are non-uniform, with a skewed distribution of flood changes towards increasingly large changes at the median and in turn the 95th percentile at increasing time horizons. In contrast the 5th percentile displays very little variability for all emissions scenarios and all time horizons. Prior to 2040/2050 the difference between each emissions scenario for a given time horizon, and the difference for the same emissions scenario at different time horizons, is likely a result of natural variability in the projection or sampling uncertainty through selecting a subset of 500 from 10,000.
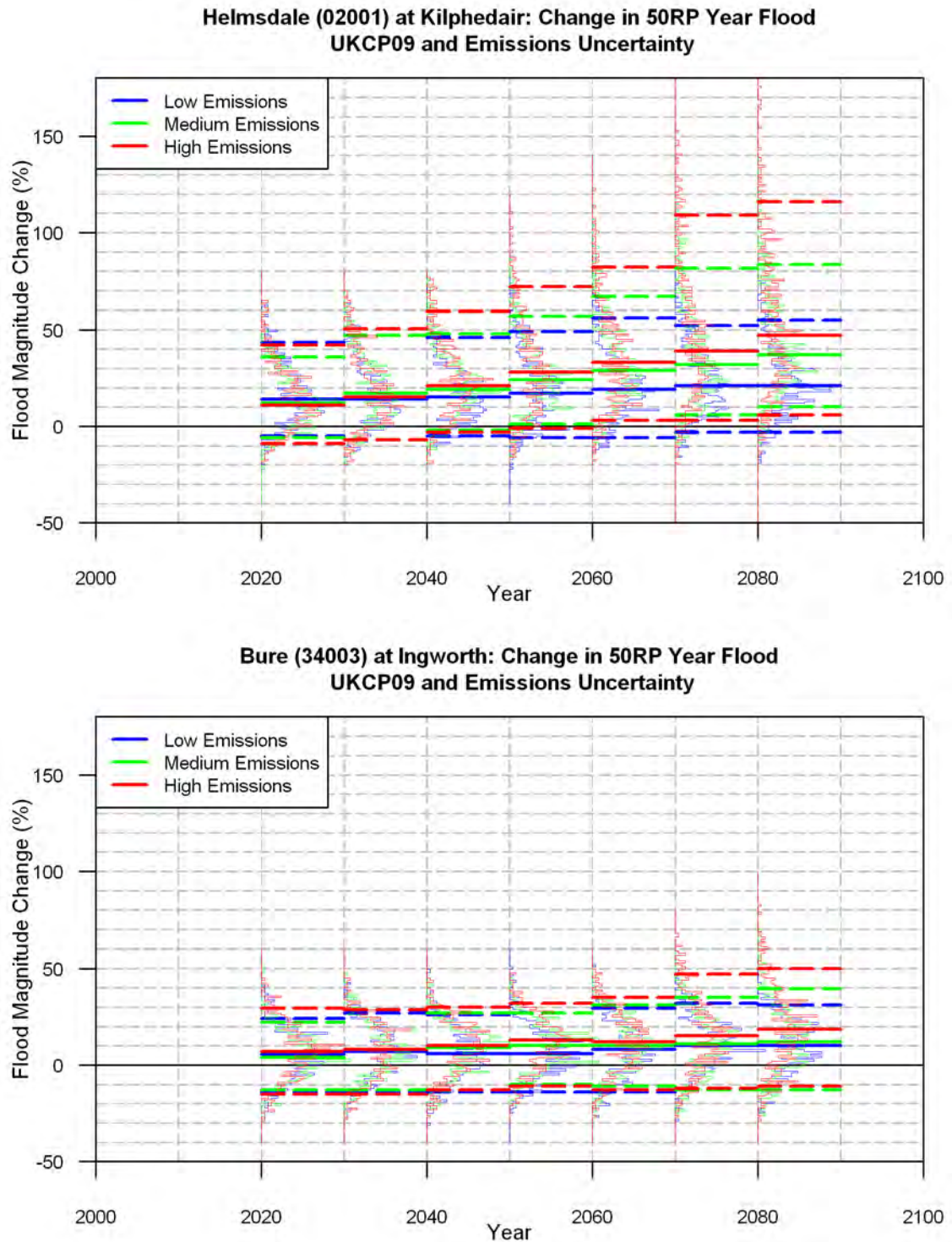
Figure 8.2 Change in 50RP in the Helmsdale (top) and Bure (bottom) catchments projected by UKCP09 precipitation changes under low (blue), medium (green) and high (red) emissions scenarios. The 5th percentile (bottom dashed), median (solid middle) and 95th percentile (dashed top) are shown for each distribution.
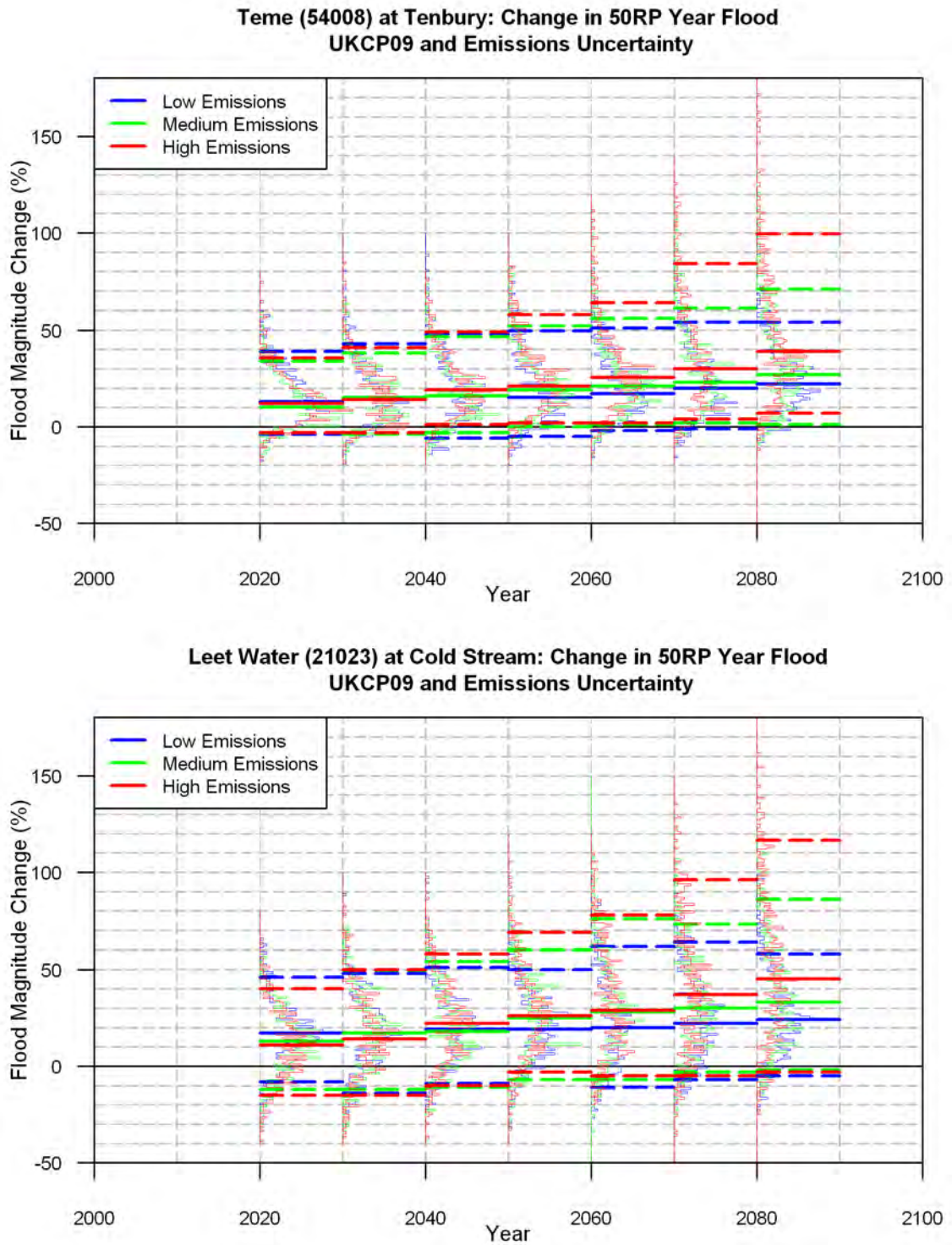
Figure 8.3 Change in 50RP in the Teme (top) and Leet Water (bottom) catchments projected by UKCP09 precipitation changes under low (blue), medium (green) and high (red) emissions scenarios. The 5th percentile (bottom dashed), median (solid middle) and 95th percentile (dashed top) are shown for each distribution.

8.3.2 Including Hydrological Model Parameter Uncertainty

For the three emissions scenarios the 500 UKCP09 change factor perturbed precipitation time series are each input in combination with 50 perturbed PDM parameter sets. The role of multiple PDM parameter sets for calculating changes in the 5RP and 50RP is shown in Figure 8.4 and Figure 8.5 respectively. The role of the hydrological parameter uncertainty is calculated by comparing the percentage difference in the range from UKCP-HP compared to UKCP for each emissions scenario.
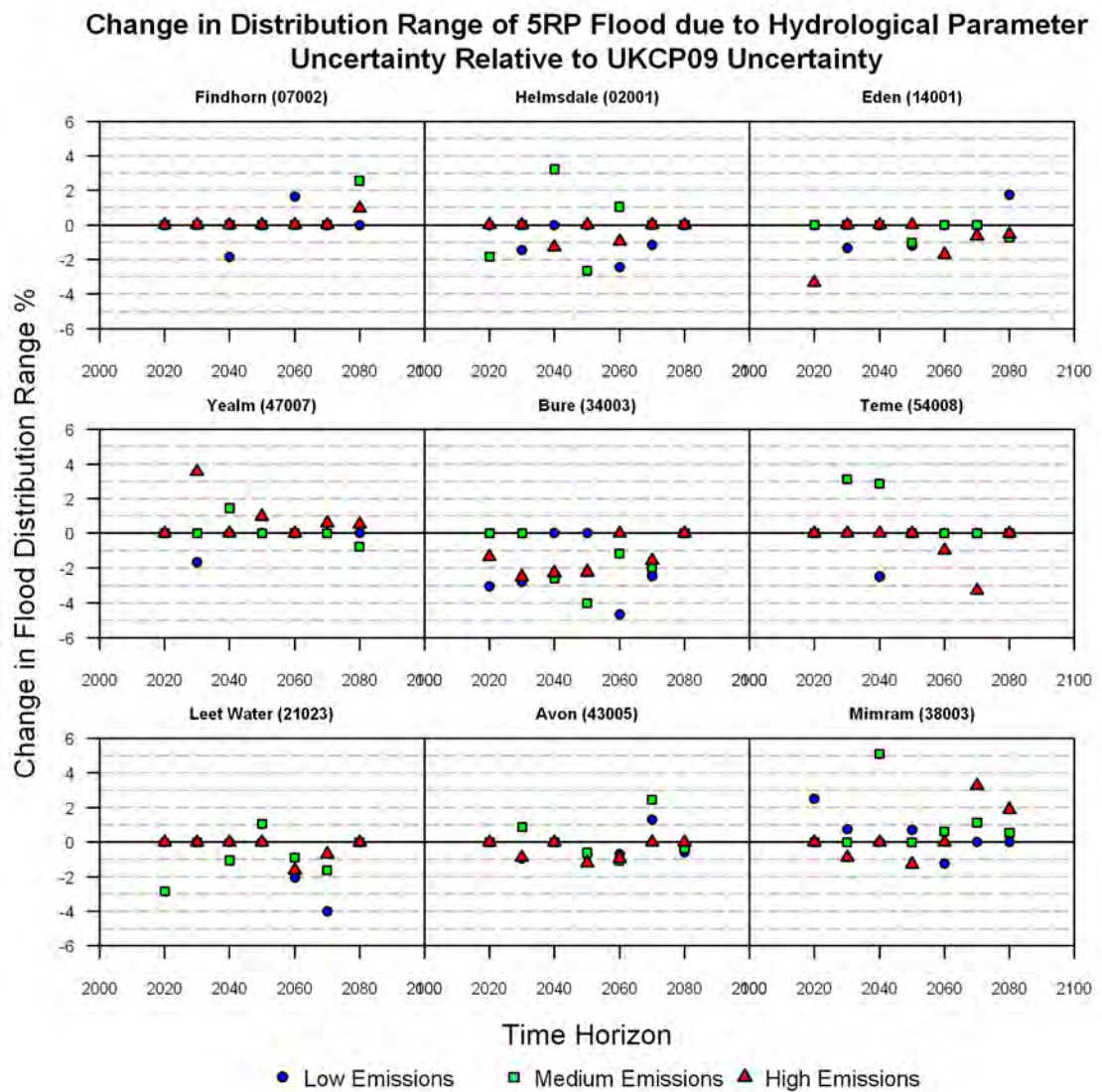
Figure 8.4 Change in the distribution range of the 5RP flood when hydrological model parameter uncertainty is included for low (blue), medium (green) and high (red) emissions.
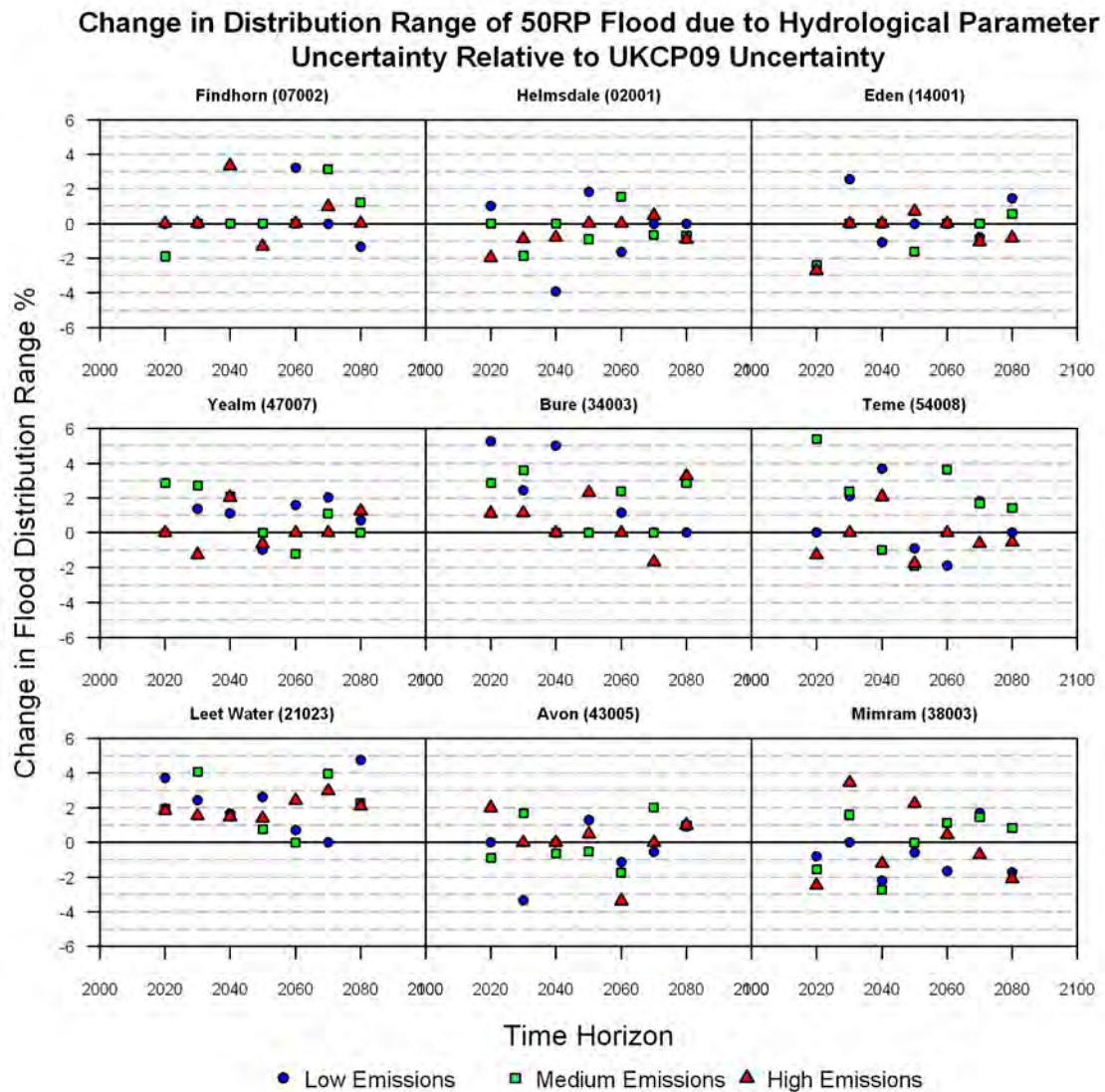
Figure 8.5 Change in the distribution range of the 50RP flood when hydrological model parameter uncertainty is included for low (blue), medium (green) and high (red) emissions.

The impact of including multiple PDM parameter sets in the combined analysis is generally small with a maximum increase in range of 5% (50RP Teme 2020s High) and a range decrease of -4.5% (5RP Bure 2060s Low) as result of a negative uncertainty from the hydrological model parameters. There are no clear patterns across the different time horizons, emissions scenario and return periods, demonstrating that including hydrological model parameter uncertainty does not systematically influence the overall distribution of change in flood quantile compared to that observed from 500 UKCP09 scenarios alone. In Chapter 5 the importance of hydrological model parameter uncertainty was found to increase as precipitation changes increased in magnitude. As only a small proportion of the UKCP09 scenarios are associated with very high precipitation changes, it is possible that their overall

impact is small in comparison to the full ensemble of 500 UKCP09 scenarios, despite possibly resulting in very large individual changes.

8.3.3 Including Hydrological Model Parameter and Flood Frequency Uncertainty

The addition of flood frequency estimation uncertainty in the modelling framework is calculated by comparing the change in distribution range of UKCP-HP-FF relative to UKCP-HP as shown in Figure 8.6.

The largest uncertainty is associated with the three catchments (Findhorn, Bure, Leet Water) identified in Chapter 6 to be sensitive to flood frequency estimation uncertainty. Across all catchments, the influence of flood frequency uncertainty on the total uncertainty range is dependent on the return period, with larger increases at higher return periods. There is also a dependence with time towards smaller relative (as opposed to absolute) uncertainty at increasing time horizons. In some cases there are decreases in the ranges from the 2060s onwards, most noticeable in the Yealm and Avon catchments. In the near term (2020-2040) including flood frequency uncertainty results in proportionately larger ranges of possible flood changes, indicating that the medium to near term time horizon is when flood frequency estimation contributes its greatest proportion of uncertainty in climate change impact studies. This is because the UKCP09 projections are associated with the smallest range of flood quantile changes in the near term (Figure 8.2 and Figure 8.3) which is a property identified in Chapter 6 as being highly influential in defining the relative magnitude of flood frequency uncertainty.

The role of incorporating flood frequency analysis uncertainty in the overall climate change impact assessment (Figure 8.6) is much larger than that of hydrological parameter uncertainty (Figure 8.4). This suggests that flood frequency estimation contributes a larger source of uncertainty than hydrological model parameters in climate change impact studies on flood peaks. There is also a stronger temporal dependence (on time horizon) of the flood frequency uncertainty which is absent in the hydrological model parameter uncertainty. The next section quantifies the relative contributions of each uncertainty component by partitioning fractions of the impact distribution to each source of uncertainty.
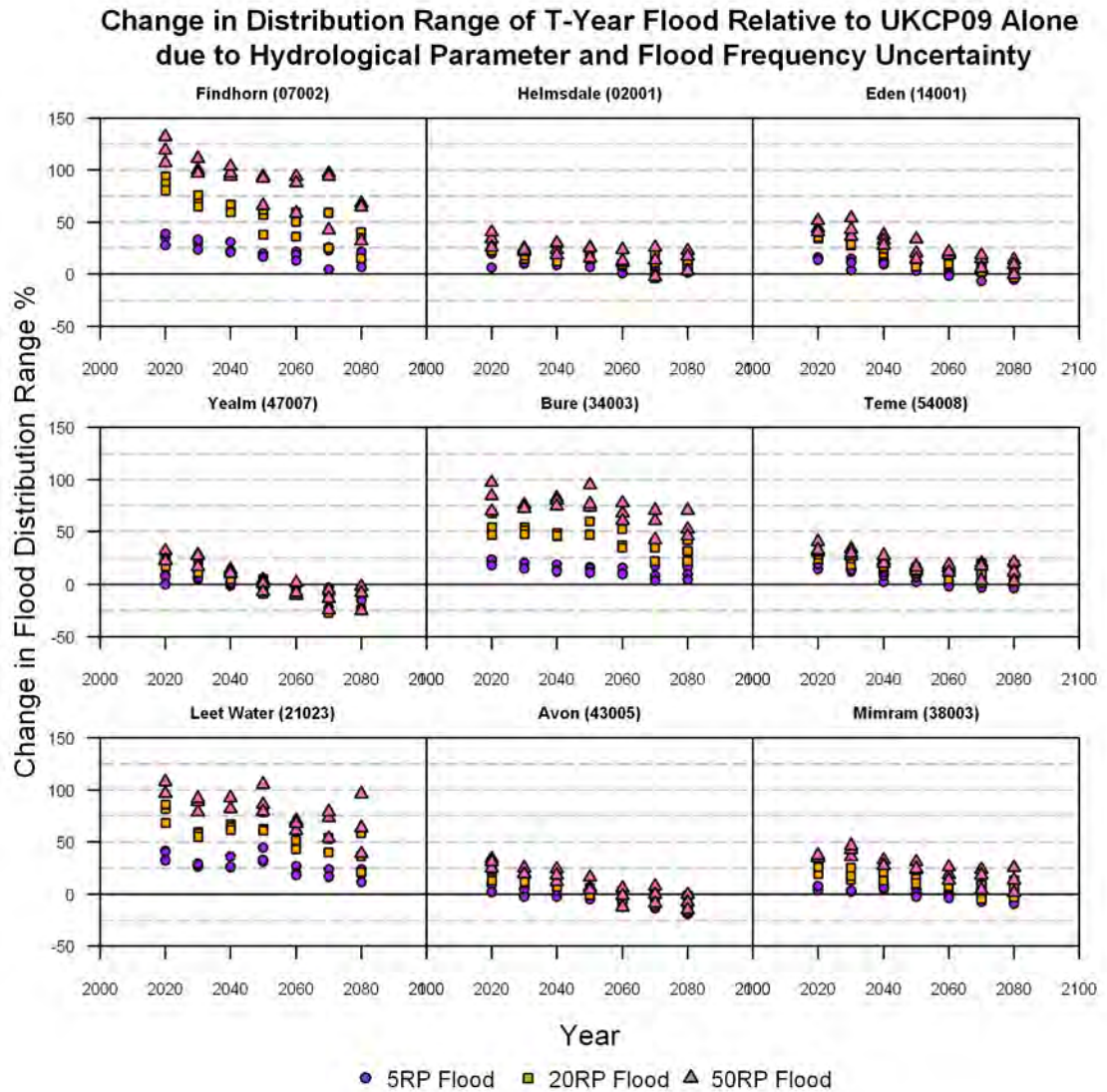
Figure 8.6 Change in the distribution range of the T-Year flood when flood frequency estimation uncertainty is included. 5RP (purple), 20RP (orange) and 50RP (pink) are all plotted for all emissions scenarios.

8.3.4 Combined Uncertainty Analysis

The methods outlined in section 8.2.2 are used here to separate the relative scales of uncertainty associated with each considered uncertainty component. This allows for the magnitude of the impact distribution (i.e. change in 5RP or 50RP) to be attributed to the different uncertainty sources. The results are presented for all nine catchments from Figure 8.7 to Figure 8.15 for the 5RP (top panels) and 50RP (bottom panels). The left hand panels show the relative fraction of uncertainty and the right hand panels display the cumulative fractions of uncertainty. A negative fraction of uncertainty indicates that the climate change impact distribution decreases in range with the addition of that component of uncertainty.
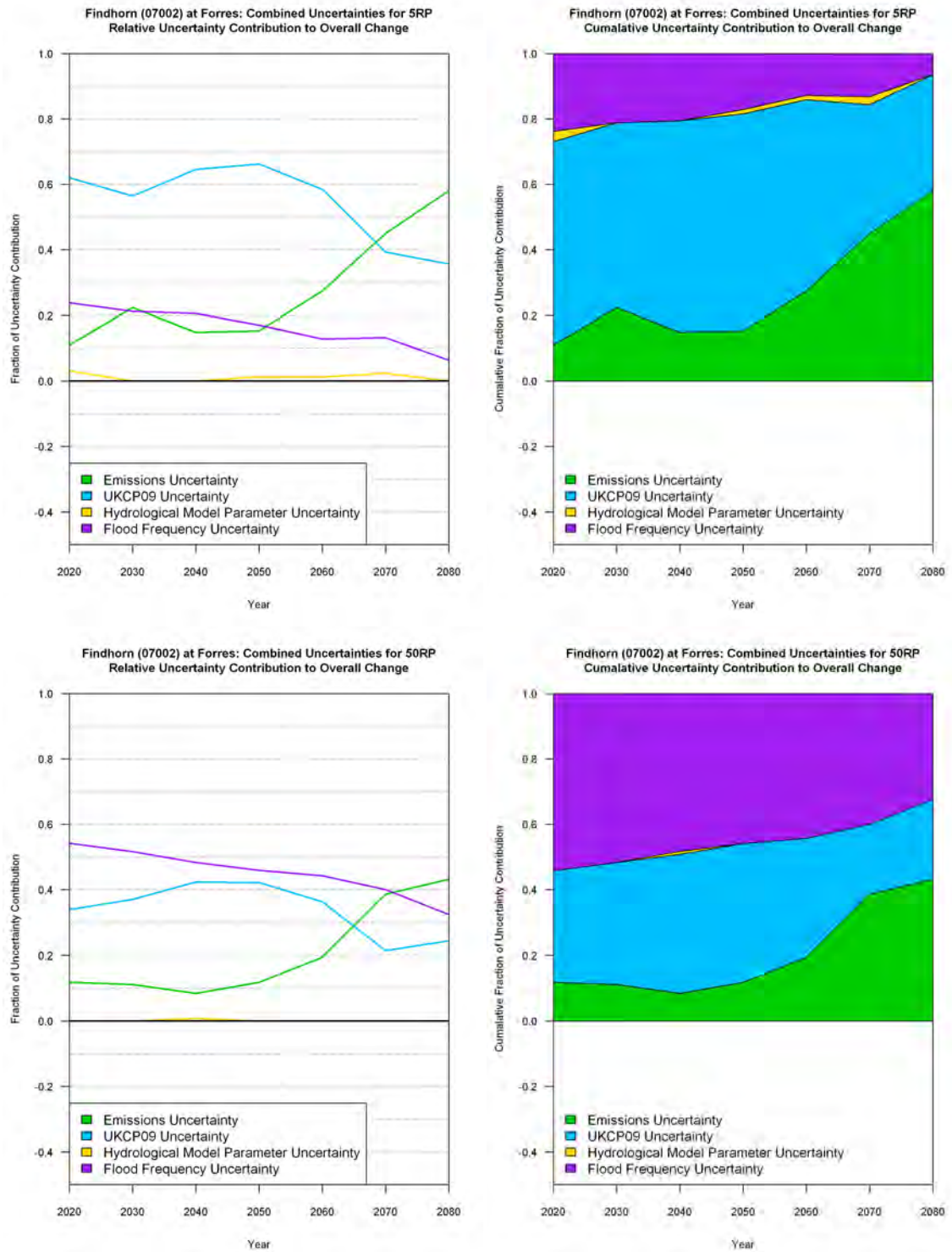
Figure 8.7 Relative (left) and cumulative (right) scales of uncertainty sources for the 5RP (top) and 50RP (bottom) in the Findhorn catchment. Uncertainty is partitioned between emissions scenarios (green), UKCP09 model uncertainty (blue), hydrological parameter uncertainty (yellow) and flood frequency uncertainty (purple).
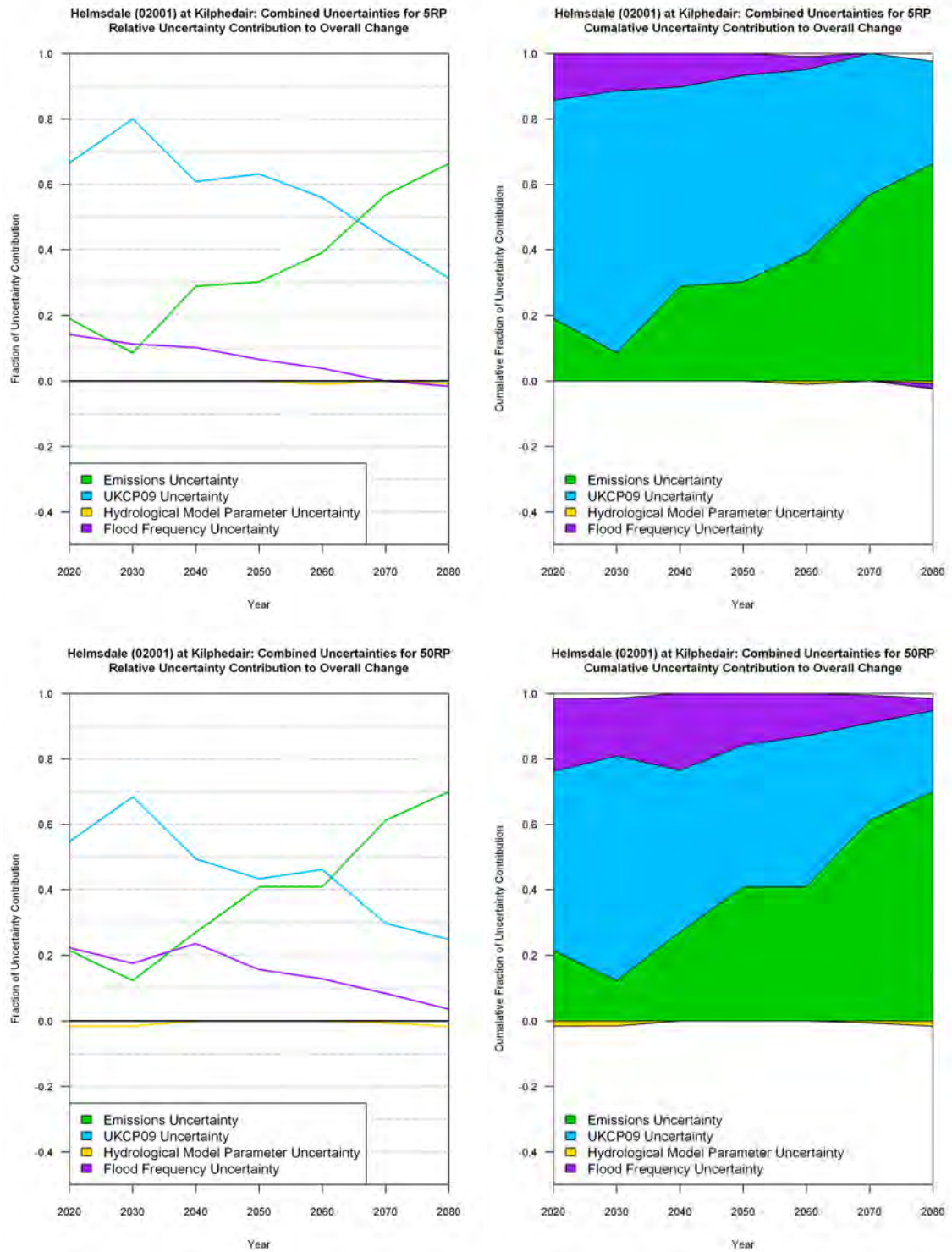
Figure 8.8 Relative (left) and cumulative (right) scales of uncertainty sources for the 5RP (top) and 50RP (bottom) in the Helmsdale catchment. Uncertainty is partitioned between emissions scenarios (green), UKCP09 model uncertainty (blue), hydrological parameter uncertainty (yellow) and flood frequency uncertainty (purple).
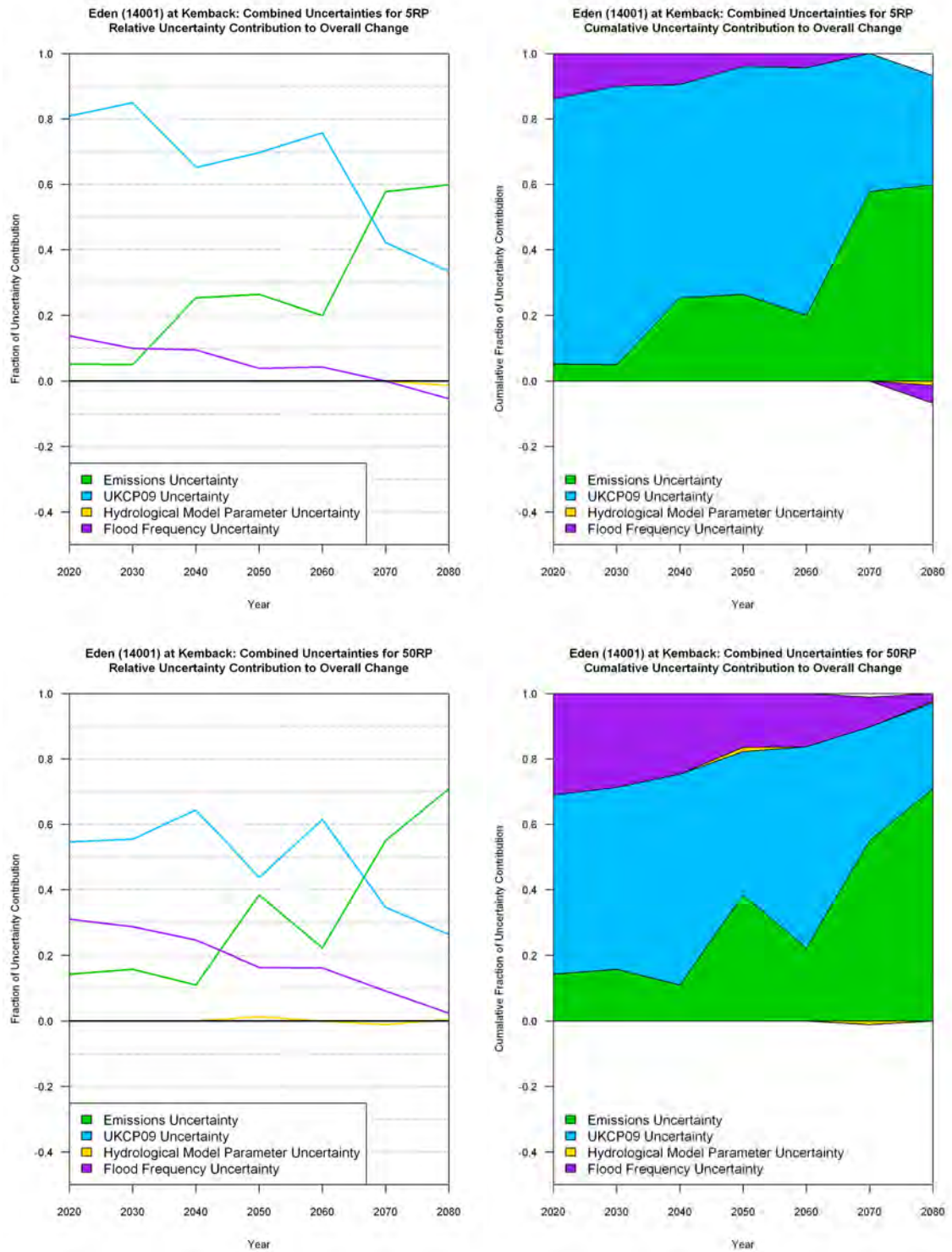
Figure 8.9 Relative (left) and cumulative (right) scales of uncertainty sources for the 5RP (top) and 50RP (bottom) in the Eden catchment. Uncertainty is partitioned between emissions scenarios (green), UKCP09 model uncertainty (blue), hydrological parameter uncertainty (yellow) and flood frequency uncertainty (purple).
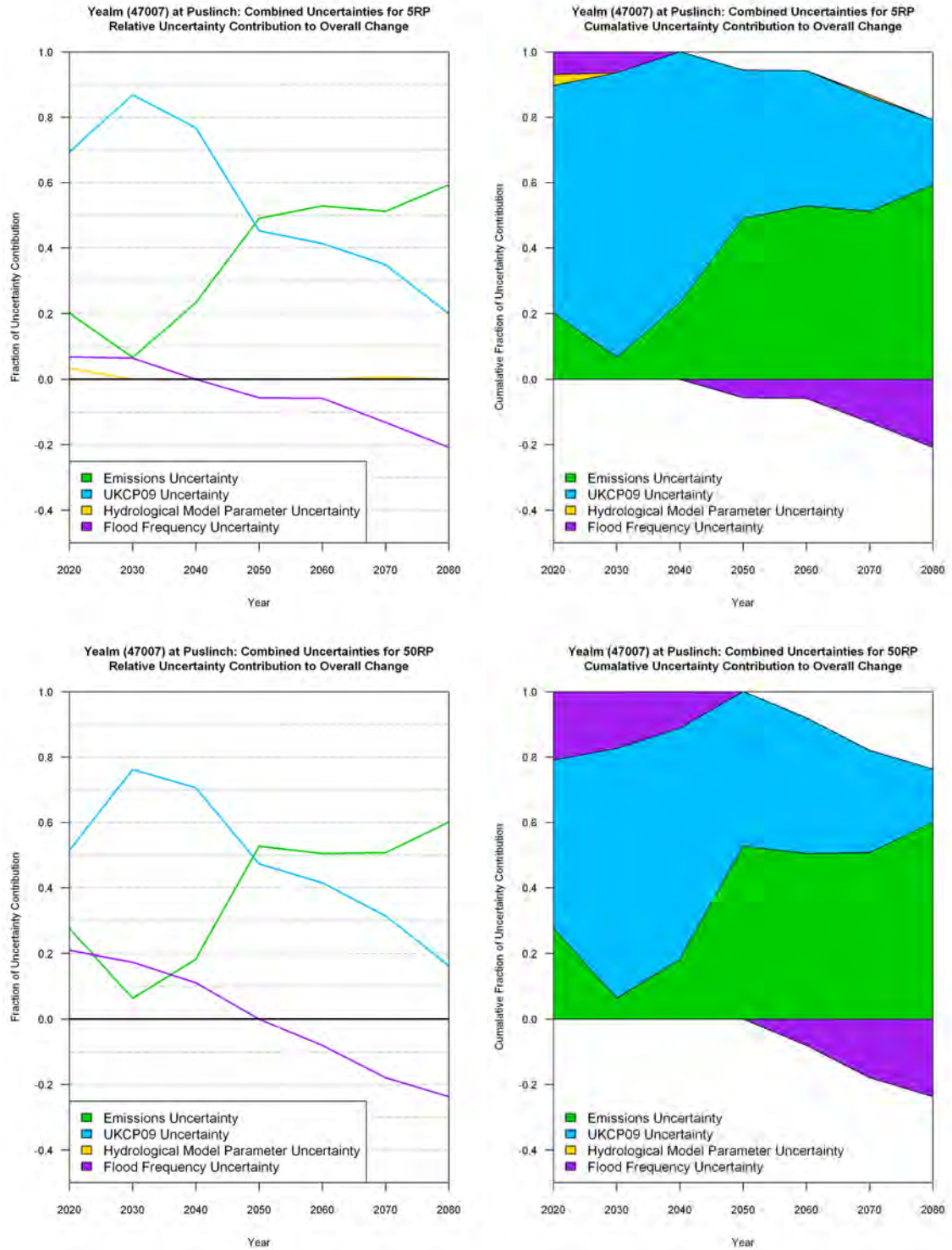
Figure 8.10 Relative (left) and cumulative (right) scales of uncertainty sources for the 5RP (top) and 50RP (bottom) in the Yealm catchment. Uncertainty is partitioned between emissions scenarios (green), UKCP09 model uncertainty (blue), hydrological parameter uncertainty (yellow) and flood frequency uncertainty (purple).
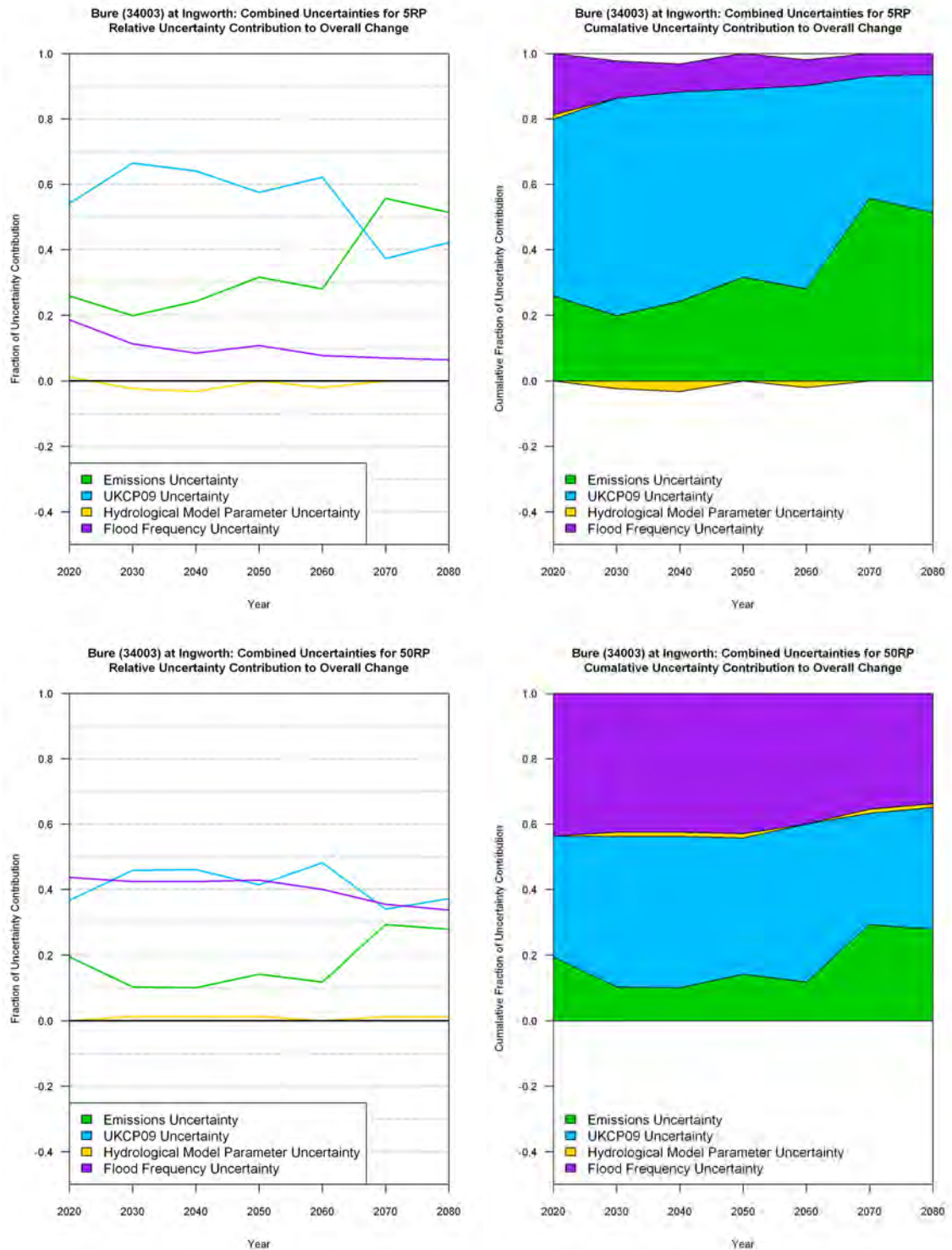
Figure 8.11 Relative (left) and cumulative (right) scales of uncertainty sources for the 5RP (top) and 50RP (bottom) in the Bure catchment. Uncertainty is partitioned between emissions scenarios (green), UKCP09 model uncertainty (blue), hydrological parameter uncertainty (yellow) and flood frequency uncertainty (purple).
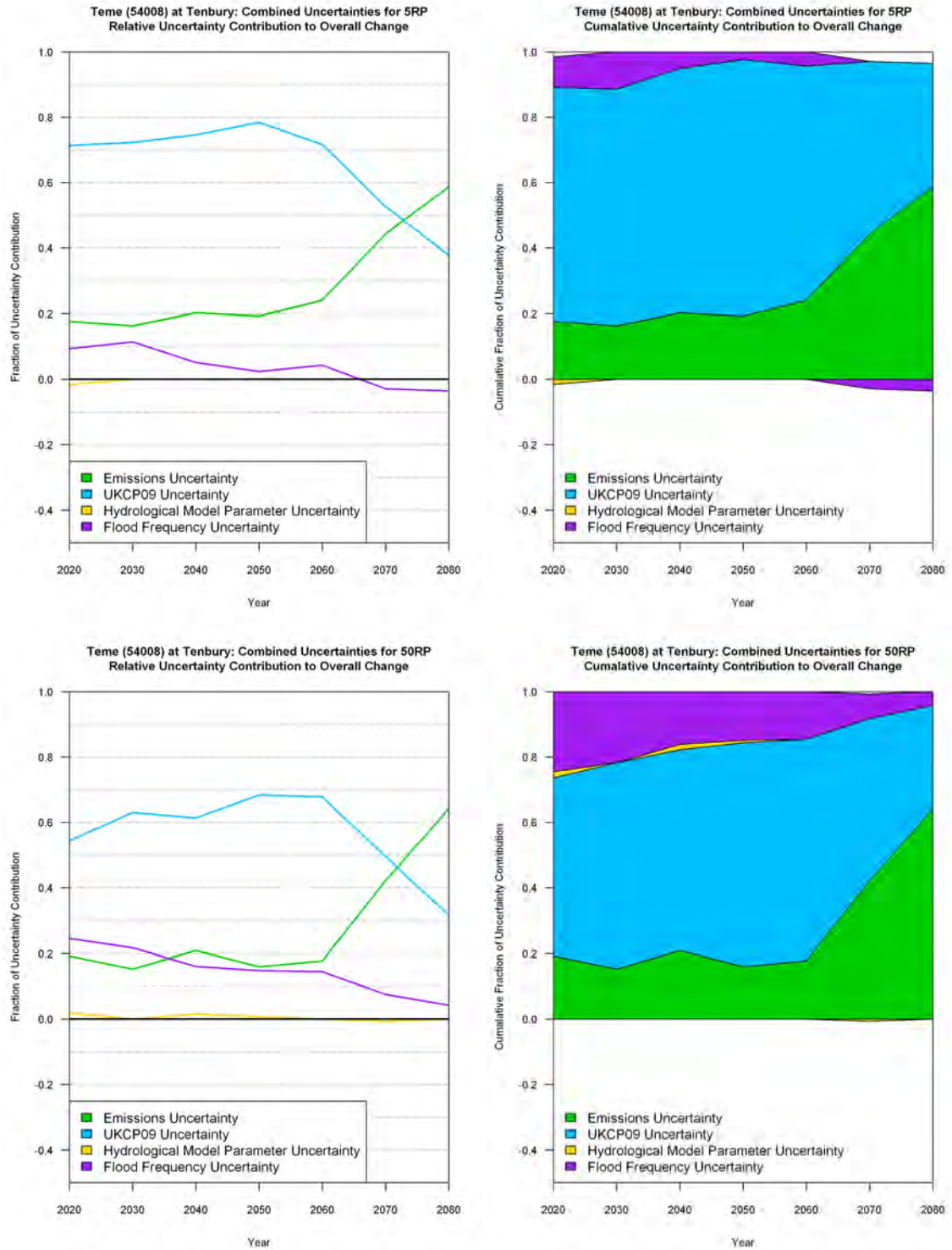
Figure 8.12 Relative (left) and cumulative (right) scales of uncertainty sources for the 5RP (top) and 50RP (bottom) in the Teme catchment. Uncertainty is partitioned between emissions scenarios (green), UKCP09 model uncertainty (blue), hydrological parameter uncertainty (yellow) and flood frequency uncertainty (purple).
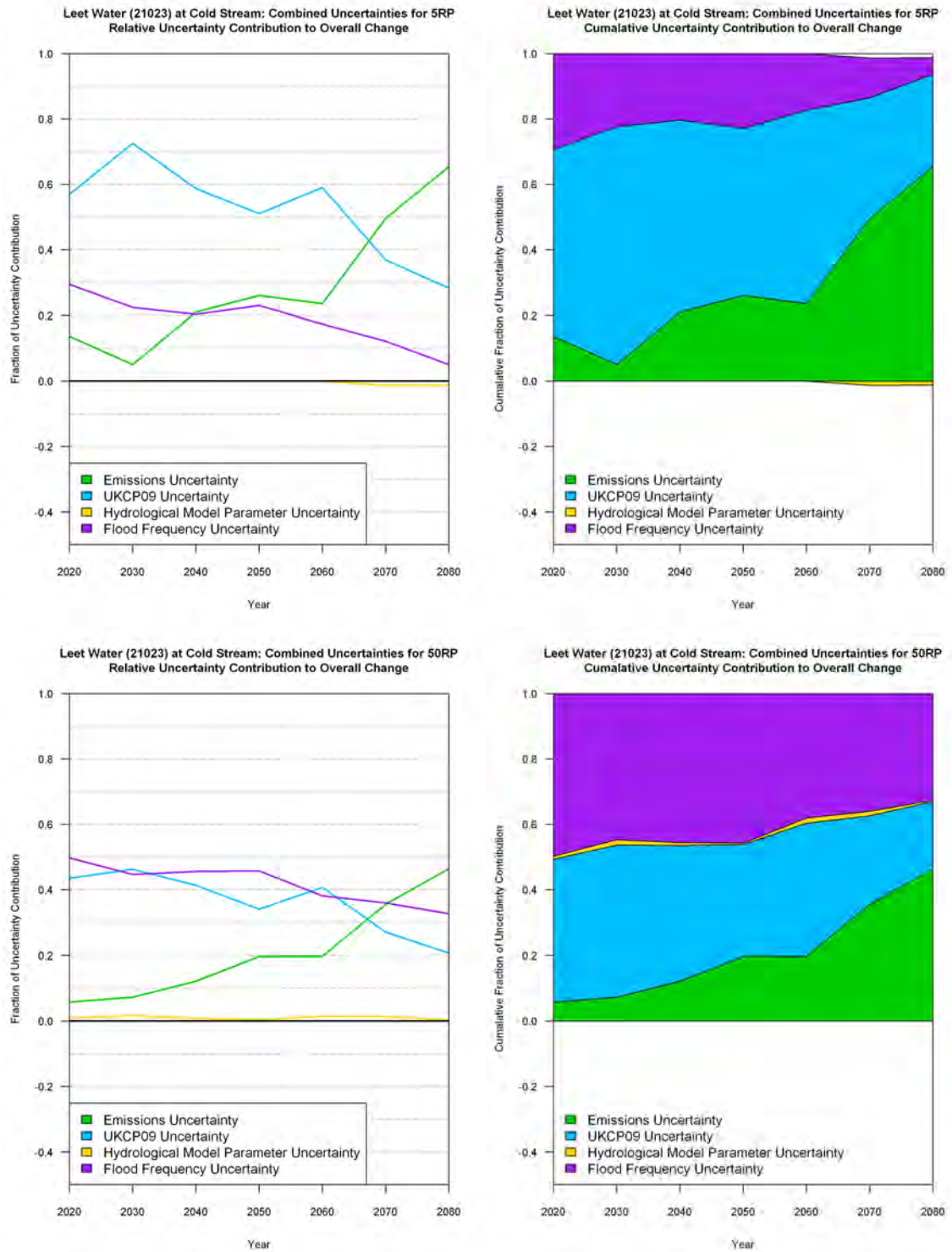
Figure 8.13 Relative (left) and cumulative (right) scales of uncertainty sources for the 5RP (top) and 50RP (bottom) in the Leet Water catchment. Uncertainty is partitioned between emissions scenarios (green), UKCP09 model uncertainty (blue), hydrological parameter uncertainty (yellow) and flood frequency uncertainty (purple)..
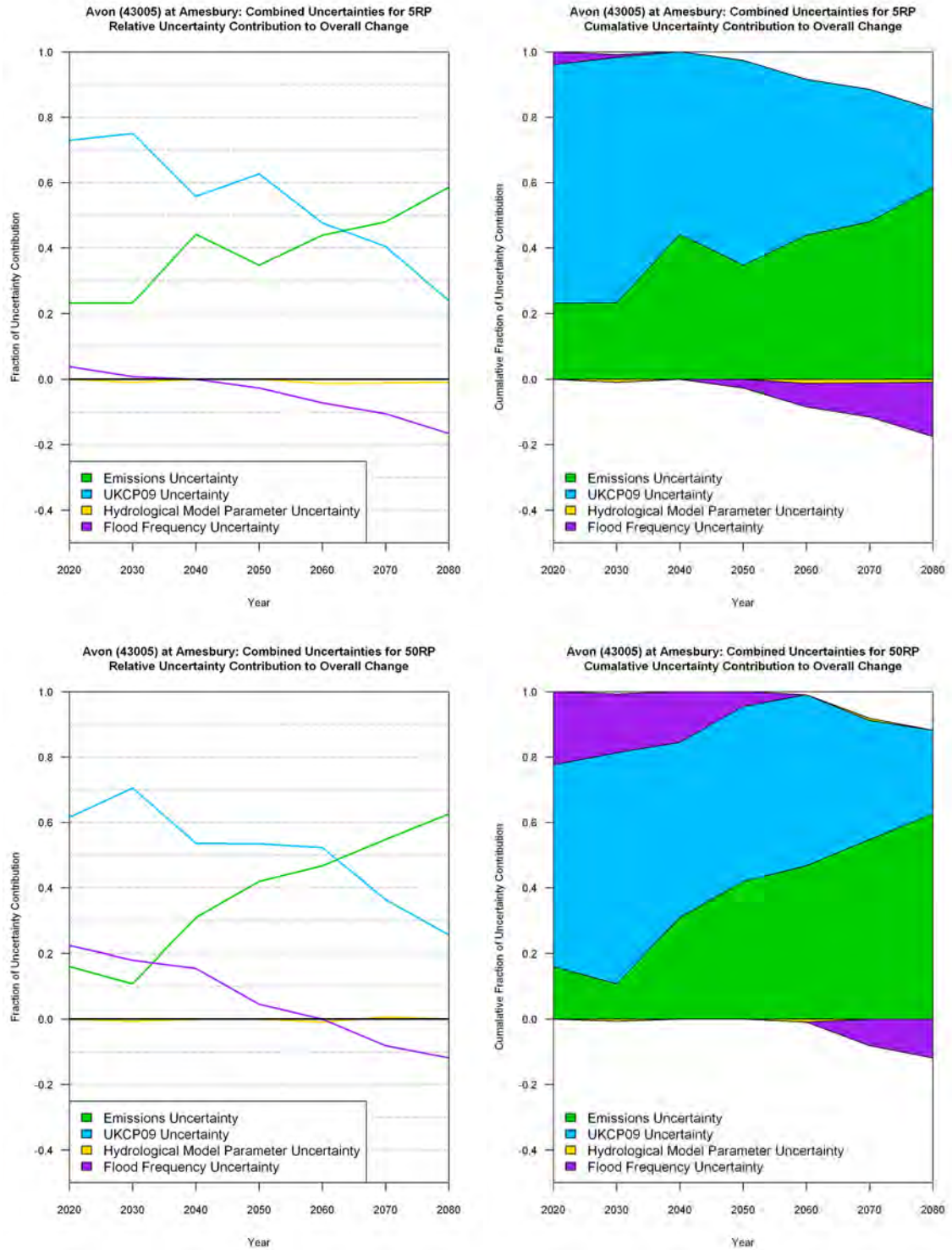
Figure 8.14 Relative (left) and cumulative (right) scales of uncertainty sources for the 5RP (top) and 50RP (bottom) in the Avon catchment. Uncertainty is partitioned between emissions scenarios (green), UKCP09 model uncertainty (blue), hydrological parameter uncertainty (yellow) and flood frequency uncertainty (purple).
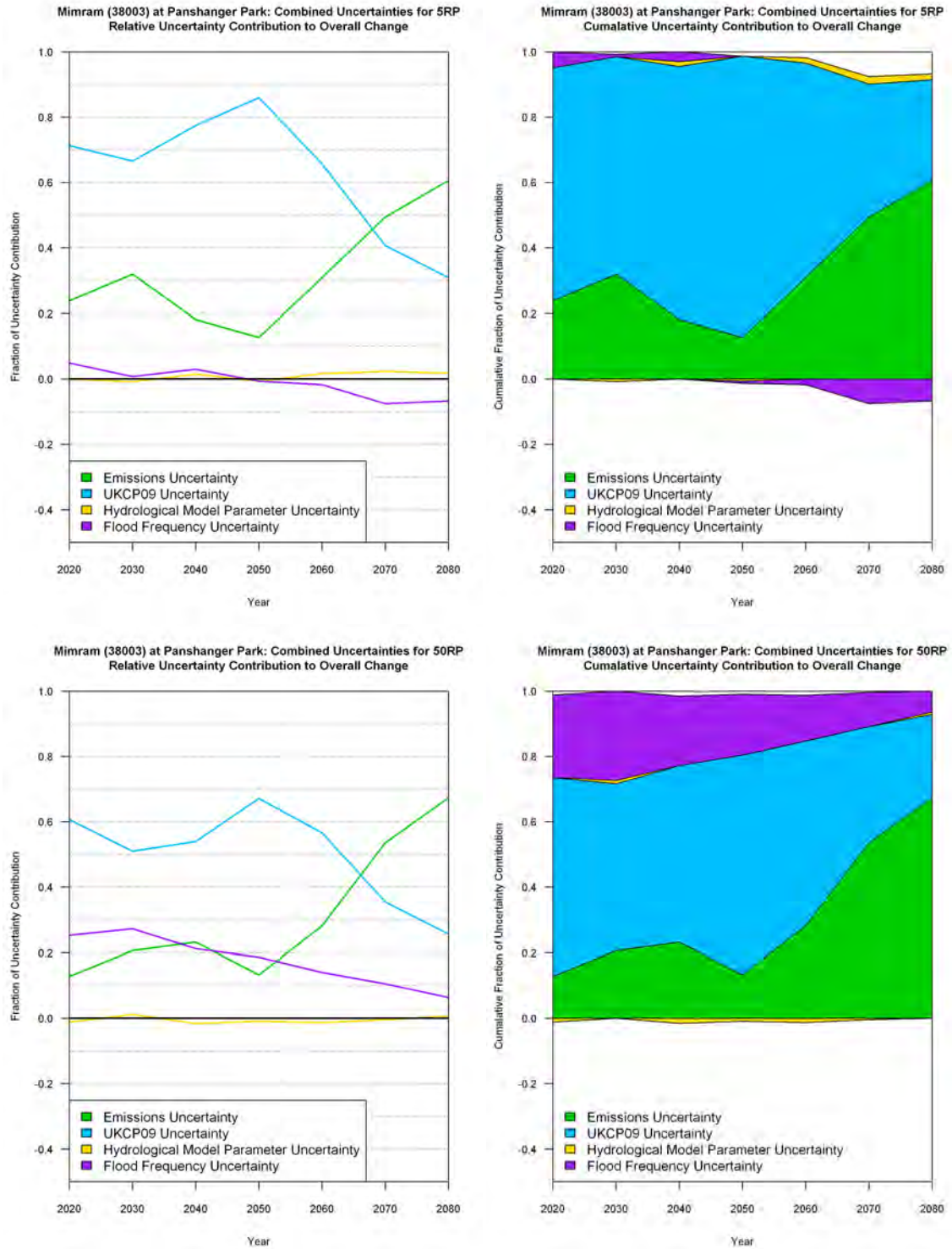
Figure 8.15 Relative (left) and cumulative (right) scales of uncertainty sources for the 5RP (top) and 50RP (bottom) in the Mimram catchment. Uncertainty is partitioned between emissions scenarios (green), UKCP09 model uncertainty (blue), hydrological parameter uncertainty (yellow) and flood frequency uncertainty (purple).

The patterns describing the relative importance of uncertainty in the nine catchments can be broadly split in to three groups.

- Group 1 - Emissions scenarios, UKCP09 modelling and flood frequency analysis all contribute a similar magnitude of uncertainty towards the end of the 21st century (Findhorn, Bure and Leet Water).

- Group 2 - Flood frequency analysis contributes a negative uncertainty towards the end of the 21st century, decreasing the range of changes in the 5RP and 50RP at these time horizons (Yealm and Avon).

- Group 3 - UKCP09 is generally the dominant source of uncertainty with emissions scenarios becoming increasingly important over time (Helmsdale, Eden, Teme and Mimram).

In all catchments the hydrological model parameters are shown to contribute only a small fraction (positive or negative) to the overall uncertainty.

For the 5RP, UKCP09 is the dominant source of uncertainty in all catchments contributing between 60% and 80% of total projection uncertainty during 2020-2060. From 2060/2070 emissions scenario uncertainty increases and becomes the dominant source of uncertainty. Flood frequency uncertainty is generally small for the 5RP and decreases in magnitude at further time horizons. In a number of catchments (Helmsdale, Eden, Yealm, Teme, Avon and Mimram) the flood frequency contribution becomes negative between 2050 and 2080, reducing the range of future changes in 5RP.

For the 50RP the UKCP09 uncertainty remains greatest for the early 21st century although with a contribution of 40%-70%, smaller compared to that from the 5RP. This smaller contribution is a result of the increased importance of flood frequency uncertainty for higher return periods which ranges from 20% to 50% for the 2020s-2060s. The contribution of flood frequency uncertainty decreases over time and becomes negative by 2060 for the Avon and Yealm catchments. The emissions uncertainty becomes more important at increasing time horizons typically becoming the dominant uncertainty beyond 2060. In the Findhorn, Bure and Leet Water catchments which are sensitive to flood frequency analysis, the flood frequency uncertainty is the dominant source of uncertainty until the 2080s when emissions uncertainty becomes dominant. In all three catchments the role of UKCP09 uncertainty is typically of a similar magnitude as the flood frequency uncertainty until the 2060s.

The results highlight that the relative importance of the different sources of uncertainty varies depending on the time horizon of interest and with catchment response type. For nearer time horizons, flood frequency estimation and UKCP09 (i.e. climate models) contribute the greatest amount of uncertainty. At more distant time horizons (2060s onwards) emissions scenario uncertainty becomes increasingly important; often the dominant source of uncertainty by 2080. The role of flood frequency uncertainty varies at different return periods; with higher return periods associated with larger uncertainty. Notably hydrological model parameter uncertainty has been shown to be small and in many cases has very little influence compared with the other sources of uncertainty.

8.4 Future Projection Uncertainty in the Context of Baseline Uncertainty

8.4.1 Rationale for Baseline Context of Future Projections

The future projections of flood changes display a wide range due to the contributions of different sources of uncertainty. Uncertainty however, does not just arise in future climate change projections; it is dealt with in present day situations. An example of this is flood frequency analysis, which was shown in Chapter 6 to have a large degree of uncertainty. Yet despite the large range of uncertainty in estimating present day design standard flood quantiles, strategic flood management decisions are still made. In light of this the aim of this section is to place the range of the future projections in the context of the baseline flood frequency estimation uncertainty. This will provide a present day context for future projections, quantifying the proportion of projections which lie beyond our current design uncertainty.

In practice a flood defence design comprises of a number of components in addition to flood frequency analysis. Hydraulic factors such as channel roughness and channel curvature also influence its design. However the uncertainty of all these factors are combined in a single value of uncertainty, known as the freeboard (Kirby and Ash, 2000). In this section, the flood design uncertainty only refers to the hydrological flood frequency uncertainty. In the context of climate change analysis the additional factors which influence the flood defence design can be assumed to be stationary.
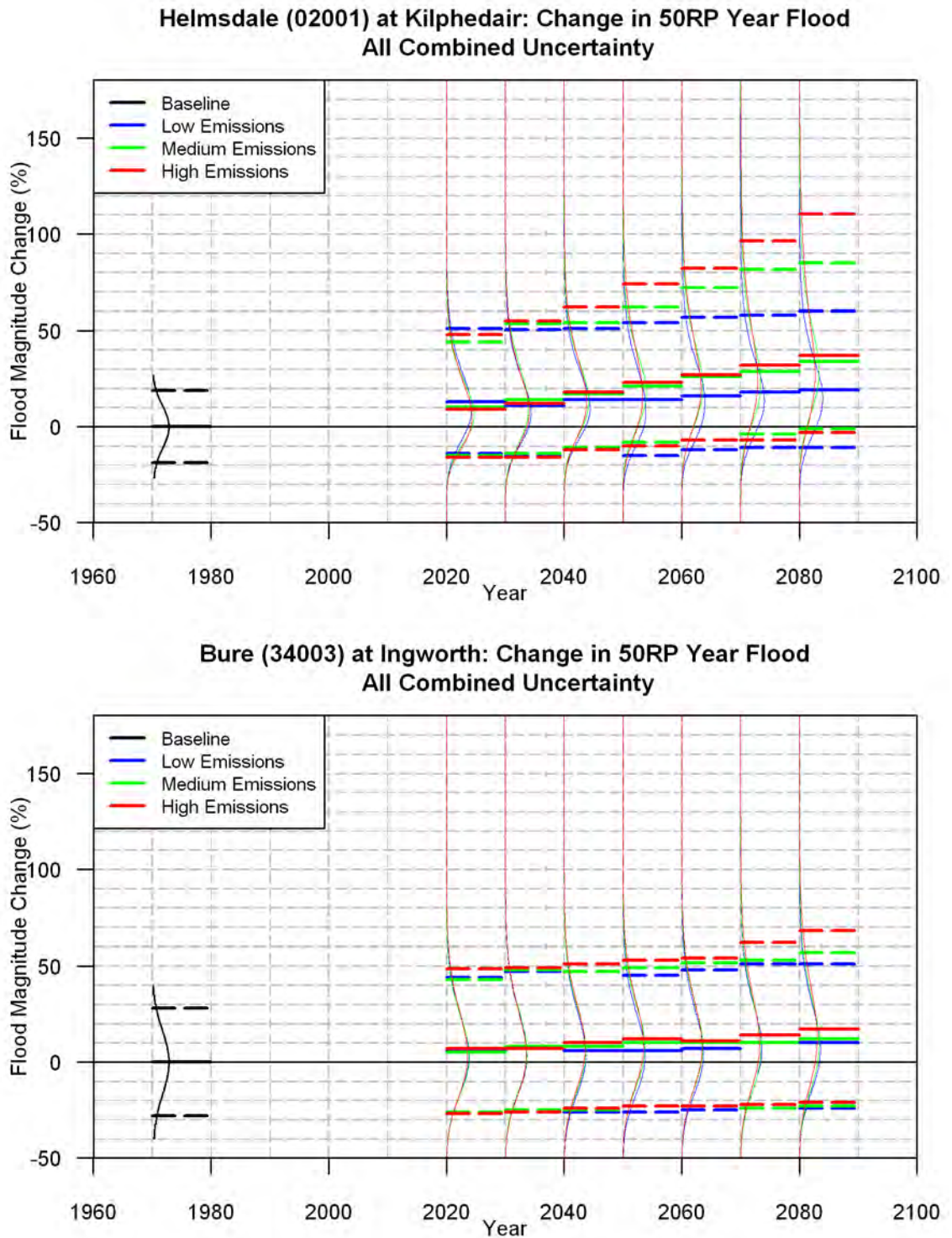
Figure 8.16 Change in 50RP in the Helmsdale (top) and Bure (bottom) catchments projected by UKCP09 precipitation changes under low (blue), medium (green) and high (red) emissions scenarios including hydrological parameter and flood frequency estimation uncertainty. The baseline flood frequency estimation uncertainty is shown in black.
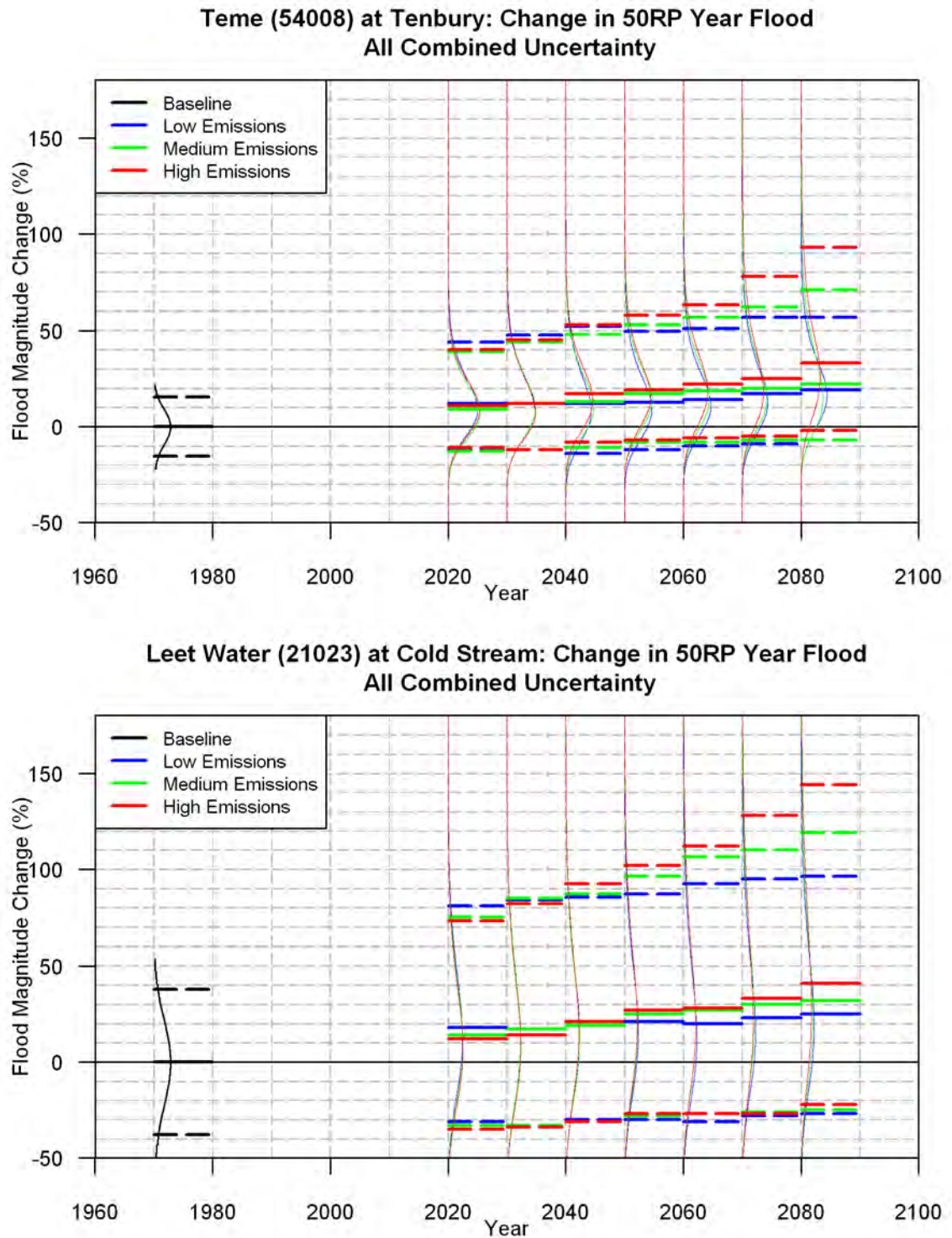
Figure 8.17 Change in 50RP in the Helmsdale (top) and Bure (bottom) catchments projected by UKCP09 precipitation changes under low (blue), medium (green) and high (red) emissions scenarios including hydrological parameter and flood frequency estimation uncertainty. The baseline flood frequency estimation uncertainty is shown in black.

8.4.2 Method for Quantifying Context of Future Projections

The future changes in 50RP are shown in conjunction with the baseline 50RP uncertainty for the Helmsdale, Bure, Teme and Leet Water in Figure 8.16 and Figure 8.17. The baseline uncertainty (black) is expressed as a percentage deviation about its central estimate (as calculated in Chapter 6); ranging from ±15% in the Teme catchment to ±40% in the Leet Water catchment. The future projections increase in range over time for all catchments, but a proportion of future projections remain within the range of the baseline uncertainty. For instance in the Bure catchment, a large proportion of the projection uncertainty lies within the baseline range even for the 2080s. For the Helmsdale catchment a large proportion of possible 50RP changes are outside the range of uncertainty associated with the baseline estimate. As current flood management plans are designed to cope with baseline uncertainty, knowing how much of the future projection is included (or excluded) by the baseline uncertainty can help inform future flood management decisions.

In practice, flood management decisions are made with regards to the baseline uncertainty. For example if the baseline uncertainty is very large, the flood estimate covering 80% of the uncertainty range (80th percentile) may have been taken as precautionary; alternatively if the uncertainty is small a less precautionary 50th percentile (i.e. the median) may be used. This present day decision influences the current level of flood protection but in turn affects the proportion of future scenarios which may be protected against by the baseline flood management decision.

Future projections can be expressed in the context of the baseline flood estimate uncertainty by taking each percentile of the baseline flood frequency uncertainty as a reference threshold. For each reference threshold, the percentage of future projections with flood peak changes that are less than or equal to the reference are calculated. This is undertaken independently for a given return period (5RP, 20RP and 50RP), emission scenario (low, medium and high) and time horizon (2020-2080). This represents the percentage of future projections that are protected against by a given reference threshold with the results shown in Figure 8.18 to Figure 8.26. Each figure includes the results from a single catchment for the 5RP (top), 20RP (middle) and 50RP (bottom) under low (left), medium (middle) and high (right) emissions scenarios. Each baseline reference threshold is plotted on the y-axis with time horizon varying on the x-axis. The percentage of future projections which do not exceed that reference threshold is calculated and displayed using colour bands (i.e. the percentage of

future projections protected against by using a given baseline percentile as a design threshold). Regions on the plots with green/blue colours indicate where a large proportion of future projections will be protected against if the corresponding reference threshold was chosen as a flood design allowance. The regions that are red/orange represent a greater proportion of future projections that will exceed the corresponding reference threshold and are therefore not covered by the baseline flood allowance.

8.4.3 Results from Baseline Context of Future Projections

In this section the term probability is used to describe the proportion of future projections which exceed (or not) a given baseline reference threshold. The probability is only relevant in the context of the total range of the future projection and does not describe a likelihood of occurrence for a projection.

The greatest probability of a future projection lying within the baseline uncertainty is for the Bure catchment. For the 50RP the median reference threshold is greater than 45% of future projections in 2020s (low emissions) decreasing to 30% by the 2080s. The maximum percentage of future scenarios protected against is between 80%-90% (depending on the time horizon) when the 95th percentile reference threshold is chosen as the flood design allowance for 50RP distribution.

In contrast the Yealm catchment displays the lowest probability that a future projection would be protected by a given baseline flood allowance. A reference threshold equal to the 95th percentile of the baseline 5RP would provide a level of protection between 40% in the 2020s (high emissions) to only 15% by the 2080s (all emissions). If the flood design allowance is taken as the 5RP estimate ignoring any uncertainty (equivalent to a reference threshold for the baseline distributions 50th percentile) all future projections exceed this threshold by 2050, suggesting that this allowance offers no protection against future climate change by the 2050s regardless of the emissions scenario.

The results vary between catchments but can be grouped according to the size of the baseline flood frequency estimation uncertainty. The three catchments with the largest baseline uncertainty (Findhorn, Bure and Leet Water) have a greater probability that the baseline uncertainty will cover the largest proportion of the future impacts of climate. Across all catchments the future changes in flood quantiles for larger return periods (e.g. 50RP) have a higher probability of exceeding a given baseline flood allowance. The three emissions

scenarios typically display similar results until the 2040s at which point the medium and high emissions show greater increases in flood changes. This in turn increases the proportion of scenarios which exceed a given baseline flood allowance or alternatively can be described as a decrease in the probability that a baseline flood design allowance provides effective future protection.

It is clear that a large proportion of future flood peak projections still lie outside the current range of baseline uncertainty in most catchments (orange and red colours in the graphs), and that this proportion increases with time horizon. The exception is for catchments with a large baseline uncertainty where baseline flood design can remain effective against future climate projections. This probability of maintaining protection is greatest in the nearer-term (i.e. 2020s-2040s) and diminishes with time horizon. The results highlight that management approaches to climate change should be designed on an individual catchment basis. In the Yealm no percentile of the baseline flood estimate offers protection against the future projections by the 2050s suggesting that keeping the baseline flood policy would not be appropriate; whereas in the Findhorn catchment the 50RP baseline estimate could potentially provide protection for between 0%-90% of future projections by the 2080s.

The probability that a baseline flood allowance can offer protection against the projected impact of climate change on flood peaks is primarily controlled by the size of the baseline flood frequency uncertainty. A larger baseline uncertainty allows a greater probability of incorporating a future flood peak change but only if it is incorporated within a design.
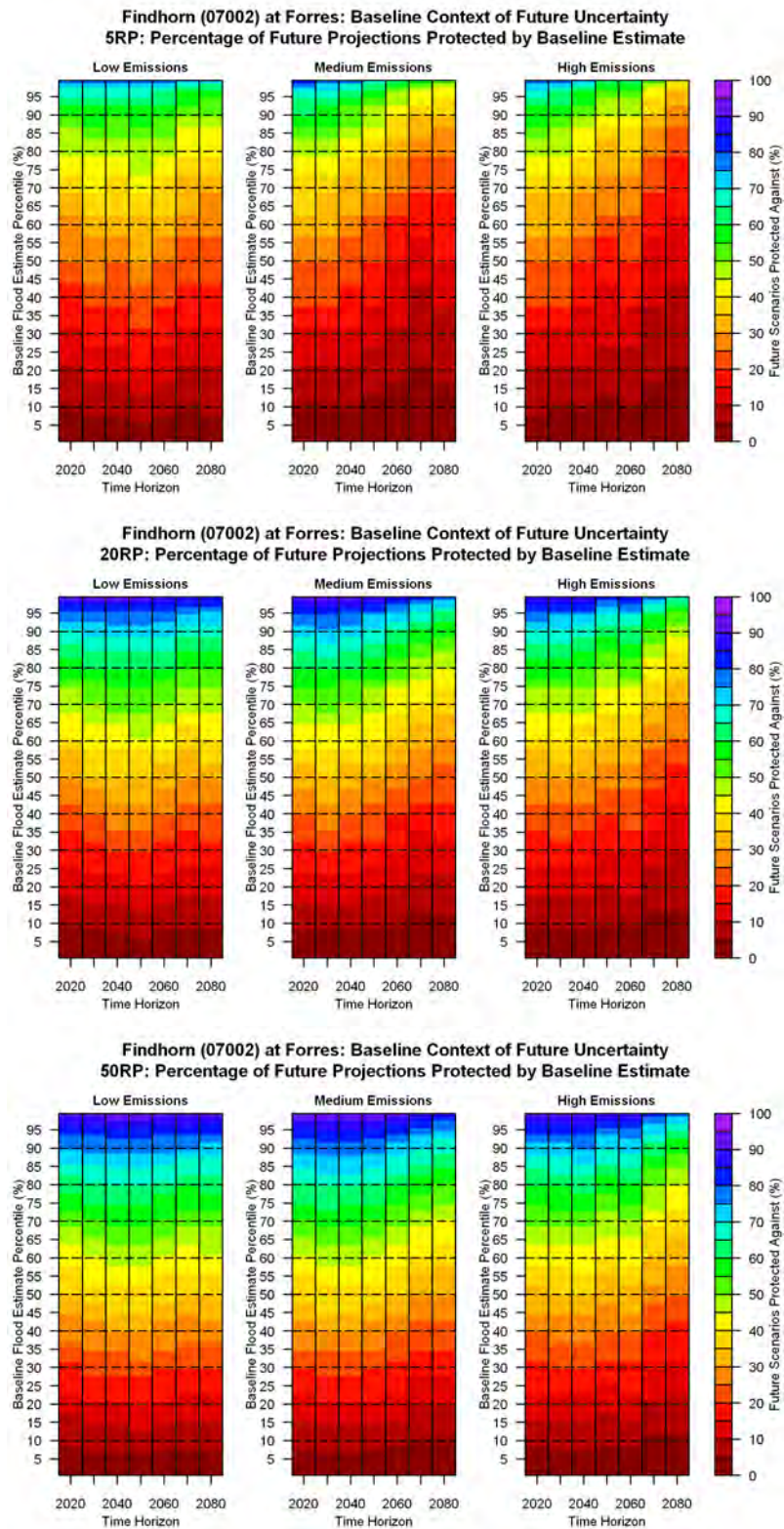
Figure 8.18 Percentage of future projections with flood changes greater than a given percentile allowance of the baseline flood estimate in the Findhorn catchment for the 5RP (top), 20RP (middle) and 50RP (bottom) under low (left), medium (middle) and high (right) emissions.
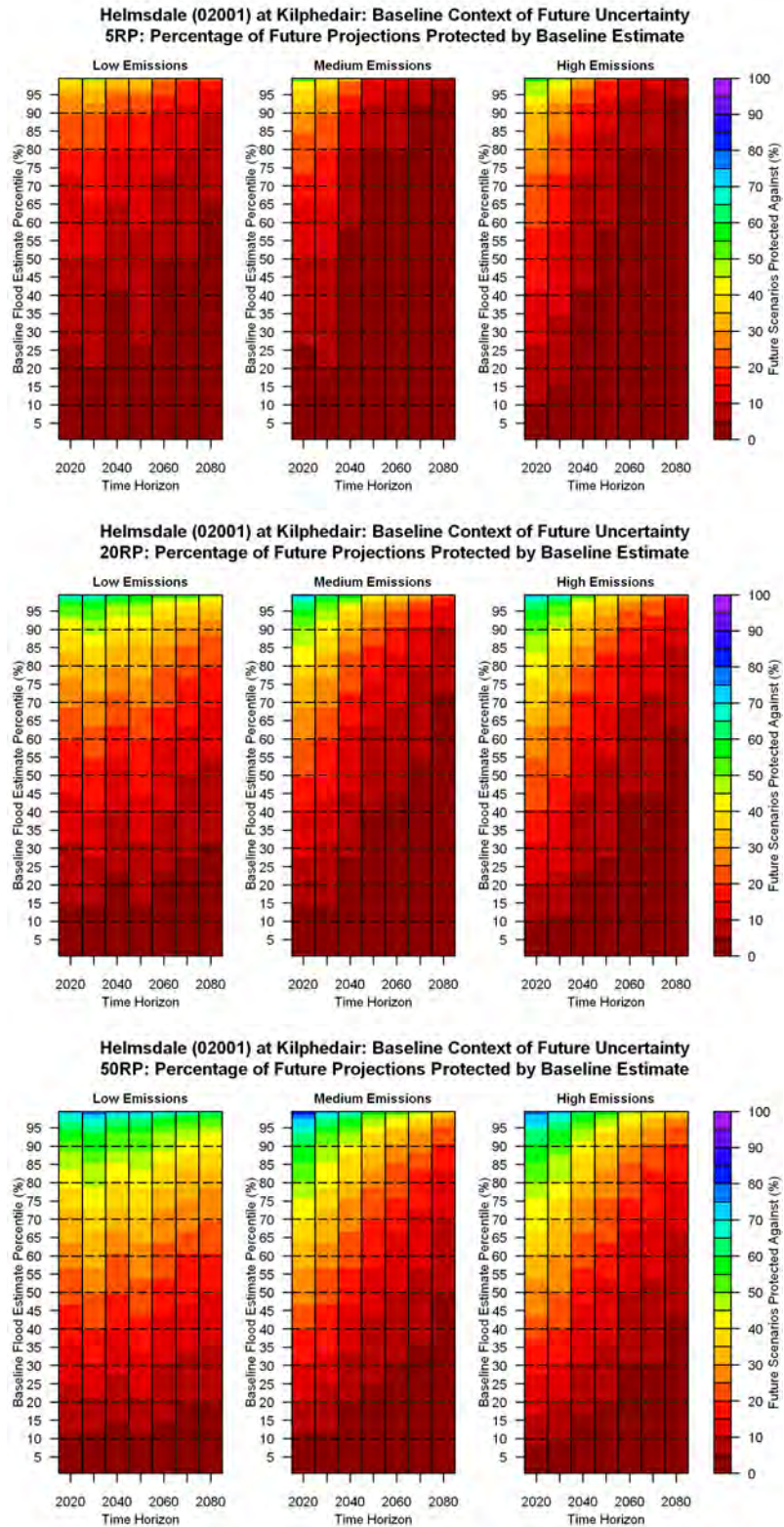
Figure 8.19 Percentage of future projections with flood changes greater than a given percentile allowance of the baseline flood estimate in the Helmsdale catchment for the 5RP (top), 20RP (middle) and 50RP (bottom) under low (left), medium (middle) and high (right) emissions.
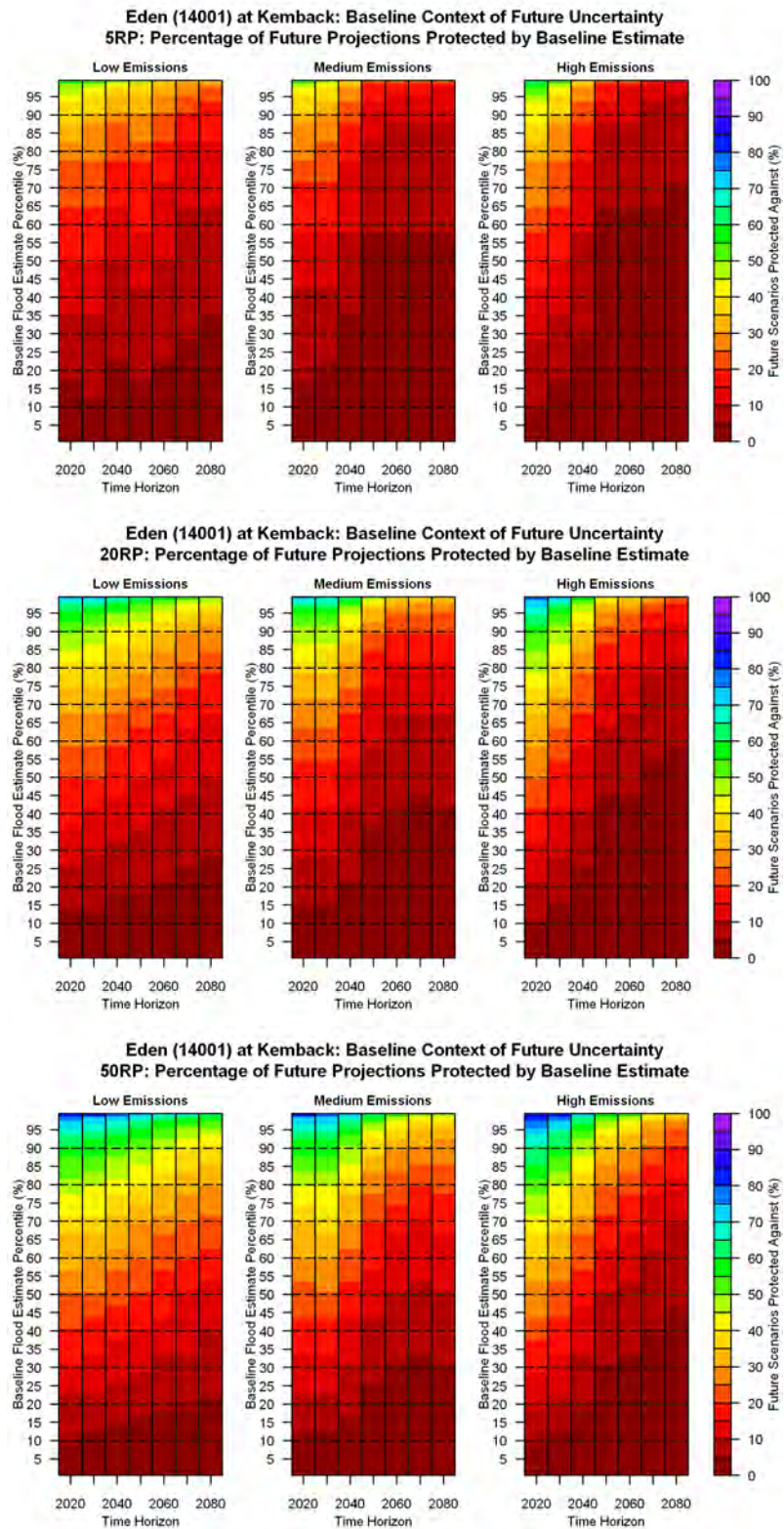
Figure 8.20 Percentage of future projections with flood changes greater than a given percentile allowance of the baseline flood estimate in the Eden catchment for the 5RP (top), 20RP (middle) and 50RP (bottom) under low (left), medium (middle) and high (right) emissions.
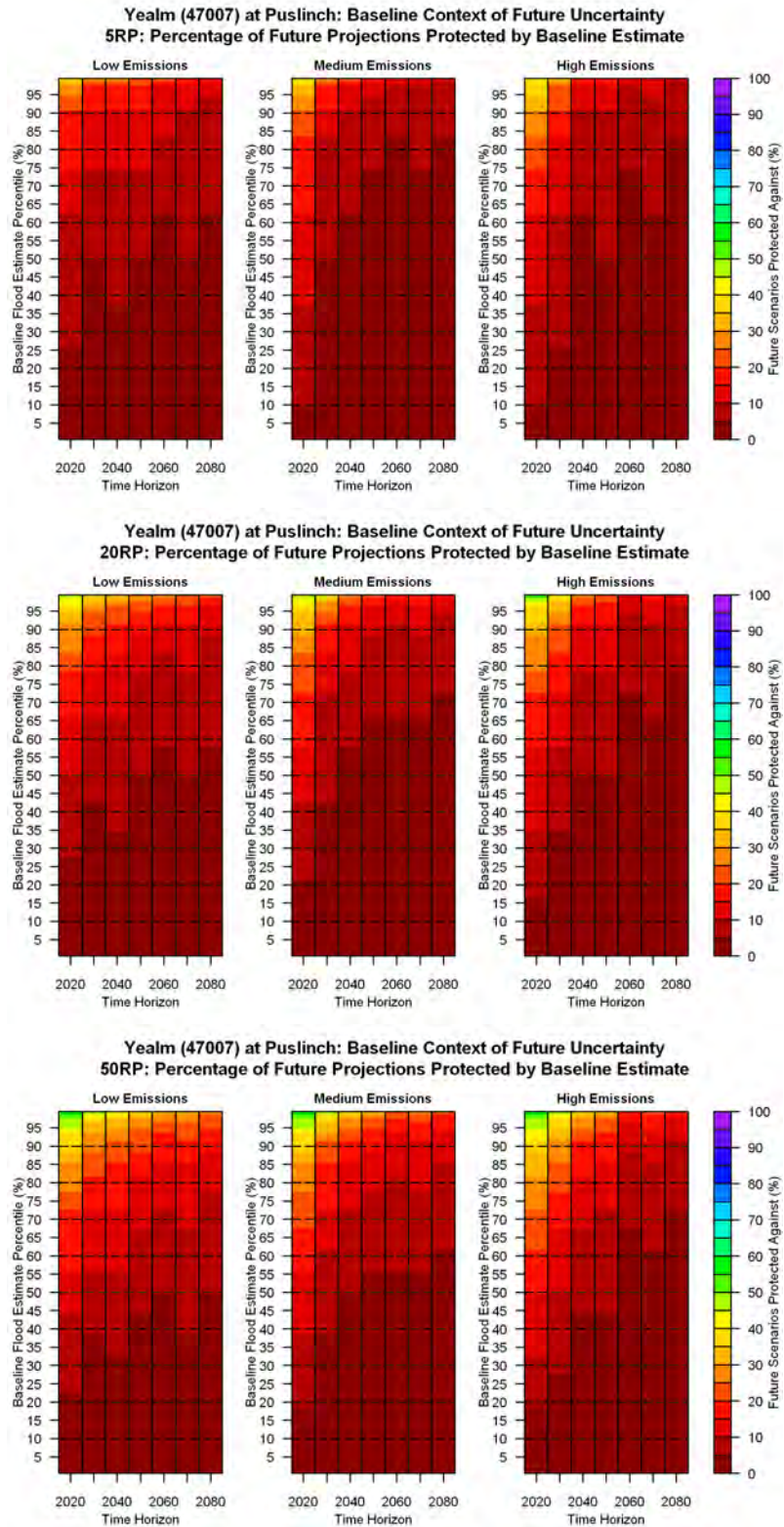
Figure 8.21 Percentage of future projections with flood changes greater than a given percentile allowance of the baseline flood estimate in the Yealm catchment for the 5RP (top), 20RP (middle) and 50RP (bottom) under low (left), medium (middle) and high (right) emissions.
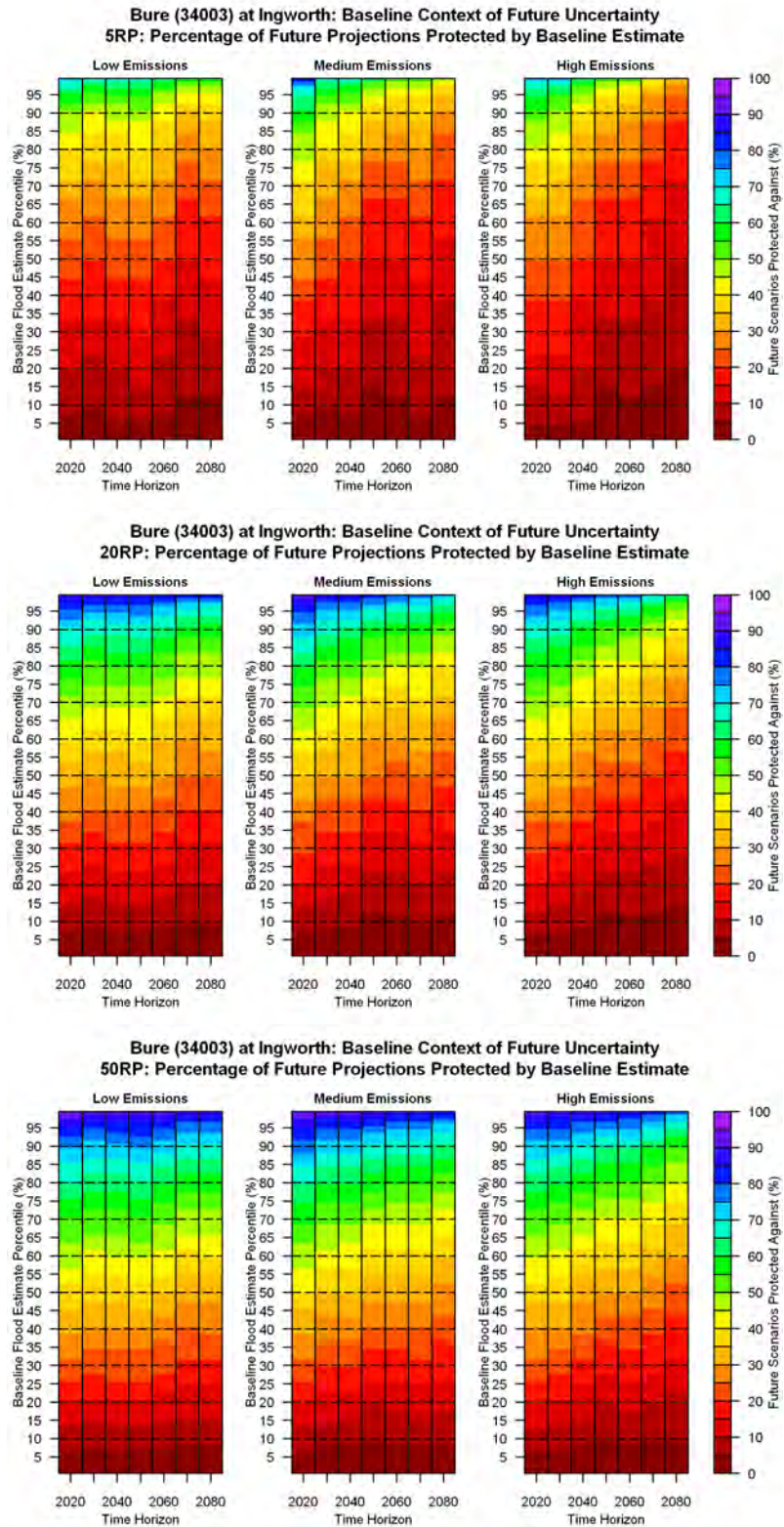
Figure 8.22 Percentage of future projections with flood changes greater than a given percentile allowance of the baseline flood estimate in the Bure catchment for the 5RP (top), 20RP (middle) and 50RP (bottom) under low (left), medium (middle) and high (right) emissions.
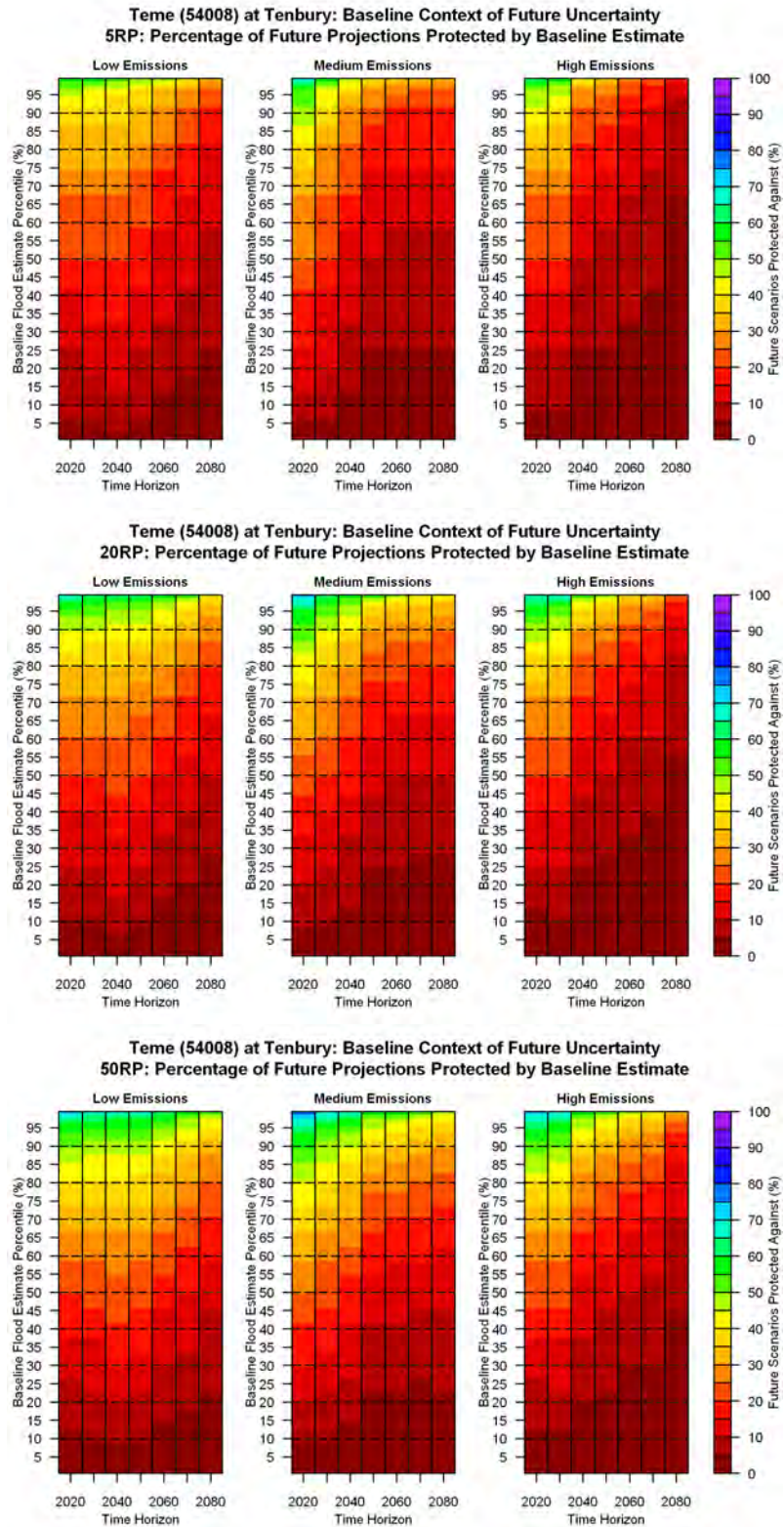
Figure 8.23 Percentage of future projections with flood changes greater than a given percentile allowance of the baseline flood estimate in the Teme catchment for the 5RP (top), 20RP (middle) and 50RP (bottom) under low (left), medium (middle) and high (right) emissions.
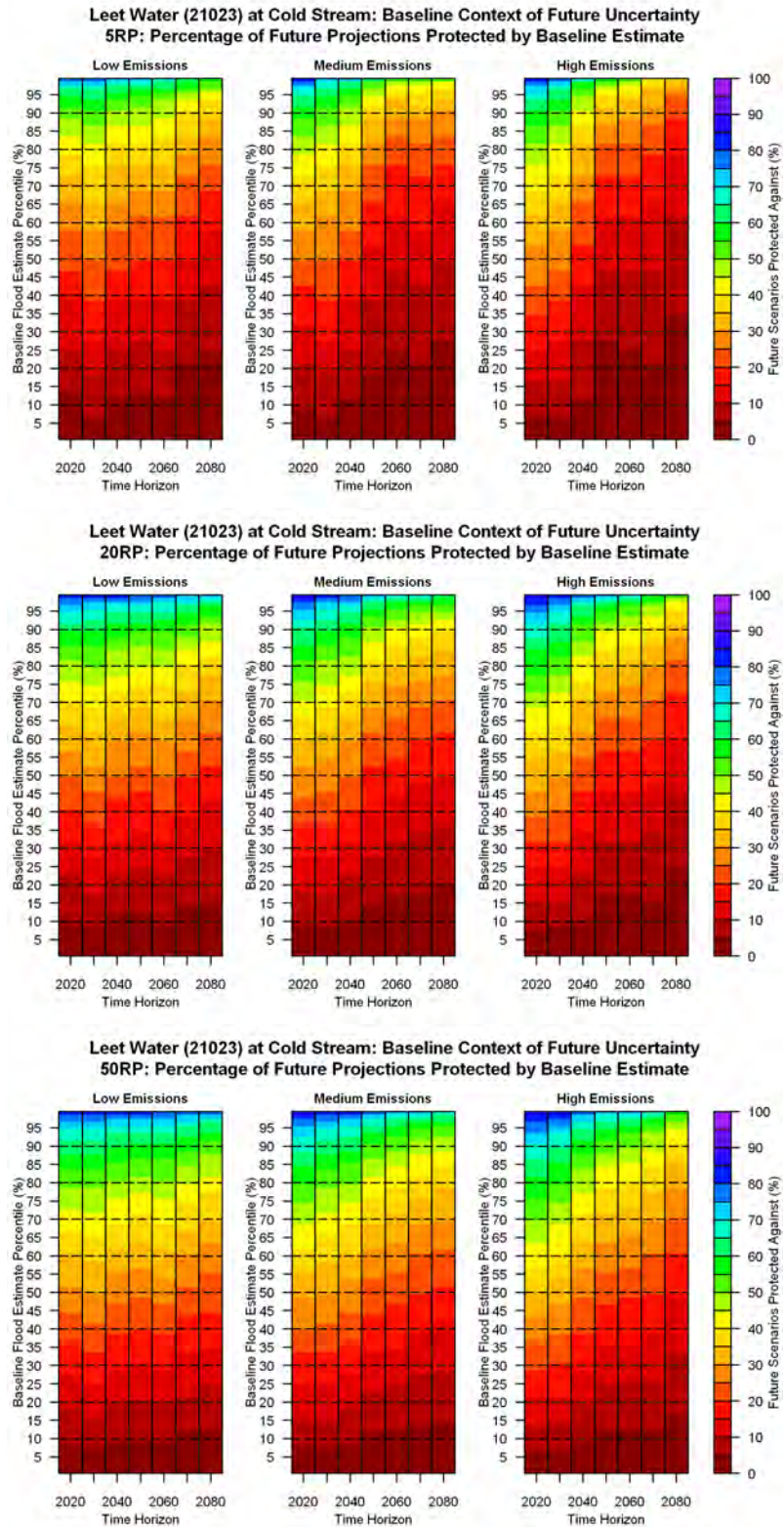
Figure 8.24 Percentage of future projections with flood changes greater than a given percentile allowance of the baseline flood estimate in the Leet Water catchment for the 5RP (top), 20RP (middle) and 50RP (bottom) under low (left), medium (middle) and high (right) emissions.
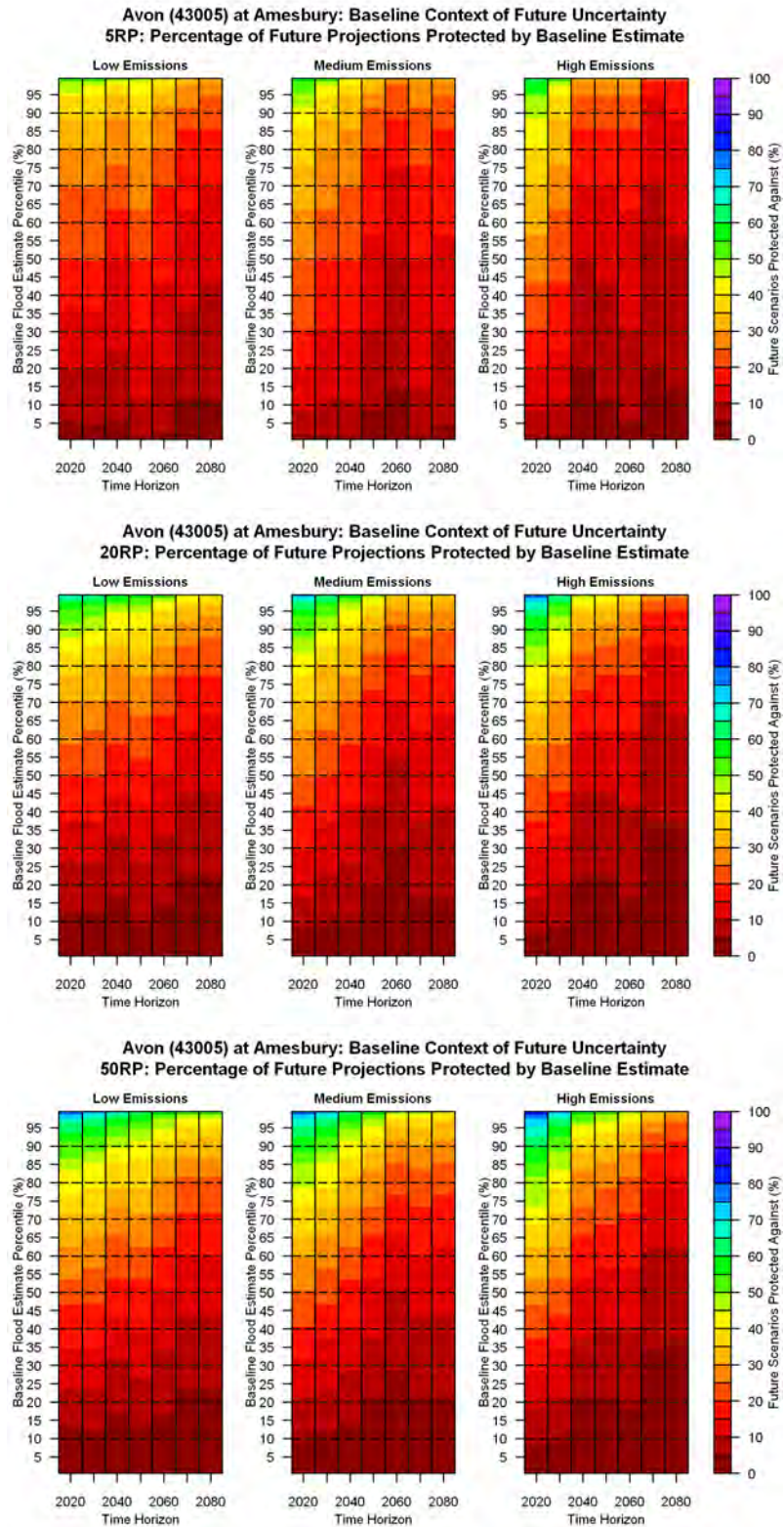
Figure 8.25 Percentage of future projections with flood changes greater than a given percentile allowance of the baseline flood estimate in the Avon catchment for the 5RP (top), 20RP (middle) and 50RP (bottom) under low (left), medium (middle) and high (right) emissions.
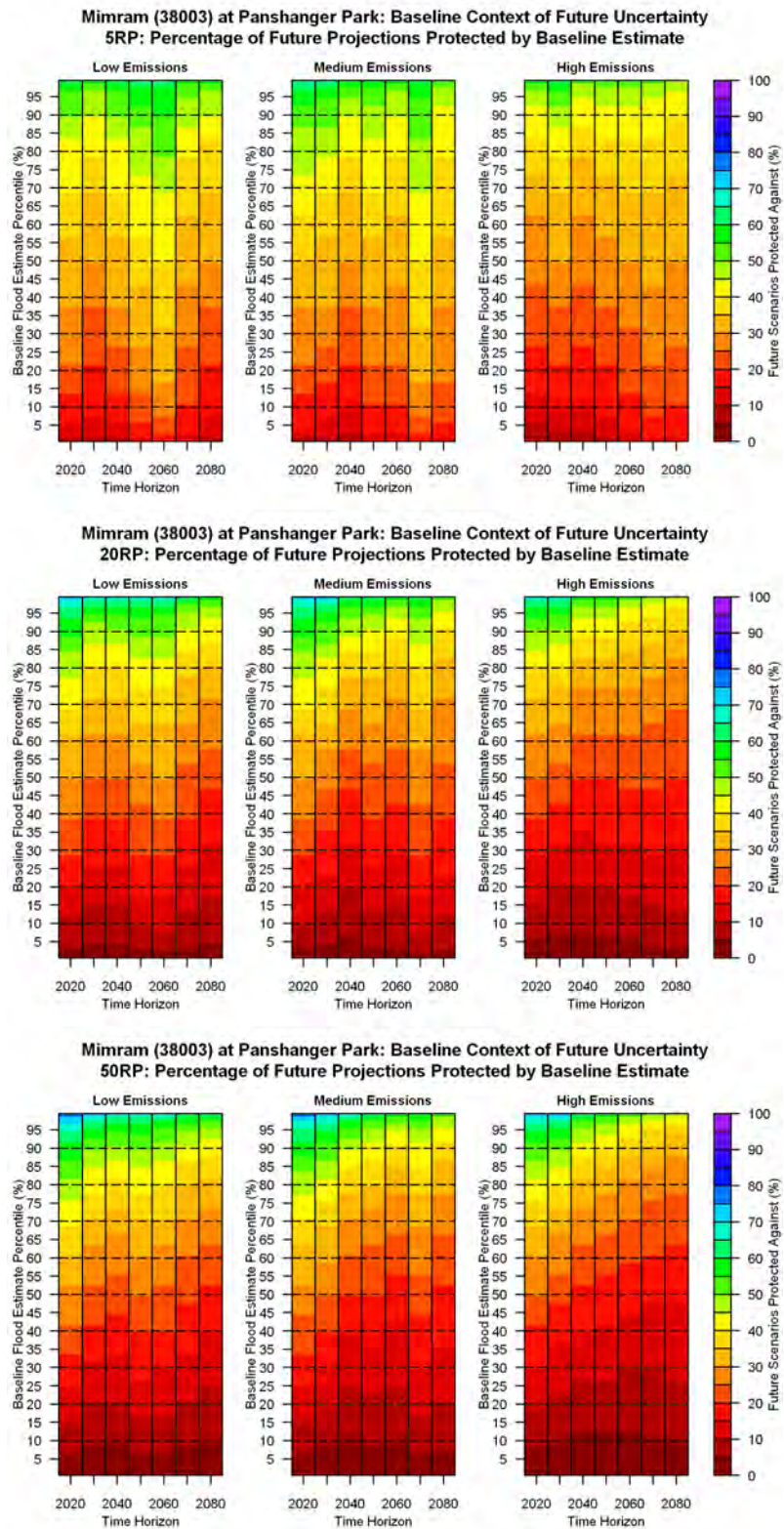
Figure 8.26 Percentage of future projections with flood changes greater than a given percentile allowance of the baseline flood estimate in the Mimram catchment for the 5RP (top), 20RP (middle) and 50RP (bottom) under low (left), medium (middle) and high (right) emissions.

8.4.4 Evaluation of Current Adaptation Allowance

The previous section evaluated the level of protection offered by a baseline flood design allowance against future projections of flooding. In the UK the currently recommended climate change adaptation allowance was, at the time of analysis, to add 20% to baseline values. This section evaluates the percentage of future projections that are protected against by the baseline estimate plus a 20% allowance (referred to as Base20). The analysis is presented for the Yealm (Figure 8.27) and Bure (Figure 8.28) catchments which previously displayed the lowest and highest levels of potential future protection respectively.

When a 20% allowance is added to all baseline percentiles the level of protection increases in the Yealm. The greatest impact is for the 5RP, with a decreasing impact as the return period increases in magnitude. For the 50RP flood the 20% allowance could add an extra protection of between 60% (low emissions) and 40% (high emissions) compared with not including an allowance. However, the way the flood design allowance is originally calculated plays an important role; the median Base20 50RP provides protection between 60%-80% until the 2040s, but reduces to only 20%-40% by the 2080s. If a different percentile is considered, such as the 75th percentile, protection could be provided against 30%-50% of future projections in the 2080s.

Adding a 20% allowance in the Bure catchment is most effective for the 5RP in the near term (2020-2040). By the 2080s a design based on the 50th percentile 5RP value is exceeded by between 60% (high) and 30% (low) of future projections. For the 50RP, protection against up to 90% of future projections is provided in the 2080s for low, medium and high emissions based on a Base20 equal to the 75th, 80th and 90th percentiles of the 50RP distribution respectively.

The results suggest that the 20% allowance can provide an adequate measure of protection in the Bure catchment but remains dependent on the threshold level of the baseline estimate. This is particularly true for catchments with a higher confidence (i.e. smaller uncertainty in flood quantile estimation) in the baseline flood quantile estimate, such as the Yealm catchment.
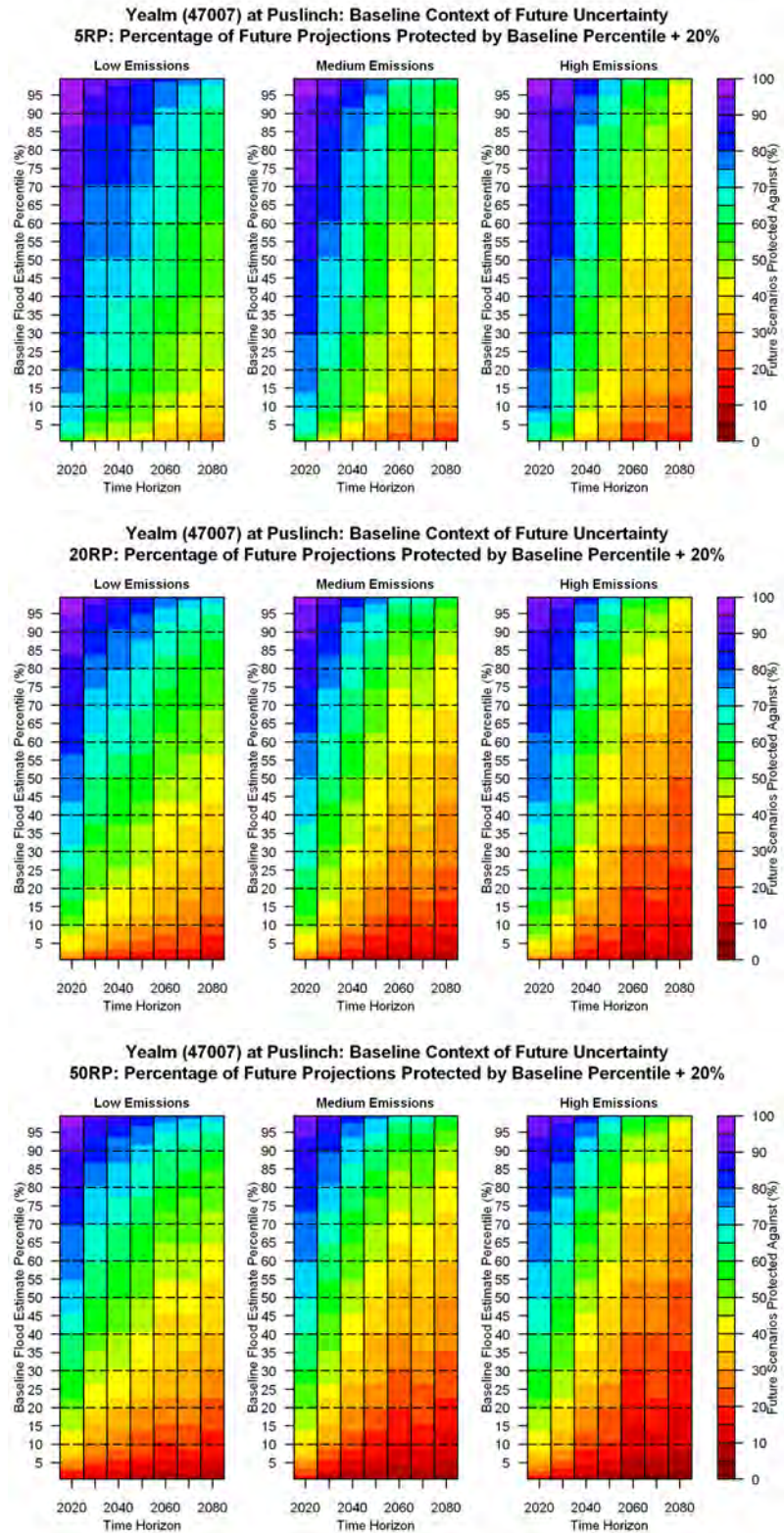
Figure 8.27 Percentage of future scenarios that the different confidence levels of the baseline flood estimate with 20% allowance offer protection against in the Yealm catchment for the 5RP, 20RP and 50RP under low (left), medium (middle) and high (right) emissions.
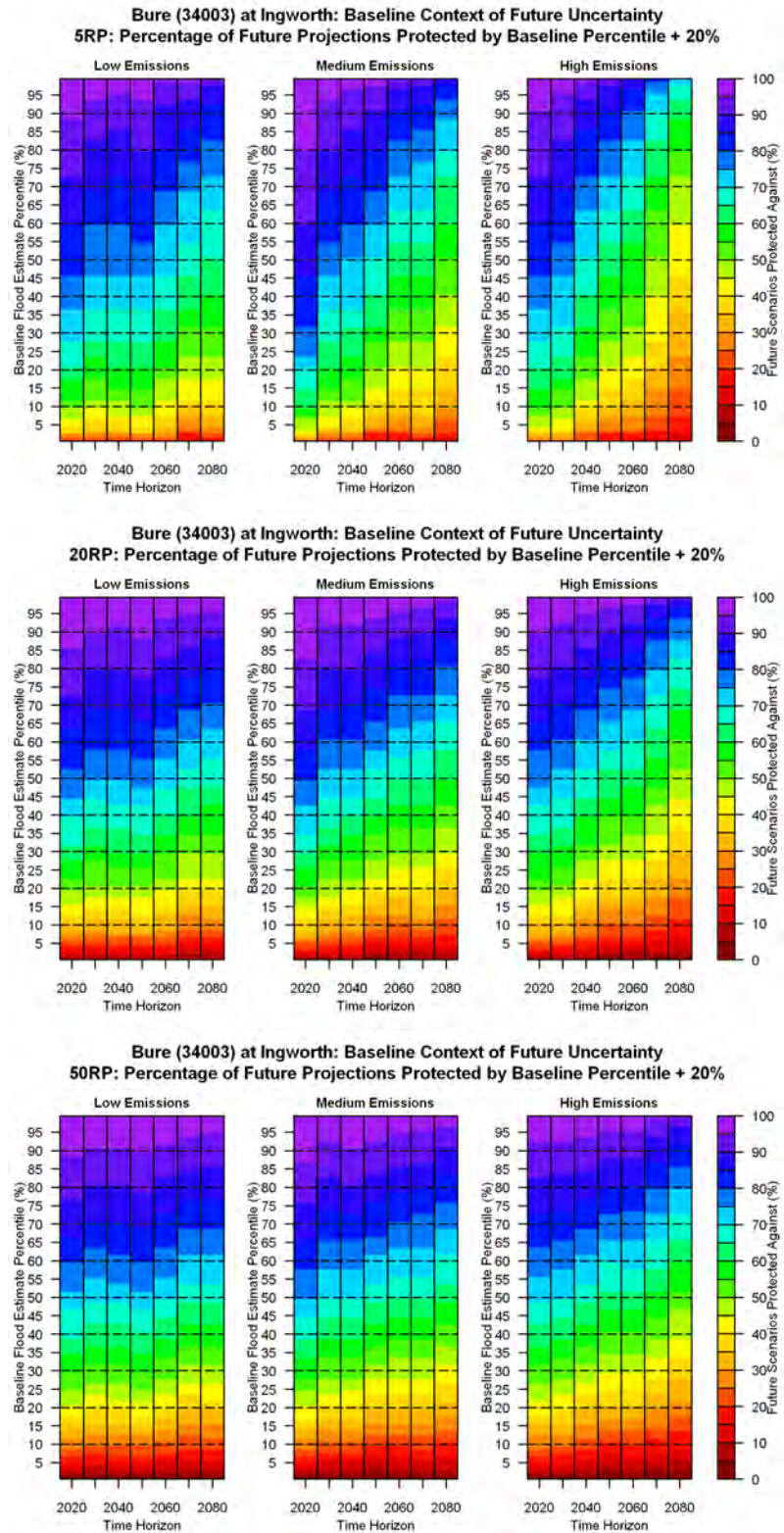
Figure 8.28 Percentage of future scenarios that the different confidence levels of the baseline flood estimate with 20% allowance offer protection against in the Bure catchment for the 5RP, 20RP and 50RP under low (left), medium (middle) and high (right) emissions.
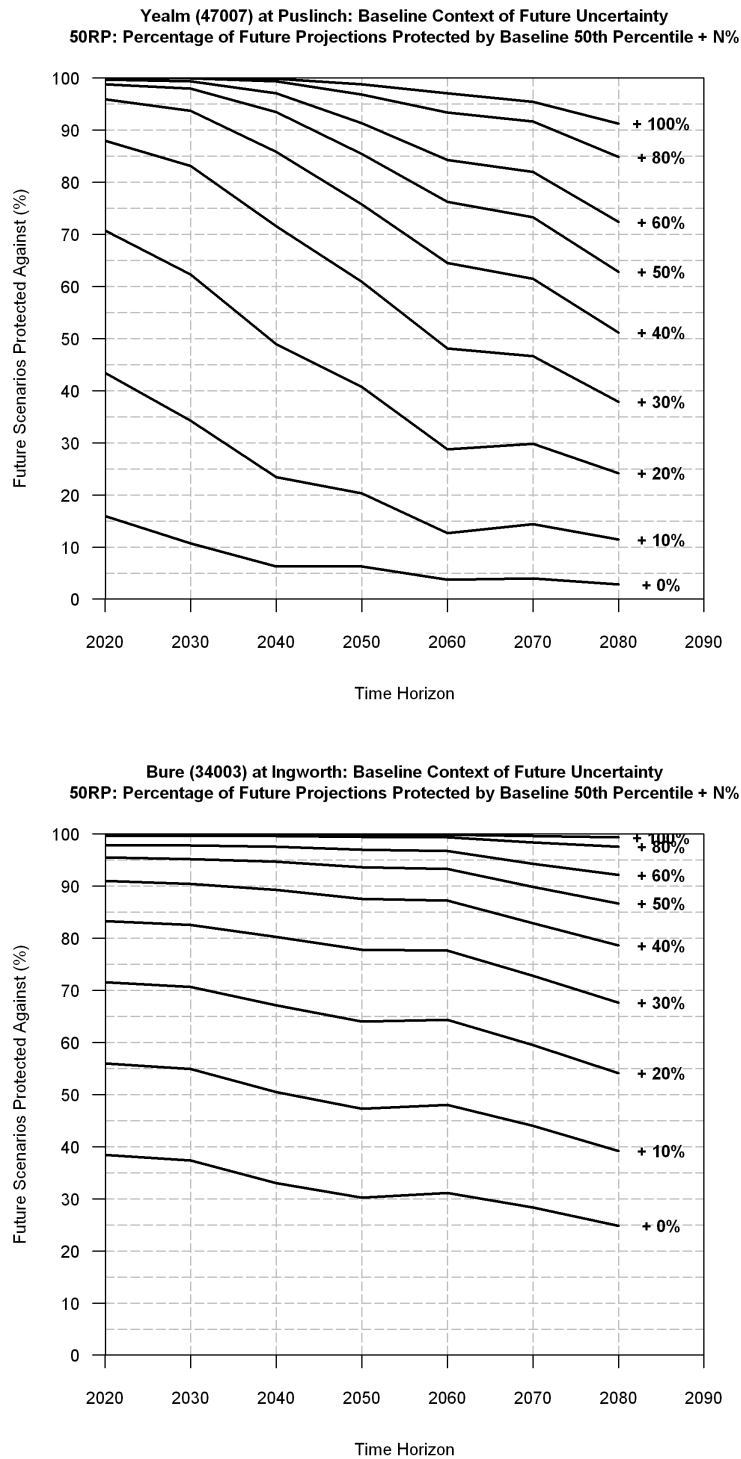
Figure 8.29 Percentage of future flood changes for a high emissions scenario which exceed the different flood allowances added to the 50th percentile of the baseline for the Yealm (top) and Bure (bottom) catchments.

The use of a blanket 20% allowance provides a different level of protection in each catchment; further evidence of this is provided by considering several alternative flood

allowances for the Yealm and Bure catchments (Figure 8.29). When the flood design is based on the 50RP flood estimate without uncertainty (i.e. the median of the 50RP baseline distribution) an allowance of +40% would protect against 80% of future projections in the Bure by 2080, whereas in the Yealm only 50% of projections would be protected against. Each increase in the flood allowance in the Bure provides a smaller increase in benefit than the previous allowance, with increases in the flood allowance above 50% adding little extra benefit.

The same pattern is evident in the Yealm for larger allowances up until 2040, after which the level of protection offered by each allowance begins to diverge. In the Yealm catchment, increasing the allowance from 0% to 30% has a large impact on the level of protection for nearer time horizons (up to 2050), with a difference of 50% in 2030. At further time horizons the difference is proportionately smaller as the 30% allowance offers a decreasing level of protection.

If a design target was set to protect against 50% of future projections, the flood allowance required in the Yealm would be +20% up to 2040, +30% up to 2060 and +40% thereafter. For the equivalent level of protection in the Bure a 10% allowance is required up to 2040 and +20% allowance thereafter. This further highlights that the application of a flood adaptation allowance needs to be considered on an individual catchment basis, taking into account the time horizon and emissions scenario

8.5 Discussion and Conclusions

The first aim of this chapter is to identify the role of uncertainty of four components of the climate change impact study; emissions scenarios, climate model, hydrological model parameters and flood frequency analysis. The importance of the different sources of uncertainty is shown to vary by catchment and time horizon. Emissions scenario uncertainty is small during the early 21st century but increases in size from the 2050s, typically becoming the dominant uncertainty source by the 2080s. UKCP09 uncertainty contributes the largest component of uncertainty prior to the 2070s, when emissions uncertainty increases. The exception to this is in catchments that are sensitive to flood frequency analysis at high return periods, where flood estimation uncertainty is large; in these instances flood frequency uncertainty can be greater or equal in magnitude to UKCP09 uncertainty. The influence of flood frequency uncertainty is greatest at closer time horizons and decreases thereafter, in some cases it contributes a negative uncertainty where the range of flood changes is reduced

through its inclusion. Hydrological parameter uncertainty is small relative to the other uncertainty sources and has no significant trends.

The results obtained here are dependent on the methods employed to analyse the uncertainty components. A number of assumptions are made to extract the different fractions of uncertainty. For instance UKCP09 model uncertainty is assumed to be equivalent to the smallest distribution of the three emissions scenarios at a given time horizon. This assumption is made due to there being no baseline UKCP09 time series for comparison but is further complicated by skewed distributions of change (i.e. high emissions have a greater distribution tail to larger flood increases). If the three emissions scenarios were compared at an individual percentile of each emissions distribution the quantified difference between the emissions scenarios would vary (e.g. the difference between emissions scenarios is larger at the 95th percentile compared to the median).

The results are also dependent on the experiment design, which is a compromise for reasons of computational resources and efficiency. A reduced number of UKCP09 scenarios were considered, which although found to be adequate through sensitivity tests, represent a compromise to the full 10,000 scenarios. Further to this assumption, only 50 hydrological parameter sets were included. Using a larger number of parameter sets may have altered the role of the model parameter uncertainty; although previous studies have also identified this as being a small component.

It is important to note that a number of uncertainty sources were not included as part of this analysis. The role of climate variability was not explicitly included, despite its importance being highlighted in Chapter 4. The UKCP09 climate scenarios include the effects of climate variability meaning that the UKCP09 uncertainty proportion could have been partitioned between climate model uncertainty and climate variability (following Chapter 4 and Hawkins and Sutton (2011)) if an ensemble of baseline climate realisation was available from UKCP09; which is not the case. Another uncertainty source not included here is the choice of downscaling method. Climate change factors are used to perturb the observed record, alternatively weather generated time series could have been used with the change factors. Lastly the influence of hydrological model structure was not included, with only the PDM hydrological model used.

The second aim of this chapter is to place the future climate projections and their uncertainties in the context of the uncertainty associated with the baseline. This was undertaken by comparing each future projections distribution with the distribution of the baseline flood frequency estimate. The percentage of future projections protected by the baseline estimate depends on the magnitude of the baseline uncertainty and the level of the baseline percentile threshold considered. Catchments with a large baseline uncertainty have the greatest potential to offer protection against future projections due to the large range of baseline uncertainty; however their effective protection depends on the adopted flood allowance. This demonstrates that considering uncertainty in the baseline flood estimate also helps to provide a level of protection against possible future flood changes.

Where the baseline flood protection is not adequate it is important to consider increasing the level of protection through the use of a climate change allowance. Including the currently recommended allowance of 20% is shown to offer increased levels of protection in the nearer term but may not be sufficient at more distant time horizons. Furthermore the use of a blanket allowance for all catchments provides a different level of future protection in each catchment. A varying allowance applied on a catchment by catchment basis would allow for the same level of protection to be attained.

8.6 Chapter Summary

The importance of the different components of uncertainty in a 'top-down' impact study framework have been analysed in this chapter. This was undertaken using three emissions scenarios, 500 randomly selected UKCP09 precipitation change factors, 50 hydrological model parameter sets and flood frequency analysis uncertainty. These components were simulated sequentially for nine catchments resulting in 75,000 future changes in the 5RP, 20RP and 50RP each with a standard error of flood frequency uncertainty for each decadal time horizon in the 21st century.

The different components of uncertainty were partitioned to calculate their relative contributions to the overall distributions of flood changes, allowing for the evaluation of their relative importance over time. While uncertainty is shown to be linked to the catchment and return period, a number of other patterns have emerged. Emissions scenarios were found to contribute a small fraction of uncertainty during the early 21st century but this contribution increased from the 2040s/2050s; becoming the dominant source of uncertainty by the 2080s. The UKCP09 (climate model) uncertainty is found to be the dominant source of uncertainty,

contributing 40%-80%, until emissions uncertainty increases (i.e. up to 2050). The influence of flood frequency is most significant at larger return periods; in three catchments it was equal to or greater than UKCP09 and emissions uncertainty for the 50RP. Overall flood frequency uncertainty was most important for the nearer term (2020-2040) and decreases in its relative contribution thereafter. In some instances incorporating flood frequency uncertainty reduced the range of changes, hence contributing a negative uncertainty component. Hydrological model parameter uncertainty was shown to be small or negligible for all catchments, displaying no spatial or temporal trends.

The future projections for changes in flooding were evaluated in the context of the baseline flood estimate uncertainty. It was found that maintaining the baseline level of protection would offer little future protection in projected changes except in catchments with a large baseline uncertainty. In these instances a precautionary baseline estimate (i.e. 95th percentile of estimate) could provide protection for up to 60% of future projected 50RP changes. Climate change adaptation guidance in the UK recommends an allowance of 20% compared with the baseline value. This is shown to offer improved levels of protection in the near term (2020-2040) but decreases thereafter. Importantly the level of protection provided by the allowance varies between catchments, suggesting that the use of a blanket allowance for all catchments is not sufficient to attain equal levels of protection.

This chapter has combined the different components of uncertainty which have been explored in this thesis. The next chapter concludes the thesis with a summary, conclusions, contributions and suggestions for future work.

CHAPTER 9

Conclusions

9.1 Introduction

The main aim of this thesis was to understand the role of uncertainty in the components of the 'top down' impact study framework when assessing the impact of climate change on UK flooding. In order to address this aim the following research objectives were formulated:

1. Explore methods for quantifying the uncertainty associated with each component of the climate change impact study framework; specifically, the role of climate variability, hydrological model parameter uncertainty and flood frequency analysis uncertainty.
2. Identify the relative importance of the uncertainty associated with each component in the 'top down' climate change impact study framework at different time horizons.
3. Develop methods for presenting future projections and their inherent uncertainties in a practical context.

This chapter provides an overview of the research in this thesis which contributed to fulfilling the research objectives. The key contributions to the science of climate change impact studies are highlighted in section 9.2. The main thesis conclusions are presented in section 9.3. There are a number of suggestions for future work made in 0; with the thesis ending with the concluding remarks 9.5.

9.2 Summary of Main Research Contributions

This section highlights the key research contributions to the field of climate change and hydrology from the work undertaken in this thesis.

1. Flood frequency estimation uncertainty has often been overlooked in climate change impact assessments. This thesis has presented methods for the explicit inclusion of flood frequency uncertainty and it has been shown, in some instances, to be the largest source of uncertainty in a climate change impact study contributing up to 50% of the total range of impacts.

2. The relative importance of the uncertainty associated with each component of the 'top down' impact study framework has been shown to vary at different time horizons. In the near term flood frequency estimation and climate model uncertainty are most important, adding up to 50% and 80% respectively to the full range of impacts. At more distant time horizons emissions scenario uncertainty becomes increasingly important with a total influence of up to 75% by the 2080s. While hydrological model parameter uncertainty is shown to be small to negligible at all time horizons.

3. A resampling methodology has been developed to address the important issue of climate variability in climate change impact studies. The methodology is applied to climate model outputs to provide multiple climate realisations when no multi-realisation model ensemble is available.

4. Considering uncertainty in present day flood frequency estimation is shown to offer a benefit for future adaptation strategies. Where a larger range of uncertainty is accounted for in the present day estimate, a greater proportion of future projections may be covered by the present day level of defence.

5. The calibrated values of specific PDM model parameters have been shown to influence the magnitude of flood quantile changes as a consequence of climate change.

9.3 Thesis Summary and Conclusions

9.3.1 Flood Frequency Analysis Uncertainty: Chapters 6, 7 & 8

Flood frequency analysis uncertainty has been shown to be an important component of uncertainty within the top down impact study framework. Previously flood frequency

analysis uncertainty has been overlooked as a source of uncertainty, often resulting in the quantification of other sources of uncertainty of lesser importance.

In Chapter 6 methods for the explicit inclusion of flood frequency uncertainty were developed. The size of the uncertainty was found to be linked to a catchment's flood peak population (POT3) and in turn it's fitted flood frequency curve. Catchments where the flood frequency curve is unbounded (i.e. The fitted distribution has increasingly large flood values at increasing return periods) were found to have the largest flood frequency uncertainty. It is important to note however that the size of uncertainty does not necessarily influence the estimated magnitude of a flood quantile. In Chapter 7 it was demonstrated that a shorter record length (with larger uncertainty) can produce the same flood quantile estimate as a longer record (with smaller uncertainty).

When flood frequency uncertainty is included in a climate change impact study, the range of 50RP flood changes in catchments with a large flood frequency uncertainty almost doubled. This highlights the importance of considering flood frequency uncertainty, however it is not always necessary to include it in all catchments. To identify when it is necessary to undertake a full flood frequency uncertainty analysis, a simple screening tool was developed in section 6.5.3 to quickly identify catchments with a large influence of flood frequency uncertainty in any climate change impact assessment.

When compared with other sources of uncertainty in the climate change impact study frame work in Chapter 8, flood frequency uncertainty was found to the dominant source of uncertainty at nearer term time horizons. At more distant time horizons it was of equal importance as climate model uncertainty in catchments with a large flood frequency uncertainty.

The results of this thesis highlight the importance of considering flood frequency analysis uncertainty as well as providing a simple screening process to identify when it must be considered. Given its influence on the climate change estimates in some catchments it should be viewed as a compulsory step in the assessment of the climate change impacts on flooding.

9.3.2 The Role of Climate Variability: Chapters 4, 5, 6, 7 & 8

Climate variability and climate change are two distinct phenomena that are implicitly intertwined making it difficult to separate one from the other. This has typically led to a focus on climate change, which is often referred to separately from climate variability despite their

co-occurrence. In this thesis the role of climate variability has manifested itself in a range of different forms throughout, resulting in a number of separate issues.

First of these issues is the role of climate variability in climate model projections. As demonstrated in Chapter 4, a climate model provides just a single realisation of climate and in turn a single realisation of the climate variability. This makes the choice of a baseline and future period within a climate model realisation for application in an impact study a somewhat arbitrary choice. To overcome this issue, as well as the fact that the model may not accurately reproduce the same climate variability compared with observations, a simple resampling methodology was developed. The resampling methodology allows for the explicit inclusion of climate variability within climate change impact studies which is not possible from single or few climate model realisations or the probabilistic UKCP09 projections.

The second issue in relation to climate variability is its role in the observed records that are used as part of the climate change impact analysis, particularly in this example of flood impact assessments. The interest in planning for flood events is a result of their destructive power, however such events by their very nature are rare. Typically in the UK hydrological records range from 30-50 years in length meaning that in most records it is unlikely that a 100-year design standard flood event has occurred. As outlined in Chapter 3 and Chapter 6 this requires the fitting of flood frequency distribution which has a degree of uncertainty that is also linked to the observed record. The occurrence (or not) of a single flood event in the observed record can in some cases influence the magnitude of estimated flood quantiles, particularly if a large extrapolation is required. This issue is also highly influential when calculating the future change in a flood quantile as a result of climate change due to the application of the change factor methodology. With longer record lengths there is a greater chance of capturing the true climate variability providing a greater confidence in any estimated flood quantiles or derived changes in flood quantile. However due to the typically short record lengths it is essential to quantify the uncertainty associated with a flood quantile estimate.

Lastly it is important to understand the combined role of variability in both the climate system and in turn its impact on the variability of the hydrological system. The translation of changes in climate through to changes in flooding has been shown in Chapters 4, 5 and 7, to be highly non-linear. This highlights that there are no short cuts between changes in climate

(either natural of anthropogenic) and changes in hydrology, demonstrating the importance of hydrological analysis and modelling.

9.3.3 Uncertainty in Climate Change Impact Studies: Chapters 4, 5, 6, 7 & 8

This thesis has demonstrated that uncertainty is present in each component of the 'top down' climate change impact study framework. The manner in which the uncertainty cascades from one component to the next has been shown to vary between catchments, time horizon and flood return period.

In Chapter 8 the different components of uncertainty were combined to assess their relative size and importance. In the near term flood frequency analysis uncertainty was shown to be the dominant source of uncertainty in a number of catchments. In catchments where flood frequency analysis uncertainty is small, climate model uncertainty was found to be the largest source of uncertainty. In Chapter 8, climate model uncertainty was incorporated using the probabilistic UKCP09 projections which do not allow for the explicit quantification of climate variability which, as discussed in section 9.3.2, is also known to be important. At further time horizons the choice of emissions scenario was shown to become more influential, becoming the dominant source of uncertainty by the 2080s in most catchments.

Hydrological model parameters were found to contribute only a small proportion of uncertainty compared with the other uncertainty sources in Chapter 8. This is likely due to the use of a large ensemble of climate change projections (500 UKCP09). If a smaller number of climate change projections were used, hydrological model parameter uncertainty becomes more important. This is particularly significant given the results in Chapter 5 demonstrate that specific PDM model parameters (C_{max} and the secondary flow routing), when combined with large precipitation increases, can influence the size of change of a flood quantile. If a smaller sub-sample of UKCP09 was selected, one of which was very wet, the derived changes in flood quantile may be viewed differently compared with the changes from the full UKCP09 ensemble. It is therefore recommended that where a larger ensemble of climate projections are used hydrological model parameter uncertainty is not essential to include, but where a smaller number of climate projections are considered so too must hydrological model parameter uncertainty be considered.

Table 9.1 Summary of uncertainties that are present in this thesis that are either explicitly quantified or implicitly embedded within the analysis.

Uncertainty	Role in Thesis	Description
Data	Implicit	- Uncertainty in measurement of river flows, in particularly peak flows. - Uncertainty in the rain gauge measurements of precipitation. - There are a number of methods for calculation of potential evapotranspiration.
Physical Processes	Implicit	An incomplete understanding of the physical processes that a computational model is representing.
Emissions Scenarios	Explicit	A range of emissions scenarios were used in this thesis.
Climate Modelling	Explicit	13 CMIP3 climate models were in Chapter 4. - The UKCP09 probabilistic climate projections were also used.
Higher Frequency Climate Variability	Explicit	- Variations in the magnitude and sequence of the climate from year to year. - Addressed through the development of the resampling methodology in Chapter 4.
Lower Frequency Climate Variability	Implicit	Variations in the climate over multiple decades due to larger scale processes such as the NAO.
Downscaling	Explicit and Implicit	- Change factors were used to perturb historic time series. - No inclusion of alternative statistical or dynamical methods.
Hydrological Model Structure	Implicit	- Only a reduced parameter version of the PDM hydrological model was used. - No alternative hydrological models were used in this thesis.
Hydrological Model Parameters	Explicit	Chapter 5 outlines the exploration and testing of PDM model parameters.
Snowmelt Modelling	Implicit	There is uncertainty in both the structure and parameters of the snowmelt module which were not explored.
Flood Frequency Analysis Distribution	Implicit	- A number of flood frequency extreme value distributions exist. - The Generalised Pareto distribution was the only distribution used in this analysis.
Flood Frequency Analysis Fitting	Explicit	The uncertainty in fitting a flood distribution was covered in detail in Chapter 6.

The quantification of uncertainty needs to be balanced with a pragmatic approach to climate change impact modelling. Table 9.1 provides a full list of the uncertainties in this thesis, many of which have been explicitly quantified. Although an impact study can never be entirely exhaustive, this thesis has demonstrated a number of methods and tools for allowing a better characterisation of uncertainty. Further to this, in Chapter 8 quantifying both baseline and future uncertainty was shown to offer potential benefits for the longer term management of flooding. Where a higher level of baseline flood frequency uncertainty is considered in present day planning, the greater the potential to provide protection against future climate change and its associated uncertainty.

9.4 Suggestions for Future Work

This thesis has explored the uncertainty associated with a number of components in the 'top down' impact study framework. In this section are a number of recommendations for future research based on the findings and conclusions of this thesis.

9.4.1 Uncertainty from Downscaling and Hydrological Model Structure

This thesis has included a number of uncertainty sources, some of which have not traditionally been considered in climate change impact studies (e.g. climate variability, flood frequency analysis). However a number of additional sources of uncertainty were not included here, most notably downscaling methods and hydrological model structure.

Both methods have previously been explored independently from other sources of uncertainty as demonstrated in the scientific overview in Chapter 2, however they need to be incorporated in a similar combined analysis as has been undertaken here. This would enable an understanding and quantification of how influential these uncertainty components are in comparison to those addressed in this thesis.

9.4.2 A Resampling Methodology for Multi-Variate and Multi-Site Application

The resampling methodology developed in Chapter 4 of this thesis was created to address the issue of climate variability in impact studies. In this example it was only applied as a sensitivity analysis to precipitation, where climate variability was shown to play an important role in defining future impacts. Further research is required to extend the resampling methodology to include multiple variables (e.g. both precipitation and temperature). This would require the temporal patterns of correlation to be analysed for all considered climatological variables. The resampling procedure would then be carried out at the highest

order temporal correlation level (i.e. monthly, seasonally, or yearly time steps) for all variables. If the sampling time step is altered, further analysis would be required to find the optimum number of resamples that are required to adequately reproduce consistent magnitudes of variability (i.e. the currently suggested 40 baseline and 40 futures may not be appropriate). This would allow for multiple variables to be resampled simultaneously creating multiple realisations of temporally coherent climate variables. This can be extended to multiple sites by using the same order of resampling at each location of interest, providing the temporal characteristics of each site are the same.

Development of the methodology in this manner would allow for temporally and spatially coherent ensembles of climate change projections for multiple variables. This is advantageous for regions outside of the UK where fully probabilistic climate projections are not available. For UK based applications, one of the main limitations of the UKCP09 scenarios is that they are not spatially coherent making comparison between locations difficult. Furthermore the UKCP09 projections do not include a baseline realisation, which as previously highlighted in this thesis, limits the analysis of climatic variability.

With the advent of CMIP5 there may be an increase in multi-realisation climate model runs. However if this is not the case or data is not available, developing spatially and temporally coherent resampled climate scenarios could represent a feasible alternative.

9.4.3 Further Tests of Hydrological Parameters

Hydrological parameter uncertainty was shown to be small in relation to other sources of uncertainty. In this thesis however, a large ensemble of climate change scenarios (500 UKCP09 change factors) were used. In applications where a smaller number of scenarios are used, hydrological parameter uncertainty will be increasingly important (as shown in Chapter 5).

This is particularly true given the evidence for some model parameters influencing the magnitude impact of climate change, which contradicts the traditional assumption of a stationary bias in a hydrological impact study (i.e. any model bias is the same for both baseline and future simulation). Further test are required to explore this further to understand the mechanism in PDM causing this, the analysis of additional climate scenarios as opposed to sensitivity based changes would contribute to understanding this.

Furthermore the role of the secondary model routing parameter was hypothesised to be linked to the non-linear interaction of the primary and secondary flow routing components. This needs to be explored through the analysis of split model hydrographs to identify the cause of this interaction.

9.5 Concluding Remarks

This thesis has demonstrated the importance of quantifying uncertainty in climate change impact studies, with particular focus on the impact of climate change on UK flooding. It is hoped that this work has highlighted the importance of quantifying uncertainty to provide a robust and defensible assessment of the impacts of climate change. Currently little consensus exists over the most appropriate methods to undertake climate change impact analysis, in part due to the diverse nature of the many impacts of interest. However, acknowledging the inherent uncertainties in climate change impact science should be viewed as a prerequisite for any climate change impact study.

References

Abbott, M. B., Bathurst, J. C., Cunge, J. A., O'connell, P. E. & Rasmussen, J. (1986) An introduction to the European Hydrological System - Systeme Hydrologique Europeen, "SHE", 2: Structure of a physically-based, distributed modelling system. *Journal of Hydrology,* 87**,** 61-77.

Abebe, N. A., Ogden, F. L. & Pradhan, N. R. (2010) Sensitivity and uncertainty analysis of the conceptual HBV rainfall-runoff model: Implications for parameter estimation. *Journal of Hydrology,* 389**,** 301-310.

Ajami, N. K., Gupta, H., Wagener, T. & Sorooshian, S. (2004) Calibration of a semi-distributed hydrologic model for streamflow estimation along a river system. *Journal of Hydrology,* 298**,** 112-135.

Anandhi, A., Frei, A., Pierson, D. C., Schneiderman, E. M., Zion, M. S., Lounsbury, D. & Matonse, A. H. (2011) Examination of change factor methodologies for climate change impact assessment. *Water Resour. Res.,* 47**,** W03501.

Arnell, N. W. (1999) The effect of climate change on hydrological regimes in Europe: a continental perspective. *Global Environmental Change,* 9**,** 5-23.

Arnell, N. W. (2003a) Effects of IPCCSRES emissions scenarios on river runoff: a global perspective. *Hydrology and Earth System Sciences,* 7**,** 619-641.

Arnell, N. W. (2003b) Relative effects of multi-decadal climatic variability and changes in the mean and variability of climate due to global warming: future streamflows in Britain. *Journal of Hydrology,* 270**,** 195-213.

Arnell, N. W. (2004) Climate-change impacts on river flows in Britain: The UKCIP02 scenarios. *Water and Environment Journal,* 18**,** 112-117.

Arnell, N. W. (2011) Uncertainty in the relationship between climate forcing and hydrological response in UK catchments. *Hydrol. Earth Syst. Sci.,* 15**,** 897-912.

Arnell, N. W. & Reynard, N. S. (1996) The effects of climate change due to global warming on river flows in Great Britain. *Journal of Hydrology,* 183**,** 397-424.

Bardossy, A., Stehlik, J. & Caspary, H.-J. (2002) Automated objective classification of daily circulation patterns for precipitation and temperature downscaling based on optimized fuzzy rules. *Climate Research,* 23**,** 11-22.

Bastola, S., Murphy, C. & Sweeney, J. (2011) The role of hydrological modelling uncertainties in climate change impact assessments of Irish river catchments. *Advances in Water Resources,* 34**,** 562-576.

Bates, B. C., Kundzewicz, Z. W., Wu, S. & Palutikof, J. P. (2008) Climate Change and Water. Technical Paper of the Intergovernmental Panel on Climate Change, IPCC Secretariat. Geneva.

Bayliss, A. C. & Jones, R. C. (1993) Peaks over threshold database: Summary statistics and seasonality. IH Report 121. Institute of Hydrology. Wallingford.

Beguería, S. (2005) Uncertainties in partial duration series modelling of extremes related to the choice of the threshold value. *Journal of Hydrology,* 303**,** 215-230.

Bell, V. A., Kay, A. L., Jones, R. G. & Moore, R. J. (2007) Use of a grid-based hydrological model and regional climate model outputs to assess changing flood risk. *International Journal of Climatology,* 27**,** 1657-1671.

Bell, V. A. & Moore, R. J. (1999) An elevation-dependent snowmelt model for upland Britain. *Hydrological Processes,* 13**,** 1887-1903.

Beven, K. (1997) TOPMODEL: A critique. *Hydrological Processes,* 11**,** 1069-1085.

Beven, K. (2001) *Rainfall-Runoff Modelling: The Primer,* Chichester, Wiley.

Beven, K. (2006) A manifesto for the equifinality thesis. *Journal of Hydrology,* 320**,** 18-36.

Beven, K. (2011) I believe in climate change but how precautionary do we need to be in planning for the future? *Hydrological Processes,* 25**,** 1517-1520.

Beven, K. & Binley, A. (1992) The future of distributed models - Model calibration and uncertainty prediction. *Hydrological Processes,* 6**,** 279-298.

Beven, K. & Freer, J. (2001) Equifinality, data assimilation, and uncertainty estimation in mechanistic modelling of complex environmental systems using the GLUE methodology. *Journal of Hydrology,* 249**,** 11-29.

Beven, K., Smith, P. & Freer, J. (2007) Comment on "Hydrological forecasting uncertainty assessment: Incoherence of the GLUE methodology" by Pietro Mantovan and Ezio Todini. *Journal of Hydrology,* 338**,** 315-318.

Beven, K. J., Smith, P. J. & Freer, J. E. (2008) So just why would a modeller choose to be incoherent? *Journal of Hydrology,* 354**,** 15-32.

Boorman, D. B., Hollis, J. M. & Lilly, A. (1995) Hydrology of soil types: a hydrologically based classification of soils in the United Kingdom. *IH Report No. 126.* Wallingford, Institute of Hydrology.

Boyle, D. P., Gupta, H. V. & Sorooshian, S. (2000) Toward improved calibration of hydrologic models: Combining the strengths of manual and automatic methods. *Water Resour. Res.,* 36**,** 3663-3674.

Cameron, D. (2006) An application of the UKCIP02 climate change scenarios to flood estimation by continuous simulation for a gauged catchment in the northeast of Scotland, UK (with uncertainty). *Journal of Hydrology,* 328**,** 212-226.

Cameron, D., Beven, K. & Naden, P. (2000) Flood frequency estimation by continuous simulation under climate change (with uncertainty). *Hydrol. Earth Syst. Sci.,* 4**,** 393-405.

Cameron, D. S., Beven, K. J., Tawn, J., Blazkova, S. & Naden, P. (1999) Flood frequency estimation by continuous simulation for a gauged upland catchment (with uncertainty). *Journal of Hydrology,* 219**,** 169-187.

Carter, T. R. (2007) General guidelines on the use of scenario data for climate impact and adaptation assessment. IPCC.

Chen, J., Brissette, F. P. & Leconte, R. (2011) Uncertainty of downscaling method in quantifying the impact of climate change on hydrology. *Journal of Hydrology,* 401**,** 190-202.

Christensen, J. H., Boberg, F., Christensen, O. B. & Lucas-Picher, P. (2008) On the need for bias correction of regional climate change projections of temperature and precipitation. *Geophys. Res. Lett.,* 35**,** L20709.

Christensen, J. H., Kjellstrom, E., Giorgi, F., Lenderink, G. & Rummukainen, M. (2010) Weight assignment in regional climate models. *Climate Research,* 44**,** 179-194.

Cloke, H. L., Jeffers, C., Wetterhall, F., Byrne, T., Lowe, J. & Pappenberger, F. (2010) Climate impacts on river flow: projections for the Medway catchment, UK, with UKCP09 and CATCHMOD. *Hydrological Processes,* 24**,** 3476-3489.

Cole, S. J. & Moore, R. J. (2008) Hydrological modelling using raingauge- and radar-based estimators of areal rainfall. *Journal of Hydrology,* 358**,** 159-181.

Conway, D. & Jones, P. D. (1998) The use of weather types and air flow indices for GCM downscaling. *Journal of Hydrology,* 212-213**,** 348-361.

Crooks, S. M., Kay, A. L. & Reynard, N. (2010) Regionalised impacts of climate change on flood flows: hydrological models, catchments and calibration. Milestone report 1., Defra.

Crooks, S. M. & Naden, P. S. (2007) CLASSIC: a semi-distributed rainfall-runoff modelling system. *Hydrology and Earth System Sciences,* 11**,** 516-531.

Cullmann, J. & Wriedt, G. (2008) Joint application of event-based calibration and dynamic identifiability analysis in rainfall-runoff modelling: implications for model parametrisation. *Journal of Hydroinformatics,* 10**,** 301-316.

Dankers, R. & Feyen, L. (2008) Climate change impact on flood hazard in Europe: An assessment based on high-resolution climate simulations. *J. Geophys. Res.,* 113**,** D19105.

Dankers, R. & Feyen, L. (2009) Flood hazard in Europe in an ensemble of regional climate scenarios. *J. Geophys. Res.,* 114**,** D16108.

Deb, K., Pratap, A., Agarwal, S. & Meyarivan, T. (2002) A fast and elitist multiobjective genetic algorithm: NSGA-II. *Ieee Transactions on Evolutionary Computation,* 6**,** 182-197.

Déqué, M., Rowell, D., Lüthi, D., Giorgi, F., Christensen, J., Rockel, B., Jacob, D., Kjellström, E., De Castro, M. & Van Den Hurk, B. (2007) An intercomparison of regional climate simulations for Europe: assessing uncertainties in model projections. *Climatic Change,* 81**,** 53-70.

Deser, C., Phillips, A., Bourdette, V. & Teng, H. (2010) Uncertainty in climate change projections: the role of internal variability. *Climate Dynamics***,** 1-20.

Dessai, S. & Hulme, M. (2004) Does climate adaptation policy need probabilities? *Climate Policy,* 4**,** 107-128.

Diaz-Nieto, J. & Wilby, R. L. (2005) A comparison of statistical downscaling and climate change factor methods: Impacts on low flows in the River Thames, United Kingdom. *Climatic Change,* 69**,** 245-268.

Durman, C. F., Gregory, J. M., Hassell, D. C., Jones, R. G. & Murphy, J. M. (2001) A comparison of extreme European daily precipitation simulated by a global and a regional climate model for present and future climates. *Quarterly Journal of the Royal Meteorological Society,* 127**,** 1005-1015.

Engen-Skaugen, T. (2007) Refinement of dynamically downscaled precipitation and temperature scenarios. *Climatic Change,* 84**,** 365-382.

Environment Agency (2005) CATCHMOD: Conceptual Rainfall Runoff Model. Technical User Guide and Software Manual for CATCHMOD v4.03. Environment Agency: UK. UK.

Evans, E. P., Simm, J. D., Throne, C. R., Arnell, N. W., Ashley, R. M., Hess, T. M., Lane, S. N., Morris, J., Nicholls, R. J., Penning-Rwosell, E. C., Reynard, N. S., Saul, A. J., Tapsell, S. M., Watkinson, A. R. & Wheater, H. S. (2008) An update of the Foresight Future Flooding 2004 qualitative risk analysis. London, Cabinet Office.

Faulkner, D., Robb, K. & Haysom, A. (2008) Return period assessment of the summer 2007 floods in central England. *BHS 10th National Hydrology Symposium.* Exeter.

Foresight (2004) Future Flooding: Executive Summary. London, Office of Science and Technology.

Fowler, H. & Kilsby, C. (2007) Using regional climate model data to simulate historical and future river flows in northwest England. *Climatic Change,* 80**,** 337-367.

Fowler, H. J., Blenkinsop, S. & Tebaldi, C. (2007) Linking climate change modelling to impacts studies: recent advances in downscaling techniques for hydrological modelling. *International Journal of Climatology,* 27**,** 1547-1578.

Fowler, H. J., Ekström, M., Kilsby, C. G. & Jones, P. D. (2005a) New estimates of future changes in extreme rainfall across the UK using regional climate model integrations. 1. Assessment of control climate. *Journal of Hydrology,* 300**,** 212-233.

Fowler, H. J. & Kilsby, C. G. (2002) Precipitation and the North Atlantic Oscillation: A study of climatic variability in northern England. *International Journal of Climatology,* 22**,** 843-866.

Fowler, H. J., Kilsby, C. G., O'connell, P. E. & Burton, A. (2005b) A weather-type conditioned multi-site stochastic rainfall model for the generation of scenarios of climatic variability and change. *Journal of Hydrology,* 308**,** 50-66.

Frei, C., Scholl, R., Fukutome, S., Schmidli, J. & Vidale, P. L. (2006) Future change of precipitation extremes in Europe: Intercomparison of scenarios from regional climate models. *Journal of Geophysical Research-Atmospheres,* 111.

Ghavidelfar, S., Alvankar, S. & Razmkhah, A. (2011) Comparison of the Lumped and Quasi-distributed Clark Runoff Models in Simulating Flood Hydrographs on a Semi-arid Watershed. *Water Resources Management,* 25**,** 1775-1790.

Giorgi, F. (1990) Simulation of Regional Climate Using a Limited Area Model Nested in a General Circulation Model. *Journal of Climate,* 3**,** 941-963.

Giorgi, F. & Mearns, L. (1999) Introduction to special section: Regional climate modeling revisited. *Journal of Geophysical Research-Atmospheres,* 104**,** 6335-6352.

Giorgi, F. & Mearns, L. O. (1991) Approaches to the simulation of regional climate change: A review. *Rev. Geophys.,* 29**,** 191-216.

Greenwood, J. A., Landwehr, J. M., Matalas, N. C. & Wallis, J. R. (1979) Probability weighted moments: Definition and relation to parameters of several distributions expressable in inverse form. *Water Resour. Res.,* 15**,** 1049-1054.

Gringorten, I. I. (1963) A plotting rule for extreme probability paper. *Journal of Geophysical Research,* 68**,** 813-814.

Hall, J. (2007) Probabilistic climate scenarios may misrepresent uncertainty and lead to bad adaptation decisions. *Hydrological Processes,* 21**,** 1127-1129.

Hannaford, J. & Marsh, T. J. (2008) High-flow and flood trends in a network of undisturbed catchments in the UK. *International Journal of Climatology,* 28**,** 1325-1338.

Hawkins, E. & Sutton, R. (2009) The Potential to Narrow Uncertainty in Regional Climate Predictions. *Bulletin of the American Meteorological Society,* 90**,** 1095-1107.

Hawkins, E. & Sutton, R. (2011) The potential to narrow uncertainty in projections of regional precipitation change. *Climate Dynamics,* 37**,** 407-418.

Hay, L. E. & Clark, M. P. (2003) Use of statistically and dynamically downscaled atmospheric model output for hydrologic simulations in three mountainous basins in the western United States. *Journal of Hydrology,* 282**,** 56-75.

Hay, L. E., Clark, M. P., Wilby, R. L., Gutowski, W. J., Leavesley, G. H., Pan, Z., Arritt, R. W. & Takle, E. S. (2002) Use of Regional Climate Model Output for Hydrologic Simulations. *Journal of Hydrometeorology,* 3**,** 571-590.

Hay, L. E., Wilby, R. J. L. & Leavesley, G. H. (2000) A comparison of delta change and downscaled GCM scenarios for three mountainous basins in the United States. *Journal of the American Water Resources Association,* 36**,** 387-397.

Haylock, M. R., Cawley, G. C., Harpham, C., Wilby, R. L. & Goodess, C. M. (2006) Downscaling heavy precipitation over the United Kingdom: A comparison of dynamical and statistical methods and their future scenarios. *International Journal of Climatology,* 26**,** 1397-1415.

Haylock, M. R., Hofstra, N., Klein Tank, A. M. G., Klok, E. J., Jones, P. D. & New, M. (2008) A European daily high-resolution gridded data set of surface temperature and precipitation for 1950 - 2006. *J. Geophys. Res.,* 113**,** D20119.

Hosking, J. R. M. & Wallis, J. R. (1987) Parameter and Quantile Estimation for the Generalized Pareto Distirbution. *Technometircs,* 29**,** 339-349.

Hough, M. N. & Jones, R. J. A. (1997) The United Kingdom Meteorological Office rainfall and evaporation calculation system: MORECS version 2.0-an overview. *Hydrol. Earth Syst. Sci.,* 1**,** 227-239.

Hulme, M. & New, M. (1997) Dependence of Large-Scale Precipitation Climatologies on Temporal and Spatial Sampling. *Journal of Climate,* 10**,** 1099-1113.

Hulme, M., Pielke, R. & Dessai, S. (2009) Keeping prediction in perspective. *Nature Reports Climate Change* 3**,** 126-127.

Huntington, T. G. (2006) Evidence for intensification of the global water cycle: Review and synthesis. *Journal of Hydrology,* 319**,** 83-95.

Hurrell, J. W. (1995) Decadal Trends in the North-Atlantic Oscillation - Regional Temperatures and Precipitation. *Science,* 269**,** 676-679.

Hurrell, J. W., Visbeck, M. H., Polvani, L. & Cullen, H. M. (2001) The North Atlantic Oscillation: Past, present, and future. *Proceedings of the National Academy of Sciences of the United States of America,* 98**,** 12876-12877.

Institute of Hydrology (1999) Flood Estimation Handbook. Crowmarsh Gifford, Wallingford, Institute of Hydrology.

Ipcc (1990) Climate Change: The IPCC Scientific Assessment

Ipcc (1992) Emissions Scenarios for the IPCC: An Update. In: Climate Change 1992: The Supplementary Report to the IPCC Scientific Assessment . Cambridge.

Ipcc (2000) Emissions Scenarios. A Special Report of Working Group II of the Intergovernmental Panel on Climate Change. Cambridge.

Ipcc (2007) Climate Change 2007: Synthesis Report. Cambridge.

Jacob, D., Bärring, L., Christensen, O., Christensen, J., De Castro, M., Déqué, M., Giorgi, F., Hagemann, S., Hirschi, M., Jones, R., Kjellström, E., Lenderink, G., Rockel, B., Sánchez, E., Schär, C., Seneviratne, S., Somot, S., Van Ulden, A. & Van Den Hurk, B. (2007) An inter-comparison of regional climate models for Europe: model performance in present-day climate. *Climatic Change,* 81**,** 31-52.

Jakeman, A. J. & Hornberger, G. M. (1993) How much complexity is warranted in a rainfall-runoff model? *Water Resour. Res.,* 29**,** 2637-2649.

Jakeman, A. J., Littlewood, I. G. & Whitehead, P. G. (1990) Computation of the instantaneous unit hydrograph and identifiable component flows with application to two small upland catchments. *Journal of Hydrology,* 117**,** 275-300.

Kay, A. L., Davies, H. N., Bell, V. A. & Jones, R. G. (2009) Comparison of uncertainty sources for climate change impacts: flood frequency in England. *Climatic Change,* 92**,** 41-63.

Kay, A. L. & Jones, D. A. (2011) Transient changes in flood frequency and timing in Britain under potential projections of climate change. *International Journal of Climatology***,** n/a-n/a.

Kay, A. L., Jones, R. G. & Reynard, N. S. (2006) RCM rainfall for UK flood frequency estimation. II. Climate change results. *Journal of Hydrology,* 318**,** 163-172.

Kendon, E. J., Rowell, D. P., Jones, R. G. & Buonomo, E. (2008) Robustness of Future Changes in Local Precipitation Extremes. *Journal of Climate,* 21**,** 4280-4297.

Kidson, R. & Richards, K. S. (2005) Flood frequency analysis: assumptions and alternatives. *Progress in Physical Geography,* 29**,** 392-410.

Kilsby, C. G., Jones, P. D., Burton, A., Ford, A. C., Fowler, H. J., Harpham, C., James, P., Smith, A. & Wilby, R. L. (2007) A daily weather generator for use in climate change studies. *Environmental Modelling & Software,* 22**,** 1705-1719.

Kirby, A. M. & Ash, J. R. (2000) Fluvial freeboard guidance note. *R&D Technical Report W187.* Environment Agency.

Kjeldsen, T. R. & Jones, D. A. (2004) Sampling variance of flood quantiles from the generalised logistic distribution estimated using the method of L-moments. *Hydrol. Earth Syst. Sci.,* 8**,** 183-190.

Kjeldsen, T. R. & Jones, D. A. (2006) Prediction uncertainty in a median-based index flood method using L moments. *Water Resour. Res.,* 42**,** W07414.

Kjeldsen, T. R. & Jones, D. A. (2009) A formal statistical model for pooled analysis of extreme floods. *Hydrology Research,* 40**,** 465-480.

Knutti, R., Furrer, R., Tebaldi, C., Cermak, J. & Meehl, G. A. (2010) Challenges in Combining Projections from Multiple Climate Models. *Journal of Climate,* 23**,** 2739-2758.

Knutti, R., Stocker, T. F., Joos, F. & Plattner, G. K. (2003) Probabilistic climate change projections using neural networks. *Climate Dynamics,* 21**,** 257-272.

Lamb, R. (1999) Calibration of a conceptual rainfall-runoff model for flood frequency estimation by continuous simulation. *Water Resources Research,* 35**,** 3103-3114.

Lamb, R. & Kay, A. L. (2004) Confidence intervals for a spatially generalized, continuous simulation flood frequency model for Great Britain. *Water Resour. Res.,* 40**,** W07501.

Latif, M., Collins, M., Pohlmann, H. & Keenlyside, N. (2006) A review of predictability studies of Atlantic sector climate on decadal time scales. *Journal of Climate,* 19**,** 5971-5987.

Ledbetter, R., Prudhomme, C. & Arnell, N. (2012) A method for incorporating climate variability in climate change impact assessments: Sensitivity of river flows in the Eden catchment to precipitation scenarios. *Climatic Change,* 113**,** 803-823.

Lee, H., Mcintyre, N., Wheater, H. & Young, A. (2005) Selection of conceptual models for regionalisation of the rainfall-runoff relationship. *Journal of Hydrology,* 312**,** 125-147.

Lindstrom, G., Johansson, B., Persson, M., Gardelin, M. & Bergstrom, S. (1997) Development and test of the distributed HBV-96 hydrological model. *Journal of Hydrology,* 201**,** 272-288.

Liu, Z., Martina, M. L. V. & Todini, E. (2005) Flood forecasting using a fully distributed model: application of the TOPKAPI model to the Upper Xixian Catchment. *Hydrol. Earth Syst. Sci.,* 9**,** 347-364.

Mantovan, P. & Todini, E. (2006) Hydrological forecasting uncertainty assessment: Incoherence of the GLUE methodology. *Journal of Hydrology,* 330**,** 368-381.

Mantovan, P., Todini, E. & Martina, M. L. V. (2007) Reply to comment by Keith Beven, Paul Smith and Jim Freer on "Hydrological forecasting uncertainty assessment: Incoherence of the GLUE methodology". *Journal of Hydrology,* 338**,** 319-324.

Marsh, T. J. (2001) The autumn 2000 floods in the UK - a brief overview. *Weather,* 56**,** 343-345.

Marshall, J., Kushner, Y., Battisti, D., Chang, P., Czaja, A., Dickson, R., Hurrell, J., Mccartney, M., Saravanan, R. & Visbeck, M. (2001) North Atlantic climate variability: Phenomena, impacts and mechanisms. *International Journal of Climatology,* 21**,** 1863-1898.

Meehl, G. A., Covey, C., Taylor, K. E., Delworth, T., Stouffer, R. J., Latif, M., Mcavaney, B. & Mitchell, J. F. B. (2007) THE WCRP CMIP3 Multimodel Dataset: A New Era in Climate Change Research. *Bulletin of the American Meteorological Society,* 88**,** 1383-1394.

Merz, B. & Thieken, A. H. (2005) Separating natural and epistemic uncertainty in flood frequency analysis. *Journal of Hydrology,* 309**,** 114-132.

Merz, R., Parajka, J. & Blöschl, G. (2011) Time stability of catchment model parameters: Implications for climate impact analyses. *Water Resour. Res.,* 47**,** W02531.

Milly, P. C. D., Betancourt, J., Falkenmark, M., Hirsch, R. M., Kundzewicz, Z. W., Lettenmaier, D. P. & Stouffer, R. J. (2008) Stationarity Is Dead: Whither Water Management? *Science,* 319**,** 573-574.

Moore, R. J. (2007) The PDM rainfall-runoff model. *Hydrology and Earth System Sciences,* 11**,** 483-499.

Moss, R., Babiker, M., Brinkman, S., Calvo, E., Carter, T., Edmonds, J., Elgizouli, I., Emori, S., Erda, L., Hibbard, K., Jones, R., Kainuma, M., Kelleher, J., Lamarque, J. F., Manning, M., Matthews, B., Meehl, J., Meyer, L., Mitchell, J., Nakicenovic, N., O'neill, B., Pichs, R., Riahi, K., Rose, S., Runci, P., Stouffer, R., Van Vuuren, D.,

Weyant, J., Wilbanks, T., Van Ypersele, J. P. & Zurek, M. (2008) Towards New Scenarios for Analysis of Emissions, Climate Change, Impacts, and Response Strategies. Geneva, Intergovernmental Panel on Climate Change.

Moss, R. H., Edmonds, J. A., Hibbard, K. A., Manning, M. R., Rose, S. K., Van Vuuren, D. P., Carter, T. R., Emori, S., Kainuma, M., Kram, T., Meehl, G. A., Mitchell, J. F. B., Nakicenovic, N., Riahi, K., Smith, S. J., Stouffer, R. J., Thomson, A. M., Weyant, J. P. & Wilbanks, T. J. (2010) The next generation of scenarios for climate change research and assessment. *Nature,* 463**,** 747-756.

Mudelsee, M., Borngen, M., Tetzlaff, G. & Grunewald, U. (2003) No upward trends in the occurrence of extreme floods in central Europe. *Nature,* 425**,** 166-169.

Murphy, J. M., Sexton, D. M. H., Barnett, D. N., Jones, G. S., Webb, M. J. & Collins, M. (2004) Quantification of modelling uncertainties in a large ensemble of climate change simulations. *Nature,* 430**,** 768-772.

Murphy, J. M., Sexton, D. M. H., Jenkins, G. J., Boorman, P. M., Booth, B. B. B., Brown, C. C., Clark, R. T., Collins, M., Harris, G. R., Kendon, E. J., Betts, R. A., Brown, S. J., Howard, T. P., Humphreys, K. A., Mccarthy, M. P., Mcdonald, R. E., Stephens, A., Wallace, C., Warren, R., Wilby, R. & Wood, R. A. (2009) UK Climate Projections Science Report: Climate change projections. Exeter, Met Office Hadley Centre.

Nash, J. E. & Sutcliffe, J. V. (1970) River flow forecasting through conceptual models. 1. A discussion of principles. *Journal of Hydrology,* 10**,** 282-290.

New, M. & Hulme, M. (2000) Representing uncertainty in climate change scenarios: a Monte-Carlo approach. *Integrated Assessment,* 1.

New, M., Lopez, A., Dessai, S. & Wilby, R. (2007) Challenges in using probabilistic climate change information for impact assessments: an example from the water sector. *Philosophical Transactions of the Royal Society a-Mathematical Physical and Engineering Sciences,* 365**,** 2117-2131.

Niel, H., Paturel, J. E. & Servat, E. (2003) Study of parameter stability of a lumped hydrologic model in a context of climatic variability. *Journal of Hydrology,* 278**,** 213-230.

Nobrega, M. T., Collischonn, W., Tucci, C. E. M. & Paz, A. R. (2011) Uncertainty in climate change impacts on water resources in the Rio Grande Basin, Brazil. *Hydrol. Earth Syst. Sci.,* 15**,** 585-595.

Noguer, M., Jones, R. & Murphy, J. (1998) Sources of systematic errors in the climatology of a regional climate model over Europe. *Climate Dynamics,* 14**,** 691-712.

Olsen, J. R., Lambert, J. H. & Haimes, Y. Y. (1998) Risk of Extreme Events Under Nonstationary Conditions. *Risk Analysis,* 18**,** 497-510.

Parker, D., Folland, C., Scaife, A., Knight, J., Colman, A., Baines, P. & Dong, B. W. (2007) Decadal to multidecadal variability and the climate change background. *Journal of Geophysical Research-Atmospheres,* 112**,** D18115.

Perrin, C., Michel, C. & Andréassian, V. (2001) Does a large number of parameters enhance model performance? Comparative assessment of common catchment model structures on 429 catchments. *Journal of Hydrology,* 242**,** 275-301.

Pitt Review (2008) The Pitt Review: Lessons learned from the 2007 floods. London, Cabinet Office.

Prudhomme, C., Jakob, D. & Svensson, C. (2003) Uncertainty and climate change impact on the flood regime of small UK catchments. *Journal of Hydrology,* 277**,** 1-23.

Prudhomme, C., Reynard, N. & Crooks, S. (2002) Downscaling of global climate models for flood frequency analysis: where are we now? *Hydrological Processes,* 16**,** 1137-1150.

Prudhomme, C., Wilby, R. L., Crooks, S., Kay, A. L. & Reynard, N. S. (2010) Scenario-neutral approach to climate change impact studies: Application to flood risk. *Journal of Hydrology,* 390**,** 198-209.

Raisanen, J. (2001) CO2-Induced Climate Change in CMIP2 Experiments: Quantification of Agreement and Role of Internal Variability. *Journal of Climate,* 14**,** 2088-2104.

Raisanen, J. & Ruokolainen, L. (2006) Probabilistic forecasts of near-term climate change based on a resampling ensemble technique. *Tellus A,* 58**,** 461-472.

Rao, A. R. & Hamed, K. H. (2000) *Flood Frequency Analysis,* Boca Raton, CRC Press.

Raupach, M. R., Marland, G., Ciais, P., Le Quere, C., Canadell, J. G., Klepper, G. & Field, C. B. (2007) Global and regional drivers of accelerating CO2 emissions. *Proceedings of the National Academy of Sciences of the United States of America,* 104**,** 10288-10293.

Reed, S., Koren, V., Smith, M., Zhang, Z., Moreda, F., Seo, D.-J. & Dmip Participants, A. (2004) Overall distributed model intercomparison project results. *Journal of Hydrology,* 298**,** 27-60.

Reynard, N. S., Crooks, S. M., Kay, A. L. & Prudhomme, C. (2010) Regionalised Impacts of Climate Change on Flood Flows: R&D Technical Report FD2020/TR. London, DEFRA.

Reynard, N. S., Prudhomme, C. & Crooks, S. M. (2001) The flood characteristics of large UK Rivers: Potential effects of changing climate and land use. *Climatic Change,* 48**,** 343-359.

Robson, A. J. (2002) Evidence for trends in UK flooding. *Philosophical Transactions of the Royal Society of London Series a-Mathematical Physical and Engineering Sciences,* 360**,** 1327-1343.

Rosbjerg, D. & Madsen, H. (1995) Uncertainty measures of regional flood frequency estimators. *Journal of Hydrology,* 167**,** 209-224.

Rummukainen, M., Räisänen, J., Bringfelt, B., Ullerstig, A., Omstedt, A., Willén, U., Hansson, U. & Jones, C. (2001) A regional climate model for northern Europe: model description and results from the downscaling of two GCM control simulations. *Climate Dynamics,* 17**,** 339-359.

Ruokolainen, L. & Raisanen, J. (2007) Probabilistic forecasts of near-term climate change: sensitivity to adjustment of simulated variability and choice of baseline period. *Tellus A,* 59**,** 309-320.

Salathe, E. P., Mote, P. W. & Wiley, M. W. (2007) Review of scenario selection and downscaling methods for the assessment of climate change impacts on hydrology in the United States pacific northwest. *International Journal of Climatology,* 27**,** 1611-1621.

Schneider, S. H. & Mastrandrea, M. D. (2005) Probabilistic assessment of "dangerous" climate change and emissions pathways. *Proceedings of the National Academy of Sciences of the United States of America,* 102**,** 15728-15735.

Shafii, M. & De Smedt, F. (2009) Multi-objective calibration of a distributed hydrological model (WetSpa) using a genetic algorithm. *Hydrol. Earth Syst. Sci.,* 13**,** 2137-2149.

Singh, V. P. & Strupczewski, W. G. (2002) On the status of flood frequency analysis. *Hydrological Processes,* 16**,** 3737-3740.

Srikanthan, R. & Mcmahon, T. A. (2001) Stochastic generation of annual, monthly and daily climate data: A review. *Hydrol. Earth Syst. Sci.,* 5**,** 653-670.

Stainforth, D. A., Aina, T., Christensen, C., Collins, M., Faull, N., Frame, D. J., Kettleborough, J. A., Knight, S., Martin, A., Murphy, J. M., Piani, C., Sexton, D., Smith, L. A., Spicer, R. A., Thorpe, A. J. & Allen, M. R. (2005) Uncertainty in predictions of the climate response to rising levels of greenhouse gases. *Nature,* 433**,** 403-406.

Stedinger, J. R., Vogel, R. M., Lee, S. U. & Batchelder, R. (2008) Appraisal of the generalized likelihood uncertainty estimation (GLUE) method. *Water Resour. Res.,* 44**,** W00B06.

Steele-Dunne, S., Lynch, P., Mcgrath, R., Semmler, T., Wang, S., Hanafin, J. & Nolan, P. (2008) The impacts of climate change on hydrology in Ireland. *Journal of Hydrology,* 356**,** 28-45.

Stewart, E. J., Morris, D. G., Jones, D. A. & Spencer, P. S. (2010) Extreme rainfall in Cumbria, November 2009 - an assessment of strom rarity. *British Hydrological Society Third International Symposium.* Newcastle.

Tebaldi, C. & Knutti, R. (2007) The use of the multi-model ensemble in probabilistic climate projections. *Philosophical Transactions of the Royal Society a-Mathematical Physical and Engineering Sciences,* 365**,** 2053-2075.

Thompson, N., Barries, I. A. & Ayles, M. (1981) The Meteorological Office Rainfall and Evaporation Calculation System: MORECS (July 1981). *Hydrological Memorandum No. 45.* Bracknell, Met Office.

Todini, E. (1996) The ARNO rainfall runoff model. *Journal of Hydrology,* 175**,** 339-382.

Todini, E. (2007) Hydrological catchment modelling: past, present and future. *Hydrol. Earth Syst. Sci.,* 11**,** 468-482.

Uhlenbrook, S., Seibert, J., Leibundgut, C. & Rodhe, A. (1999) Prediction uncertainty of conceptual rainfall-runoff models caused by problems in identifying model parameters and structure. *Hydrological Sciences Journal-Journal Des Sciences Hydrologiques,* 44**,** 779-797.

Van Vuuren, D., Edmonds, J., Kainuma, M., Riahi, K., Thomson, A., Hibbard, K., Hurtt, G., Kram, T., Krey, V., Lamarque, J.-F., Masui, T., Meinshausen, M., Nakicenovic, N., Smith, S. & Rose, S. (2011) The representative concentration pathways: an overview. *Climatic Change***,** 1-27.

Vaze, J., Post, D. A., Chiew, F. H. S., Perraud, J. M., Viney, N. R. & Teng, J. (2010) Climate non-stationarity - Validity of calibrated rainfall-runoff models for use in climate change studies. *Journal of Hydrology,* 394**,** 447-457.

Vidal, J. P. & Wade, S. (2008) A framework for developing high-resolution multi-model climate projections: 21st century scenarios for the UK. *International Journal of Climatology,* 28**,** 843-858.

Villarini, G., Smith, J. A., Serinaldi, F., Bales, J., Bates, P. D. & Krajewski, W. F. (2009) Flood frequency analysis for nonstationary annual peak records in an urban drainage basin. *Advances in Water Resources,* 32**,** 1255-1266.

Visser, H., Folkert, R. J. M., Hoekstra, J. & De Wolff, J. J. (2000) Identifying Key Sources of Uncertainty in Climate Change Projections. *Climatic Change,* 45**,** 421-457.

Wagener, T., Mcintyre, N., Lees, M. J., Wheater, H. S. & Gupta, H. V. (2003) Towards reduced uncertainty in conceptual rainfall-runoff modelling: Dynamic identifiability analysis. *Hydrological Processes,* 17**,** 455-476.

Wagener, T., Sivapalan, M., Troch, P. A., Mcglynn, B. L., Harman, C. J., Gupta, H. V., Kumar, P., Rao, P. S. C., Basu, N. B. & Wilson, J. S. (2010) The future of hydrology: An evolving science for a changing world. *Water Resour. Res.,* 46**,** W05301.

Weigel, A. P., Knutti, R., Liniger, M. A. & Appenzeller, C. (2010) Risks of Model Weighting in Multimodel Climate Projections. *Journal of Climate,* 23**,** 4175-4191.

Wilby, R. L. (2005) Uncertainty in water resource model parameters used for climate change impact assessment. *Hydrological Processes,* 19**,** 3201-3219.

Wilby, R. L. (2006) When and where might climate change be detectable in UK river flows? *Geophysical Research Letters,* 33.

Wilby, R. L., Beven, K. J. & Reynard, N. S. (2008) Climate change and fluvial flood risk in the UK: more of the same? *Hydrological Processes,* 22**,** 2511-2523.

Wilby, R. L. & Harris, I. (2006) A framework for assessing uncertainties in climate change impacts: Low-flow scenarios for the River Thames, UK. *Water Resources Research,* 42**,** 10.

Wilby, R. L., Hay, L. E. & Leavesley, G. H. (1999) A comparison of downscaled and raw GCM output: implications for climate change scenarios in the San Juan River basin, Colorado. *Journal of Hydrology,* 225**,** 67-91.

Wilby, R. L., Tomlinson, O. J. & Dawson, C. W. (2003) Multi-site simulation of precipitation by conditional resampling. *Climate Research,* 23**,** 183-194.

Wilby, R. L., Troni, J., Biot, Y., Tedd, L., Hewitson, B. C., Smith, D. M. & Sutton, R. T. (2009) A review of climate risk information for adaptation and development planning. *International Journal of Climatology,* 29**,** 1193-1215.

Wilks, D. S. (1998) Multisite generalization of a daily stochastic precipitation generation model. *Journal of Hydrology,* 210**,** 178-191.

Wood, A. W., Leung, L. R., Sridhar, V. & Lettenmaier, D. P. (2004) Hydrologic implications of dynamical and statistical approaches to downscaling climate model outputs. *Climatic Change,* 62**,** 189-216.

Woollings, T. (2010) Dynamical influences on European climate: an uncertain future. *Philosophical Transactions of the Royal Society A: Mathematical, Physical and Engineering Sciences,* 368**,** 3733-3756.

Xu, C. Y. (1999) From GCMs to river flow: a review of downscaling methods and hydrologic modelling approaches. *Progress in Physical Geography,* 23**,** 229-249.

Xu, H., Taylor, R. G. & Xu, Y. (2011) Quantifying uncertainty in the impacts of climate change on river discharge in sub-catchments of the Yangtze and Yellow River Basins, China. *Hydrology and Earth System Sciences,* 15**,** 333-344.

Yip, S., Ferro, C. A. T., Stephenson, D. B. & Hawkins, E. (2011) A Simple, Coherent Framework for Partitioning Uncertainty in Climate Predictions. *Journal of Climate,* 24**,** 4634-4643.

Zhang, X., Srinivasan, R. & Liew, M. V. (2010) On the use of multi-algorithm, genetically adaptive multi-objective method for multi-site calibration of the SWAT model. *Hydrological Processes,* 24**,** 955-969.

Zorita, E. & Von Storch, H. (1999) The Analog Method as a Simple Statistical Downscaling Technique: Comparison with More Complicated Methods. *Journal of Climate,* 12**,** 2474-2489.